# Nontypeable *Haemophilus influenzae*-Induced Inflammation, Corticosteroids Unresponsiveness and Functional Polarisation in COPD Alveolar Macrophages

A thesis submitted to The University of Manchester for the degree of Doctor of Philosophy in the Faculty of Medical and Human Sciences

**2016**

**Rana Muhsin Khalaf**

**School of Medicine**

## List of Contents                                           Page

### Chapter One: Introduction

**Chapter Two: Materials and Methods**

## Chapter Three: NTHi Induced Cytokine Release in Human Alveolar Macrophages

**Chapter Four: The Effects of Corticosteroids and Kinase Inhibitors on NTHi Stimulation in Human Alveolar Macrophages**

**Chapter Five: Alveolar Macrophage Functional Polarisation in Response to NTHi Infection**

**Chapter Six: General Discussion**

**Final word count: 42,945**

**List of Tables:**

**List of Figures:**

## List of abbreviations:

| | |
|---|---|
| **µg** | Microgram |
| **µl** | Microlitre |
| **µM** | Micromolar |
| **ANOVA** | Analysis of Variance |
| **AP-1** | Activator Protein 1 |
| **APS** | Ammonium Per Sulphate |
| **AIs** | Autoinducers |
| **AI2** | Autoinducer-2 |
| **AZD6244** | Selumetinib (ARRY-142886) |
| **BAC CHOC** | Bacitracin Chocolate Agar |
| **BAL** | Bronchoalveolar Lavage |
| **Birb-796** | 1-5-tert-butyl-2-p-tolyl-2H-pyrazol-3-yl)-3- [4- (2-morpholin-4-yl-ethoxy) naphthalen-1-yl] urea. |
| **BHI** | Brain Heart Infusion |
| **BMS-345541** | (4 (2′-aminoethyl) amino-1,8-dimethylimidazo (1,2-a) quinoxaline) |
| **BSA** | Bovine Serum Albumin |
| **BSAC** | British Society for Antimicrobial Chemotherapy |
| **cAMP** | Cyclic Adenosine Monophosphate |
| **CAT** | COPD Assessment Test |
| **CBA** | Colombia Blood Agar |
| **CBP** | cAMP Response Element Binding Protein |
| **CCL1** | Chemokine C-C Motif Ligand 1 |
| **CCL13** | Chemokine C-C Motif Ligand 13 |

| | |
|---|---|
| **CCL16** | Chemokine C-C Motif Ligand 16 |
| **CCL17** | Chemokine C-C Motif Ligand 17 |
| **CCL18** | Chemokine C-C Motif Ligand 18 |
| **CCL24** | Chemokine C-C Motif Ligand 24 |
| **CD14** | Cluster of Differentiation 14 |
| **CD163** | Cluster of Differentiation 163 |
| **CD36** | Cluster of Differentiation 36 |
| **CD38** | Cluster of Differentiation 38 |
| **CD80** | Cluster of Differentiation 80 |
| **CD86** | Cluster of Differentiation 86 |
| **cDNA** | Complementary Deoxyribonucleic Acid |
| **CFU** | Colony Forming Unit |
| **CHO** | Chinese Hamster Ovary |
| **CHOC** | Columbia Agar Chocolate |
| **$CO_2$** | Carbon Dioxide |
| **COPD** | Chronic Obstructive Pulmonary Disease |
| **CR** | Complement Receptor |
| **CSE** | Cigarette Smoke Extract |
| **Ct** | Cycle Threshold |
| **CXCL10** | Chemokine C-X-C Motif Ligand 10 |
| **CXCL5** | Chemokine C-X-C Motif Ligand 5 |
| **CXCL8** | Chemokine C-X-C Motif Ligand 8 |
| **CXCL9** | Chemokine C-X-C Motif Ligand 9 |
| **CXCR1** | Chemokine C-X-C Motif Receptor 1 |
| **CXCR2** | Chemokine C-X-C Motif Receptor 2 |

| | |
|---|---|
| **DAPI** | 4',6-Diamidino-2-Phenylindole |
| **DMSO** | Dimethyl Sulphoxide |
| **DNA** | Deoxyribonucleic Acid |
| **DTT** | Dithiothreitol |
| **dUTP** | Deoxythymidine Analog 5-Bromo-2´-Deoxyuridine 5´-Triphosphate |
| **ECM** | Extracellular Matrix |
| ***E. coli*** | *Escherichia coli* |
| **EDTA** | Ethylenediaminetetraacetic Acid |
| **EGF** | Epidermal Growth Factor |
| **EGFR** | Epidermal Growth Factor Receptor |
| **ELISA** | Enzyme Linked Immunosorbent Assay |
| **ERK** | Extracellular Signal-Regulated Kinase |
| **FBS** | Foetal Bovine Serum |
| **FcR** | Immunoglobulin Receptors |
| **FEV1** | Forced Expiratory Volume in 1 Second |
| **FVC** | Forced Vital Capacity |
| **GAPDH** | Glyceraldehyde-3-Phosphate Dehydrogenase |
| **G-CSF** | Granulocyte-Colony Stimulating Factor |
| **GM-CSF** | Granulocyte Macrophage-Colony Stimulating Factor |
| **GOLD** | Global Initiative for Obstructive Lung Disease |
| **GR** | Glucocorticoid Receptor |
| **GRE** | Glucocorticoid Response Element |
| **GRO** | Growth Related Oncogene |
| **$H_2O_2$** | Hydrogen Peroxide |

| | |
|---|---|
| **Hap** | *Haemophilus* Adhesion and Penetration |
| **HDAC2** | Histone Deacetylase 2 |
| **Hib** | *Haemophilus influenzae* Serotype b |
| **HLA-DR** | Human Leukocyte Antigen-DR |
| **HMW proteins** | High Molecular Weight Proteins |
| **HSP 90** | Heat Shock Protein |
| **HTM** | Haemophilus Test Medium |
| **ICAM-1** | Intercellular Adhesion Molecule-1 |
| **ICS** | Inhaled Corticosteroids |
| **IgA** | Immunoglobulin A |
| **IKK 1** | IκB Kinase 1 |
| **IKK 2** | IκB Kinase 2 |
| **IL-10** | Interleukin-10 |
| **IL-12** | Interleukin-12 |
| **IL-13** | Interleukin-13 |
| **IL-1β** | Interleukin-1β |
| **IL-4** | Interleukin-4 |
| **IL-5** | Interleukin-5 |
| **IL-6** | Interleukin-6 |
| **IFN-γ** | Interferon Gamma |
| **IP-10** | Inducible Protein-10 |
| **I-TAC** | Interferon-Inducible T-cell α-Chemoattractant |
| **IκB** | Nuclear Factor-Kappa B Inhibitor |
| **JNK** | c-Jun amino (N)-Terminal Kinases |
| **KC** | Keratinocyte-Derived Cytokine |

| | |
|---|---|
| **L** | Litre |
| **LOS** | Lipooligosaccharide |
| **LPS** | Lipopolysaccharide |
| **LTB4** | Leukotriene B4 |
| **MAPK** | Mitogen-Activated Protein Kinase |
| **MAPKAPK** | MAPK Activated Protein Kinases |
| **MAPKK** | MAPK Kinase |
| **MAPKKK** | MAPKK Kinase |
| **MDM** | Monocyte Derived Macrophage |
| **mg** | Milligram |
| **MHC II** | Class II Major Histocompatibility Gene Complex |
| **Mig** | Monokine-Induced by Interferon- $\gamma$ |
| **MIP-2** | Macrophage Inflammatory Protein |
| **MKP-1** | MAPK Phosphatase-1 |
| **ml** | Millilitre |
| **mm** | Millimetre |
| **MMP-12** | Matrix Metalloproteinase-12 |
| **MMP-2** | Matrix Metalloproteinase-2 |
| **MMP-7** | Matrix Metalloproteinase-7 |
| **MMP-9** | Matrix Metalloproteinase-9 |
| **mMRC** | Modified British Medical Research Council |
| **MOI** | Multiplicity of Infection |
| **MR** | Mannose Receptor |
| **MRC1** | Mannose Receptor C1 |
| **MSA** | Mannitol Salt Agar |

| | |
|---|---|
| **MUC2** | Mucin 2 |
| **MUC5AC** | Mucin 5AC |
| **NaCl** | Sodium Chloride |
| **NAD** | Nicotinamide Adenine Dinucleotide |
| **NF-κB** | Nuclear Factor Kappa-Light-Chain-Enhancer of Activated B-Cells |
| **ng** | Nanogram |
| **NGF** | Nerve Growth Factor |
| **NIK** | NF-κB Inducing Kinase |
| **NO** | Nitric Oxide |
| **Nrf2** | Nuclear Factor Erythroid 2–Related Factor 2 |
| **NTHi** | Nontypeable *Haemophilus influenzae* |
| **OD** | Optical Density |
| **OMP P2** | Outer Membrane Proteins P2 |
| **OMP P5** | Outer Membrane Proteins P5 |
| **OMP P6** | Outer Membrane Proteins P6 |
| **PAF** | Platelet-Activating Factor |
| **PAMPs** | Pathogen- Associated Molecular Patterns |
| **PBMCs** | Peripheral Blood Mononuclear Cells |
| **PBS** | Phosphate Buffered Saline |
| **PCho** | Phosphorylcholine |
| **PCR** | Polymerase Chain Reaction |
| **PDE-4** | Phosophodiesterase 4 |
| **PDGF** | Platelet-Derived Growth Factor |
| **PHE** | Public Health England |

| | |
|---|---|
| **PI3 kinase** | Phosphatidylinositol-3-Kinase |
| **PMNs** | Polymorphonuclear Leukocytes |
| **Poly I:C** | Polyinosinic: polycytidylic Acid |
| **PRR** | Pattern Recognition Receptors |
| **qPCR** | Quantitative Polymerase Chain Reaction |
| **QS** | Quorum Sensing |
| **RANTES** | Regulated Upon Activation Normal T-Cell Expressed and Secreted |
| **RIPA** | Radioimmunoprecipitation Assay |
| **RNA** | Ribonucleic Acid |
| **RNS** | Reactive Nitrogen Species |
| **ROS** | Reactive Oxygen Species |
| **RPM** | Revolutions Per Minute |
| **RT** | Room Temperature |
| **RT-PCR** | Reverse Transcription Polymerase Chain Reaction |
| **SDS** | Sodium Dodecyl Sulfate |
| **SLPI** | Secretory Leukocyte Protease Inhibitor |
| **TAK1** | TGF-β Activated Kinase 1 |
| **TBS** | Tris-Buffered Saline |
| **TdT** | Terminal Deoxynucleotidyl Transferase |
| **TEMED** | Tetramethylethylenediamine |
| **TGF-β** | Transforming Growth Factor- β |
| **TGS** | Tris-Glycine SDS |
| **Th1** | T Helper Cells Type 1 |
| **Th2** | T Helper Cells Type 2 |

| | |
|---|---|
| **TIMP** | Tissue Inhibitor of Metalloprotease |
| **TLR 2** | Toll-Like Receptors 2 |
| **TLR 4** | Toll-Like Receptors 4 |
| **TMB** | 3, 3', 5, 5' Tetramethylbenzidine |
| **TNF-α** | Tumour Necrosis Factor-α |
| **TUNEL** | Transferase dUTP Nick End Labelling |
| **UV** | Ultraviolet |

The University of Manchester
Rana Muhsin Khalaf
Doctor of Philosophy
Nontypeable *Haemophilus influenzae*-induced inflammation, corticosteroids unresponsiveness and functional polarisation in COPD alveolar macrophages.
2016

## Abstract:

COPD is a chronic inflammatory disease of the airways where many patients have recurrent lower airway bacterial infection, most commonly nontypeable *Haemophilus influenzae* (NTHi). Corticosteroids are commonly used anti-inflammatory drugs in COPD with limited clinical benefit. Previous studies focused on corticosteroid responsiveness in COPD did not consider the role of airway NTHi infection. Alveolar macrophages are the main inflammatory cells in COPD pathogenesis, a shift in their phenotype was highlighted in COPD patients. Some bacteria can modify alveolar macrophage phenotype to persist in the lower airways.

I have optimised a clinically relevant *in vitro* model of NTHi infection; human alveolar macrophages were stimulated with an increasing load of live NTHi clinical isolate (R2846). NTHi provoked time-dependent release of TNF-$\alpha$, IL-6, CXCL8 and IL-10 from alveolar macrophages, which was correlated with bacterial growth, lysis and phagocytosis in the model. Furthermore, NTHi load was inversely correlated with IL-10 release. These findings suggest that NTHi infection is a dynamic inflammatory process in human alveolar macrophages and pointed to the possible role of IL-10 in the NTHi persistence in the lower airways.

NTHi-induced cytokines in alveolar macrophages showed reduced corticosteroid responsiveness, CXCL8 was particularly corticosteroid unresponsive cytokine. NTHi-induced glucocorticoid receptor (GR) phosphorylation at ser 226 residue, which would encourage GR nuclear exportation. This might be one possible mechanism of reduced corticosteroid response in the model. In line with the latter finding, NTHi impaired the corticosteroid-induced GR nuclear localisation, which was partially reversed by p38 MAPK inhibitor (BIRB-796). These results suggest the role of NTHi in corticosteroid unresponsiveness in COPD alveolar macrophages. NTHi-induced cytokine release in alveolar macrophages was mediated by NF-$\kappa$B, p38 and ERK MAPK pathways. Combination of corticosteroid (dexamethasone) with p38 and ERK MAPK inhibitors (BIRB-796 and AZD6244 respectively) showed a potential synergistic anti-inflammatory effect in the model. Therefore, inhibitors of MAPK pathways might serve as future anti-inflammatory therapies in NTHi-infected COPD patients.

NTHi *in vitro* infection caused upregulation of the pro-inflammatory (TNF-$\alpha$, CXCL8, CD38) and the anti-inflammatory (IL-10) markers' mRNA levels in COPD alveolar macrophages. Meanwhile, NTHi downregulated the antigen-presentation molecule (HLA-DR) and the scavenger receptors (CD14, CD36, CD163 and CD206) mRNA levels in COPD alveolar macrophages. Moreover, sputum macrophages from NTHi-infected stable COPD patients showed lower mRNA levels of CD36 and HLA-DR. These findings suggest that the NTHi modification of alveolar macrophage functions, especially antigen presentation and efferocytosis, might be a possible mechanism of NTHi chronic infection and COPD disease progression.

## Declaration:

No portion of the work referred to in the thesis has been submitted in support of an application for another degree or qualification of this or any other university or other institute of learning.

## Statement of Originality

All work in this thesis was conducted by the author. The only exception was the optimisation of bacterial work in our lab which was assisted by Dr. Hannah Metcalf and Dr. Sarah Jackson.

## Publications Related to this Thesis

R Khalaf, S Lea, H Metcalf, D Singh. *Haemophilus influenzae* stimulation of alveolar macrophages from COPD patients; effects of corticosteroids. Thorax 2013; 68: A59.

## The author

I am a medical doctor holding M.B.Ch.B degree and M.Sc degree in clinical pharmacology from Al-Nahrain College of Medicine/Iraq. My previous research interest was drugs-induced nephrotoxicity. However, I have started new research interest in my PhD program involving inflammatory mechanisms in COPD.

## Acknowledgement:

I would like to express my sincere thanks to my main supervisor Professor Dave Singh, for his knowledge, guidance and critical comments throughout my work and thesis writing. I am deeply grateful for my co-supervisor Dr. Simon Lea, for his valuable support, guidance and patience since my first steps in this study.

I also would like to acknowledge the support of my advisor Dr. Jonathan Plumb, and the members of airway pharmacology team in Education and Research Centre for providing me with the necessary skills and facilities for my research.

I am extremely thankful to Dr. Hannah Metcalf, Dr. Justyna Sutula and Dr. Sarah Jackson, for their great help in optimising my bacterial work, and to Dr. Nicola High (Faculty of Life Sciences) for providing me with the standard bacterial strains for this research.

I would like to thank the medical statistician, Mr. Philip Foden, who advised on all statistical analysis and data representation in this thesis.

I also would like to thank all members of the recruitment team in Medicine Evaluation Unit, for helping me to get my study samples.

## Dedication:

I dedicate my thesis to my family in Iraq; my parents, sisters, brothers and friends, who were supporting me with their encouraging words and prayers.

I dedicate my work to my husband Hayder, who gave me all the encouragement and help throughout my work. I would not finish my PhD without him.

Last but not least, I dedicate this thesis to my lovely daughters Zainab and Khadeejah, whose sentence "Mom, don't give up, you are nearly there" kept me going all the way through, and to my unborn son, whose kicks helped speed up my thesis writing.

# Chapter one

# Introduction

---

### 1.1: Chronic obstructive pulmonary disease (COPD):

### 1.1.1. Definition:

COPD is a clinical entity characterised by slowly progressive airway obstruction that is not fully reversible (1). The airflow limitation in COPD is associated with an abnormal inflammatory response of the airways to noxious particles and gases (2,3). Disease exacerbations and comorbidities contribute to the overall severity in individual patients (4).

### 1.1.2. Risk factors

Worldwide, cigarette smoking is the most commonly encountered risk factor for COPD (2). The risk of COPD is proportional to the burden of tobacco smoking which is defined by the duration and amount of cigarettes smoked (5). Industrial dust and chemicals , and in many countries, air pollution has also been identified as a COPD risk factor (2). It is noteworthy that not all smokers develop COPD. This points to the role  of host factors in the development of the disease, that may include genetic predisposition, inherited α1-antitrypsin deficiency, history of asthma and childhood respiratory illnesses (5).

### 1.1.3. Burden of the disease:

COPD is a major cause of chronic morbidity and mortality throughout the world, resulting in an increasing economic and social burden. Estimates predict that COPD will become the third leading cause of death worldwide in 2030 (2,6,7). Prevalence, morbidity and mortality vary across countries. However,  prevalence is directly related to the prevalence of tobacco smoking (2).

### 1.1.4. COPD exacerbation:

An exacerbation is defined as an event in the natural course of the disease characterised by a change in the patient's baseline dyspnoea, cough, and sputum

production that is beyond normal day-to-day variations. The change in symptoms is acute in onset, and may warrant a change in regular medication in a patient with underlying COPD (8,9). The impact of exacerbations is significant and a patient's symptoms and lung function may both take several weeks to recover to the baseline values (10).

The main etiologic factors in acute exacerbations are thought to be respiratory tract infections and air pollution (11). Infectious agents, such as bacteria, viruses, and atypicals are currently implicated in up to 80% of these episodes. Bacteria is possibly playing a role in 50% of exacerbations (12). The spectrum of bacterial pathogens isolated from respiratory secretions changes with the severity of underlying airflow obstruction (13–15). Nontypeable *Haemophilus influenzae* (NTHi) is the most commonly isolated bacterium in all severities of COPD. *Moraxella catarrhalis* and *Streptococcus pneumoniae* are less frequently isolated, while Gram-negative bacilli, predominantly *Pseudomonas aeruginosa* , are more often isolated from patients with very severe COPD (16).

### 1.1.5. Pathogenesis:

The main pathogenic events in COPD are: inflammation, protease-antiprotease imbalance and oxidative stress.

### 1.1.5.1. Inflammation:

Airway inflammation is the primary pathogenic mechanism in the development of COPD. It is present in small airways of all smokers, but in COPD there is an abnormal and enhanced inflammatory response to inhaled toxins, leading to tissue destruction (emphysema), mucus hypersecretion (chronic bronchitis) and small airway inflammation and fibrosis (Bronchiolitis) (17). This inflammatory response

is characterised by increased numbers of inflammatory cells, namely neutrophils, macrophages, and T lymphocytes (CD8+ more than CD4+) in the lungs. These inflammatory cells release a variety of cytokines and mediators that participate in the disease process (17). In general, the extent of inflammation is related to the degree of airflow obstruction. It is known that airway inflammation persists in spite of smoking cessation through an unknown mechanism. Although autoantigens and persistent microorganisms may play a role (18).

### 1.1.5.2. Proteases-antiprotease imbalance:

The imbalance between lung tissue destruction by proteases and the protective effect of antiproteases in the lung is a widely accepted mechanism of pulmonary emphysema (19). COPD lungs show an increased production (or activity) of proteases which damage the connective tissue components. This increase is associated with inactivation (or reduced production) of antiproteases which protect the tissue from the damaging effect of proteases (2). This state of imbalance is mediated by cigarette smoke and inflammation-induced oxidative stress, which primes several inflammatory cells to release a combination of proteases and inactivates several antiproteases by oxidation (5). The protease destruction of elastin, which is the major component of lung parenchyma, would result in emphysema that is likely to be irreversible (2). Proteases are mainly produced by neutrophils and alveolar macrophages (20). The main proteases produced by neutrophils are serine proteases (neutrophil elastase, cathepsin G, and protease 3), which were found to produce emphysema in experimental animals (21–23). Furthermore, inhibition of neutrophil elastase was reported to reduce cigarette smoke-induced emphysema in guinea pigs (24). Neutrophil elastase activity in the bronchoalveolar lavage (BAL) fluid from COPD patients showed a positive

correlation with the severity of emphysema (25). Likewise, proteases released by alveolar macrophages, like cathepsin B and matrix metalloproteases (MMP), were identified as important mediators of airway remodelling and development of emphysema (19,26). Expression of MMP-1, MMP-2, MMP-8 and MMP-9 was reported to be increased in alveolar macrophages and lung tissue from emphysema patients (27,28). As a result of the abundance of neutrophils and macrophages in the COPD lung, a proteases-rich milieu will be generated causing lung tissue destruction (20,29). On the other hand, impaired antiprotease function, such as α1-antitrypsin deficiency (30,31) and tissue inhibitors of metalloproteases (TIMP) polymorphism (19) was linked to the development of emphysema. Moreover, α1-protease inhibitor activity was found to be inversely correlated with severity of emphysema in COPD patients (25). Secretory leukocyte protease inhibitor (SLPI), which is a potent inhibitor of neutrophil elastase, was reported to be decreased in sputum of patients with chronic bronchitis (32). These data indicate that the proteases-antiproteases imbalance in the COPD lung is a major factor in disease pathogenesis.

### 1.1.5.3. Oxidative stress:

The oxidative burden is increased in COPD. Sources of oxidants include cigarette smoke and reactive oxygen (ROS) and nitrogen species (RNS) released from inflammatory cells (33). Also, there is a reduction in endogenous antioxidants due to downregulation of the transcription factor Nuclear factor erythroid 2–related factor 2  (Nrf2) that regulates the transcription of antioxidants genes (34). This imbalance in oxidants and antioxidants results in increased oxidative stress which can inactivate antiproteases or stimulate mucus production (17). ROS and aldehydes play a crucial role in enhancing the inflammation. This is achieved through the activation of mitogen-activated protein kinases (MAPK) and

transcription factors such as nuclear factor-kappa-light-chain enhancer of activated B-cells (NF-κB) and activator protein-1 (AP-1). Oxidative stress also alters nuclear histone acetylation and deacetylation leading to increased gene expression of pro-inflammatory mediators in the lung (33).

### 1.1.6. Pathophysiology:

The above mentioned pathogenic factors result in the characteristic abnormal features of the disease, including air flow limitation, mucus hypersecretion, gas exchange defects and systemic features.

### 1.1.6.1. Airway obstruction and hyperinflation:

Small airways obstruction is the consequence of chronic airway inflammation, fibrosis and luminal inflammatory exudates. Airways obstruction will ultimately result in expiratory air trapping and hyperinflation (17). Emphysema contributes to hyperinflation and it is believed that hyperinflation develops early in the course of the disease. Moreover, hyperinflation is a major contributor to the dyspnoea and exercise intolerance seen in COPD patients (2).

### 1.1.6.2. Gas exchange abnormalities:

Oxygen and carbon dioxide ($CO_2$) transfer in the COPD lung are impaired, resulting in arterial hypoxemia and hypercapnia (17). The gas exchange defect results from abnormal ventilation/perfusion ratio. This is related to structural changes in the lung (2).

### 1.1.6.3. Mucus hypersecretion and ciliary dysfunction:

Chronic productive cough is a feature of chronic bronchitis. However, not all COPD patients have symptomatic mucus overproduction. The mechanisms of mucus hypersecretion include squamous metaplasia, goblet cell hyperplasia and

hypertrophy of bronchial submucosal glands. These pathological changes are due to chronic irritation by noxious particles (2,35). In addition, different mediators and proteases stimulate mucus secretion through activation of epidermal growth factor receptors (EGFR) (2).

Ciliary dysfunction is another feature of the disease which results from squamous metaplasia. This dysfunction could impair the mucociliary escalator and the normal mucus clearance (17).

### 1.1.6.4. Pulmonary hypertension:

Pulmonary hypertension occurs in advanced disease due to hypoxic pulmonary vascular constriction, endothelial dysfunction and loss of pulmonary capillary bed in emphysematous lung tissue (36). Progressively increased pressure in the pulmonary circulation could eventually lead to right-sided heart failure (17).

### 1.1.6.5. Systemic manifestations:

COPD comorbid conditions affect the patient's quality of life and mortality rate (4). Airway remodelling could affect gas exchange and cardiac function. Moreover, chronic systemic inflammation associated with the disease could initiate cardiovascular complications, skeletal muscle wasting, diabetes, osteoporosis and depression (2).

### 1.1.7. COPD diagnosis:

Clinical diagnosis of COPD is considered in any patient with dyspnoea, chronic cough or sputum production who had a history of exposure to any of the disease risk factors. In this clinical context, spirometry is needed to confirm airflow limitation which is defined as the ratio of post-bronchodilator forced expiratory volume in one second/forced vital capacity (FEV1/FVC) <0.70 (2).

### 1.1.8. Classification of severity of airflow limitation in COPD:

According to the Global Initiative for Obstructive Lung Disease (GOLD), the severity of airflow limitation is divided into four stages depending on spirometric endpoints. FEV1 measurement after inhalation of short acting bronchodilator is used to determine the severity of the disease as shown in Table 1.1 (37).

**Table 1.1:** **Classification of severity of airflow limitation in COPD.**

| COPD stage | Description | Post-bronchodilator FEV$_1$ (% predicted) | Post-bronchodilator FEV$_1$/FVC ratio (%) |
|---|---|---|---|
| GOLD 1 | Mild | FEV$_1 \geq 80\%$ | <70% |
| GOLD 2 | Moderate | 50%≤ FEV$_1 <80\%$ | <70% |
| GOLD 3 | Severe | 30%≤ FEV$_1 <50\%$ | <70% |
| GOLD 4 | Very severe | FEV$_1 <30\%$ | <70% |

**Abbreviations:** FEV$_1$= Forced expiratory volume in one second, FVC= Forced vital capacity

### 1.1.9. Assessment of COPD:

The goals of COPD assessment, defined by GOLD strategy in 2011, are to determine the severity of the disease, its impact on patient's health status, and the risk of future events (exacerbations, hospital admission and death). Eventually, this assessment will help to guide therapy. Different aspects of the disease are assessed separately. These include the degree of airflow limitation, the risk of exacerbation, comorbidities and symptoms (38). Furthermore, symptoms can be assessed by either COPD Assessment Test (CAT) or modified British Medical Research Council (mMRC). Table 1.2 summarises the combined assessment of COPD.

**Table1.2: Combined assessment of COPD**
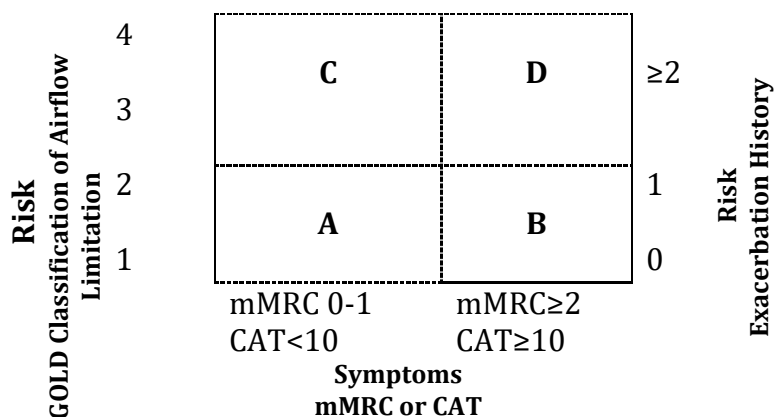


| Patient | Characteristics | Spirometric Classification | Exacerbations per year | mMRC | CAT |
|---|---|---|---|---|---|
| A | Low risk Less symptoms | GOLD 1-2 | ≤ 1 | 0-1 | CAT<10 |
| B | Low risk More symptoms | GOLD 1-2 | ≤ 1 | ≥ 2 | CAT≥10 |
| C | High risk Less symptoms | GOLD 3-4 | ≥ 2 | 0-1 | CAT<10 |
| D | High risk More symptoms | GOLD 3-4 | ≥ 2 | ≥ 2 | CAT≥10 |

**Abbreviations:** CAT= COPD Assessment Test, mMRC= Modified British Medical Research Council

## 1.1.10. Pharmacotherapy of stable COPD:

According to the GOLD strategy, the objectives of pharmacotherapy in COPD are to relieve symptoms, reduce severity and frequency of exacerbation, and improve exercise tolerance and health status. To date, no medication has been proven to modify the long-term decline in lung function (2).

Drugs that are used in the treatment of stable COPD include bronchodilators, corticosteroids, methylxanthines and phosphodiesterase-4 inhibitors.

### 1.1.10.1. Inhaled bronchodilators

Bronchodilators are drugs that reduce the bronchial muscle tone and improve $FEV_1$. They include $\beta_2$ agonists and anticholinergics. $\beta_2$ agonists relax the airway smooth muscles by stimulation of $\beta_2$ receptors. Short-acting agonists with 4-6 hours duration of action, like salbutamol and terbutaline, could improve symptoms and FEV1 when used as needed or on a regular basis (39). On the other hand, long-acting agonists, like salmeterol and formoterol, produce a longer duration of effect on symptom relief and FEV1. These drugs improve health status and exacerbation frequency. However, they have no effect on mortality rate and the decline in lung function (40–42).

Anticholinergic bronchodilators act by blocking muscarinic cholinergic receptors in the airways. Short-acting anticholinergics, like ipratropium bromide, cause symptomatic relief for up to 8 hours. However, the effect of the long-acting anticholinergic, tiotropium, lasts for 24 hours. It improves health status and reduces exacerbation frequency (43–45). The combination of bronchodilators with different mechanisms induces greater bronchodilation with fewer side effects. Combining short-acting or long-acting $\beta_2$ agonists with an anticholinergic improve FEV1 and symptoms greater than each compound does alone (46,47).

### 1.1.10.2.  Inhaled corticosteroids (ICS):

The use of inhaled corticosteroids (ICS) in stable COPD is reserved for patients with severe disease and frequent exacerbation (48). Regular use of ICS improves symptoms, lung function and quality of life, and decreases the frequency of exacerbation in COPD patients with FEV1< 60% predicted (40,49–51). Nevertheless, it does not improve long-term decline in lung function or mortality (2,52,53). An updated meta-analysis showed a significant increase in the risk of pneumonia with the

ICS fluticasone and budesonide (54). The benefits of ICS should, therefore, be balanced against the risk of a higher incidence of pneumonia. ICS can be combined with long-acting β2-agonists (with or without long-acting anti-cholinergics) in moderate to severe COPD. Such combination improves lung function, symptoms and exacerbation rate better than individual drug does alone (40,49,51). In addition to the risk of pneumonia, ICS prolonged use is associated with oral candidiasis, skin bruising and osteoporosis (2,55).

### 1.1.10.3. Methylxanthines:

Methylxanthines are non-selective phosphodiesterase inhibitors, with bronchodilator and non-bronchodilator effects. Theophylline is the most commonly used methylxanthine. It has been shown to improve lung function and gas exchange compared to placebo (56). Theophylline may be added if symptomatic control is suboptimal despite triple inhaler therapy in severe COPD. It is not used as a first line bronchodilator because its effects are modest, and its therapeutic index is narrow (2).

### 1.1.10.4. Phosphodiesterase-4 (PDE-4) Inhibitors

PDE-4 inhibitors reduce inflammation by inhibiting the breakdown of intracellular cyclic adenosine monophosphate (cAMP). Roflumilast, a highly selective PDE-4 inhibitor, has been shown to improve lung function and reduce exacerbation rate in severe COPD (57), and in patients with chronic bronchitis (58). However, the side effects of the drug including nausea, diarrhoea, weight loss and headache may be a problem for some patients (59). In general, PDE-4 inhibitors should be used in combination with at least one long-acting bronchodilator (2).

### 1.1.11. Pharmacotherapy of exacerbation:

Three main drug categories are used in the treatment of COPD exacerbation; bronchodilators, corticosteroids and antibiotics. Short-acting $\beta_2$ agonists, with or without short-acting anticholinergics, are the first choice bronchodilators (60). Systemic corticosteroids are recommended during exacerbation as they reduce recovery time, improve lung function, improve arterial hypoxaemia, and minimise the risk of early relapse and treatment failure. Oral prednisolone at a dose of 40 mg/day for five days is recommended (61).

Antibiotics are recommended in bacterial exacerbations. Studies showed that antibiotic use reduces mortality rate and improves symptoms in a considerable proportion of patients (62,63). Patients with increased dyspnoea, sputum volume and sputum purulence require antibiotic therapy (2). Duration of antibiotic therapy is 5-10 days, and the choice of antibiotic depends on the bacterial resistance pattern.

Hospitalisation of patients with COPD may be necessary to provide antibiotic therapy, appropriate supportive care and monitor oxygen status. Oxygen supplementation via external devices or mechanical ventilation may be indicated to maintain oxygen delivery to vital tissues (64).

## 1.2. Airway inflammatory profile in stable and exacerbated COPD:

Airways of COPD patients are infiltrated by different inflammatory cells which release a variety of inflammatory mediators. The abundance of the inflammatory cells during the stable disease is different from that during an exacerbation.

### 1.2.1. Airway inflammation in stable COPD:

COPD is a heterogeneous inflammatory disease in which different inflammatory cells are involved in mediating disease development and progression. Studies showed increased numbers of alveolar macrophages, neutrophils, T and B lymphocytes in the alveoli and airways of COPD patients (3).

### 1.2.1.1. Alveolar macrophages:

Alveolar macrophages play a central role in the pathophysiology of COPD. They account for most of the pathogenic features of the disease (3,65). There is 5-10 fold increase in alveolar macrophages in the airways of COPD patients compared to healthy controls (3). Alveolar macrophages are the cells of interest in this thesis, therefore, detailed explanation of its role in disease pathophysiology will be discussed in a separate section.

### 1.2.1.2. Neutrophils:

Circulating neutrophils are recruited to the lungs in response to cigarette smoking by the chemotactic factors Chemokine C-X-C Motif Ligand 8 (CXCL8) and Leukotriene B4 (LTB4). These chemokines are released from alveolar macrophages and airway epithelial cells (66,67). Neutrophils were found to increase in sputum and BAL fluid from COPD patients, and their number correlated with disease severity (68–70). Neutrophils secrete the serine proteases MMP-8 and 9, which are involved in alveolar destruction and mucus hypersecretion (3).

### 1.2.1.3. T lymphocytes:

T lymphocytes are increased in the lung parenchyma (71) and peripheral blood (72,73) of COPD patients, with a greater increase in CD8 positive than CD4 positive cells (74–76). There is a positive correlation between the number of T lymphocytes and the degree of alveolar destruction and airflow limitation (71,74). The increase in T lymphocytes indicates chronic immune stimulation in the airways. This might be attributed to chronic lower airway colonisation with bacteria (77), or due to continuous parenchymal damage exposing new sites to the immune system as autoantigens (78).

### 1.2.1.4. Eosinophils:

The role of eosinophils in COPD pathophysiology is unclear, some studies revealed increased eosinophil count in the airways of stable COPD patients which contributes to airflow obstruction (79). However, others did not report such an increase (80). Increased eosinophil is observed during disease exacerbation more than during stable state (81,82). In the stable state, eosinophil count might predict the response to corticosteroids and the presence of coexisting asthma (79,83).

### 1.2.1.5. Epithelial cells:

Airway epithelial cells are involved in the innate and adaptive immune defences of the lung (3). They release different inflammatory mediators such as tumour necrosis factorα (TNF-α), CXCL8, granulocyte macrophage-colony stimulating factor (GM-CSF) and interleukin-1β (IL-1β) (84–86). Also, they produce transforming growth factor-β (TGF-β) which is involved in local fibrosis (87). Moreover, epithelial cells release antimicrobial molecules and mucus which are involved in defence against inhaled bacteria. Furthermore, they release antioxidants and antiproteases which are involved in tissue repair (88,89). Cigarette smoke

exposure could damage the innate immune defence of the epithelial cells resulting in increased susceptibility to infection (3). In COPD patients, epithelial cells showed higher expression of growth factor receptors. This might explain the squamous metaplasia seen in the airways of smokers and COPD patients, indicating increased risk of bronchial carcinoma (90).

### 1.2.2. Airway inflammation in COPD acute exacerbation:

The current understanding of acute exacerbation indicates that airway inflammation increases from the stable state. Investigation of inflammatory mechanisms could help to identify potential therapies which could modify airway inflammation and improve patient symptoms (91).

Below is a brief description of the changes in inflammatory cells and their mediators during acute exacerbations.

### 1.2.2.1. Macrophages:

Observational studies during acute exacerbation did not reveal any increase in alveolar macrophages (11,92,93). One study had even shown a significant reduction in the sputum macrophages during exacerbation (94). However, this reduction was in the percentage rather than the absolute number, which could be only a reflection of an increase in another cell type, especially neutrophils.

### 1.2.2.2. Neutrophils:

Neutrophils were found to increase in sputum and bronchial biopsy during acute exacerbations (95,96). In addition, increased neutrophilic inflammation markers, like myeloperoxidase, neutrophil elastase and CXCL8, was associated with an increase in sputum purulence (97). This association was prominent during acute exacerbation (98). The percentage of neutrophils in distal airways was negatively correlated with airflow obstruction during acute exacerbation (99). Neutrophil

recruitment appears to be mediated by the upregulation of neutrophil chemoattractants, CXCL5 and CXCL8, and their receptors (CXCR1 and CXCR2). The upregulation of these moleculaes was observed in bronchial biopsies from exacerbating COPD patients (96).

### 1.2.2.3. Lymphocytes:

CD8 positive T-lymphocytes were increased in the airways and lung tissue from COPD patients as compared to the healthy controls (74,100). Furthermore, an increase in CD8 positive cells in sputum and BAL fluid has been correlated with the severity of airflow limitation (101). During COPD exacerbation, CD4 positive/CD8 positive ratio in the sputum samples was reported to be significantly lower than that during the stable state. Moreover, type-2 CD8 positive cells, which produce IL-4, were found to be the predominant subtype during exacerbation (94). This evidence suggests that an imbalance in T lymphocyte subpopulations, with the predominance of CD8 positive type-2 cells, might be associated with the development of severe acute exacerbations (94).

### 1.2.2.4. Eosinophil:

During COPD exacerbations, it is recognised that an "asthma-like" inflammatory pattern in the airways may exist with increased numbers of eosinophils (81,102). The eosinophil attracting chemokines, regulated upon activation normal T-cell expressed and secreted (RANTES), eotaxin and IL-5 have been reported to be increased during acute exacerbations (93,103–105).

### 1.2.2.5: Inflammatory mediators:

Several inflammatory markers are increased in the respiratory tract during the acute exacerbation. TNF-α is increased in sputum during acute exacerbation (106,107). This could contribute to the upregulation of endothelial adhesion

molecules, thus facilitating cell migration as well as activating neutrophils directly (69). TNF-α may also increase the expression of RANTES to modulate eosinophil recruitment during exacerbation (105).

CXCL8 and LTB4 sputum levels were increased during acute exacerbation of chronic bronchitis. This increase was correlated with sputum purulence, increased neutrophil elastase and myeloperoxidase levels (98).

GM-CSF was found to be increased in BAL fluid during exacerbations (108). This cytokine stimulates differentiation of granulocytes and macrophages and can activate them directly. The effect of GM-CSF provides another mechanism whereby neutrophils, as well as eosinophils and macrophages can contribute to inflammatory changes within the airways (108).

Sputum IL-6 was increased during an exacerbation, and its level was higher when exacerbations were associated with symptoms of common cold. Interestingly, experimental rhinovirus infection has shown to increase sputum IL-6 levels in healthy subjects and patients with asthma (109,110).

Airway inflammation during exacerbation could worsen the protease-antiprotease balance. Degranulation of neutrophils and macrophages increased, resulting in the release of elastases and other proteases. Sputum MMP-9 level was correlated with increased neutrophil and lymphocyte counts during exacerbation (95). Also, neutrophil elastase was reported to increase in exacerbation episodes characterised by purulent sputum (98). In addition, a study showed reduced TIMP-1 level in sputum from exacerbated COPD patients, which was associated with an increase in MMP-9 (95). Impaired protease-antiprotease balance during exacerbation can cause epithelial damage and reduce ciliary beat frequency (111). Furthermore, the protease-antiprotease imbalance stimulates mucus secretion by goblet cells and increase the permeability of the bronchial mucosa resulting in

airway oedema and protein exudation into the airway (112) . These changes, especially in the small airways, may adversely affect airflow and lead to increased breathlessness, as well as to the increased mucus secretion and purulence which are characteristic features of acute exacerbations (98).

## 1.3. Alveolar macrophages:

Alveolar macrophages play a critical role in the pathophysiology of COPD (65). Macrophages are recruited to the lung as the first line immune response to inhaled toxins and pathogens. These cells have the ability to engulf toxic, pathogenic and allergic particles. Consequently, the number of recruited macrophages is increased several fold in the lung of smokers and COPD patients (113). Alveolar macrophages are localised to the areas of lung tissue destruction, and their number is positively correlated with the degree of emphysema and severity of COPD (71,114). Furthermore, alveolar macrophages were reported to survive for months to few years in COPD lung (115).

Possible mechanisms of increased alveolar macrophage count in COPD lung include increased monocyte recruitment from the circulation (67,116), increased alveolar macrophage proliferation (117,118), prolonged survival (115,117) and impaired mucociliary and lymphatic clearance of alveolar macrophages (65,119,120).

Alveolar macrophages have a significant role in maintaining pulmonary homeostasis through their diverse role in inflammation, antigen presentation, phagocytosis and tissue remodelling. In order to perform its versatile function, alveolar macrophages are programmed to a spectrum of phenotypes in response to their microenvironmental signals (121).

### 1.3.1. Alveolar macrophage functional polarisation:

Macrophages are a dynamic and heterogeneous cell population which responds to the microenvironment by changing their functional polarisation state (122). *In vivo* environmental stimuli could induce a reversible macrophage functional polarisation state rather than inducing a distinct polarisation state (121).

50

There are two principal polarisation states or phenotypes; the classical activation or M1 macrophage and the alternative activation or M2 macrophage. These phenotypes represent the two poles of the macrophage activation spectrum and mirroring the T helper (Th) 1/ 2 dichotomy (121,123). They are distinctive in their activation stimulus, released mediators, expressed surface markers and effector function (122). Table 1.3 summarises the characteristics of each phenotype.

The classically activated M1 macrophage is activated by IFNγ, TNF-α and the bacterial component lipopolysaccharide (LPS). This phenotype releases pro-inflammatory cytokines like TNF-α, IL-12, IL-6, IL-1β; chemokines like CXCL8, CXCL9, CXCL10; as well as MMPs like MMP-9 and MMP-7. Moreover, it releases low levels of IL-10 (122). M1 macrophages are involved in Th1 activation, and the production of copious pro-inflammatory cytokines with microbicidal and antigen presenting function. Therefore, they are involved in host protection against infection (121,122,124). However, excessive or prolonged M1 response may result in serious damage to the host (125).

Alternative activation programme encompasses three distinct phenotypes, M2a, M2b and M2c. M2a macrophages are induced by IL-4 and IL-13. Meanwhile, M2b macropahges are induced by immune complexes, Toll-like receptors (TLR) and IL-1 receptor ligands. On the other hand, M2c macrophages are activated by IL-10 and glucocorticoids (124). M2 macrophages are immunoregulatory cells; they release high levels of IL-10 and low levels of pro-inflammatory cytokines (except M2b) (126). They are implicated in Th2 response (especially M2a) (124), tissue remodelling and phagocytosis of apoptotic cells (efferocytosis) (123). Alternatively activated macrophages have poor microbicidal efficacy, this can permit intracellular

growth of pathogens consequently resulting in chronicity of some bacterial infections (127,128).

A detailed transcriptome analysis of alveolar macrophages from COPD, healthy smokers and non-smokers control showed that smoking was associated with the downregulation of some M1 genes and upregulation of some M2 genes. This change in M1 and M2 genes was progressive with the development of COPD (129). These data suggest a possible role of dysregulated macrophage phenotype in smoking-induced lung disease.

**Table 1.3: Macrophage phenotype characteristics and biomarkers**

| Criteria | Classical activation M1 | Alternative activation | | |
|---|---|---|---|---|
| | | **M2a** | **M2b** | **M2c** |
| **Stimulating factor** | INF-γ + TNF-α or LPS | IL-4, IL-13 | Immune complex +TLR/IL-1R ligands | IL-10, glucocorticoids |
| **Cytokines/ Chemokines** | TNF-α, IL-12, IL-6, IL-1β, CXCL8, CXCL9, CXCL10, CCL5, CCL3 | IL-10, CCL18, CCL17, CCL24 | TNF-α, IL-6, IL-1, IL-10, CCL1 | IL-10, TGF-β, CCL16, CCL18, CXCL13 |
| **Surface receptors** | MHC II, CD80, CD86 | Mannose receptor, Scavenger receptor, MHC II, CD163 | MHC II, CD86, CD80 | Mannose receptor, Scavenger receptor, CD14 |
| **Function** | Pro-inflammatory Microbial killing Antigen presentation | Th2 responses, allergy, encapsulation of parasites | Immunoregulat-ion | Immunoregulat-ion Matrix deposition Tissue remodelling |

**Abbreviations:** IFN-γ= Interferon γ, TNF-α= Tumour necrosis factor-α, LPS= Lipopolysaccharide, IL (-4, -13, -10, -1, -6, -12) = Interleukin (-4, -13, -10, -1, -6, -12), TLR= Toll-like receptors, IL-1R= IL-1 receptor, TGF-β= Transforming growth factor-β, MHC II= Major histocompatibility complex class II, Th2= T helper type 2, CD= Cluster of differentiation, CCL= Chemokine C-C Motif Ligand, CXCL= Chemokine C-X-C Motif Ligand.

## 1.3.2. Heterogeneous role of alveolar macrophages in healthy and diseased lung

Alveolar macrophages have versatile functions in the lung and their dysregulated functions are thought to be an important pathogenic event in COPD development and progression. Figure 1.1 summarises the role of alveolar macrophages in COPD pathogenesis.
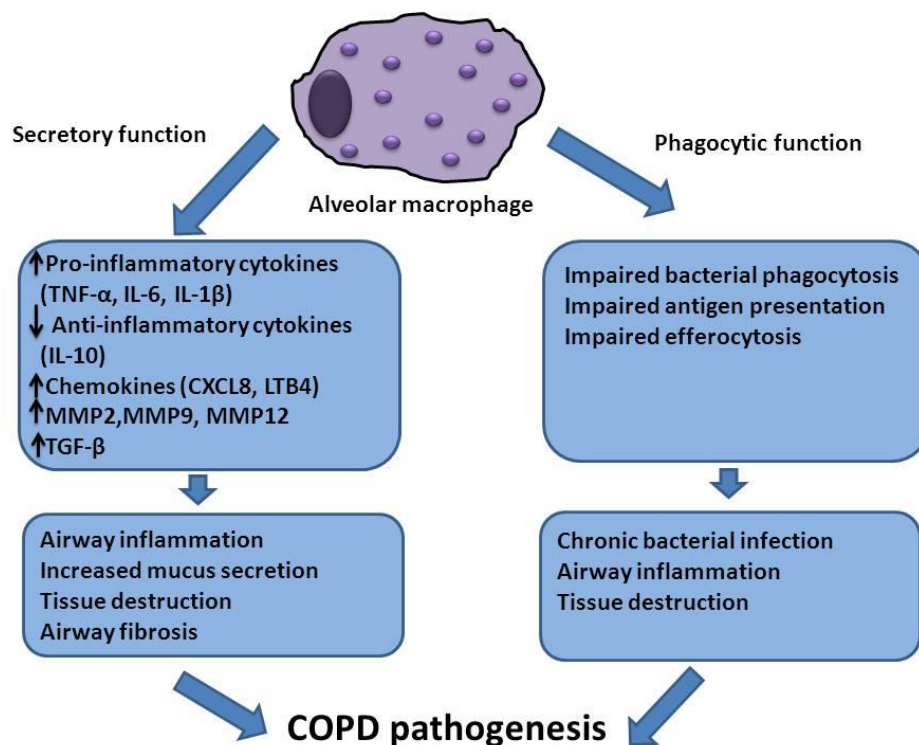


**Figure 1.1: Alveolar macrophage dysfunction in COPD.** Alveolar macrophage secretory and phagocytic functions are impaired in COPD. Increased pro-inflammatory mediators, decreased anti-inflammatory cytokines together with impaired bacterial phagocytosis and efferocytosis contribute to COPD pathogenesis and disease progression. TNF-α= Tumour necrosis factor-α, IL= Interleukin, LTB4= Leukotriene B4, TGF-β= Transforming growth factor- β, CXCL= Chemokine C-X-C Motif Ligand.

### 1.3.2.1. Role of alveolar macrophages in defence against inhaled pathogens:

Alveolar macrophages stand as the first line of defence against inhaled pathogens. These cells phagocytose the pathogen and present its antigens to T cells which in turn stimulate microbial killing by the macrophages (130).

#### 1.3.2.1.1. Phagocytosis of inhaled pathogen:

Alveolar macrophages are the main resident phagocytes in the lung. They phagocytose opsonised and non-opsonised pathogens through the expression of phagocytic receptors like immunoglobulin receptors (FcR), complement receptor (CR), mannose receptor (MR) and a group of scavenger receptors (131). Moreover, alveolar macrophages express a number of TLRs which recognise specific domain on the pathogen surface and induce the release of cytokines and other mediators to orchestrate cellular host defence (132). Cigarette smoke was reported to impair alveolar macrophage phagocytosis of live bacteria in mice (133). Moreover, alveolar macrophages from COPD patients showed reduced phagocytosis of potentially pathogenic bacteria like NTHi and *Streptococcus pneumonia in vitro* (134,135). Impaired macrophage phagocytosis in COPD could be one explanation of recurrent bacterial exacerbation and airway bacterial colonisation.

#### 1.3.2.1.2. Antigen presentation:

Alveolar macrophages represent a link between innate and acquired immunity. After phagocytosis of an antigen, alveolar macrophages present the antigen to T cells to initiate cell-mediated immunity (136). Antigen presentation is mediated through the surface marker human leukocyte antigen-DR (HLA-DR), which is a class II major histocompatibility gene complex (MHC II) molecule (137). Nevertheless, numerous studies indicate that alveolar macrophages do not present antigen effectively to T cells and could induce antigen-specific immune tolerance in

T cells (138,139). In the context of COPD, HLA-DR expression was downregulated in BAL-derived alveolar macrophages (140,141), suggesting hypoactivation of macrophages which could predispose to immunological tolerance and development of airway infection (142,143).

### 1.3.2.1.3. Microbicidal activity:

After pathogen phagocytosis, alveolar macrophages initiate phagolysosomal killing of the pathogen through the release of ROS, Nitric oxide (NO) and some proteases like lysozymes (65,144). Some respiratory pathogens like *Mycobacterium* species could survive and multiply in the phagosome by inhibiting phagolysosomal fusion and killing of the pathogen (145). Macrophages have a load-limited microbicidal capacity in human and mice (146). When the phagolysosomal killing mechanism is overwhelmed by a high bacterial load, macrophages would apply another killing strategy, the apoptosis-associated killing, which was demonstrated against intracellular bacteria like *Mycobacterium tuberculosis* and *Streptococcus pneumoniae* (127,147). COPD alveolar macrophages showed less mitochondrial ROS release and impaired apoptosis-associated killing following *in vitro* challenge with *Streptococcus pneumonia* (148). This suggests defective intracellular killing in COPD alveolar macrophages that could predispose to airway bacterial persistence.

## 1.3.2.2. Role of alveolar macrophages in the pro-inflammatory response:

Alveolar macrophages have a potent pro-inflammatory effect through the release of cytokines, chemokines and lipid mediators, which help in recruitment or activation of other immune cells during inflammation (149). In addition, some of the released pro-inflammatory mediators might act as a direct microbial killing agents (150). Release of inflammatory mediators from alveolar macrophages is triggered

by microbial molecules or other stimuli, through the activation of pattern recognition receptors (PRR) (149).

### 1.3.2.2.1. Release of the pro-inflammatory cytokines and chemokines:

Alveolar macrophages contribute to COPD-airway inflammation through the release of different pro-inflammatory cytokines and chemokines Like TNF-α, IL-6, IL-1β, IL-12 and CXCL8 (3).

TNF-α exerts a broad inflammatory effect in COPD, including activation of neutrophils, macrophages, monocytes, epithelial cells, mucus secretion and destruction of lung parenchyma (3). TNF-α could amplify airway inflammation through the activation of transcription factor NF-κB and p38 MAPK pathway. These pathways will, in turn, switch on different inflammatory genes (3). TNF-α is increased in sputum of COPD patients especially during disease exacerbations (69,106).

IL-6 has both pro-inflammatory and fibrotic actions that are implicated in the pathogenesis of COPD and lung fibrosis (151,152). IL-6 levels were reported to increase in sputum and exhaled breath of COPD patients, particularly during exacerbations (92,153). Furthermore, COPD monocytes released more IL-6 in response to LPS stimulation than non-COPD controls (154).

IL-1β has a similar inflammatory action to TNF-α (155), it stimulates MMP-9 release from different cell types (156). Studies on IL-1β receptor knockout mice supported its important role in the development of emphysema (22). In COPD, IL-1β was reported to increase in serum and it was negatively correlated with FEV1 (157). In addition, sputum levels of IL-1β were reported to increase in COPD especially during exacerbations (158).

Alveolar macrophages have the capacity to recruit several cell types from the circulation, including monocytes, neutrophils and T-lymphocytes via the release of multiple chemokines (3). The best-studied chemokine is CXCL8 (IL-8) (159). Other chemokines include, inducible protein (IP)-10 (CXCL10), interferon-inducible T-cell α-chemoattractant (I-TAC) (CXCL11) and monokine-induced by interferon- γ (Mig) (CXCL9) (160).

CXCL8 is a potent neutrophil chemoattractant which is released from alveolar macrophages in response to cigarette smoke, bacterial products, LPS and viruses (3). CXCL8 was found to be increased in induced sputum and BAL fluid from COPD patients. This increase was correlated with elevated neutrophil count (69,161,162). During bacterial exacerbation, CXCL8 was further increased in induced sputum and it was positively correlated to sputum bacterial load (98,106,163–165). This evidence indicates that bacterial infection in COPD induces neutrophilic inflammation, at least partly, by inducing CXCL8 release. In addition, development of emphysema was linked to CXCL8 (66). Taken together, these findings suggest the role of bacteria-induced neutrophilic inflammation in airway tissue destruction.

Some studies reported increased basal release of TNF-α and CXCL8 from COPD alveolar macrophages  as compared to healthy controls (166,167). However, other studies have shown that alveolar macrophages from COPD patients and smoking controls released  less cytokines ( such as TNF-α, IL-6 and CXCL8) upon LPS stimulation, as compared to healthy non-smokers (168). Furthermore, BAL-derived macrophages from cigarette smoke-exposed mice showed reduced TNF-α and IL-6 release in response to Polyinosinic:polycytidylic acid (poly I:C) and LPS (169). In line with these findings, exposure to cigarette smoke extract (CSE) was

reported to impair the release of IL-1β, IL-2 and TNF-α from human peripheral blood mononuclear cells (PBMCs) (170). Also, CSE downregulated the gene expression of some cytokines and chemokines like IL-1β and IL-6 in COPD-monocyte derived macrophages (MDMs) (171). On the other hand, cigarette smoke exposure was reported to be a potent inducer of CXCL8 release from COPD MDMs (171) and BAL-derived macrophages (172). Moreover, CSE further increased the LPS-induced CXCL8 release from human monocytic cell line (THP-1) (173). These findings imply that smoking can impair the innate immune response to infecting pathogen. However, acute exposure to cigarette smoke can upregulate the neutrophil recruitment by CXCL8 (168,171).

### 1.3.2.2.2. *Release of Leukotriene B4 (LTB4):*

Alveolar macrophages release lipid mediators upon activation, like LTB4. LTB4 is involved in neutrophil chemotaxis (3,174). LTB4 is increased in the exhaled breath condensate in stable COPD and was reported to increase further during exacerbation both in breath condensate and sputum (163,175,176).

### 1.3.2.3. Role of alveolar macrophages in immunoregulation:

Alveolar macrophages release a potent anti-inflammatory cytokine, IL-10, in response to inflammatory stimuli (3,121). It was reported that IL-10 release follows the acute pro-inflammatory response to LPS (177) and it acts as a negative regulator of the pro-inflammatory cytokines including TNF-α, IL-6 and CXCL8 (177,178). Furthermore, IL-10 inhibits MMP-9 release from COPD monocytes and at the same time activates TIMP-1, the natural endogenous inhibitor of MMP-9 (179,180). In the context of COPD, impaired IL-10 release was reported; sputum samples from COPD patients had less IL-10 levels than healthy non-smokers (181,182). Moreover, IL-10

release from LPS-stimulated lung explants from COPD patients was less than that released from healthy non-smokers (177).

### 1.3.2.4. Role of alveolar macrophages in Efferocytosis:

Efferocytosis is an important function of alveolar macrophages by which apoptotic cells are removed from lung tissue (183). Ingestion of apoptotic cells would help to prevent their secondary necrosis and release of their pro-inflammatory contents. These contents could disrupt tissue homeostasis and stimulate both innate and adaptive immunity against autoantigens promoting autoimmunity (183,184). In COPD, there is a higher burden of apoptotic cells than in healthy controls (183). *In vitro* studies reported defective efferocytosis in COPD alveolar macrophages (140,185). Moreover, impaired expression of efferocytosis receptors, cluster of differentiation (CD)31, CD44 and CD91, was reported in alveolar macrophages from smokers with COPD (186).

### 1.3.2.5. Role of alveolar macrophages in Tissue remodelling:

The airways of COPD patients are characterised by two main pathological events, which are lung parenchymal destruction and airway wall fibrosis. These changes result in airflow obstruction. Alveolar macrophages are believed to mediate tissue remodelling in the lung (187).

#### *1.3.2.5.1. Extracellular matrix destruction:*

Destruction of extracellular matrix (ECM) in the lung parenchyma (proteolysis) is one of the pathological features of COPD lung that eventually leads to emphysema  (155). ECM is a complex mixture of proteins including elastin, gelatin, collagen and laminin (188). Alveolar macrophages release a variety of proteases which are implicated in  degradation of elastin and other components of ECM (113). These proteases include; serine proteases, like neutrophil elastase;

cysteine proteases, like cathepsins B, L and S (21,189); and MMPs, like MMP-2 (gelatinase A), MMP-9 (gelatinase B) and MMP-12 (155,190). However, the most relevant elastolytic enzyme in COPD appears to be MMP-9 (27,191).

MMP release from alveolar macrophages is regulated by exposure to endotoxins, cytokines, phagocytosis and growth factors. MMPs degrade the ECM and also help to activate some cytokines like TGF-β, IL-1β and membrane-bound TNF-α (113). MMP-9 levels and elastolytic activity were increased in COPD alveolar macrophages when compared to healthy controls (155). Moreover, alveolar macrophages in COPD lung showed higher expression of MMP-9, MMP-1 and MMP-2 than healthy lung (27,28). Furthermore, macrophage count was increased at the site of emphysematous changes (71,114) and their role was verified in smoke-induced emphysema in mice (26). Overall, these results point to the pivotal role of alveolar macrophages in the development of emphysema.

### 1.3.2.5.2. Airway wall fibrosis:

Chronic inflammation in COPD airways can result in airway fibrosis due to excessive deposition of ECM in bronchi and bronchioles (192). Alveolar macrophages release growth factors like TGF-β and extracellular glycoproteins, like fibronectin, which have a fibrogenic potency (193,194). COPD alveolar macrophages release higher levels of TGF-β and fibronectin than non-COPD controls (194). Therefore, it appears that alveolar macrophages may contribute to airway fibrosis in COPD.

### 1.4. Nontypeable *Haemophilus influenzae* (NTHi) infection in COPD:

### 1.4.1. Microbiology:

*Haemophilus influenzae* is a small (1 μm X 0.3 μm), pleomorphic, gram-negative coccobacillus. It is a non-motile, non–spore-forming, fastidious, facultative anaerobe. It requires hemin (X) and β-nicotinamide adenine dinucleotide (NAD or V) for its aerobic growth (195). Figure 1.2 shows the microscopical and colonial morphology of *Haemophilus influenzae.*

*Haemophilus influenzae* is classified according to the presence or lack of polysaccharide capsule into typeable (encapsulated) and nontypeable (non-encapsulated) strains (NTHi). The most important encapsulated serotype is *Haemophilus influenzae* serotype b (Hib), which was responsible for bacteraemia, meningitis, and other invasive infections before the routine use of Hib conjugate vaccines in children (196). On the other hand, the non-encapsulated serotypes (NTHi) cause non- systemic infections including airway infections (195).
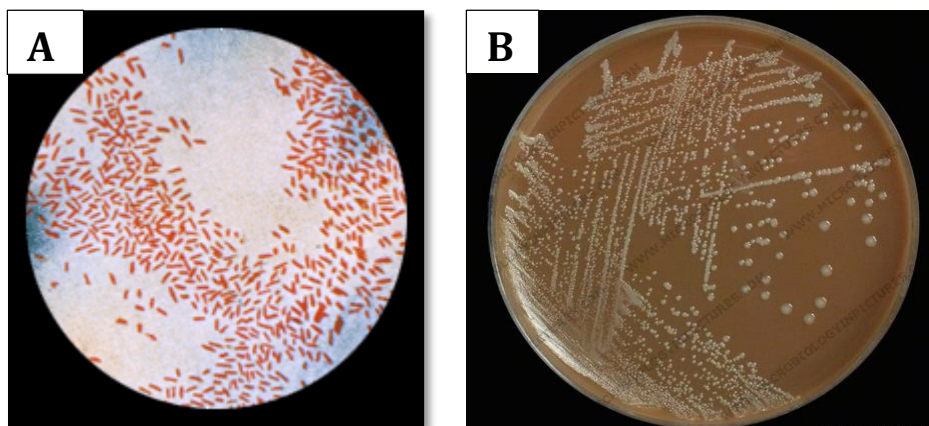


**Figure 1.2:** **Microscopical features and colonial morphology of *Haemophilus influenzae.*** Microscopically, *Haemophilus influenzae* is a gram-negative, pleomorphic coccobacillus (A) (197) *.* Colonies appear as convex, smooth, pale, grey or transparent colonies on Chocolate agar (B) (198).

### 1.4.2. Epidemiology:

*Haemophilus* species constitute approximately 10% of the upper respiratory tract normal flora in human (199) and is transmitted from person to person via airborne droplets and direct contact with respiratory secretions (200). NTHi is an opportunistic human respiratory tract pathogen, which can be either asymptomatic or can cause local infections like otitis media, acute pneumonia and sinusitis (201). However, recent findings indicate that NTHi can cause invasive infection such as meningitis, septic arthritis and bacteraemia (202). NTHi asymptomatic infection is referred to as colonisation. It has been reported that 44% of children below two years were colonised with NTHi with higher carriage rate in older children (201,203).

### 1.4.3. Role of NTHi in stable COPD:

Lower airway NTHi colonisation is potentially harmful and participate in COPD pathogenesis and progression (204). NTHi is present frequently in the lower airways of about 30% of adults with COPD at any time, and with serial sampling NTHi is detected in about 60% (205–208). Studies using molecular diagnosis of NTHi revealed that some COPD patients are persistently colonised by NTHi despite negative sputum cultures (204).

Chronic NTHi infection can serve as a primary inflammatory stimulus and can potentiate the damaging effect of cigarette smoke (16). Neutrophilic airway inflammation with elevated inflammatory mediators, like TNF-α, CXCL8, MMP-9 and LTB4, was reported in NTHi colonised COPD patients and healthy smokers (207–210). Also, NTHi colonisation was associated with worse health status, more frequent exacerbations and accelerated decline in lung function (208).

NTHi- induced inflammation could contributes to the progression of COPD at all stages, through inducing neutrophil influx into the airways (208). Neutrophil necrosis will release its elastases and proteases as well as oxygen radicals resulting in lung parenchymal damage and a decline in lung function (211). In support of this concept, an animal study showed that exposure of mice to NTHi lysates resulted in an airway inflammatory profile similar to that seen in COPD, with increased neutrophil count, TNF-α, IL-6, IL-12 and IFNγ in BAL fluid (212). Furthermore, chronic NTHi exposure resulted in structural changes similar to that seen in COPD, including airway inflammatory cell infiltrate, lymphoid aggregates and airway fibrosis (212).

### 1.4.4. Role of NTHi in disease exacerbation:

Bacterial infection causes 30-50% of all COPD exacerbations with NTHi being the most commonly isolated bacteria (213). Frequency and severity of exacerbations are associated with airway colonisation (208). NTHi was isolated from the bronchial tissues of 87% of patients with exacerbations. On the other hand, it was isolated from 33% of stable COPD patients and 0% of healthy controls (206). The adaptive immune response after an exacerbation seems to be strain-specific and protects against recurrent exacerbation due to the homologous strain, but leaves the patient vulnerable to exacerbations caused by heterologous strains (214). This could be one mechanism of recurrent airway infections.

The exact mechanism by which NTHi could precipitate exacerbation in the course of its chronic colonisation state is not fully understood; some studies suggested increased bacterial concentration (or load) in the airways as one proposed mechanism of exacerbation (215,216). However, another study reported only a small rise in the airway bacterial load during exacerbation (217).

Nonetheless, the calculation of this study was reinterpreted by another group, who submitted a letter to explain that there was a mathematical error. Upon reinterpretation, there was a considerable increase in bacterial load during exacerbation (218). However, the mechanisms underlying these changes in bacterial load are unclear (219).

Another well-accepted explanation of exacerbation is the acquisition of new strains of NTHi either from the upper respiratory tract or developed from pre-existing strains (220).

### 1.4.5. Pathogenesis of NTHi infection in COPD:

The pathogenesis of NTHi infection begins with bacterial colonisation of the nasopharynx, a process that involves establishment on the mucosal surface and evasion of local immune mechanisms (221). A combination of virulent bacterial mechanisms and defective host immunity contributes to lower airway infection, resulting in inflammation and disease progression (195). Figure 1.3 shows the mechanisms of NTHi infection in COPD.
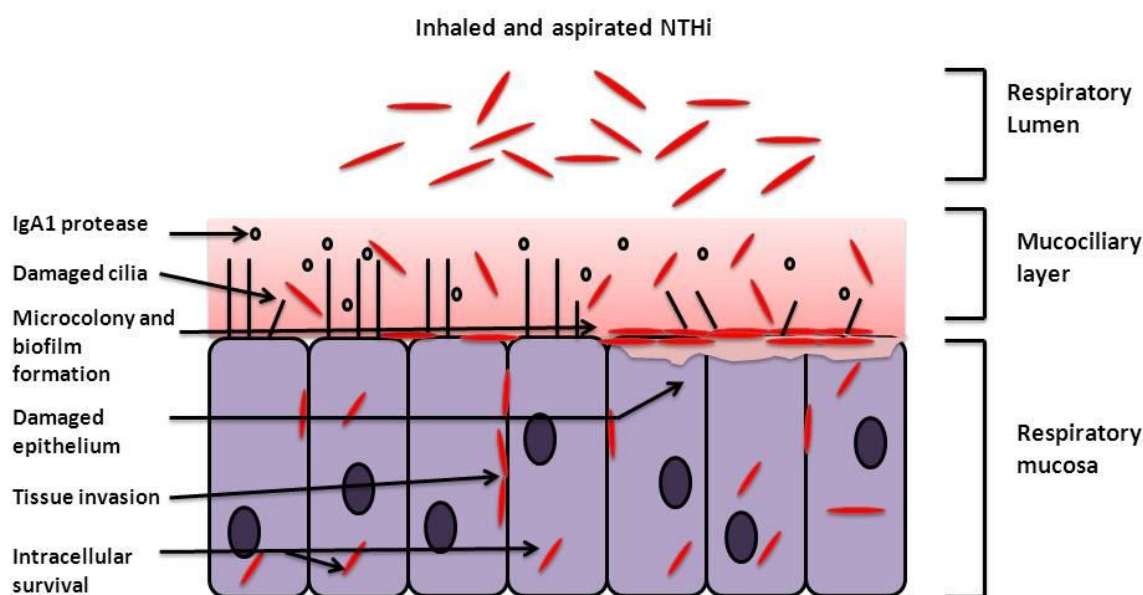
**Figure1.3:** **Mechanisms of NTHi infection and persistence in COPD lung**. Impaired phagocytosis and mucociliary dysfunction in COPD lung are the main predisposing factors involved in NTHi colonisation. NTHi tends to adhere to areas of epithelial damage and establish itself as microcolonies and biofilms. NTHi release immunoglobulin A1 (IgA1) protease to protect itself from the mucosal host immune response, and could damage respiratory cilia to avoid mucociliary clearance. NTHi can invade the mucosal layer and survive both intercellularly and intracellularly to evade the hostile respiratory environment and persist in the lower airways.

### 1.4.5.1. Bacterial virulence mechanisms:

#### 1.4.5.1.1. Mucociliary interaction:

NTHi infection has its direct effects on mucociliary function. Bacteria bind initially with the mucus layer to establish itself and induce ciliary dysfunction. Major outer membrane proteins (OMP) and lipooligosaccharide (LOS) are the main bacterial surface molecules implicated in mucociliary interaction (195,222).

OMP P2 and P5 facilitate binding of NTHi to human nasopharyngeal mucin (222–224). OMP P2 is the most abundant major OMP in NTHi constituting ~50% of the protein content and is strongly immunogenic (225). Both P2 and P5 are highly variable between strains. This variation allows the organism to evade clearance by potentially protective antibodies and contributes to the development of chronic infection (226). On the other hand, OMP P6, which is a peptidoglycan-associated lipoprotein, shows a high degree of sequence conservation among strains (227) making it as a potential vaccine candidate (228). OMP P6 presents in the outer membrane of all strains of NTHi (229). Evidence suggests that P6 elicits bactericidal antibody responses (229,230). Also, this protein evokes lymphocyte proliferative responses *in vitro* that correlate with relative protection from COPD exacerbations in humans (231). The exact function of P6 has not been fully determined, but results from experiments performed on a P6 knock-out strain of NTHi suggest that it is important in maintaining the integrity of the bacterial outer membrane (232).

NTHi can induce ciliotoxicity in epithelial cells by its LOS (233). LOS is a NTHi outer membrane component which lacks a repeating O-antigen and instead contains non-repeating oligosaccharides consisting of glucose, galactose, N-acetylglucosamine, phosphorylcholine (PCho) and sialic (N-acetyl-neuraminic) acid in varying combinations (222,234,235). Functionally, LOS is similar to LPS from Enterobacteriaceae; its heterogeneous structure allows bacteria to evade host immune response (236). LOS binds TLR4 and induces an inflammatory response in the host (237). This response is characterised by rapid recruitment of polymorphonuclear leukocytes (PMNs) to the lung (238,239). PCho component of LOS is a phospholipid acquired from the host cell surface and incorporated into bacterial cell membrane. Growing evidence suggests its role in NTHi pathogenicity. PCho has been linked to NTHi resistance to respiratory antimicrobial peptides

(240). In addition, PCho was implicated in NTHi colonisation in a murine model of pulmonary infection (241). Moreover, PCho was contributed to NTHi invasion and biofilm formation (242,243). The latter role of PCho will be discussed later in this section.

### 1.4.5.1.2. Adhesion to respiratory mucosa:

NTHi has evolved specific adherence mechanisms that facilitate its continued close association with epithelial surfaces, and prevent its removal by mechanical forces, thus sustaining successful colonisation of the human respiratory tract (244). NTHi appears to have a preference towards nonciliated cells or damaged mucosa (195). A number of adhesive factors exist, like OMP P5, adhesins and pili, each of which recognises a distinct host cell structure and influences cellular binding specificity (222).

### OMP P5:

Studies in human oropharyngeal cells showed that OMP P5 plays a significant role in adhesion of NTHi to epithelial cells, and contributes to NTHi recognition and phagocytosis by murine alveolar macrophages (245). It was observed that P5-deficient strains demonstrated minimal adherence to Chinese hamster ovary (CHO) cells (224). Furthermore, NTHi adhesion to epithelial cells was mediated by the specific interaction between OMP P5 and intercellular adhesion molecule-1 (ICAM-1), which was upregulated by NTHi in respiratory epithelial cells. Therefore, blocking the OMP P5-ICAM-1 interaction may reduce respiratory colonisation by NTHi (246).

### Adhesins:

NTHi express high molecular weight proteins (HMW) on its surfaces which facilitate its adherence to epithelial cells. Two main types of HMW have been

identified, namely; HMW1 and HMW2 proteins. NTHi strains lacking these proteins showed low adherence capacity to the human epithelium. Therefore, it was suggested that HMW proteins are important colonising factors (247).

*Pili:*

Some isolates of NTHi are capable of expressing pili, which are rod-like projections from the bacterial surface that promote agglutination of erythrocytes and adherence to respiratory epithelial cells (248). Pilin-mediated binding occurs only to sialic acid-containing lactosylceramide structures (GM3) on oropharyngeal epithelial cells and erythrocytes. In addition, pili were shown to play a role in biofilm formation by NTHi (249). In conditions where the clearance of tracheobronchial secretions is impaired (i.e., cystic fibrosis and chronic bronchitis), pilin-mediated NTHi adherence and biofilm formation may mediate a state of chronic colonisation (248).

*Other factors:*

About 25% of NTHi strains lack adhesins and pili but are still capable of efficient adhesion to respiratory mucosa. These strains express different adhesion molecules like *Haemophilus* adhesion and penetration (Hap), Hia/Hsf proteins, protein E and protein D (222,250–252). Hap is a monomeric autotransporter protein which has serine protease activity and undergoes autoproteolytic cleavage (253). It was identified as an important factor in bacterial interaction with respiratory epithelium, by promoting bacterial adherence to extracellular matrix proteins, namely fibronectin, laminin and collagen IV (254,255). Protein D and protein E are surface proteins which have been recognised as adhesion and invasion molecules in monocytic and epithelial cell lines (251,252).

69

### 1.4.5.1.3. Evasion of host immunity:

### 1.4.5.1.3.1. Immunoglobulin A1 (IgA1) protease activity

Immunoglobulin A (IgA) is the primary immunoglobulin at mucosal surfaces which is produced by mucosal lymphocytes (256,257). IgA represents an important part of the innate immune response in the lung against inhaled pathogens (258). It binds to bacteria and prevents their attachment to epithelial cells, inactivates their toxins and facilitates bacterial killing (195). There are two main IgA subclasses in the lung; IgA1 and IgA2 (256,258). Nearly all NTHi strains express proteases that cleave and neutralise IgA1 to colonise the human respiratory mucosa (259,260). IgA1 proteases cleave IgA1 at the hinge region of the $\alpha$-heavy chain, resulting in loss of its antibacterial activity (261). On the other hand, IgA2 lacks most of the hinge region making it less susceptible to bacterial IgA proteases (256–258). IgA1 proteases produced by NTHi isolated from sputum of exacerbated COPD patients showed a higher cleavage activity of human IgA than IgA1 proteases produced by other colonising strains (262). In addition, genomic studies have identified two variants of IgA1 protease, type I IgA1 protease which is produced by nearly all NTHi strains, and type II IgA1 protease which is produced by NTHi isolated during COPD exacerbation. The type II variant is homologous to IgA1 protease of pathogenic *Neisseria,* which interferes with the lysosomal killing of the bacteria and promotes intracellular survival (263,264). This suggests a possible role of type II IgA1 protease in bacterial survival in the lung. However, further investigations are needed to identify clearly the role of this protease during NTHi infection. Therefore, IgA1 protease is an important virulence factor in NTHi infection, and hence, could be a candidate target for future therapies.

### 1.4.5.1.3.2. Microcolony formation:

NTHi have the ability to form microcolonies on the mucosal surface as a protective mechanism against bacteriostatic and bactericidal products like lactoferrin, lysozymes and antibodies (265). Bacterial aggregation in microcolonies is promoted by Hap protein and potentiated by the host SLPI, which inhibits Hap autoproteolysis (266).

### 1.4.5.1.3.3. Phase variation and antigenic drift of virulence determinants:

NTHi has evolved adaptive means to survive in the highly immunogenic respiratory tract. It can upregulate or downregulate its surface antigens, a property called phase variation. This involves changes in the key structures involved in disease pathogenesis like LOS, pili and adhesins. Ultimately, phase variation will modify antibody function (267).

Some strains of NTHi could change their surface epitopes by undergoing point mutation of the encoding genes. Therefore, the antibody binding sites will be modified. This process is called antigenic drift. The most common structures involved in antigenic drift are OMP P2, P5 and IgA1 protease (268,269).

Co-colonisation by more than one NTHi strain facilitates horizontal transfer of genes by providing a supply of potentially diverse deoxyribonucleic acid (DNA) that can be taken up by the colonizing strains and incorporated into the bacterial genome. It appears that NTHi applies two or three of the above genetic mechanisms to alter a single antigen like pili (268).

### 1.4.5.1.3.4. Biofilm formation and immune evasion:

A biofilm is a structured community of bacterial cells enveloped in a self-produced polymeric matrix, which is adherent to an inert or living surface

(270,271). Bacteria growing in biofilms are more resistant to immune clearance mechanisms and to antibiotics compared to planktonic bacteria (272,273).

Growing evidence suggests a propensity of NTHi to form biofilms in the respiratory tract (204,274). Monthly sputum cultures from COPD patients revealed negative cultures in spite of continuous colonisation by NTHi proven by molecular typing (204). Likewise, middle ear fluids from children with otitis media were sterile by culture. However, molecular assays showed that NTHi DNA was detectable in a substantial proportion of these samples (274). These observations suggest that NTHi persists in the respiratory tract as biofilms, which are a biologically active, but non-culturable form of bacterial growth. Moreover, it has been demonstrated that NTHi isolated from patients with cystic fibrosis and otitis media grown as biofilms *in vitro*. Bacteria growing in biofilms were more resistant to a broad range of antibiotics than planktonic bacteria (275,276). Therefore, different antibiotic regimens should be studied to treat NTHi persistent infection.

Investigation of NTHi biofilms *in vitro* suggested the importance of an epitope on LOS in biofilm formation (277). Subsequent studies showed that sialic acid (278,279) and PCho (242) components of LOS are essential for biofilm formation both *in vitro* and in an experimental animal model of infection. Moreover, PCho-expressing NTHi strains formed significantly thicker biofilms with more surface coverage and total biomass than PCho deficient mutants (242). NTHi pili were also demonstrated to be essential for biofilm formation (249,277), and antibodies directed against pili were protective even against established NT*Hi* biofilms (280). Although Hap and OMP P5 were recognised in the biofilm extracellular matrix (281), they were not required for NTHi biofilm growth *in vitro* (245).

NTHi produces extracellular DNA that is necessary for biofilm formation (282). In addition, NTHi produce DNA binding protein DNABII, which is important

in stabilising extracellular DNA in the biofilm matrix, and was reported to keep the structural integrity of biofilms (283). Antibodies against DNABII were found to cause debulking of NTHi biofilms both *in vitro* and in an experimental model of otitis media. In addition, these antibodies showed synergism with antibiotics in clearance of pre-formed NTHi biofilms *in vivo* (284).

Further characterisation of the composition of NTHi biofilm may improve the current understanding of NTHi pathogenesis in COPD and possibly highlight some therapeutic or vaccine targets.

### 1.4.5.1.3.5. Quorum sensing and biofilm formation:

Quorum sensing (QS) is a bacterial cell to cell communication process that involves the production, detection, and response to extracellular signalling molecules called autoinducers (AIs). AIs accumulate in the environment as the bacterial population density increases, and bacteria monitor this information to track changes in their cell numbers and alter their own gene expression. QS controls genes that govern activities which are beneficial when performed by groups of bacteria acting in synchrony. Processes regulated by QS include biofilm formation, sporulation, competence and virulence factors secretion (285,286). Bacteria also use QS signals to modify the transcriptional program in other bacterial species in the same microenvironment (287,288). NTHi produces autoinducer-2 (AI2) quorum signal, a family of derivatives of dihydroxypentanedione, which is a metabolic byproduct of homocysteine (289). NTHi mutants of AI2 gene (LuxS) showed impaired biofilm formation in chinchilla model of otitis media (290). Moreover, it was observed that AI2 quorum signals from NTHi promote biofilm formation and persistence of *Moraxella catarrhalis* forming together polymicrobial biofilms in experimental animals (291).

These data suggest the importance of quorum signals as potential targets for treatment of persistent NTHi infection.

### *1.4.5.1.4. Local tissue invasion and intracellular survival:*

A potentially very important pathogenic feature of NTHi is its ability to invade local tissue and survive intracellularly in the respiratory tract. This feature allows NTHi to persist in the lung and cause recurrent infection despite antibiotic therapy and development of bactericidal antibodies (292). The interaction between NTHi and host cells is a complex and dynamic process. Hence different pathways have been implicated in NTHi tissue invasion and survival inside host cells (292,293). These pathways are described below and summarised in Figure 1.4.
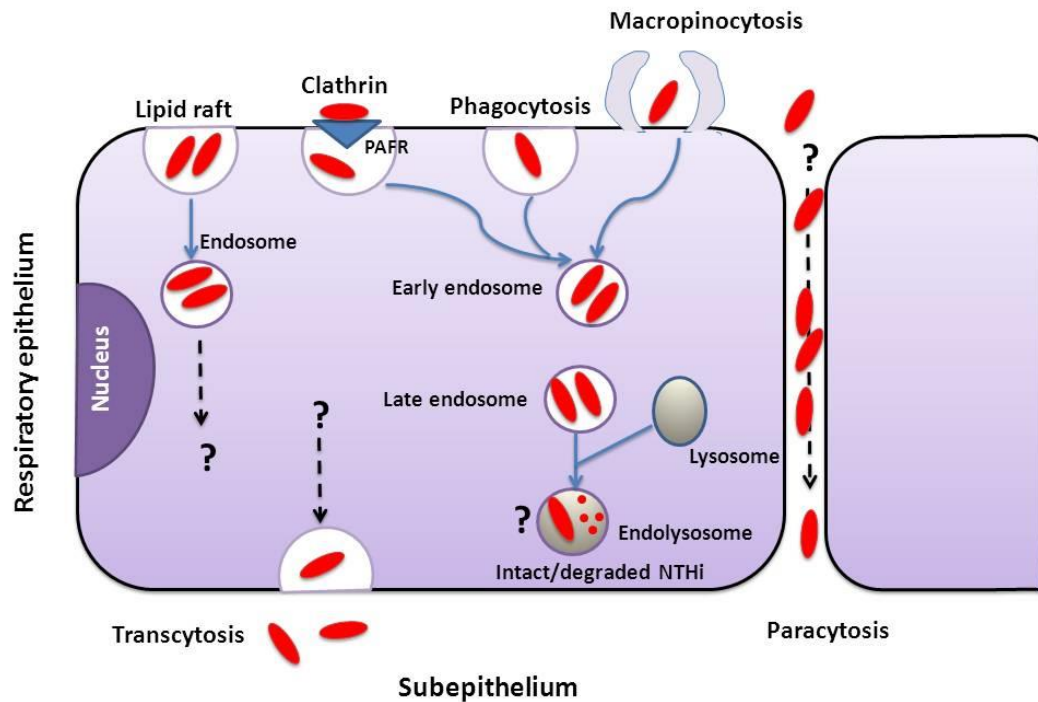
**Figure 1.4: Mechanisms of NTHi tissue invasion and intracellular trafficking.** Intraepithelial invasion by NTHi occur through different pathways; macropinocytosis, phagocytosis, clathrin-mediated and lipid raft-mediated endocytosis. The resultant endosome is trafficked to the endolysosomal pathway except for lipid raft-mediated endosome which is trafficked to different unrecognised pathway. The fate of NTHi inside endolysosomes is not fully understood. However, small count of viable bacteria was recovered from endolysosomes (294). Interepithelial and subepithelial NTHi invasion occurs by processes of paracytosis and transcytosis respectively. Bacterial factors involved in these processes are not identified yet. Unknown or not fully understood processes are marked with question marks. PAFR= platelet–activating factor receptor.

### 1.4.5.1.4.1. Phagocytosis and macropinocytosis:

Phagocytosis and macropinocytosis are processes by which macrophages internalise particles and they both involve membrane dynamics. However, the main difference between the two mechanisms is that phagocytosis is receptor dependent, while macropinocytosis is an actin-dependent process (292,295). Phagosomes and macropinosomes are inconsistently trafficked to the endolysosomal pathway (292). An *in vitro* study found that intraepithelial NTHi was protected from antibiotics and bactericidal antibodies for at least 24 hours (296). Therefore, it was suggested that NTHi phagocytosis was a protective mechanism from immune clearance. Furthermore, NTHi was reported to survive *in vitro* for up to 72 hours inside murine alveolar macrophages (297). In addition, *ex vivo* studies have recovered viable NTHi from mononuclear cells in excised adenoid tissue (298) and detected NTHi inside epithelial cells in 87% of subjects who had exacerbations of chronic bronchitis (206).

Experiments exploring the interaction between human bronchial epithelial cells and NTHi revealed that NTHi induced cytoskeletal rearrangement in the infected cells, including actin polymerisation and increased cortical actin. These changes resulted in the extension of host cell microvilli and the formation of lamellipodia, which surround adherent bacteria and form a membrane-bound vacuole. These findings suggested internalisation of bacteria by the process of macropinocytosis (299).

### 1.4.5.1.4.2. Clathrin-mediated endocytosis (receptor-mediated endocytosis)

Clathrin-mediated endocytosis produces endosomes which are eventually trafficked by endolysosomal pathway (300). Both platelet-activating factor (PAF) receptors and β-glucan receptors mediate NTHi internalisation into epithelial cells.

In addition, β-glucan receptor mediates non-opsonic internalisation of NTHi into macrophages (243,251,301). PAF receptor interacts with PCho residue of bacterial LOS to enhance respiratory epithelial cell adherence and invasion (246). Therefore, PCho is an important virulence factor due to its contribution to NTHi colonisation and biofilm formation. PAF receptor-mediated endocytosis appears to be independent of macropinocytosis and may be the predominant invasion pathway for most strains (222,251).

### 1.4.5.1.4.3. Lipid raft-mediated endocytosis

Lipid rafts are plasma membrane microdomains enriched in cholesterol, glycosphingolipids, and glycosylphosphatidylinositol-anchored molecules, with roles in signal transduction and bacterial trafficking (302). Lipid raft-mediated endocytosis produces endosomes that are trafficked in a pathway avoiding the endolysosomal killing; hence lipid raft-mediated endocytosis is a less microbicidal mechanism of internalisation (303). Inhibitors of lipid raft significantly impaired NTHi invasion of murine alveolar macrophages and human airway epithelial cells (133,294). Therefore, it was suggested that the integrity of lipid raft is an important factor in NTHi invasion.

### 1.4.5.1.4.4. Endolysosomal trafficking

NTHi was reported to undergo endolysosomal trafficking in human airway epithelial cells. It was observed that the majority of intracellular NTHi was metabolically active but non-replicating inside acidic intracellular vacuoles, which showed features of early and late endosomes (294). Moreover, NTHi was co-localised with cathepsin D, a protease that marks endolysosomal fusion. Nevertheless, the percentage of cathepsin D-associated NTHi was significantly lower than a standard strain of *Salmonella typhimurium* known to traffic to the

lysosome. This indicates that NTHi may not traffic to the lysosomes or cannot survive inside them (294). However, the exact mechanism of bacterial avoidance or survival in the lysosomes remains to be identified.

### 1.4.5.1.4.5. Paracytosis and transcytosis:

Paracytosis or NTHi penetration between lung epithelial cells was suggested as an important mechanism of bacterial persistence in the lung (296,304). NTHi was able to disrupt epithelial tight junctions and cluster between epithelial cells in human nasopharyngeal tissue culture (305). In addition, NTHi was extensively identified in the epithelium, submucosa, interstitium, and the alveolar epithelium of lung explants from patients with end-stage lung disease, including COPD and cystic fibrosis (306). Visualisation of NTHi in lung epithelium by transmission electron microscopy showed that intracellular NTHi was degraded, while the intercellular NTHi was intact (296,304). This observation suggests the role of paracytosis in NTHi survival. The exact mechanism of NTHi paracytosis is poorly understood. However, a hypothetical bacterial protein was suggested to act as paracytin (296).

Trancytosis is a possible mechanism by which NTHi traverse through the airway epithelial cells to the subepithelium. Nonetheless, bacterial factors involved in trancytosis have yet to be recognised (293).

### 1.4.5.2. Host and microenvironmental factors in NTHi colonisation:

In the absence of lung disease, the natural course of infection with NTHi is colonisation of the upper respiratory tract (16). However, in COPD patients, exposure to cigarette smoke results in goblet cell hyperplasia, mucus hypersecretion, and decreased respiratory epithelial cell ciliary function. These effects increase the likelihood of acute NTHi bronchitis and pneumonia (221,307,308). Furthermore, in established disease, defective immune

responsiveness and impaired phagocytosis by alveolar macrophages might provide an immunologic basis for the persistence of NTHi in the airways of adults with COPD (134,135). Moreover, Specific immune defects, such as hypogammaglobulinemia and other deficiencies in humoral immunity also increase host susceptibility to disease due to NTHi, including both localised respiratory tract and systemic disease (309–311).

*In vitro* studies suggest that NTHi preferentially adheres to respiratory epithelial cells that either lack cilia or are structurally damaged (305,312). Cellular damage in the host may occur as a result of numerous factors unrelated to the presence of bacteria. However, the presence of NTHi can cause stasis and loss of cilia, as well as damage and sloughing of epithelial cells (233,313).

### 1.4.6. Host immune response to NTHI infection:

Host immune response to NTHi determines the fate of infection and affects its pathogenesis (195).

#### 1.4.6.1. Innate immune response:

NTHi causes intense stimulation of cellular innate immune response in the lung. The main innate immune cells involved in defence against NTHi are macrophages, neutrophils and epithelial cells (195). NTHi surface epitopes or pathogen-associated molecular patterns (PAMPs) are recognised by TLR expressed on innate immune cells (314). OMP, especially P6, is recognised by TLR2 receptor and is capable of inducing CXCL8 and TNF-α from human alveolar macrophages (228), and is important for dendritic cell migration (315). LOS is primarily recognised by TLR4 receptors and causes release of different inflammatory cytokines and chemokines like CXCL8, TNF-α, IL-1β and IL-12 from human alveolar

macrophages (316). TLR4 mediated inflammatory response was recognised as an important pathway in innate immune response to NTHi in mice (317,318).

Alveolar macrophages from COPD patients showed a reduced pro-inflammatory response to NTHi. This would promote NTHi survival and provide a source for on-going inflammatory stimuli for non-macrophage immune mediators (316).

### 1.4.6.2 Adaptive immune response:

Adaptive immune response to NTHi infection follows the innate response and is mediated by B and T lymphocytes (195). Studies revealed strong antibody response to NTHi which activates complement-mediated bacterial killing (319). This limits NTHi to mucosal rather that systemic infection (195).

T cells play a central role in defence against intracellular bacteria. T helper and cytotoxic T cells secrete a number of inflammatory mediators which govern cytotoxic mechanisms (195). T cell activation in response to NTHi infection could affect the clinical outcome of the disease. Nevertheless, studies in COPD patients have revealed a defective T cell response to NTHi as a possible mechanism of chronic infection (205,320,321).

## 1.5. Signalling pathways in airway inflammation:

Inflammation is a protective mechanism against tissue damage by infectious or toxic agents (322). Innate immune cells ,like macrophages, recognise PAMPs by their PRR and subsequently initiate intracellular signalling cascades to induce the release of inflammatory mediators that promote pathogen killing and tissue repair (323). Nevertheless, uncontrolled or ineffective inflammatory response results in excessive tissue destruction. Important pro-inflammatory signalling pathways in COPD are MAPK and NF-κB pathways.

### 1.5.1. Mitogen-Activated Protein Kinase (MAPK) pathway

MAPKs are cascades of sequentially phosphorylated intracellular enzymes, which translate extracellular stimuli into a vast array of cellular responses. There is growing research interest in investigating the role of MAPKs in COPD pathogenesis as a candidate targets for novel anti-inflammatory therapies (324,325). All eukaryotic cells possess a number of MAPK pathways, which co-ordinately regulate gene expression, mitosis, metabolism, motility, survival, apoptosis, and differentiation (326).

The most studied MAPKs in human are p38, extracellular signal-regulated kinases (ERK) and c-Jun amino (N)-terminal kinases (JNK). Each group composed of three sequentially acting kinases, a MAPK, a MAPK kinase (MAPKK), and a MAPKK kinase (MAPKKK) (326). Individual kinases for each pathway are shown in Figure 1.5.

The activation process starts when an extracellular stimulus interacts with transmembrane receptors, such as receptor tyrosine kinases and G-protien coupled receptors, causing activation of MAPKKK. MAPKKK are protein Ser/Thr kinases, which phosphorylate and activate MAPKK. This in turn activates MAPK by dual

phosphorylation at Thr and Tyr residues within a conserved Thr-X-Tyr motif located in the activation loop of the kinase domain subdomain VIII. Activation of MAPKs will subsequently activate a number of protein kinases termed MAPK activated protein kinases (MAPKAPK) (Figure 1.5). These kinases control a broad range of biological processes in the cell (325,326). Below is a brief description of MAPK modules.
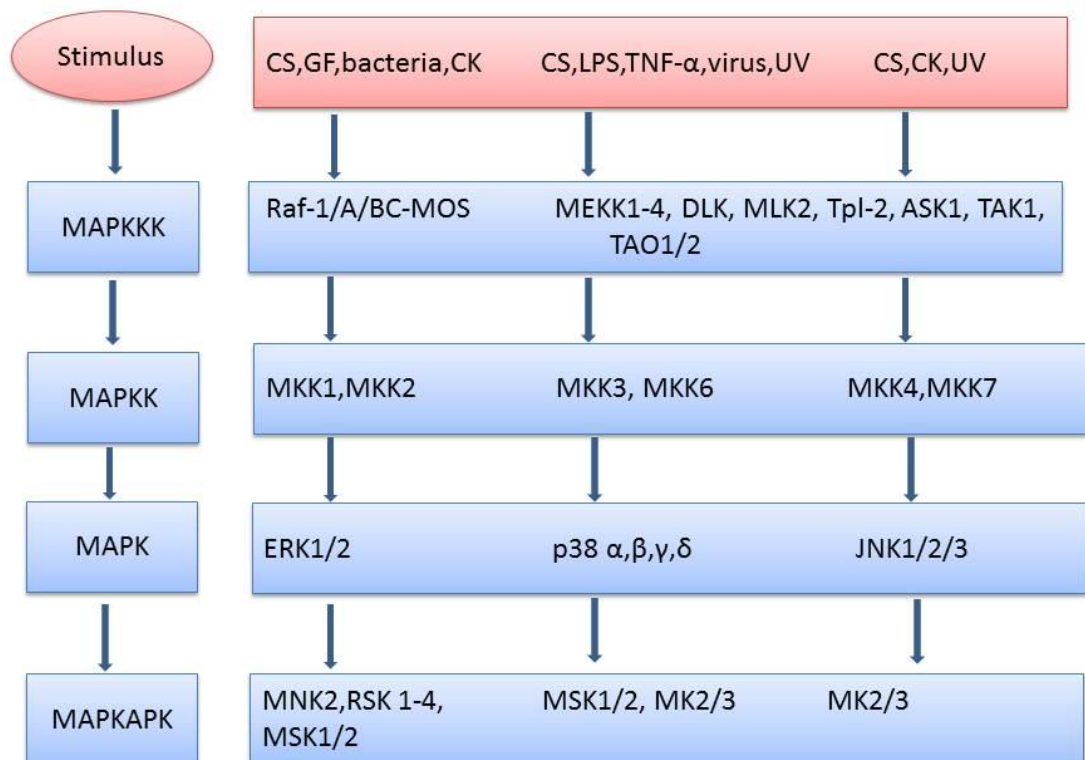


**Figure 1.5: Mitogen-Activated Protein Kinase (MAPK) pathways.** Extracellular stimuli bind to membrane receptors causing activation of MAPK kinase kinases (MAPKKK), which in turn activate MAPK kinases (MAPKK), then MAPKs. MAPKs will activate a number of MAPK activated protein kinases (MAPKAPK) resulting in cellular responses. ERK= Extracellular regulated kinase, JNK= c-Jun N-terminal kinase, MNK= MAP kinase-interacting kinase, MOS= Mouse sarcoma, MSK= Mitogen- and stress-activated protein kinase 1, RAF= Rapidly accelerated fibrosarcoma kinase, RSK= Ribosomal S6 kinase, TAO= Serine/Threonine-protein kinase, TPL= Tumour progression locus, MLK= Mixed lineage kinase, CS= Cigarette smoke, CK= Cytokines, LPS= Lipopolysaccharide, TNF-α= Tumour necrosis factor alpha, UV= Ultraviolet.

### 1.5.1.1. p38 MAPK pathway; relevance in COPD:

p38 MAPK is one of the widely studied pathways in COPD. Four isoforms have been identified, p38α, p38β, p38γ and p38δ. p38α and p38β are highly expressed in tissue. Meanwhile, p38γ and p38δ have more restricted tissue expression which highlights more specialised functions (327,328). p38α appears to be the main isoform involved in inflammatory responses, and higher levels were detected in lungs of COPD than non-COPD controls (329).

Different stimuli have been implicated in p38 MAPK activation, including oxidative stress (e.g. cigarette smoke), viral infection, ultraviolet (UV) irradiation, hypoxia, ischemia, bacterial LPS, IL-1, and TNF-α (328). Most stimuli that activate p38 MAPKs also stimulate JNK isoforms, and many MAPKKKs in the p38 module control the JNK module (326). Furthermore, p38α can be autophosphorylated by interaction with TGF- β -activated protein 1-binding protein 1 and the activation of tyrosine kinases as occurs with the stimulation of the T-cell antigen receptor (330).

The p38 module plays a critical role in normal immune and inflammatory responses (328). The p38 isoforms regulate cytokine expression in response to various stimuli. The mechanisms of p38-mediated cytokine release are either controlling transcription factors such as NF-κB (331), post-trancriptional stabilisation of the mRNA of inflammatory mediators (332,333) or at the level of protein translation (334,335). Therefore, deletion of p38 MAPK from epithelial cells was reported to reduce pro-inflammatory gene expression (336). The p38 MAPKs have also been shown to play roles in cell proliferation and survival (326).

The relevance of p38 in COPD has been suggested by the reported higher p38 activation in COPD alveolar macrophages, alveolar wall and CD8 positive and CD20

positive lymphocytes than non-COPD controls (329,337). Figure 1.6 summarises the potential role of p38 and other MAPK pathways in COPD.

The p38 pathway is a core mediator of airway inflammation; this role was highlighted in LPS-induced GM-CSF, CXCL8 and MMP-9 release from human macrophages (338–340). In addition, sputum analysis of COPD patients revealed a positive association between sputum phospho-p38 levels, sputum neutrophil count, CXCL8 and lower FEV1 (341). The latter finding suggests that p38 can mediate inflammatory cell migration in the airways, such as neutrophils and eosinophils. This role is believed to be due to the p38 effect on actin cytoskeleton that is necessary for cell migration (342–344). Furthermore, an animal study investigating ozone-induced airway hyperresponsiveness showed that airway smooth muscle contraction was mediated by p38 MAPK. Pretreatment of the animals with a p38 MAPK inhibitor reversed the airway hyperresponsiveness (345). These data suggest a possible p38 MAPK-mediated mechanism in bronchoconstriction in airway diseases

Recently, growing evidence supports the role of p38 MAPK in airway corticosteroid insensitivity. However, investigations were done mostly on corticosteroid resistant asthma. p38 MAPK was reported to phosphorylate glucocorticoid receptor (GR) in peripheral blood monocytes from asthma patients, causing less steroid responsiveness (346). Moreover, alveolar macrophages from corticosteroid insensitive asthma patients showed higher levels of activated p38 and lower levels of dexamethasone-induced MAPK phosphatase-1 (MKP-1) expression (347) . In addition, p38γ isoform reduced corticosteroid response in PBMCs from asthma patients (348). Similar studies in COPD patients have highlighted the possible role of p38 MAPK in corticosteroid resistance. p38 MAPK inhibition by BIRB-796 synergistically enhanced corticosteroid sensitivity of LPS-

stimulated alveolar macrophages from COPD patients (349). Likewise, p38 MAPK inhibitor (SB706504) showed a combined inhibitory effect with dexamethasone on LPS-induced TNF-α release from COPD alveolar macrophages, and LPS-induced transcription of inflammatory genes from COPD MDMs (350). Taken together, these data suggest the importance of p38 inhibitors in improving steroid sensitivity in chronic airway diseases.
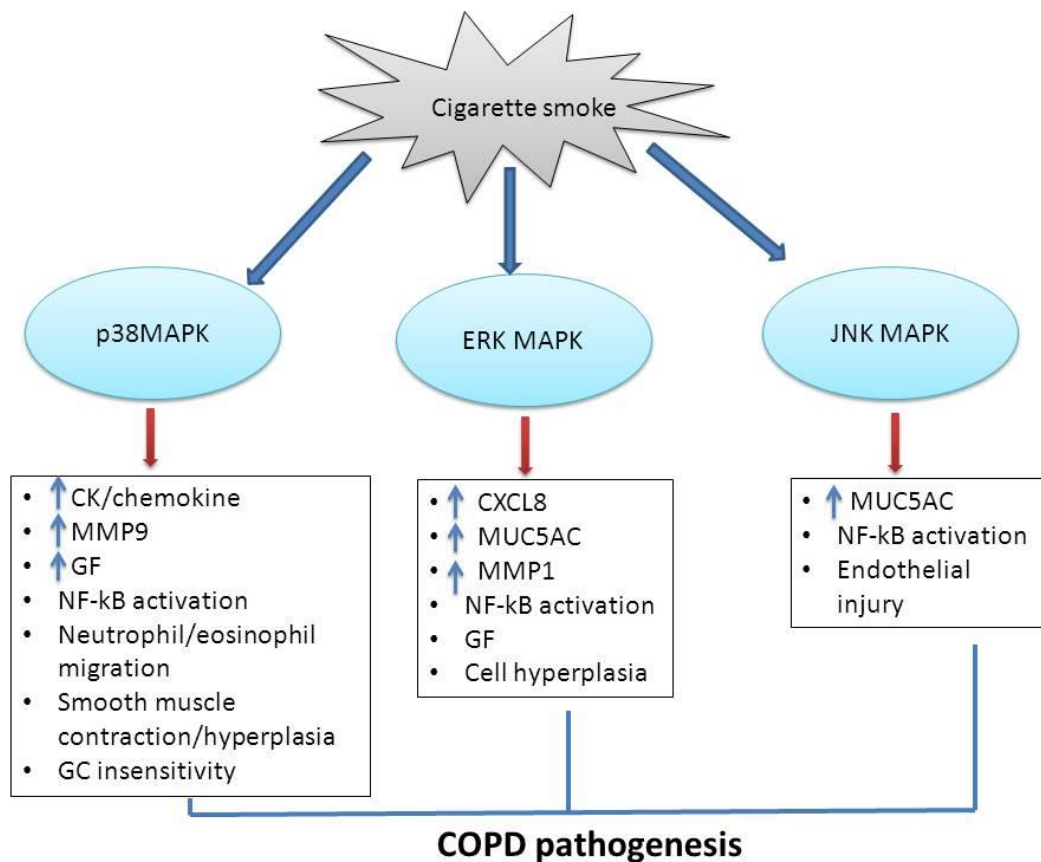


**Figure 1.6: Potential role of MAPK pathways in COPD pathogenesis**. Cigarette smoke induces p38, ERK and JNK MAPKs activation. Each pathway mediates airway changes contributing to COPD pathophysiology. MUC5AC= Mucin 5AC gene, MMP= Matrix metalloproteinase, CK= Cytokine, GF= Growth factor, GC= Glucocorticoids, NF-κB= Nuclear factor kappa B.

### 1.5.1.2. Extracellular signal-regulated kinase MAPK pathway; relevance in COPD:

There are two ERK isoforms, ERK1 and ERK2. Both isoforms are activated by growth factors, like platelet-derived growth factor (PDGF), epidermal growth factor (EGF) and nerve growth factor (NGF). Also, cytokines, osmotic stress, insulin and microtubule disorganisation can activate ERK MAPK pathway (351,352). ERK MAPK importantly controls cell proliferation, therefore, it has a direct role in tumorigenesis (326,353).

The importance of ERK pathway in COPD pathogenesis came from the finding that airway epithelial and alveolar cells from patients with emphysema have higher levels of activated ERK1/2 than non-emphysematous controls. This suggests the importance of ERK MAPK pathway in lung tissue remodelling in COPD (354).

*In vitro* studies have shown that cigarette smoke-induced MMP-1 and CXCL8 secretion was mediated by ERK pathway in human epithelial cells and alveolar macrophages respectively (339,354). Other studies showed that mucin 5AC (MUC5AC) gene expression induced by smoke and ROS traverse through the JNK and ERK MAPK pathways (355) (Figure 1.6). Moreover, ERK was identified as an important pathway mediating LPS-induced lung injury in mice (356).

The role of ERK MAPK in corticosteroid insensitivity in the airways has yet to be investigated. However, in human lymphoblastic cells, ERK MAPK was reported to decrease corticosteroid-induced apoptosis by reducing GR phosphorylation at serine (ser) 211 residues. This phosphorylation site is responsible for corticosteroid transcriptional activity (357). Therefore, this observation suggests a possible role of ERK MAPK in reducing corticosteroid anti-inflammatory effect, which requires further investigation as a potential mechanism of corticosteroid resistance in COPD.

### 1.5.1.3. JNK MAPK pathway; relevance in COPD:

JNK has three known isoforms, JNK1, JNK2 and JNK3. JNK 1 and 2 have wide tissue distribution, whereas JNK 3 is primarily localised to neuronal tissue, testis and cardiac myocytes (358).

As with p38, JNK MAPK is activated by various cellular stresses, including heat shock, ionising radiation, oxidative stress, DNA-damaging agents, cytokines, UV irradiation, DNA and protein synthesis inhibitors (which stresses the cells), growth factor deprivation, and to a lesser extent by growth factors (359). Activation of this pathway leads to phosphorylation of several additional substrates, including those of the early-response proto-oncogene family c-fos. This leads to the formation of Jun-Fos heterodimers or Jun homodimers to create the AP-1 transcription factor (360).

JNK1 and JNK2 have been shown to play a crucial role in the control of cell proliferation, differentiation of hematopoietic populations as well as the apoptotic response to cellular stresses (361,362).

JNK pathway mediates some cigarette smoke-induced changes in the lung such as mucin production from epithelial cells and endothelial cell injury (355,363). Furthermore, JNK activates NF-κB transcription factor in human monocytes (364). This indicates that JNK activation could induce a pro-inflammatory response through a positive crosstalk with NF-κB (Figure 1.6).

Studies have linked JNK activation with glucocorticoid insensitivity in HeLa cells. This effect is believed to be due to JNK-mediated phosphorylation of the GR at ser 226 enhancing GR nuclear export which may contribute to termination of GR-mediated transcription (365,366).

### 1.5.2. Nuclear Factor-κB (NF- κB):

NF-κB is a crucial regulator of the inflammatory response which is involved in the evolution as well as resolution of inflammation (322). NF-κB controls a broad range of biological activities including immune responses, cell proliferation, differentiation, and tissue remodelling (367). NF-κB is expressed by a variety of inflammatory cells and its role has been highlighted in the pathogenesis of asthma and COPD (368). Increased expression of NF-κB pathway markers was reported in sputum macrophages from exacerbated COPD patients (369)and bronchial biopsies during stable state (370).

NF-κB is a dimeric transcription factor composed of p50 (NF-κB1) and p65 (RElA) subunits (371). In resting cells, NF-κB is retained in the cytoplasm by an inhibitory molecule, the IκB. Inflammatory stimuli, including bacterial infections, oxidative stress and cytokines, cause dissociation of NF-κB from its inhibitory molecule to enter the nucleus and switch on target genes (322). NF-κB translocation requires IκB degradation by some kinases like IκB kinase (IKK) 1 and IKK2. These kinases are activated in turn by upstream kinases like NF-κB inducing kinase (NIK) (371).

*In vitro* studies demonstrate the anti-inflammatory effect of NF-κB inhibitors, although their potential role in COPD and asthma have been questioned due to their inhibition of the beneficial host immune response against viral and bacterial infections (368).

### 1.5.3. Signalling pathways of NTHI infection:

Like most other bacterial infections, NTHi infection induces inflammation with prominent release of cytokines and chemokines. NTHi-induced inflammation is mostly activated by its binding to TLRs (317). Evidence supports the role of TLR4

and TLR2 in the effective innate immune response to respiratory tract infection caused by NTHi (317,372).

The downstream signalling pathways and transcription factors have recently been investigated in the pathogenesis of NTHi infection; the transcription factor NF-κB and MAPK signalling pathways were the most widely studied pathways of infection. NF-κB activation was identified to mediate NTHi-induced inflammatory response via TLR4 binding in murine airway epithelial cells, suggesting NF-κB role in innate immune response to *H.influenzae* (317). In addition, OMP P6 binding to TLR2 in human epithelial cells was associated with NF-κB activation (373). This activation was mediated by two pathways, the activation of NIK- IKKα/β complex leading to IκBα degradation, and the activation of MKK3/6-p38 MAPK. Moreover, TLR2-dependent activation of TGF-β activated kinase 1 (TAK1) appears to mediate the activation of the above signalling pathways (373). In another study, activation of EGFR by NTHi was linked to NF-κB mediated release of TNF-α, IL-1β and macrophage inflammatory protein 2 (MIP-2) in human epithelium and in a mouse model of middle ear and lung infection (374).

p38 and ERK MAPK pathways were identified as mediators of NTHi induced CXCL8 in human epithelial cells (375). Furthermore, p38MAPK activation was reported to mediate NF- κB-dependent inflammation in NTHi infection (373,374).

Mucus production is a characteristic feature of NTHi airway infection, NTHi might signal through different pathways to express mucin genes. In one study the TGF-β-SMAD signalling pathway together with TLR2-TAK1-NIK-IKKβ/γ-IκBα pathway were used by NTHi lysate to stimulate NF-κB-dependent MUC2 mucin gene transcription in human epithelial cells (376). Moreover, cytoplasmic proteins of NTHi was reported to induce MUC5AC mucin transcription in human epithelial cells through the activation of the p38MAPK pathway, whereas activation of

phosphoinositide-3 (PI3) kinase pathway caused a reduction in NTHi-induced MUC5AC transcription through a negative crosstalk with p38MAPK (377). Figure 1.7 summarises the mentioned signalling pathways.
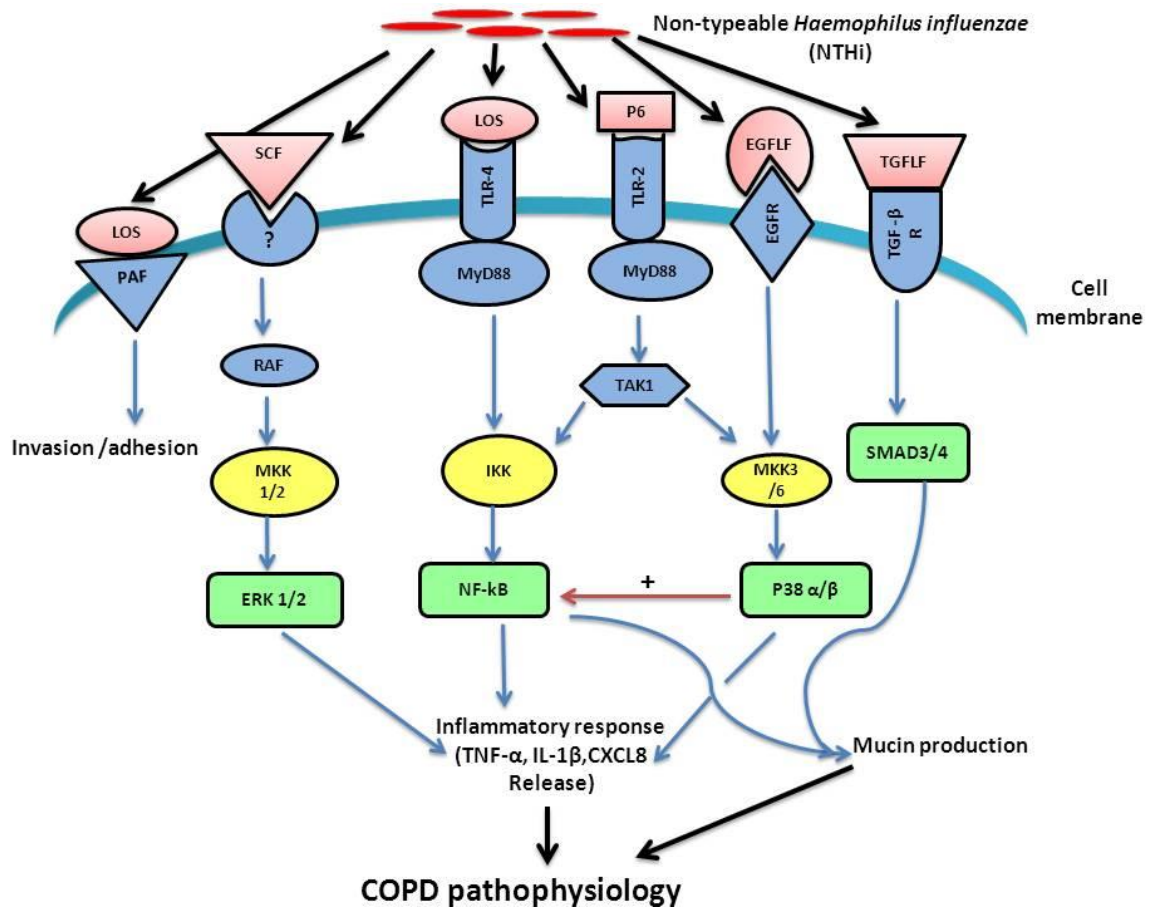


**Figure 1.7: Signalling pathways of NTHi infection.** Different NTHi ligands bind to surface receptors and activate the downstream signalling pathways. NTHi induces pro-inflammatory cytokines and chemokines release through activation of NF-κB, p38 and ERK MAPK pathways. Activation of these pathways is mediated by phosphorylation of their upstream kinases. NTHi-induced mucin production is mediated by NF-κB and SMAD signalling pathways. Both inflammation and mucus production contribute to COPD development and progression. LOS= Lipooligosaccharide, SCF= Soluble cytoplasmic fraction, P6= Outer membrane protein P6, EGFLF= Epidermal growth factor like factor, TGFLF= Transforming growth factor like factor, PAF= Platelet-activating factor, TLR= Toll-like receptors, EGFR= Epidermal growth factor receptor, TGF-βR= Transforming growth factor-β receptor. RAF= Rapidly accelerated fibrosarcoma kinase, ERK= Extracellular signal- regulated Kinase, IKK= IκB kinase, NF-κB= Nuclear factor-κB, TAK1= TGF-β activated kinase 1, MKK= Mitogen- activated protein kinase kinase, TNFα= Tumour necrosis factor α, IL= Interleukin.

## 1.6. Corticosteroids in COPD:

Corticosteroids (glucocorticoids or steroids) are anti-inflammatory drugs used in the treatment of a variety of inflammatory diseases including COPD. However, many COPD patients respond poorly to high doses of inhaled or oral corticosteroids (378).

### 1.6.1. Molecular mechanism of corticosteroid action:

Corticosteroids diffuse through the cell membrane and bind to glucocorticoid receptors (GR) in the cytoplasm. Corticosteroid-receptor complex translocates to the nucleus and binds to glucocorticoid response elements (GREs) on the promoter region of steroid-responsive genes (379).

Transactivation of target genes can be mediated by the interaction of DNA-bound GR with co-activator molecules, like cyclic adenosine monophosphate (cAMP) response element binding protein (CBP). This interaction causes acetylation of the core histone of the target genes and recruits chromatin remodelling engines resulting in gene activation (380). Genes that are switched on by corticosteroids include those encoding β2-adrenoceptors, SLPI and MKP-1 (378,381).

The main anti-inflammatory action of corticosteroids is to switch off the activated inflammatory genes encoding cytokines, chemokines, adhesion molecules and receptors (382). Activated GR interacts with the recruited co-repressor molecule, histone deacetylase 2 (HDAC2), to reduce histone acetylation and chromatin remodelling. Subsequently, the inflammatory genes will be effectively suppressed (383). Moreover, corticosteroids can directly interact with transcription factors, like NF-κB and AP-1, to transrepress inflammatory genes transcription (384).

### 1.6.2. Glucocorticoid receptor (GR):

GR is an intracellular phosphor-protein which mediates the corticosteroid actions. There are two main isoforms of GR, α and β. Corticosteroids bind to GR-α to exert their effects. In contrast, GR-β acts as a negative inhibitor of corticosteroids by interfering with DNA binding of activated GRα (385). GR can be activated by ligand and non-ligand dependent mechanisms. The inactive GR is sequestrated in the cytoplasm by heat shock protein (HSP 90) chaperone complex. This prevents nuclear translocation of the inactive GR (386).

GR is a modular protein composed of an N-terminal domain which carries transactivation region (AF-1), a central Zinc finger DNA binding domain (DBD) responsible for GRE binding and nuclear export, and a C-terminal domain containing ligand-dependent transcriptional activation function (AF-2) which is responsible for receptor dimerisation (387).

Corticosteroids binding to GR results in conformational changes by phosphorylation of the GR at multiple serine/threonine residues. This activation step will release the GR from HSP90 complex and facilitate its nuclear translocation (386,388).

Depending on the activation level, GR is present in both phosphorylated and unphosphorylated state within the cell. This suggests that GR undergoes auto-dephosphorylation by phosphatases binding to the C-terminal domain of the receptor (386). Growing evidence supports the relation between different phosphorylation sites on GR and its transcriptional activation. Furthermore, interdependence between the various phosphorylation sites was reported (389). In human GR, the most widely studied phosphorylation sites are ser 203, ser 211 and ser 226. GR has a basal and stimulated level of ser 203 phosphorylation, and it is

reported to be confined to the cytoplasm only. Therefore, ser 203 phosphorylated GR might be transcriptionally inactive receptor (386,390). On the other hand, the activity of GR is linked to phosphorylation at ser 211 site in human. Higher ser 211 phosphorylation correlates with more GR transcriptional activity and is found in both cytoplasm and nucleus (390). This form of activated GR is recruited to GRE of different corticosteroid-responsive genes. On the other hand, GR phosphorylation at ser 226 results in a reduction in the GR transcriptional activity by enhancing its nuclear export. In general, GR activity is correlated to ser 211 phosphorylation exceeding that of ser 226 (386).

Crosstalk between GR and MAPK signalling has been reported, p38 MAPK was highlighted to cause GR phosphorylation and reduce corticosteroid effect in steroid resistant asthma, which was restored by p38 MAPK inhibition (346). Moreover, p38 MAPK inhibition improved GR nuclear translocation and partially reduced its phosphorylation at ser 226 in PBMCs from severe asthma (348). ERK and JNK MAPKs also affect GR function by reducing ser 211 phosphorylation in lymphoid cells. Also, JNK can phosphorylate ser 226 residue in human and monkey cell lines (365). Moreover, ERK and JNK inhibitors restored the sensitivity of lymphoid cells to corticosteroid-induced apoptotic action (357).

### 1.6.3. Corticosteroid resistance in COPD:

Corticosteroids improve COPD symptoms and mortality with a small reduction in exacerbation frequency (391). Some studies showed that corticosteroids have an anti-inflammatory effect in stable COPD patients, by reducing sputum chemotactic activity and increasing neutrophil elastase inhibition (392). In addition, preincubation of neutrophils with corticosteroid reduced their chemotactic response and fibronectin degradation ability (393). In contrast, other studies

showed a lack of corticosteroid anti-inflammatory effect in the stable state. It was observed that a high dose of inhaled corticosteroids did not reduce the number of inflammatory cells and mediators in the airways and sputum of stable COPD patients (394,395).

Investigations of corticosteroid resistance in COPD have suggested different possible mechanisms. Several disease-relevant inflammatory elements were tested for their corticosteroid response *in vitro.* Studies on alveolar macrophages from COPD subjects have identified a subset of steroid-resistant cytokines, particularly CXCL8 (167,168), GM-CSF and G-CSF (168). Moreover, microarray analysis of inflammatory genes from COPD MDMs revealed a group of steroid-resistant genes including CXCL8, IL-1β, IL-18 and growth-related oncogenes (GRO) (350). These steroid-resistant cytokines are of critical importance in disease pathogenesis and progression (67,69,157,396). As a result of the increased number of alveolar macrophages in COPD airways (113,114), there will be more steroid-resistant mediators that cannot be suppressed by the administered corticosteroids (168). Alveolar macrophage sensitivity to corticosteroids was found to be less in COPD than in smokers (166,167). However, more recent studies revealed no difference in corticosteroid response between alveolar macrophages from COPD and healthy controls (168,397).

Neutrophils secrete a number of cytokines and chemokines which are involved in COPD pathophysiology (398). Airway neutrophils, but not peripheral blood neutrophils, showed reduced GR expression in COPD and healthy controls, resulting in impaired corticosteroid suppression of CXCL8 and TNF-α release from neutrophils (399). Moreover, IFN-γ production by airway lymphocytes was reported to be steroid-resistant in COPD patients  (400).

It is well known that one of the molecular mechanism of the anti-inflammatory action of corticosteroids is the recruitment, by activated GR, of HDAC2 to the activated inflammatory genes, thus reversing the acetylation of these genes and silencing their transcription (380,401). HDAC2 activity and expression were reduced in alveolar macrophages, airways and peripheral lung of COPD patients, which was linked to disease severity (166,402). This was possibly triggered by oxidative and nitrative stress (403,404). HDAC2 dysfunction is therefore highlighted to be one possible mechanism of corticosteroid resistance in COPD patients (405)

Another mechanisms of corticosteroids resistance include impairment in GR nuclear translocation and its ligand binding affinity. However, it was only reported in steroid resistant asthma patients (346,406).

## 1.7.    Hypothesis:

NTHi is the most common airway infection in stable and exacerbated COPD, contributing to serious morbidity, mortality and disease progression. Corticosteroids are widely used anti-inflammatory drugs during COPD exacerbations. However, corticosteroids do not completely suppress airway inflammation. Therefore, investigation of the innate immune response to NTHi in a relevant *in vitro* model would help to understand the molecular basis of NTHi infection in COPD. Furthermore, assessment of the anti-inflammatory effect of corticosteroids in this *in vitro* model could test the potential clinical benefit of corticosteroids during NTHi infection. Furthermore, this investigation could highlight potential therapeutic targets for future therapy.

Modulation of alveolar macrophage phenotype by some bacteria was highlighted as a possible mechanism of chronic infections. Therefore, NTHi modulation of M1/M2 markers could be an important mechanism of bacterial persistence in the lower airways of COPD patients.

## 1.8.    Aims and objectives:

The general aim of this thesis is to investigate COPD alveolar macrophage inflammatory response to NTHi infection *in vitro* and test the anti-inflammatory effect of corticosteroids and kinase inhibitors on this response. Moreover, I aimed at investigating alveolar macrophage functional polarisation in response to NTHi infection. These aims were achieved through the following steps:

1.  Optimise the *in vitro* model of NTHi infection by:

- Culturing alveolar macrophages with live NTHi and investigating the resultant inflammatory response in terms of cytokine release over 24 hours.

- Monitoring NTHi survival in the culture and the macrophage viability in response to an increasing bacterial concentration.

- Comparing alveolar macrophage inflammatory response triggered by standard NTHi strain (R2846) with that triggered by NTHi isolates from stable COPD patients.

2. Study the effect of anti-inflammatory compounds on NTHi-induced inflammatory response by:

- Studying corticosteroid responsiveness of NTHi-induced cytokines in alveolar macrophages from COPD versus non-COPD controls.

- Investigating the signalling pathways mediating NTHi inflammatory response in alveolar macrophages from COPD patients. Also, studying the effect of corticosteroids on the activated pathways.

- Assessing the anti-inflammatory effect of compounds that knock down the signalling pathways of NTHi-induced inflammation in COPD alveolar macrophages.

- Investigating the potential synergistic effect of kinase inhibitors with corticosteroids.

- Examining the effect of NTHi on GR phosphorylation and nuclear translocation as a possible mechanism of reduced corticosteroid responsiveness.

- Assessing the role of p38 MAPK in NTHi-induced GR phosphorylation and nuclear translocation.

3. Investigate the role of NTHi in modulating alveolar macrophage functional polarisation as a possible mechanism of NTHi chronic infection in COPD by:

    - Monitoring the change in mRNA levels of macrophage (M1/M2) phenotype markers in response to NTHi infection *in vitro*.

    - Comparing the mRNA levels of sputum macrophage (M1/M2) markers in NTHi-infected COPD patients versus non-infected controls.

# Chapter two

# Materials and Methods

## 2.1. Isolation of alveolar macrophages and cell culture:

### 2.1.1. Isolation of alveolar macrophages from resected lungs:

Alveolar macrophages were obtained from peripheral airways of lung tissue resected from surgically excised lung lobe or segment. Lung tissue was cut from areas distal to the tumour and perfused with sterile 0.15 M Sodium Chloride (NaCl) to isolate macrophages. The retrieved fluid was centrifuged (400g, 10 minutes, room temperature (RT)). The resulting cell pellet was resuspended in RPMI 1640 media (Sigma Chemical, Dorset, UK). The cell suspension was layered over Ficoll-Paque (GE Healthcare, Buckinghamshire, UK) and centrifuged (400g, 30 minutes, 4°C). Ficoll-Paque is a density gradient media which allows differential migration of different cell types; mononuclear cells will form a layer at the interface between plasma and Ficoll. Alveolar macrophages were collected and resuspended in RPMI 1640 medium supplemented with 10% foetal bovine serum (FBS) (Life Technologies, Warrington, UK), 1% penicillin/streptomycin (Sigma), and 1% L-glutamine (Life Technologies). Cells were washed with non-supplemented RPMI 1640 medium (400g, 10 minutes, 4°C). Cells were resuspended in supplemented RPMI 1640 and viable cells were counted by Trypan blue exclusion on a Neubauer haemocytometer. Cells were resuspended at a concentration of $1\times10^6$ macrophages per ml in supplemented RPMI 1640 medium.

Alveolar macrophages were seeded on appropriate culture plate, as stated for each experiment, and incubated at 37 °C and 5% $CO_2$ for a minimum of 18 hours to allow alveolar macrophages to adhere to the plate. Non-adherent cells were removed by washing with pre-warmed supplemented RPMI 1640 medium (without antibiotic) before infection experiments.

### 2.1.2. Isolation of alveolar macrophages from induced sputum:

### 2.1.2.1. Sputum induction:

Subjects were assessed for their lung function at the beginning of the visit. Spirometry was done after inhalation of 200 μg of salbutamol (Stockport Pharmaceuticals, Stockport, UK) and the FEV1 was recorded as the baseline reading. FEV1 of ≥50% predicted permits the patient to carry on sputum induction process. Subjects were asked to inhale an increasing concentration of sterile hypertonic saline (3, 4 and 5%) via an ultrasonic nebuliser (Ultraneb 2000, Medix, Harlow, UK), each for 5 minutes. To exclude any bronchospasm due to the procedure, spirometry was repeated after each inhalation. If FEV1 dropped by less than 10% of the baseline level, the subject was asked to inhale the next concentration of hypertonic saline. On the contrary, if the FEV1 drop was ≥ 10% but still ≤20%, the subject was asked to inhale the same concentration of hypertonic saline. If FEV1 dropped by >20%, the process was stopped and the subject was given another dose of salbutamol (200 μg), rested for 20 minutes before repeating the spirometry, and discharged. After each inhalation subjects had been asked to blow their nose and wash their mouth with water before they were asked to cough in to a sterile container. The sample was kept on ice to maintain cell viability until the time of processing.

### 2.1.2.2. Sputum processing:

Sputum was processed within 2 hours of induction. Sputum was placed in a sterile petri dish and inspected against a black background to identify sputum plugs. Plugs were separated from saliva by a sterile forceps and collected into a sterile, pre-weighed tube. The sample was weighed and part of the sample used for sputum bacteriology (minimum weight 0.1 g). The remaining sputum was used for macrophage isolation.

### 2.1.2.3. Sputum macrophage isolation:

Dithiothreitol (DTT) (0.1%) in phosphate buffered saline (PBS) was added to sputum sample at a volume of four times the sample weight, e.g., (400ul:100 mg). The sample was vortexed and placed on a rolling mixer (15 minutes, RT). PBS at a volume of four times the sample weight was added, and the sample was filtered using sterile nylon gauze with pore size 48μm. The filtrate was centrifuged (790g, 10 minutes, 4°C), cell pellets were resuspended in supplemented RPMI 1640 medium and viable cells were counted by Trypan blue exclusion on a Neubauer haemocytometer. Cells were adjusted to a concentration of $1 \times 10^6$ cells per ml and were plated on 6 well plates and cultured for 24 hours at 37 °C and 5% $CO_2$. Non-adherent cells were removed by washing with supplemented RPMI 1640 to leave macrophages.

### 2.2. Bacterial preparation:

### 2.2.1: Bacterial culture:

The two strains of bacteria used in this study were *Escherichia coli* (*E. coli*) (strain ATCC 11775/ NCTC 9001) and NTHi (R2846 or strain 12). Both were kindly provided by Dr Nicola High (Faculty of Life Sciences-University of Manchester). *E. coli* (ATCC 11775/ NCTC 9001), a urinary isolate, was grown from frozen stock on Columbia blood agar (CBA) (E&O Laboratories, Scotland) and incubated at 37 °C and 5% $CO_2$ for 16 hours. Under aseptic conditions, multiple colonies were recovered from culture plates and inoculated in sterile Brain Heart Infusion (BHI) broth (Sigma).

NTHi R2846 is a well-characterised strain that is isolated from middle ear fluid of a child with otitis media (407). NTHi frozen stocks were streaked on Columbia

agar chocolate (CHOC) (E&O Laboratories) and incubated at 37 $^{o}$C and 5% $CO_2$ for 16 hours. Under aseptic conditions, individual colonies were harvested and inoculated in BHI broth supplemented with hemin and β-NAD (Sigma Aldrich, UK) each at 10μg/ml (408).

Broths of both bacteria were incubated in the shaking incubator (311DS Labnet) at 200 revolutions per minute (RPM) and 37 °C for 16 hours. The bacterial suspension was centrifuged (4000 RPM, 10 minutes, RT) and the resulting bacterial pellets were washed twice in sterile Dulbecco's PBS (Sigma). Bacterial pellets were resuspended in sterile PBS and the optical density was measured at 600 nm ($OD_{600}$) using plate reader (POLARstar Omega, BMG LABTECH). The broth was then diluted to 1.2±0.02 $OD_{600}$. Bacterial viability and count were confirmed each time by Miles-Misera plate counting as described below.

### 2.2.2. Bacterial quantification:

Quantification of viable bacteria was determined by Miles-Misera protocol (409). Eight tenfold serial dilutions were prepared from 1.2 $OD_{600}$ bacterial suspension in sterile PBS. Two CHOC plates (at RT) were divided by an imaginary line into four quadrants and three 10 μl drops of each dilution were plated on a quadrant (Figure 2.1). Plates were incubated overnight at 37 $^{o}$C and 5% $CO_2$. Developed colonies were counted in the quadrant with the highest number of colonies that were still easily discernible. The average colony count was corrected to the dilution factor and multiplied by 1000 to give the number of colony forming unit per millilitre (CFU/ml).

For example, in the Miles-Misera test result shown in Figure 2.1, the quadrant with $10^{-6}$ dilution (Figure 2.1 B) contains the highest number of colonies that are easily discernible. The calculation below uses the count from this quadrant.

Average bacterial count /µl= 17+18+21/30= 1.9 CFU/µl

Bacterial count /ml of 1.2 $OD_{600}$ suspension= $1.9 \times 10^6 \times 1000 = 1.9 \times 10^9$ CFU/ml
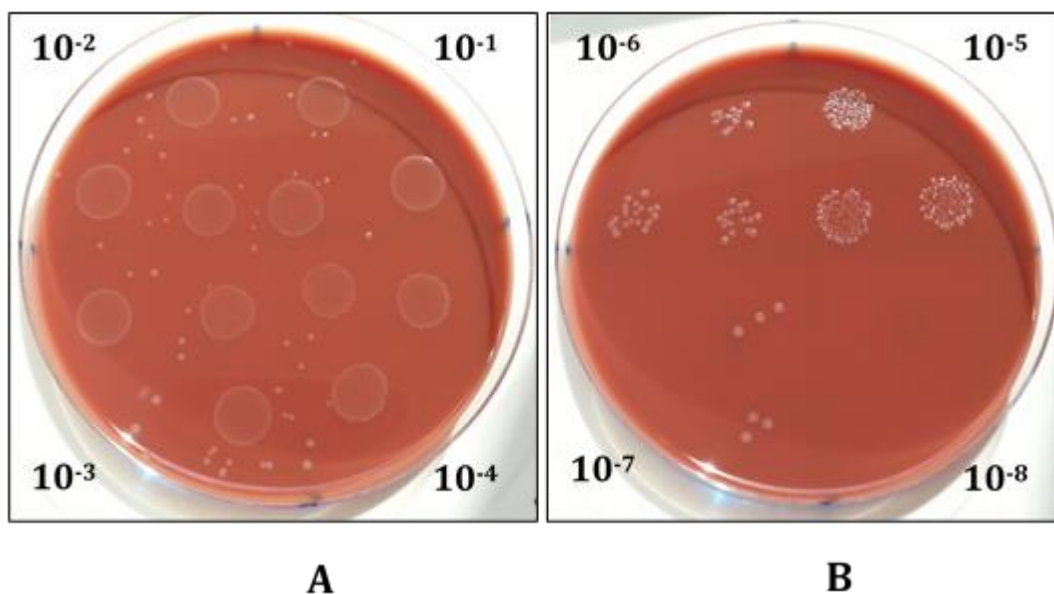


**Figure 2.1: NTHi quantification by Miles- Misera plate counting**. Two chocolate agar plates A and B were divided into four quadrants. Each quadrant was plated with the labelled bacterial dilution. In this figure, quadrant with $10^{-6}$ bacterial dilution is ideal for colony count.

### 2.2.3. Setting Multiplicity of infection (MOI):

To present bacterial load in a more understandable and convenient way, and to keep the bacterial load consistent throughout my experiments, Multiplicity of Infection (MOI) was used. MOI is the ratio of live bacteria per cell (bacteria: macrophage).

NTHi viable count in 1.2 $OD_{600}$ suspension was calculated in 4 different experiments, the average was calculated and rounded to the closest $10 \times 10^9$ CFU/ml. This count was set to be the expected count for each experiment. However, NTHi count was confirmed every time to eliminate any significant difference in the experimental conditions that might affect bacterial growth. Tenfold difference in

NTHi count between experiments was accepted. MOI was pre-set to 1:1, 3:1, 10:1, 30:1, 100:1, 300:1 and 1000:1 MOI.

Target MOI was achieved on culture plate using the following equation:

NTHi viable count in 1.2 $OD_{600}$ suspension (**A**) = $\sim10\times10^9$ CFU/ml

CFU/well (**B**) =Target MOI x alveolar macrophages per well x 10 (dilution factor in the well)

Target CFU/ml (**C**) = (**B**)/media volume per well

Dilution from 1.2 $OD_{600}$ suspension = (**A**)/ (**C**)

Dilution factor for each target MOI is calculated, and sub-stocks from 1.2 $OD_{600}$bacterial suspensions were prepared in supplemented RPMI 1640.

**Example:** To achieve 10:1 MOI in a well containing $10^5$ alveolar macrophages with media volume of 0.2 ml.

 (**A**)= 10 x $10^9$ CFU/ml

 (**B**)= 10 x $10^5$x10 = $10^7$

 (**C**)= $10^7$/0.2 ml=5 x$10^7$

Dilution from 1.2 $OD_{600}$ suspension =10 x $10^9$/5 x$10^7$=200 (dilution factor)


## 2.3. Isolation of NTHi from sputum samples of stable COPD patients:

Sputum samples were induced and processed as detailed in sections 2.1.2.1 and 2.1.2.2. 1% DTT (Sigma-Aldrich) was used to homogenise sputum plugs. DTT was sterilised by filtering through a syringe filter (0.2 μm pore size). A working DTT concentration of 0.1% was freshly prepared. An equal volume of 0.1% DTT was

added to the sputum sample and vortexed for 1 minute. The sample was incubated for 15 minutes at 37 $^{\circ}$C. After incubation the sample was vortexed for an additional 1 minute. The sputum homogenate was plated, as detailed below, to detect the infecting bacteria.

Various agar plates were used to help identify different respiratory pathogens. The details of the plates and characteristics of the isolated pathogens are summarised in Table 2.1. The plates are categorised into two groups, streak plates and spread plates (Table 2.2).

Streak plates gave a semi-quantitative estimate of all bacterial species in a sputum sample. Sputum homogenates were streaked on three different plates, Columbia blood agar (CBA), Bacitracin Chocolate agar (BAC CHOC) and Mannitol salt agar (MSA). Using standard four quadrants dilution of the sample on the plate, 5µl of the homogenate was sub-streaked through four quadrants of each plate using a sterile loop for each quadrant dilution. Optochin disc (Oxoid, Hampshire, UK) was placed on CBA between the first and second streaks to help identify *Streptococcus pneumonia* from other α-haemolytic streptococci (Figure 2.2).

Spread plates allow further identification and quantification of the predominant bacterial species in the sample. These include three CBA and three CHOC (E&O Laboratories) (Figure 2.2). Five tenfold serial dilutions of sputum homogenate were prepared with sterile PBS. 10µl of each $10^{-3}$, $10^{-4}$ and $10^{-5}$ dilutions was plated on individual CBA and CHOC spread plates using L-spreader (Lab-M, Lancashire, UK). Both streak and spread plates were incubated for 24 hours at 37 $^{\circ}$C and 5% $CO_2$.

**Table 2.1: Agar plates selectivity for bacterial species and their characteristic appearance.**

| Agar type | Isolated pathogen | Colony appearance |
|---|---|---|
| **Columbia agar chocolate (CHOC)** | *Haemophilus* species | Grey colonies |
| | *Moraxella catarrhalis* | White dry colonies |
| | *Neisseria* species | Grey colonies |
| | *Streptococcus pneumonia* | Green colonies with α-haemolysis |
| **Columbia blood agar (CBA)** | *Streptococcus pneumonia* | Grey/green colonies with α-haemolysis |
| | *Streptococcus pyogenes* | White colonies with β-haemolysis |
| | *Moraxella catarrhalis* | White dry colonies |
| **Chocolate agar with Bacitracin (BAC CHOC)** | *Haemophilus* species | Grey colonies |
| **Mannitol salt agar (MSA)** | *Staphylococcus aureus* | Yellow colonies |

**Table 2.2: Agar plates groups in sputum bacteriology identification.**

| Group of plates | Type of plates in a group | Number | Role in identification |
|---|---|---|---|
| **Streak plates** | Columbia blood agar (CBA) | 1 | Semi-quantitative estimate of all bacterial pathogens |
| | Chocolate agar with Bacitracin (BAC CHOC) | 1 | |
| | Mannitol salt agar (MSA) | 1 | |
| **Spread plates** | Columbia blood agar (CBA) | 3 | Identification and quantification of the predominant bacterial pathogens |
| | Columbia agar chocolate (CHOC) | 3 | |

### 2.3.1. Reading the plates:

The bacterial growth in quadrant dilutions on streak plates was recorded as scores after 24 hours, which correspond to an approximate number of the total bacterial count in the sample (Figure 2.2). Plates were re-read after 48 hours to detect the growth of underdeveloped colonies at 24 hours. Table 2.3 shows bacterial count in CFU/ml that is equivalent to the scores of bacterial growth.

Spread plates were read after 24 hours of incubation, the number of viable bacteria was calculated by counting the number of colonies of same morphology. The number was corrected to the dilution factor and sample volume (10µl), and presented as CFU/ml of the original sample. The bacterial species with the highest count was considered as the infecting pathogen (Figure 2.2).

**Table 2.3: Semi-quantitative scoring of sputum bacterial growth.**

| Total number of colonies | Score | Correspondent CFU/ml |
|---|---|---|
| <10 | + | $<10^3$ |
| 10-100 | ++ | $10^3\text{-}10^4$ |
| >100 | +++ | $10^4\text{-}10^5$ |
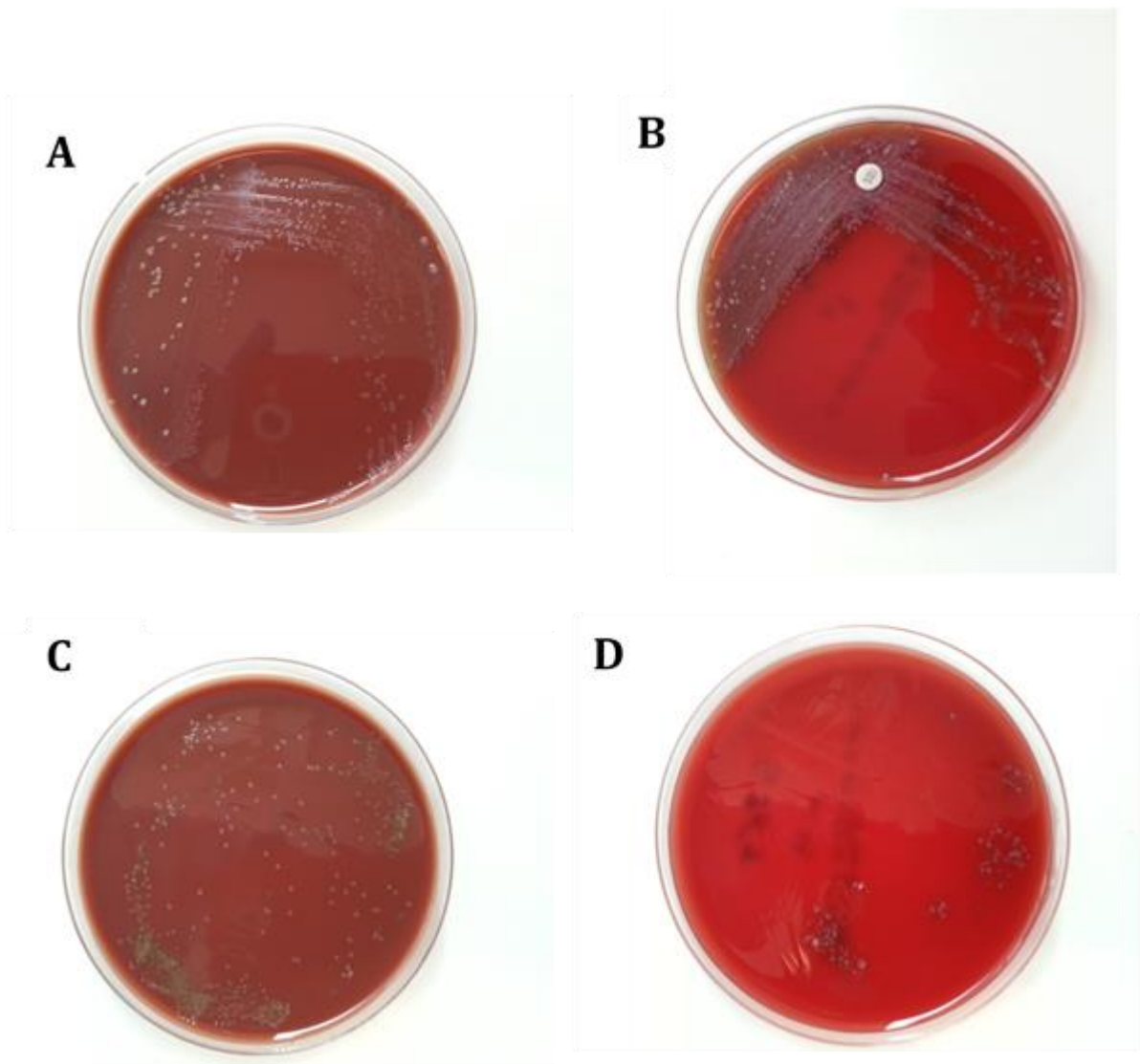
**Figure 2.2: Representative sputum culture from NTHi infected COPD subject.** Sputum homogenate was streaked on two sets of plates, streak plates (A and B) and spread plates (C and D). Mixed colony growth on streak plates (A and B) gave an estimated bacterial load of $10^3$-$10^5$ CFU/ml. Positive growth around Optochin disc between first and second streaks on blood agar (B) suggests negative culture for *Streptococcus pneumonia.* At $10^{-3}$ sputum dilution, a predominant growth of small, grey, mucoid colonies on the spread chocolate agar (C) but not on the blood agar (D) suggests *Haemophilus influenzae* infection which is countable on plate (C).

## 2.3.2. Bacterial identification:

Colonial morphology on the spread plates was highly suggestive of the pathogen (Figure 2.3). Potential pathogens were subcultured on an appropriate agar plate and incubated for 24 hours at 37 °C and 5% $CO_2$. Pure culture was used for further identification tests. Table 2.4 summarises the identification criteria.
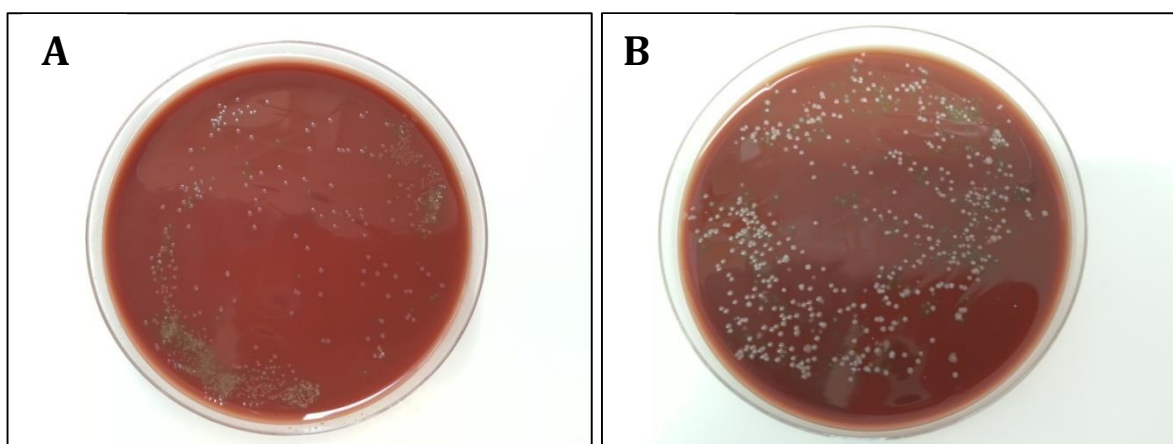


**Figure 2.3:** **Bacterial colonial morphology. A:** NTHi appears as small, grey and mucoid colonies on chocolate agar. **B:** *Moraxella catarrhalis* appears as white and dry colonies on chocolate agar.

**Table 2.4: Sputum bacterial identification criteria.**

| Microorganism | Culture medium | Colony morphology | Identification tests |
|---|---|---|---|
| *Haemophilus influenzae* | CHOC | -Small, concave, grey and mucoid. | - XV test: bacteria grow around XV discs. |
| *Moraxella (Branhamella) catarrhalis* | CHOC, CBA | -White, grey or pinkish dry.<br>- hockey-puck test: colony can be easily pushed across the plate | -Tributyrin test positive.<br>-oxidase and catalase positive. |
| *Streptococcus pneumonia* | CHOC, CBA | -clear concave colonies.<br>-α-haemolysis appearing as a green zone around the colony | -Optochin sensitivity (>14mm zone of inhibition) while other α-haemolytic *Streptococci* are resistant.<br>-Catalase negative |
| *Pseudomonas aeruginosa* | CHOC, CBA | -Irregular, translucent mucoid colonies with bluish-green pigmentation. | Oxidase and catalase positive. |
| *Staphylococcus aureus* | MSA | -Medium sized, golden buff/yellow colonies | Catalase and coagulase positive. |

**Abbreviations:** CHOC= Columbia agar chocolate, CBA= Columbia blood agar, MSA= Mannitol salt agar

### 2.3.2.1. X-V test:

X (hemin) and V (NAD) factors are used to identify *Haemophilus* species depending on their nutritional requirements.

Under sterile conditions, colonies were picked from the pure culture plate by sterile swab and dissolved in 1 ml of sterile PBS to prepare bacterial suspension equivalent to 0.5 McFarland standard (ProLab, Merseyside, UK). This standard is intended to be part of a quality control programme for adjusting densities of bacterial suspensions that are used for identification and susceptibility testing. The

bacterial suspension was streaked with a sterile swab on ISA sensitivity test agar 25ml (E&O Laboratories) and the X, V and XV discs (Oxoiod) were placed around the agar plate periphery with good spacing between the discs. The plate was incubated at 37 °C and 5% $CO_2$ for 24 hours. The growth around each disc was recorded after incubation.

Bacterial growth around XV disc only (Figure 2.4 A) indicates they need both X and V factors for their growth, like *Haemophilus influenzae.* Bacteria requiring X factor for their growth will grow around X and XV discs like *Haemophilus ducreyi.* Bacteria requiring V factor will grow around both V and XV discs like *Haemophilus parainfluenzae* (Figure 2.4 B).
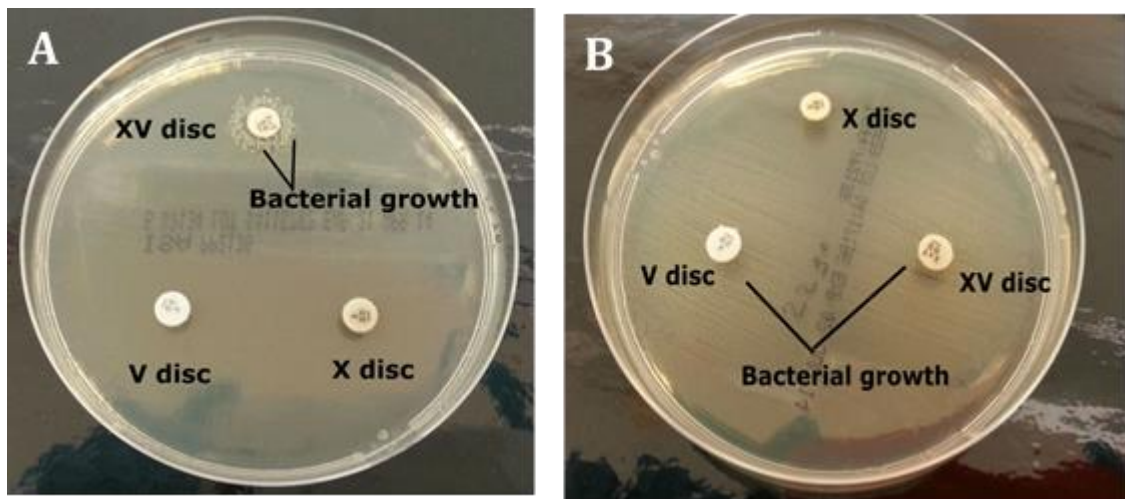


**Figure 2.4: X-V test. A:** *Haemophilus influenzae* grows around XV disc. **B:** *Haemophilus parainfluenzae* grows around V and XV discs.

### 2.3.2.2. Tributyrin test:

Tributyrin test is chromogenic test that helps in differentiation between *Moraxella (Branhamella) catarrhalis* and *Neisseria* species. The test principle is that an enzyme hydrolysis of tributyrin causes colour change of the acidobasic indicator.

Colonies were picked from the pure culture by a sterile swab, and dissolved in 1 ml sterile PBS to give bacterial suspension equivalent to 0.5 McFarland standard (Prolab). A Tributyrin stip (Sigma) was picked by a sterile needle and dropped in the suspension. The suspension was incubated at 37 °C and 5% $CO_2$ for 18-20 hours. A colour control tube was run with the sample for colour comparison. Colour change to yellow is positive for *Moraxella catarrhalis* (Figure 2.5 A). A negative orange colour indicates *Neisseria* species (Figure 2.5 B).
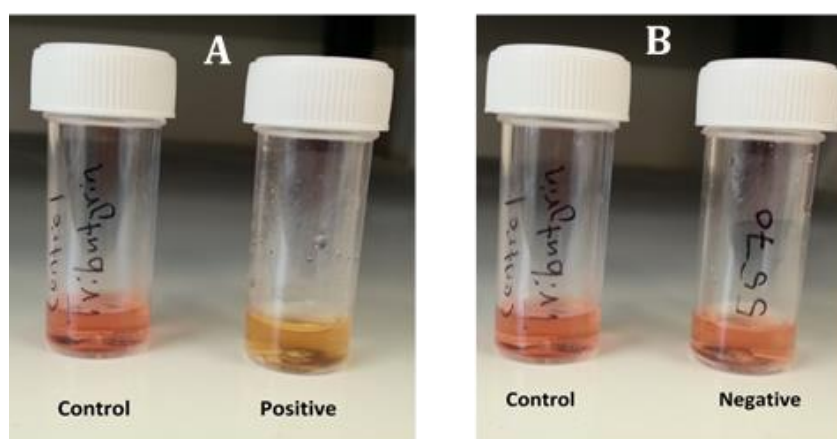


**Figure 2.5: Tributyrin test. A:** positive test indicates *Moraxella catarrhalis.* **B:** negative test indicates *Neisseria* species*.*

### 2.3.2.3. Catalase test:

This test is used to identify catalase producing bacteria like *Moraxella catarrhalis*, *Staphylococcus aureus* and *Pseudomonas aeruginosa* from those which are non-catalase producing as *Streptococcus pneumonia*. Catalase enzyme catalyses the breakdown of hydrogen peroxide ($H_2O_2$) releasing free oxygen (appears as

113

bubbles). To observe the action of the enzyme, $H_2O_2$ was added to pure bacterial colonies; any immediate bubbling is indicative of a positive result.

### 2.3.2.4. Oxidase test:

Oxidase test is used to identify oxidase producing gram-negative bacteria. In the presence of the enzyme cytochrome oxidase, the N, N-dimethyl-p-phenylenediamine oxalate and α-naphthol react to indophenol blue. One colony was picked by a sterile wooden pick and placed on oxidase disc (Sigma). Colour change was observed within 10 seconds, blue colour change indicates positive oxidase test, as in *Haemophilus influenzae*, *Moraxella catarrhalis* and *Pseudomonas aeruginosa*.

### 2.3.3. Preservation of NTHi clinical isolates:

Bacteria proven to be NTHi by positive XV test were preserved for future experiments and biotyping. Colonies were recovered from a pure culture by a sterile loop and inoculated in Microbank tubes (Prolab). The tubes were frozen at -80 °C for future experiments.

### 2.3.4. Biotyping of NTHi:

Frozen NTHi isolates were sub-cultured on CHOC plates and incubated for 24 hours at 37 °C and 5% $CO_2$. Grown bacteria were subjected to biotyping under sterile conditions including three tests, urease test, spot indole test and ornithine decarboxylase test.

### 2.3.4.1. Urease test:

In this test, urea broth, containing the phenol red colour indicator, was used. Some bacteria have a urease enzyme which can split urea in the presence of water to release ammonia and $CO_2$. The ammonia combines with $CO_2$ and water to form

ammonium carbonate, which turns the medium alkaline thus turning the indicator phenol red from its original orange-yellow colour, to bright pink.

Urea broth (Fluka-Sigma-Aldrich) was supplemented with hemin and β-NAD at 10 μg/ml. 2 ml tube of the broth was inoculated with 4-10 colonies to prepare bacterial suspension equivalent to 0.5 McFarland standard (Prolab). The broth was incubated for 18-24 hours at 37 °C and 5% $CO_2$. The colour change was recorded at the end of incubation. Pink-red change in colour indicate positive reaction (Figure 2.6).
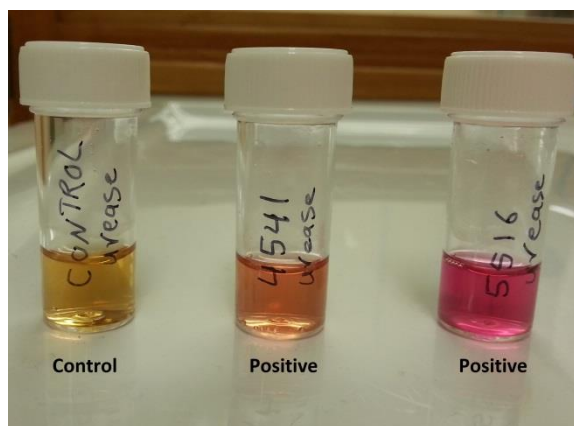


**Figure 2.6: Urease test.** Pink-red change in colour indicates a positive response.

## 2.3.4.2. Spot indole test:

Spot indole reagent is used in the qualitative method to determine bacterial ability to split indole from the tryptophan molecule. The amino acid tryptophan can be oxidised by tryptophanase enzyme produced by certain bacteria, resulting in the production of indole. The indole is detected by the p-dimethylaminocinnamaldehyde in the indole reagent producing a distinct blue colour.

Colonies were picked by a sterile wooden pick and transferred to a filter paper. One drop of indole reagent (Kovac's reagent, Remel) was added to the transferred

colonies. Colour change was observed within 1 minute, blue change in colour indicates positive indole test (Figure 2.7).
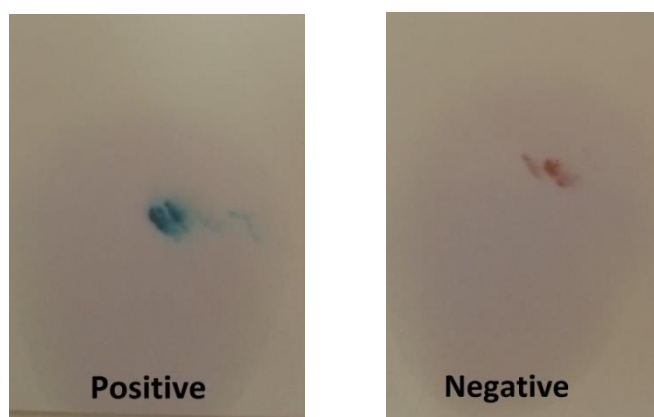


**Figure 2.7:** **Spot indole test.**

### 2.3.4.3. Ornithine decarboxylase test:

Ornithine decarboxylase test is recommended for the detection of the ability of microorganisms to decarboxylate ornithine. In the initial stages of incubation, glucose is fermented by the organisms with acid production. The glucose fermentation will result in a colour change in the Bromo Cresol Purple pH indicator to yellow. If ornithine is decarboxylated, there will be an alkaline reaction causing further change in colour to purple.

Ornithine decarboxylase broth (Fluka-Sigma-Aldrich) was supplemented with hemin and β-NAD at 10 μg/ml. 2 ml tube of the broth was inoculated with 4-10 colonies to prepare bacterial suspension equivalent to 0.5 McFarland standard (Prolab). Ornithine decarboxylase broth was covered with sterile mineral oil, this promotes fermentation by locking out oxygen, and it also prevents false alkalinisation at the surface of the medium. Broth incubated at 37 °C and 5% $CO_2$. Results were recorded at 24 and 48 hours of incubation. After 24 hours, colour

change to yellow indicates that the bacteria ferment glucose. After 48 hours, further change in colour to purple indicates ornithine decarboxylation. Failure of colour change after 48 hours indicates negative test (Figure 2.8).
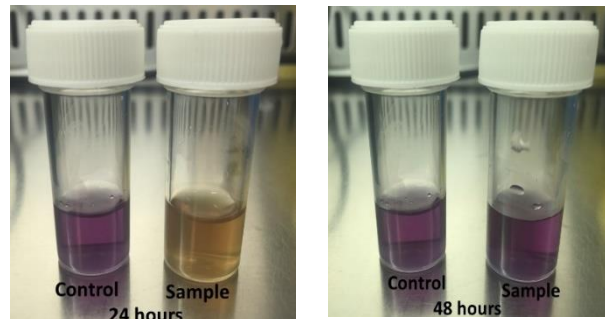


**A. Positive**
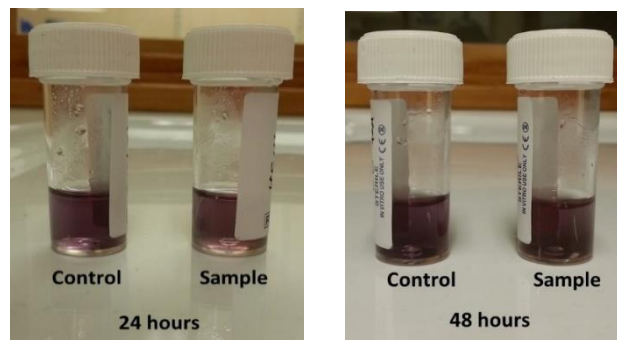


**B. Negative**
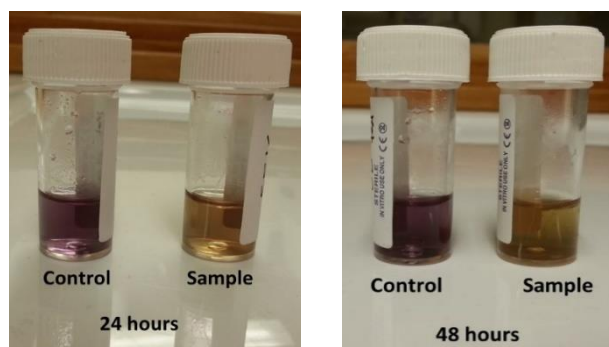


**C. Negative**

**Figure 2.8:** **Ornithine decarboxylase test. A:** Colour change to yellow at 24 hours and further change in colour to purple at 48 hours indicates positive reaction. **B:** No colour change at 24 and 48 hours indicates a negative reaction. C: Persistent colour change at 24 and 48 hours indicates a negative reaction

### 2.3.4.4. Recording and interpretation of the results:

The results were recorded and interpreted as shown in the Table 2.5:

**Table 2.5:** Bacterial biotyping

| Test | Biotype | | | | | | | |
|---|---|---|---|---|---|---|---|---|
| | I | II | III | IV | V | VI | VII | VIII |
| Urease | + | + | + | + | - | - | - | - |
| Indole | + | + | - | - | + | - | + | - |
| Ornithine decarboxylase | + | - | - | + | + | + | - | - |

### 2.3.5. Antibiotic testing of NTHi (antibiogram):

Antibiotic sensitivity testing for *Haemophilus influenzae* was established in our lab according to the British Society for Antimicrobial Chemotherapy (BSAC) guidelines (410).

Standard strains (NCTC 11931 and NCTC 12699) were obtained from Public Health England (PHE) and were used to validate test procedures. Procedures were tested monthly to ensure quality control.

Clinical NTHi isolates, as well as NTHi (R2846), were freshly subcultured from frozen stocks on CHOC agar plate. The plates were incubated for 24 hours at 37 °C and 5% $CO_2$. Colonies from each strain were suspended in 2 ml sterile PBS to create suspension equivalent to 0.5 McFarland standard (Prolab). A sterile swab was dipped once in the suspension and streaked on one Haemophilus Test Medium (HTM) plate (E &O Laboratories). The swab was spread across the plate in two perpendicular directions and was continuously turned while spreading to ensure even bacterial growth.

The antibiotic discs (Oxoid) listed in Table 2.6 were used; no more than three discs were placed on one HTM plate. Plates were incubated for 18-20 hours at 37 $^{o}$C and 5% $CO_2$. Zones of inhibitions were noted and measured by a ruler. The readings were compared to the values listed in Table 2.6 to determine antibiotic sensitivity. All results were tabulated in a work sheet for future analysis.

**Table 2.6: Antibiotics used in antibiogram and interpretation of their zones of inhibition.** R=resistance, S=sensitive, I=intermediate.

| Antimicrobial agent | Abbreviation | Disc potency (in µg unless stated) | Interpretation of zone of inhibition (mm) | | |
|---|---|---|---|---|---|
| | | | R ≤ | I | S ≥ |
| **Penicillins** | | | | | |
| Amoxicillin | AML | 2 | 13 | - | 14 |
| Ampicillin | AMP | 2 | 17 | - | 18 |
| Amoxicillin–clavulanic acid | AMC | 3 | 13 | - | 14 |
| **Cephalosporins** | | | | | |
| Cefaclor | CEC | 30 | 14 | - | 15 |
| Cefotaxime | CTX | 5 | 24 | – | 25 |
| Ceftriaxone | CRO | 30 | 24 | | 25 |
| Ceftazidime | CAZ | 30 | 14 | 15-17 | 18 |
| **Carbapenems** | | | | | |
| Imipenem | IPM | 10 | 22 | - | 23 |
| **Macrolides** | | | | | |
| Azithromycin | AZM | 15 | 19 | - | - |
| Erythromycin, | E | 5 | 14 | - | - |
| Clarithromycin | CLR | 2 | 8 | - | - |
| **Quinolones** | | | | | |
| Moxifloxacin | MXF | 5 | 17 | | 18 |
| Ciprofloxacin | CIP | 1 | 27 | - | 28 |
| Levofloxacin | LEV | 1 | 19 | - | 20 |
| Tetracyclines | | | | | |
| Tetracycline | TE | 10 | 17 | 18-21 | 22 |
| **Others** | | | | | |
| **Chloramphenicol** | C | 10 | 24 | - | 25 |
| **Sulfamethoxazole–trimethoprim** | SXT | 25 | 17 | 18-20 | 21 |

## 2.4. Cell viability assessment by Transferase dUTP Nick End Labelling (TUNEL assay):

Alveolar macrophage DNA fragmentation was measured by *In Situ* Cell Death Detection Kit, Fluorescein kit (Roche Diagnostic Ltd, Burgess Hill, UK). Cellular destruction by apoptosis results in DNA fragmentation. DNA breaks expose a large number of 3´-hydroxyl ends, which can then serve as starting points for terminal deoxynucleotidyl transferase (TdT). TdT adds deoxyribonucleotides in a template-independent fashion. The addition of the deoxythymidine analog 5-bromo-2´-deoxyuridine 5´-triphosphate (dUTP) to the TdT reaction serves to label the break sites. Once incorporated into the DNA, dUTP can be detected by fluorescence microscopy (411,412). Figure 2.9 outlined the principle of TUNEL assay.

Alveolar macrophages were plated on chamber slides at $1x10^5$ cells per well and incubated at 37 °C and 5% $CO_2$ overnight. Cells were fixed with 4% paraformaldehyde (1 hour, RT) and permeabilised by permeabilisation buffer (0.1% Triton-X in 0.1% sodium citrate), which was added to the cells for 2 minutes on ice. Cells were washed with PBS. 50µl of TUNEL reaction mix or label solution, for negative controls, was added to the cells and incubated at 37 °C in the dark for 1 hour. Cells were washed with PBS and counterstained with 4', 6-diamidino-2-phenylindole (DAPI) stain (Invitrogen) at 0.002% in PBS (5 minutes, RT).

Slides were visualised by fluorescence microscopy (Nikon Eclipse 80 i-Nikon UK Ltd, Surry, UK), equipped with QImagining digital camera (Media Cybernetics, Marlow, UK). TUNEL mix stains fragmented apoptotic nuclei green while DAPI stains all nuclei blue. Each field was examined for TUNEL, DAPI and macrophage auto-fluorescence (red). Images were analysed using Image-pro plus version 5.1 software (Media Cybernetics, Marlow, UK) and the percentage of apoptotic cells was

counted. Examples of apoptotic (TUNEL positive) cells and normal (TUNEL negative) cells are shown in Figure 2.10.
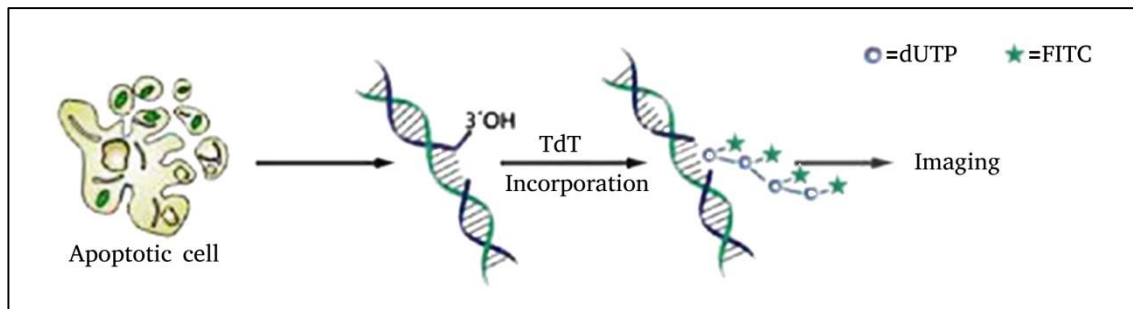


**Figure 2.9: TUNEL assay principle.** DNA fragmentation in apoptotic cells can be detected by TdT-mediated dUTP nick end labelling (TUNEL). dUTP is labelled by FITC and the labelled fragments are detected by fluorescence microscopy. TdT= terminal deoxynucleotidyl transferase, dUTP= deoxythymidine analog 5-bromo-2´-deoxyuridine 5´-triphosphate, FITC= fluorescein isothiocyanate. Adapted from www.biotool.com (413).
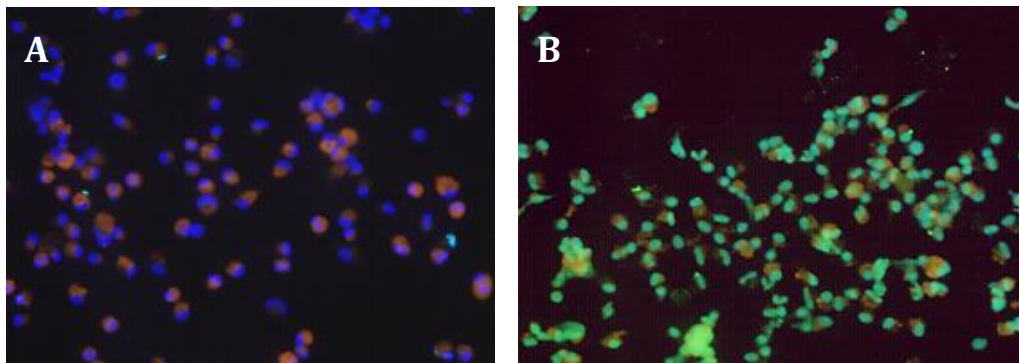


**Figure 2.10: Detection of alveolar macrophage apoptosis by TUNEL assay.** Alveolar macrophages were labelled and fluorescently stained for DNA fragmentation by TUNEL assay. A: cells with blue nuclei are viable (TUNEL negative). B: cells with green nuclei are apoptotic (TUNEL positive) due to pretreatment with Triton-X. Magnification power 20X.

## 2.5. Cytokine measurement by Enzyme-Linked Immunosorbent Assay (ELISA):

Culture supernatants were analysed for cytokines levels by ELISA. TNF-α, IL-6 and CXCL8 levels were measured using R&D system kits (R&D system, Abingdon, UK) and IL-10 was analysed by eBioscience kit (eBioscience Ltd, Hatfield, UK) according to manufacturer's instruction.

Capture antibodies of TNF-α, IL-6 and CXCL8 (R&D system) were diluted in PBS and plated on Immulon 2HB immunoassay plates (Fisher Scientific, Loughborough, UK). Captured plates were incubated overnight at RT. Unbound capture antibody was washed with wash buffer (0.05 % Tween-20 in PBS, pH 7.2-7.4).

Blocking of the non-specific binding sites on the plates was performed by using 1% bovine serum albumin (BSA) (Sigma-Aldrich) in PBS. BSA was added to the wells for 1 hour at RT. Plates were washed with wash buffer; samples and standards were prepared in supplemented medium without antibiotics and added to the plate for 2 hours at RT. Plates were washed and the biotin-linked detection antibody diluted in assay diluent was added for 2 hours RT. Excess antibody was washed off, and the horseradish peroxidase-conjugated streptavidin was added for 20 minutes at RT. The plates were washed and substrate of 1:1 mixture of $H_2O_2$ and 3, 3', 5, 5' tetramethylbenzidine (TMB) was applied for 15-20 minutes at room temperature, with light protection, for colour development.

Capture antibody of IL-10 (eBioscience) was diluted in PBS and plated on Nunc plates (Fisher Scientific). Captured plates were incubated overnight at 4 °C. Unbound capture antibody was washed with wash buffer (0.05% Tween-20 in PBS, pH 7.2-7.4).

Plates were blocked by 1 X assay diluent, included in the kit, for 1 hour at RT. Plates were washed with wash buffer. Samples and standards were prepared in 1 X assay diluent and added to the plates for 2 hours at RT. Plates were washed, and the biotin-linked detection antibody, diluted in assay diluent, was added for 1 hour at RT. Excess antibody was washed off, and the horseradish peroxidase-conjugated streptavidin was added for 30 minutes at RT. The plates were washed and the substrate of 1:1 mixture of $H_2O_2$ and TMB was applied for 15-20 minutes at room temperature, with light protection for colour development.

Reaction in both protocols was stopped by sulphuric acid (Sigma-Aldrich), and the optical density was measured by BMG microplate reader at 450 nm with wavelength correction set to 540 nm. A standard curve was generated using a four parameter logistic curve fit (OPTIMA Software). An example standard curve is shown in Figure 2.11. Samples, with mediator levels above the maximum concentration of the standard curve, were diluted to give a measureable level that could be read from the linear section of the standard curve (Figure 2.11). The subsequent mediator concentration was then multiplied by the dilution factor to give the mediator concentration for the parent sample. Values below the lower level of quantification were assigned a value of half the lowest concentration of the standard curve (414).

The working concentrations of capture and detection antibodies, as well as the limits of detection, are listed for all cytokines in Table2.7.
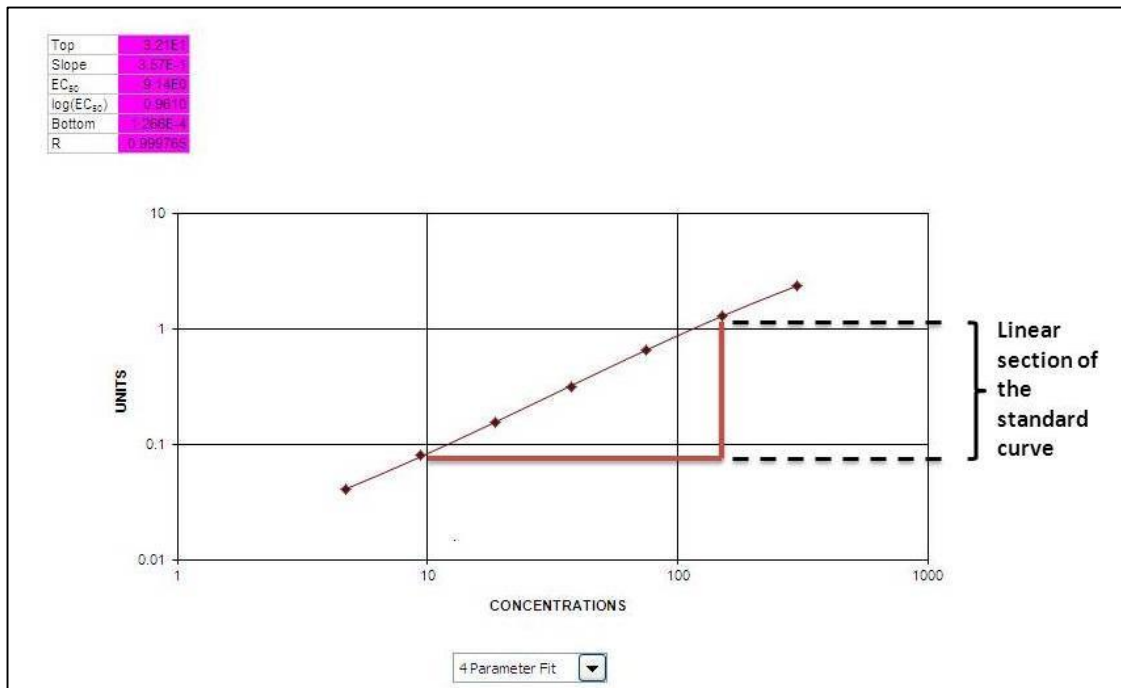
**Figure 2.11: Standard curve (four parameter fit):** A representative standard curve from IL-10 ELISA generated using a four parameter logistic curve fit. Samples concentration was read from the linear section of the standard curve. Standard concentrations are 4.688, 9.375, 18.750, 37.500, 75, 150 and 300 pg/ml.

**Table 2.7:** **ELISA antibody concentrations and limits of detection.**

| Cytokine | Assay kit | Capture antibody (µg/ml) | Detection antibody (ng/ml) | Assay diluent | Limits of detection (pg/ml) |
|---|---|---|---|---|---|
| **TNF-α** | R&D systems | 4 | 500 | 1%BSA in PBS pH 7.2-7.4 | 15.6-1000 |
| **IL-6** | R&D systems | 2 | 50 | 1%BSA in PBS pH 7.2-7.4 | 9.4-600 |
| **CXCL8** | R&D systems | 4 | 20 | 0.1%BSA, 0.05 % Tween-20 in Tris-buffered saline pH 7.2-7.4 | 31.25-2000 |
| **IL-10** | eBioscience | 1 times dilution from 250 times stock | | 1 X assay diluent | 4.6875-300 |

## 2.6. Protein extraction and Western Blot analysis:

### 2.6.1. Cells lysis:

Alveolar macrophages were lysed with radioimmunoprecipitation assay (RIPA) buffer (10 mM Tris-HCl, pH 7.4, 150 mM NaCl, 1 mM Ethylenediaminetetraacetic acid (EDTA), 0.1% Nonidet P-40). RIPA buffer contains phosphatase inhibitors (Sigma-Aldrich) and protease inhibitors (inhibitors of aspartic, cysteine, serine proteases and aminopeptidases) (Calbiochem, Nottingham, UK). Cell lysates were centrifuged (5000 RPM, 5 minutes, 4 °C). Supernatants were aspirated and stored at -80 °C for future analysis by Western blot.

### 2.6.2. Western Blot:

Cell lysate supernatants were defrosted on ice and diluted in loading buffer (62.5 mM Tris, 10% glycerol, 1% sodium dodecyl sulfate (SDS), 1% β-mercaptoethanol, and 0.01% bromphenol blue, pH 6.8). Cell lysates were sonicated

(10 minutes, 4 °C) in sonicating water bath and lysates were boiled (5 minutes, 90 °C).

SDS-polyacrylamide gel (10%) was prepared as stacking gel and separating gel as detailed in Table 2.8. Samples were loaded on SDS-polyacrylamide gel (10%). Precision Plus protein™ Kaleidoscope™ standard (Bio-Rad Laboratories Ltd, Hampshire, UK) was run to help identifying the bands' molecular weight. Protein bands were transferred to Protran standard nitrocellulose membrane (GE healthcare lifescience, Whatman™, UK) in transfer buffer (20% methanol in Tris-glycine-SDS (TGS)) for 1 hour. Membranes were blocked with 5% dried milk in Tris-buffered saline (TBS) containing 0.1% Tween-20 (1 hour, RT). Membranes then incubated with rabbit primary antibodies diluted in block buffer overnight at 4 °C. Membranes were washed three times with washing buffer (TBS containing 0.1% Tween-20) and incubated with horseradish peroxidase-linked goat anti-rabbit IgG (Cell Signalling Technology, UK) diluted 1/1000 in wash buffer (1 hour, RT). Protein bands were visualised by enhanced chemiluminescence. Densitometric analysis was performed by normalising band densities to β-actin loading control using Quantity One version 4.6.1 software (Bio-Rad Laboratories, Hemel, Hempstead, UK). Table 2.9 shows the target proteins with the primary antibodies used.

**Table 2.8: Components of SDS-polyacrylamide (10%) stacking and separating gel.**

| Gel | Components | Company |
|---|---|---|
| **Stacking gel** | 5ml deionised $H_2O$ | |
| | 1.875ml Buffer A (Trizma base-SDS pH 6.8) | Sigma-Aldrich |
| | 565 ul acrylamide-bis solution | Sigma-Aldrich |
| | 75ul APS (10% in $dH_2O$) | Sigma-Aldrich |
| | 7.5ul TEMED | Sigma-Aldrich |
| **Separating gel** | 6.125ml de-ionised $H_2O$ | |
| | 3.125 ml Buffer B (Trizma basa-SDS pH 8.8) | Sigma-Aldrich |
| | 3.125 acrylamide-bis solution | Sigma-Aldrich |
| | 125ul APS (10% in $dH_2O$) | Sigma-Aldrich |
| | 12.5ul TEMED | Sigma-Aldrich |

**Abbreviations:** APS= Ammonium per sulphate, TEMED= Tetramethylethylenediamine

**Table 2.9: Target proteins and their antibodies in Western blot.**

| Target protein | Molecular weight (kDa) | Primary antibody | Dilution factor | company |
|---|---|---|---|---|
| NF-kB p65 | 65 | Rabbit anti-human Phospho- (ser468) NF-κB p65 Antibody | 1/1000 | Cell Signaling Technology, UK |
| p38 MAPK | 43 | Rabbit anti-human phospho- (Thr180/Tyr182) p38 MAPK antibody | 1/1000 | Cell Signaling Technology, UK |
| ERK MAPK | 42, 44 | Rabbit anti-human phospho- (P44/42) MAPK antibody | 1/1000 | Cell Signaling Technology, UK |
| β- actin | 42 | Rabbit anti-β actin antibody | 1/1000 | Abcam, Cambridge, UK |
| Glucocorticoid receptor ser 211 | 95 | p- Glucocorticoid receptor ser 211 rabbit antibody | 1/1000 | Cell Signaling Technology, UK |
| Glucocorticoid receptor ser 226 | 85 | p- Glucocorticoid receptor ser 226 rabbit antibody | 1/500 | Abcam, Cambridge, UK |

### 2.6.3. Stripping and reprobing of nitrocellulose membrane:

The process of stripping and reprobing a membrane allows detecting the overlapped protein bands of close molecular weight. Membranes were stripped and reprobed for different proteins. Stripping buffer was prepared (62.5mM Tris-HCL, 2% SDS, PH 6.8) and heated to 60 °C before adding 10mM 2-beta-mercaptoethanol. Membranes were placed in the heated stripping buffer (30 minutes, 50 °C). Membranes were washed twice with washing buffer (TBS containing 0.1% Tween-

20), blocked with blocking buffer (5% dried milk in TBS containing 0.1% Tween-20) (1 hour, RT), and incubated with primary antibody overnight. Membranes were developed and analysed as per section 2.6.2.

## 2.7. Quantification of gene expression:

### 2.7.1. RNA extraction:

Ribonucleic acid (RNA) was extracted from cell lysates using RNeasy kits (Qiagen, Crawley, UK) according to manufacturer's instructions. Cell lysates were defrosted on ice before homogenisation with 21 G needle attached to 1 ml syringe. Samples were mixed with 70% ethanol at a ratio of 1:1 volume to facilitate RNA attachment to the columns' membrane. Samples were added to RNeasy spin columns and centrifuged (10000 RPM, 15 seconds) to help RNA bind to the silica-based membrane. Columns were washed using RW1 buffer to remove biomolecules such as carbohydrates, proteins, and fatty acids. To eliminate DNA contaminants, on column DNase digestion was applied using RNase-free DNase diluted in RDD buffer at 1:7 ratio (15 minutes, RT). DNase was removed by spinning the column with RW1 washing buffer (10000 RPM, 15 seconds). Columns were washed twice with RPE buffer (10000 RPM, 15 seconds then 2 minutes) and were placed in a new RNase-free Eppendorf, RNA was eluted by adding 50µl of RNase-free water to the column and centrifuged (10000 RPM, 1 minute). Resultant RNA was stored at -80 °C for future reverse transcription-polymerase chain reaction (RT-PCR).

### 2.7.2. Reverse transcription-polymerase chain reaction (RT-PCR) (cDNA synthesis):

RNA was quantified by the plate reader (POLARstar Omega, BMG LABTECH) at 260 nm. RNA purity from nucleotides and proteins was assessed by calculating the ratio of RNA absorbance at 260/280 nm; pure RNA has a ratio of 1.7-2.0. RNA

samples were diluted accordingly with molecular water (Sigma). This dilution step is to yield 50 ng/µl (for *in vitro* effect of NTHi on M1/M2 markers' experiment), or 12 ng/ µl (for sputum macrophage phenotype experiment) in the complementary DNA (cDNA) reaction mix. 12 ng/µl was the maximal RNA concentration that could be obtained from all sputum samples.

cDNA was synthesised by RT-PCR using the Verso™ 2-Step QRT-PCR kit (Thermo Scientific, Surry, UK) according to manufacturer's instruction. The cDNA reaction mix (20µl) is composed of Verso enzyme mix, cDNA synthesis buffer, dNTP mix, RNA primer (random hexamer) and RT enhancer. RNA was added to the reaction mix, and the amplification was facilitated using thermal cycler with reverse transcription cycling program specified by the manufacturer as shown in Table 2.10. Controls with no Verso enzyme and no template were included to exclude any DNA amplification. Synthesised cDNA was stored at -20 °C for future quantitative polymerase chain reaction (qPCR) analysis.

**Table 2.10: Reverse transcription cycling program**

| Step | Temperature | Time | Number of cycles |
|---|---|---|---|
| **cDNA synthesis** | 42 °C | 30 minutes | 1 cycle |
| **Inactivation** | 95 °C | 2 minutes | 1 cycle |

### 2.7.3. Quantitative polymerase chain reaction (qPCR)

cDNA was analysed for gene expression using Taqman qPCR. cDNA (1 μl) was used in 25 μl reaction mix. The reaction mix contains primer-probes for macrophage M1/M2 markers (TNF-α, CXCL8, HLA-DR, CD38, IL-10, CD14, CD163, CD206 (mannose receptor C1) and CD36), or the endogenous control glyceraldehyde-3-phosphate dehydrogenase (GAPDH) (Applied Biosystems, Warrington, UK), as listed in Table 2.11. Thermal cycling was carried out on a Stratagene MX3005P (Agilent Technologies, West Lothian, UK) according to manufacturer's recommendations as shown in Table 2.12. Relative levels of M1/M2 markers' mRNA in response to NTHi and LPS *in vitro* were determined using the $2^{-\Delta\Delta \text{ Cycle threshold}}$ ($2^{-\Delta\Delta Ct}$) method normalising to the endogenous control (GAPDH) and unstimulated levels [415,416]. Relative levels of M1/M2 markers' mRNA in sputum macropahges from NTHi-infected COPD and non-infected controls were assessed by $2^{-\Delta Ct}$ method normalising to GAPDH. Six-point efficiency curves were generated for each primer-probe set with using RNA extracted from untreated alveolar macrophages to confirm efficiencies were between 90-110%. However, due to practical reasons efficiency curves were not carried out on each sample run and therefore not used to correct for PCR efficiency, hence the use of $2^{-\Delta\Delta Ct}$ method and not Pfaffl method.

**Table 2.11: Primers used in qPCR for gene expression analysis with their reference numbers (Applied Biosystem)**

| Gene | Applied Biosystem reference number |
|---|---|
| GAPDH | Hs02758991_g1 |
| TNF-α | Hs99999043_m1 |
| CXCL8 | Hs00174103_m1 |
| CD38 | Hs01120071_m1 |
| HLA-DR | Hs00219575_m1 |
| IL-10 | Hs00961622_m1 |
| CD36 | Hs00354519_m1 |
| MRC1 (CD206) | Hs00267207_m1 |
| CD14 | Hs00169122_g1 |
| CD163 | Hs00174705_m1 |

**Table 2.12: qPCR thermal cycling program**

| Cycle | Temperature | Time | Number of cycles |
|---|---|---|---|
| Thermo-start activation | 95 °C | 15 minutes | 1 cycle |
| Denaturation | 95 °C | 15 seconds | 40 cycles |
| Annealing/Extension | 60 °C | 60 seconds | 40 cycles |

## 2.8. Glucocorticoid receptor translocation assay

Alveolar macrophages from a healthy non-smoker subject were cultured on chamber slides at $3x10^5$ cells per well. Cells were incubated overnight at 37 °C and 5% $CO_2$. The media were aspirated and replaced by serum-free media; the cells were reincubated overnight. Non-adherent cells were washed away, and the adherent cells were treated accordingly. The effect of NTHi on dexamethasone-induced GR translocation was studied by infecting the cells with NTHi (at 10:1 MOI) for 30 minutes, with or without dexamethasone pretreatment (at 1 μM) for 30 minutes.

The role of p38 MAPK pathway in GR nuclear translocation was next investigated. Cells were pretreated with p38 MAPK inhibitor (BIRB-796) (at 1 µM) for 30 minutes before adding NTHi (at 10:1 MOI), dexamethasone (at 1 µM), or NTHi and dexamethasone for another 30 minutes. Unstimulated basal control and NTHi-infected cells control were run alongside other conditions.

Cells were fixed with 4% paraformaldehyde (10 minutes, RT), and washed twice with PBS. Cells were incubated in 1.5% goat serum (Vector Laboratories Ltd, Peterborough, UK) in PBS (30 minutes, RT). Cells were incubated with primary antibody, purified mouse anti-glucocorticoid receptor clone 41 (BD Transduction Laboratories ™, Oxford, UK), diluted 1/200 in PBS containing 0.5% Triton-X overnight at 4 °C. Cells were washed twice with PBS and incubated with the secondary antibody, alexa 488 conjugated goat anti-mouse antibody (Life Technologies Ltd, Paisley, UK), diluted 1/200 in PBS for 90 minutes at 37 °C. Cells were then washed twice with PBS and mounted with Vectashield mounting medium with DAPI (Vector Laboratories Ltd). Alveolar macrophages were examined by fluorescence microscopy (Nikon Eclipse 80) equipped with the QImaging digital camera (Media Cybernetics). Four hundred cells were counted per condition, and GR localisation was categorised as either being all cytoplasmic, cytoplasmic and nuclear or nuclear. Images were digitally merged and analysed using Image Pro Plus 5.1 software. Representative images are shown in Figure 2.12.
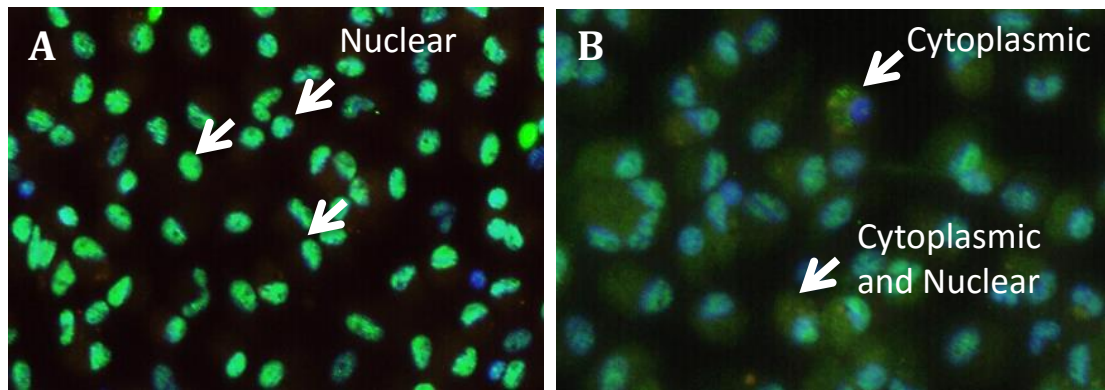
**Figure 2.12: Glucocorticoid receptors (GR) distribution:** GR were fluorescently stained and their cellular localisation was visualised by fluorescence microscopy. A: the majority of GR were localised inside the nucleus (nuclear). B: GR were either localised in the cytoplasm (cytoplasmic) or both in the cytoplasm and the nucleus (cytoplasmic and nuclear). Representative cells for each GR localisation state are pointed by arrows.

## 2.9. Statistical analysis:

Data were analysed using GraphPad instat version 3.06 (GraphPad Software, Inc., San Diego, CA, USA). Normality of data was assessed by Kolmogorov-Smirnov test.

Parametrically distributed paired data were analysed depending on the number of groups. Repeated measures ANOVA with Dunnett or Bonferroni multiple comparisons post-test were used to compare more than two groups. Paired t-test (two-tailed) was used to compare two groups of parametrically distributed data. Paired data, which were nonparametrically distributed, were compared either by Friedman test with Dunn multiple comparisons post-test (for more than two groups comparison) or by Wilcoxon matched-pairs signed-ranks test (two-tailed) (for two groups comparison).

Unpaired data which were parametrically distributed were compared using unpaired t-test (two-tailed). Unpaired data which were nonparametrically distributed were compared by Mann-Whitney test (two-tailed). $p < 0.05$ was considered significant, unless otherwise stated. Detailed statistics section was included in each chapter.

# Chapter Three

# NTHi Induced Cytokine Release in

# Human Alveolar Macrophages

## 3.1. Introduction:

NTHi has developed several mechanisms to evade host immunity and to persist in the lower airways. These mechanisms involve its ability to survive in the tissue (306) and inside epithelial cells and macrophages (297,417). Once established in the lower airways, NTHi will be in a continuous state of turnover releasing antigens such as LOS, peptidoglycan and cytoplasmic molecules, which will result in airway inflammation and tissue injury (375,418). In animal studies, exposure to NTHi lysate resulted in airway inflammation and structural changes similar to COPD (212).

Clinically, NTHi airway colonisation is linked to airway and systemic inflammation with a reduced quality of life (419). Moreover, a clinical study confined to ex-smokers, with and without COPD, showed that higher levels of IL-1$\beta$, CXCL8, MMP-9 and neutrophils in bronchoalveolar lavage (BAL) fluid were significantly associated with NTHi colonisation (208). These data support the hypothesis that NTHi colonisation causes an ongoing chronic inflammatory process. This may cause COPD disease progression independently of the effects of cigarette smoke (420).

Increased airway bacterial load and new strain acquisition are currently the proposed mechanisms of acute bacterial exacerbations (16,215) . Increased NTHi load in the lower airways caused significantly higher neutrophil count, IL-1$\beta$ and IL-12 in the sputum samples of stable COPD patients (421). Furthermore, NTHi colonisation was associated with more frequent and severe exacerbations (165).

Evidence from an *in vitro* study suggests a role for the interaction between NTHi antigens and blood monocyte-derived macrophages (MDMs) in the pathogenesis of tissue inflammation through provoking release of TNF-$\alpha$ and CXCL8

(228). Therefore, studying alveolar macrophage inflammatory response to NTHi or its antigens can help in understanding the pathogenesis of COPD exacerbation and airway colonisation. Also, it may help to test current and potential COPD therapies.

To date, *in vitro* models of inflammation in COPD widely use the Gram-negative bacterial cell wall component LPS (349,350,397). LPS is purified from *E. coli*, a less relevant bacterium in COPD. Therefore, more relevant *in vitro* models are required. Recent studies applied purified P6 (the outer membrane protein) and LOS (the endotoxin of NTHi), to stimulate human MDMs and BAL-derived macrophages (228,316). In addition, one study used live NTHi to investigate cytokine release in murine alveolar macrophages (133). However, using live whole NTHi to infect human alveolar macrophages would be more clinically relevant.

The aim of this chapter is to study human alveolar macrophage inflammatory responses to clinical isolates of NTHi, in order to characterise this relevant *in vitro* model of infection.

### 3.2. Materials and Methods:

### 3.2.1. Study subjects:

Twenty-six patients undergoing lung resection surgery for suspected or confirmed lung cancer were recruited for different experiments (see Table 3.1 for detailed demographics). Samples from subgroups of these patients were used for individual experiments, with numbers described in figure legends. Details of patients involved in each experiment are available in Table 3.2. Patients were categorised as either COPD (according to GOLD criteria) (38) or smokers with normal lung function. Both groups included current and ex-smokers. Written informed consents were obtained from all patients and the research was approved by South Manchester Research Ethics Committee.

**Table 3.1: Patients' demographic data.**

| Criteria | COPD | Smokers |
|---|---|---|
| **Smoking history (Current/Ex)** | (10/3) | (8/5) |
| **Gender (male/female)** | (7/6) | (8/5) |
| **Age (years)** | 69.2±5 | 67±6 |
| **FEV1 (L)** | 1.7±0.6 | 2.4±0.5 |
| **FEV1% predicted** | 67.4±16.5 | 94.5±16.2 |
| **FVC (L)** | 2.9±0.7 | 3.3± 1.0 |
| **FEV1/FVC ratio (%)** | 60.3±10.4 | 72.8±11.5 |
| **Pack-year history** | 52.6±10.6 | 38.5±19.1 |

Data are presented as mean±SD. FEV1= Forced expiratory volume in 1 second, FVC= Forced vital capacity, L= Litre.

**Table 3.2: Patients' categorisation per experiments.**

| Experiment | COPD | Smokers | Total |
|---|---|---|---|
| Effects of *E. coli*, NTHi and LPS on TNF-α release from human alveolar macrophages | 1 | 3 | 4 |
| NTHi-induced cytokine release in alveolar macrophages | 4 | 7 | 11 |
| Effect of NTHi on alveolar macrophage viability in the model | 1 | 2 | 3 |
| NTHi survival in the *in vitro* model | 2 | 2 | 4 |
| Alveolar macrophage inflammatory response to NTHi clinical isolates from COPD patients | 5 | 1 | 6 |

### 3.2.2. Alveolar macrophage TNF-α release in response to live *E. coli* and NTHi:

In this chapter, I investigated the time course of alveolar macrophage inflammatory response to NTHi and the effect of different bacterial concentrations regardless of the disease state. For practical reasons, I used mixed populations of COPD patients and smokers with normal lung function for statistical power. The issue of differences between COPD and controls is dealt with later in the thesis.

Preliminary experiments were carried out to assess the response of alveolar macrophages to live bacteria. Two types of bacteria, *E. coli* and NTHi, were used as stimuli for TNF-α release.

### 3.2.2.1. Alveolar macrophage culture:

Alveolar macrophages were isolated from resected lung tissue of COPD and smokers and were plated on 96 well culture plates at a concentration of $1x10^5$ cells per well. Cells were incubated overnight at 37 °C and 5% $CO_2$, non-adherent cells were washed with RPMI 1640 without antibiotics, and fresh media was added at 180 µl per well.

### 3.2.2.2. Bacterial preparation:

NTHi (R2846) and *E. coli* (ATCC 11775/ NCTC 9001) suspensions were prepared and set to $1.2 \pm 0.02$ OD$_{600}$ as detailed in methods chapter in section 2.2.1. From each bacterial suspension, five tenfold serial dilutions (1/10-1/100000) were prepared in supplemented RPMI 1640. Each bacterial dilution was used to infect alveolar macrophages. Bacterial count was verified each time by Miles- Misra plate counting as detailed in methods chapter in section 2.2.2.

### 3.2.2.3. Infection of alveolar macrophages with live bacteria:

Alveolar macrophages in triplicates were infected with either *E. coli* or NTHi at five different bacterial dilutions. 20 µl of each bacterial dilution was added to each well. LPS at 1µg/ml was used as a positive control of stimulation. After 2, 6 and 24 hours of infection, cell culture plates were spun and the supernatants were aspirated for TNF-α measurement by ELISA according to manufacturers' instruction, as detailed in materials and methods chapter in section 2.5.

### 3.2.2.4. Preliminary monitoring of bacterial survival in the culture plate:

To estimate bacterial survival in the culture over the duration of the experiment, bacterial counts were performed at 0 hours and 24 hours of infection. 10 µl from each well were aspirated and Miles-Misra plate counting was performed, the bacterial count was expressed as CFU/ml.

### 3.2.3. NTHi induced cytokine release in alveolar macrophages

In order to express bacterial concentration in a microbiologically convenient way, I used bacterial calculations different from the calculation I used in section 3.2.2, as detailed in materials and methods chapter in section 2.2.3. NTHi load was calculated per alveolar macrophage, which is known as MOI. Alveolar macrophages in triplicates were infected with 20 µl of a different bacterial concentration to set a

range of MOI (1:1, 3:1, 10:1, 30:1, 100:1, 300:1 and 1000:1). LPS at 1µg/ml was used as a positive control of stimulation. Cells were incubated at 37 °C and 5% $CO_2$ for 24 hours. Supernatants were aspirated at 2, 6 and 24 hours of infection, and analysed for TNF-α, IL-6, CXCL8 and IL-10 by ELISA according to manufacturers' instruction as detailed in materials and methods chapter in section 2.5.

### 3.2.4. Cell viability assessment by Transferase dUTP Nick End Labeling (TUNEL) assay:

Alveolar macrophages were cultured on chamber slides at $1x10^5$ cells per chamber, and infected with NTHi at MOI of 10:1, 100:1, 1000:1 and 4000:1 for 24 hours. Triton-X (0.1%) was used as a positive control of apoptosis. After overnight culture, cells were fixed and stained with TUNEL mix as detailed in materials and methods chapter in section 2.4. Immunofluorescence was detected and 400 cells per condition were counted. The percentages of TUNEL positive (apoptotic) cells were calculated and compared to unstimulated cells.

### 3.2.5. NTHi survival in the model:

In order to have more detailed monitoring of NTHi survival extracellularly and intracellularly in the model, I amended the technique mentioned in section 3.2.2.4. Alveolar macrophages were plated on 4 wells of 24 well plates at $4 \times 10^5$ cells per well, NTHi was added to each well at 10:1 MOI for 24 hours. The extracellular and intracellular viable bacterial count per well was measured at 0, 2, 6 and 24 hours of infection. Extracellular counts were performed by aspirating all media from the well at each time point, washing the cells twice with sterile PBS and collecting the wash fluid to get all the extracellular bacteria in one vial. Bacterial count in the collected fluid was quantified by Miles-Misra plate counting method.

Intracellular bacterial counts at each time point were performed by lysing the cells with sterile deionised water for 20 minutes at 37 °C and 5% $CO_2$. Cell lysates were collected and the wells were washed twice with PBS and added to the lysate. The collected fluid was plated for the intracellular bacterial count. Extracellular and intracellular NTHi counts were expressed as CFU per well. These counts were added to give the total viable NTHi per well.

### 3.2.6. Isolation of NTHi from sputum samples of stable COPD:

NTHi clinical isolates were recovered from sputum samples of stable COPD patients. NTHi was identified by the colonial morphology and the X-V test. Clinical isolates biotypes were identified by applying urease, indole and Ornithine decarboxylase tests. Furthermore, antibiotic sensitivity test was performed for further characterisation of the isolates. The details of the bacteriological test were mentioned in materials and methods chapter in section 2.3.

### 3.2.7. Alveolar macrophage inflammatory response to NTHi clinical isolates:

Alveolar macrophages were plated on 96 well culture plates at $1x10^5$ cells per well. NTHi clinical isolates were grown from frozen stocks and processed as detailed in methods chapter. Alveolar macrophages were infected in triplicates with each NTHi isolate and with NTHi R2846 at 10:1 and 100:1 MOI. Culture supernatants were aspirated after 2, 6 and 24 hours of infection and analysed for TNF-α, CXCL8, IL-6 and IL-10 by ELISA according to manufacturers' instruction.

### 3.2.8. Statistics:

Normality of data was assessed by Kolmogorov-Smirnov test. The initial data of TNF-α release by NTHi, *E. coli* and LPS were nonparametrically distributed. Friedman test with Dunn's multiple comparisons test was performed to compare NTHi and *E. coli*-induced TNF-α level versus time-matched unstimulated control.

Wilcoxon matched-pairs signed-ranks test (two-tailed) was used to compare LPS-induced TNF-α levels versus time-matched unstimulated control. TNF-α induced by *E. coli* was compared to TNF-α induced by NTHi at each time point using Wilcoxon matched-pairs signed-ranks test (two-tailed).

In the subsequent experiment, NTHi and LPS-induced TNF-α, IL-6, CXCL8 and IL-10 data were parametrically distributed. For NTHi model, at all MOIs, cytokines' levels were compared to time-matched unstimulated control using repeated measures ANOVA with Dunnett multiple comparisons test. Comparisons between different MOIs were performed by Bonferroni multiple comparisons test. Two-way ANOVA was performed to compare cytokines levels at each time point (2, 6 and 24 hours) for all MOIs. Cytokines induced by NTHi clinical isolates were compared to cytokines induced by NTHi (R2846) using Dunnett multiple comparisons test.

For LPS model, cytokines' levels were compared to time-matched unstimulated control using paired t-test (two-tailed). Comparison of LPS-induced cytokines at 2, 6 and 24 hours was performed by repeated measures ANOVA with Bonferroni multiple comparisons test.

Data of alveolar macrophage apoptosis and NTHi survival were nonparametrically distributed. The percentages of apoptotic cells for each condition were compared to unstimulated control and intracellular and extracellular bacterial counts for each condition were compared to 0 hours control using Friedman test with Dunn's multiple comparisons test. For all comparisons $p < 0.05$ was considered statistically significant.

### 3.3. Results:

### 3.3.1. Effects of E. coli, NTHi and LPS on TNF-α release from human alveolar macrophages:

I conducted an initial pilot experiment to investigate the inflammatory response of alveolar macrophages to live *E. coli* and live NTHi. LPS stimulation, which is a well-established model of cell stimulation, was used as a positive control for the purpose of comparison. Alveolar macrophages from 4 subjects (3 smokers and 1 COPD) were cultured with either NTHi or *E. coli,* each at tenfold serial dilutions (1/10- 1/100000) of the 1.2 $OD_{600}$ bacterial stock, LPS (1μg/ml) or left unstimulated for 2, 6 and 24 hours.

*E. coli* at the lowest dilutions (1/100 and 1/10) caused significantly greater TNF-α release compared to time-matched unstimulated control after 2 hours (p<0.05, Figure 3.1 A). However, higher *E. coli* dilutions (1/100000- 1/1000) significantly induced TNF-α above time-matched unstimulated control after 6 and 24 hours of culture (p<0.05).

After 2 hours, NTHi at the lowest dilution (1/10) caused significantly greater TNF-α release than time-matched unstimulated control (p<0.05, Figure 3.1B). NTHi (at 1/1000- 1/10 dilutions) caused significantly greater release of TNF-α than time-matched unstimulated control at 6 and 24 hours (p<0.05).

LPS-inducedTNF-α was not different from time-matched unstimulated controls (Figure 3.1 A and B).

NTHi-induced TNF-α was not different from *E. coli*-induced TNF-α at all-time points.
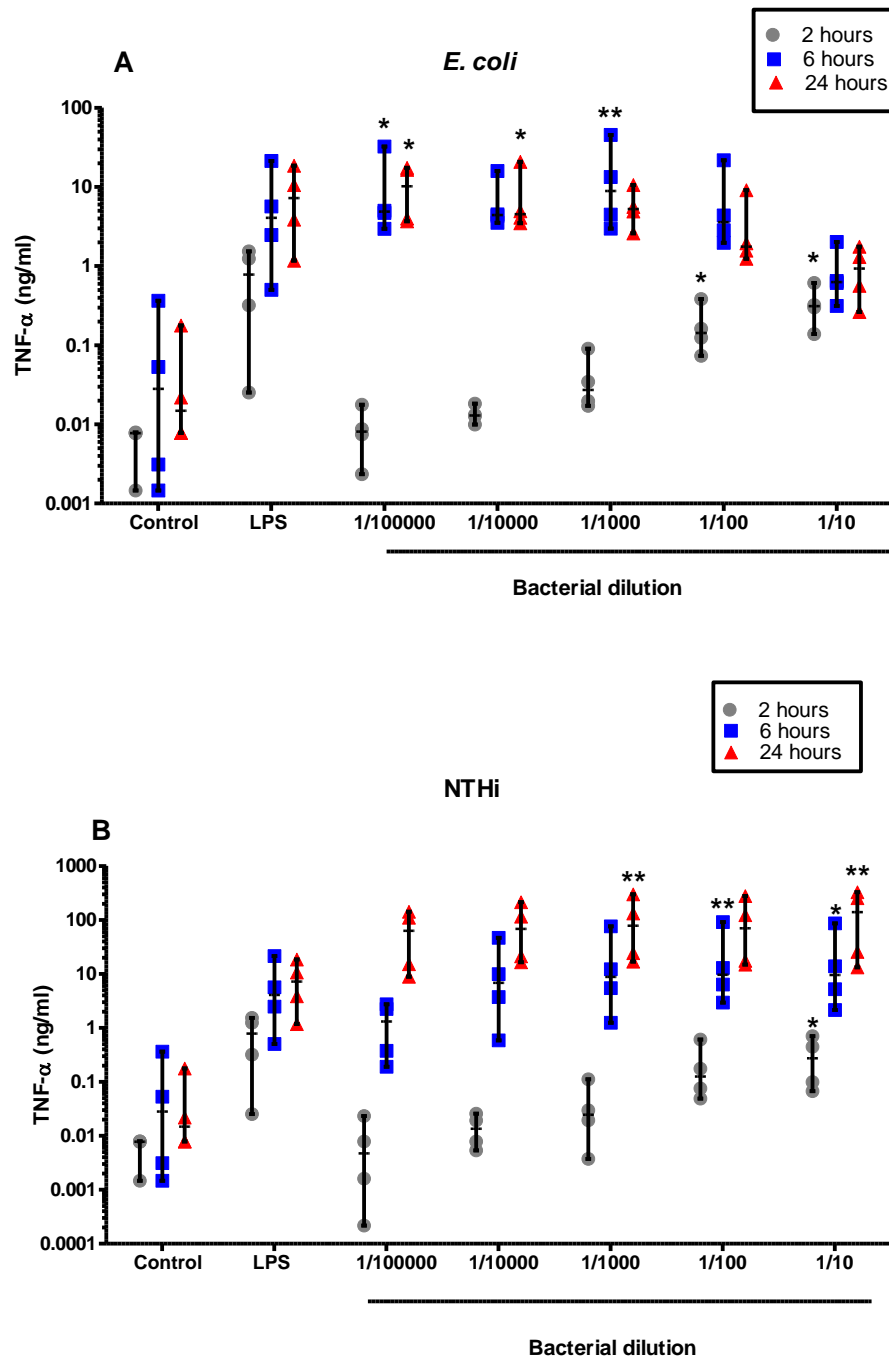
**Figure 3.1:** **Effects of *E. coli*, NTHi and LPS on TNF-α release from human alveolar macrophages.** Alveolar macrophages from 4 subjects (3 smokers and 1 COPD) were cultured with either LPS (1μg/ml), live *E. coli* (A) or live NTHi (B) both at five tenfold serial dilutions. Supernatants were recovered after 2, 6 and 24 hours of culture and analysed for TNF-α by ELISA. Data show individual subjects with median value represented as horizontal line and total range by error bars. *, ** represent significantly greater NTHi or *E. coli*-induced TNF-α than time-matched unstimulated control (p<0.05, <0.01 respectively, Friedman test followed by Dunn's multiple comparisons test).

### 3.3.2. *E. coli* and NTHi survival in the model:

Viable *E. coli* and NTHi counts were measured initially and after 24 hours by Miles-Misra plate counting (Table 3.3). Each count represents the average of 2 separate experiments. *E. coli* count after 24 hours was much higher than the initial bacterial input. In contrast, NTHi count was reduced over the 24 hours. Due to the continuous uncontrolled growth of *E. coli* in the culture, which might affect alveolar macrophage viability, I decided not to use *E. coli* in my further experiments.

**Table 3.3: *E. coli* and NTHi survival in the model.**

| Bacterial dilution from 1.2 $OD_{600}$ stock | Live *E. coli* (CFU/ml) | | Live NTHi (CFU/ml) | |
|---|---|---|---|---|
| | 0 hours | 24 hours | 0 hours | 24 hours |
| 1/100000 | $0.1525 \times 10^6$ | $2075 \times 10^6$ | $0.103 \times 10^6$ | $0.06 \times 10^6$ |
| 1/10000 | $0.113 \times 10^6$ | $53000 \times 10^6$ | $0.63 \times 10^6$ | $0.93 \times 10^6$ |
| 1/1000 | $1.8 \times 10^6$ | $97900 \times 10^6$ | $3.2 \times 10^6$ | $1.47 \times 10^6$ |
| 1/100 | $12.15 \times 10^6$ | $22733.35 \times 10^6$ | $33.7 \times 10^6$ | $3.17 \times 10^6$ |
| 1/10 | $125 \times 10^6$ | $68433.35 \times 10^6$ | $300 \times 10^6$ | $66.67 \times 10^6$ |

### 3.3.3. NTHi-induced inflammatory response in alveolar macrophages

Alveolar macrophages from 11 subjects (7 smokers and 4 COPD) were infected with live NTHi (R2846) for 24 hours. From this experiment on, NTHi concentration was set as MOIs, as this is a conventional way of standardising experiments. A range of 1:1-1000:1 MOI (NTHi: alveolar macrophage) was used. Culture supernatants were aspirated at 2, 6 and 24 hours of infection for TNF-α, IL-6, CXCL8 and IL-10 analysis by ELISA. LPS (1μg/ml) was used as a positive control of stimulation.

NTHi induced significantly greater release of TNF-α, IL-6, CXCL8 and IL-10 from alveolar macrophages compared to time-matched unstimulated controls (p<0.05 for all comparisons, Figure 3.2 A-D). After 2 hours of infection, NTHi caused significantly greater release of TNF-α (at 10:1-1000:1 MOI), IL-6 (at 100:1 MOI) and CXCL8 (at 100:1-1000:1) compared to time-matched unstimulated controls (p<0.05 for all comparisons, Figure 3.2 A-C). At 6 hours, there was a significantly greater release of TNF-α, IL-6 and CXCL8 at 3:1-1000:1 MOI than time-matched unstimulated controls (p<0.05 for all comparisons). After 24 hours all MOIs (1:1-1000:1) induced significantly greater TNF-α, IL-6 and CXCL8 release compared to unstimulated controls (p<0.05 for all comparisons, Figure 3.2 A-C). The NTHi-induced release of TNF-α, IL-6 and CXCL8 was time-dependent. Cytokine levels observed at 24 hours of infection were significantly greater than MOI-matched levels at 2 and 6 hours (p<0.01 for all comparisons).

The levels of TNF-α, IL-6 and CXCL8 induced by all MOIs at 24 hours were not significantly different from each other.

NTHi caused no change from unstimulated IL-10 release after 2 hours (Figure 3.2 D). However, after 6 hours, a significant release of IL-10 was reported at all MOIs (1:1-1000:1) (p<0.05 for all MOIs versus time-matched unstimulated control). A

significant increase from unstimulated control was observed after 24 hours by NTHi (at 1:1-100:1 MOI) (p<0.05 for all MOIs). IL-10 levels induced by all MOIs after 24 hours were significantly higher than MOI-matched levels at 2 and 6 hours (p<0.01 for all comparisons). Of note, IL-10 release by higher MOIs (300:1 and 1000:1) at 24 hours was not different from time-matched unstimulated control. Also, these levels were significantly lower than levels induced by lower MOIs (1:1-30:1) (p<0.05 for all intergroup comparisons).

Cytokine release was mostly similar in COPD and smokers, although with only 4 COPD patients the sample size was too small for statistical analysis (Appendix 1).

LPS caused a significant time-dependent release of TNF-α, IL-6, CXCL8 and IL-10 (p<0.05 versus time-matched unstimulated control), with maximal stimulation at 24 hours (p<0.05 versus 2 and 6 hours' levels, Figure 3.2 A-D).

For this experiment, data are presented as bar chart versus dot plot in Figure 3.1. This difference in presentation is due to higher sample size in this experiment (N=11 versus N=4 for Figure 3.1). Thus, data in Figure 3.2 are parametrically distributed. Meanwhile, data are nonparametrically distributed in Figure 3.1.

**A**

TNF-α (ng/ml)

2 hours
6 hours
24 hours

Control LPS   1:1   3:1   10:1   30:1   100:1   300:1   1000:1

**Multiplicity of infection**

**B**

IL-6 (ng/ml)

Control LPS   1:1   3:1   10:1   30:1   100:1   300:1   1000:1

**Multiplicity of infection**

**C**

CXCL8(ng/ml)

Control LPS   1:1   3:1   10:1   30:1   100:1   300:1   1000:1

**Multiplicity of infection**

151
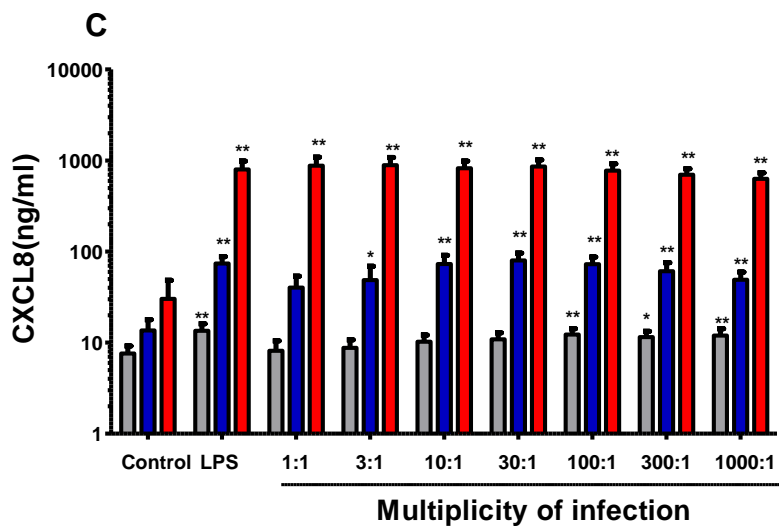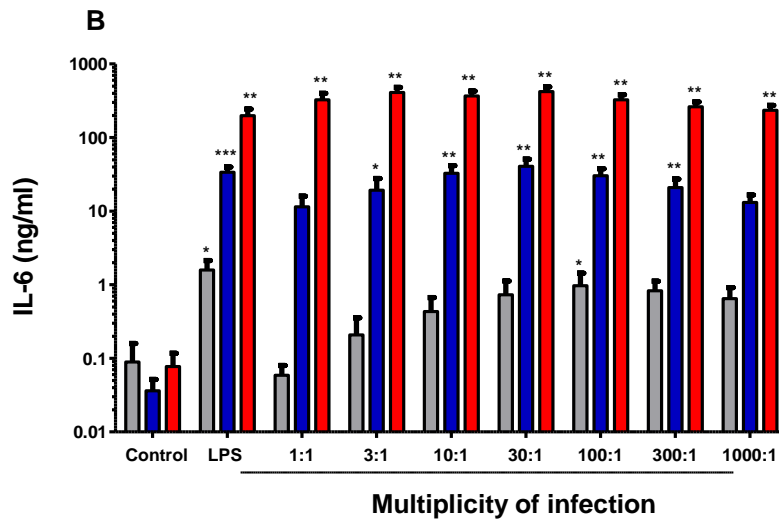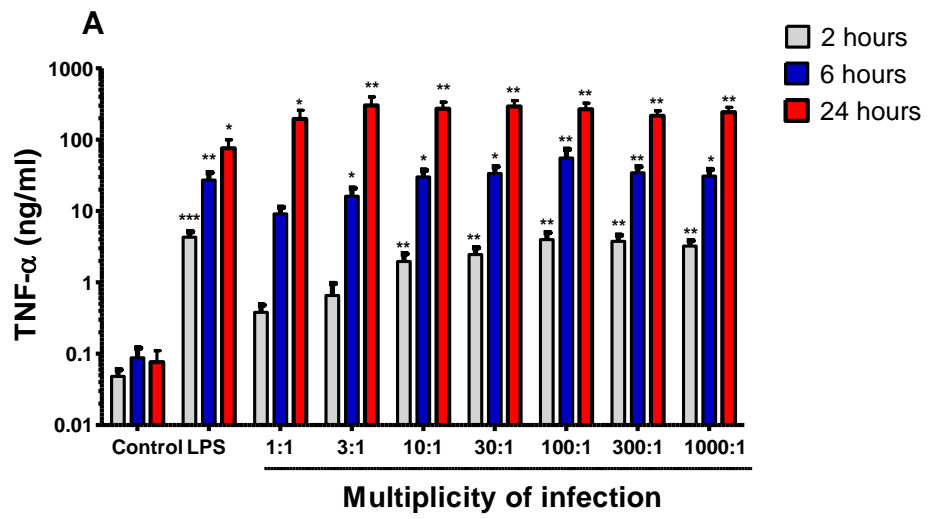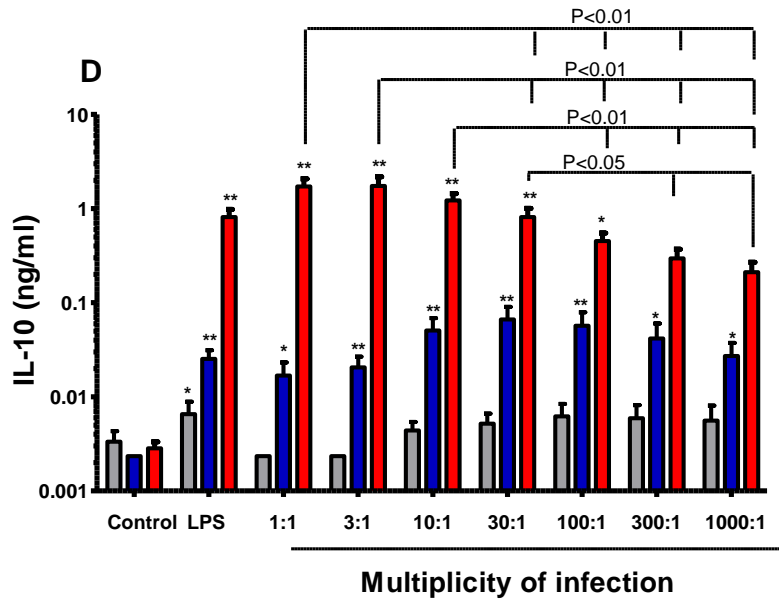
**Figure 3.2: NTHi provokes cytokine release from alveolar macrophages.** Alveolar macrophages from 11 subjects (7 smokers and 4 COPD) were either infected with live NTHi (R2846), at MOI of 1:1-1000:1, or stimulated with LPS (1µg/ml). TNF-α (A), IL-6 (B), CXCL8 (C) and IL-10 (D) release was measured by ELISA at 2, 6 and 24 hours of infection. The levels after NTHi infection were compared to unstimulated time-matched control. Data are presented as mean+SEM. *, ** represent significantly greater than time-matched unstimulated control (p<0.05, 0.01 respectively, either Repeated measures ANOVA followed by Dunnett multiple comparisons test (for NTHi) or paired t-test (for LPS). The difference between MOIs is shown above the corresponding bars (Bonferroni multiple comparisons test).

### 3.3.4. Effect of live NTHi on alveolar macrophage viability in the model:

Alveolar macrophages from 3 subjects (1 smoker and 2 COPD patients) were incubated for 24 hours either with media, live NTHi (at MOI of 10:1, 100:1, 1000:1, and 4000:1) or with Triton-X (0.1%) as a positive cell death control. The percentage of apoptotic cells was 4% in unstimulated cells. Triton-X caused significant (100%) cell apoptosis after 24 hours ($p < 0.05$ versus unstimulated control), however NTHi at 10, 100, 1000 and 4000:1 MOI caused 2%, 7%, 2.5% and 4.5% cell apoptosis respectively, which were not different from the unstimulated cells (Figures 3.3).
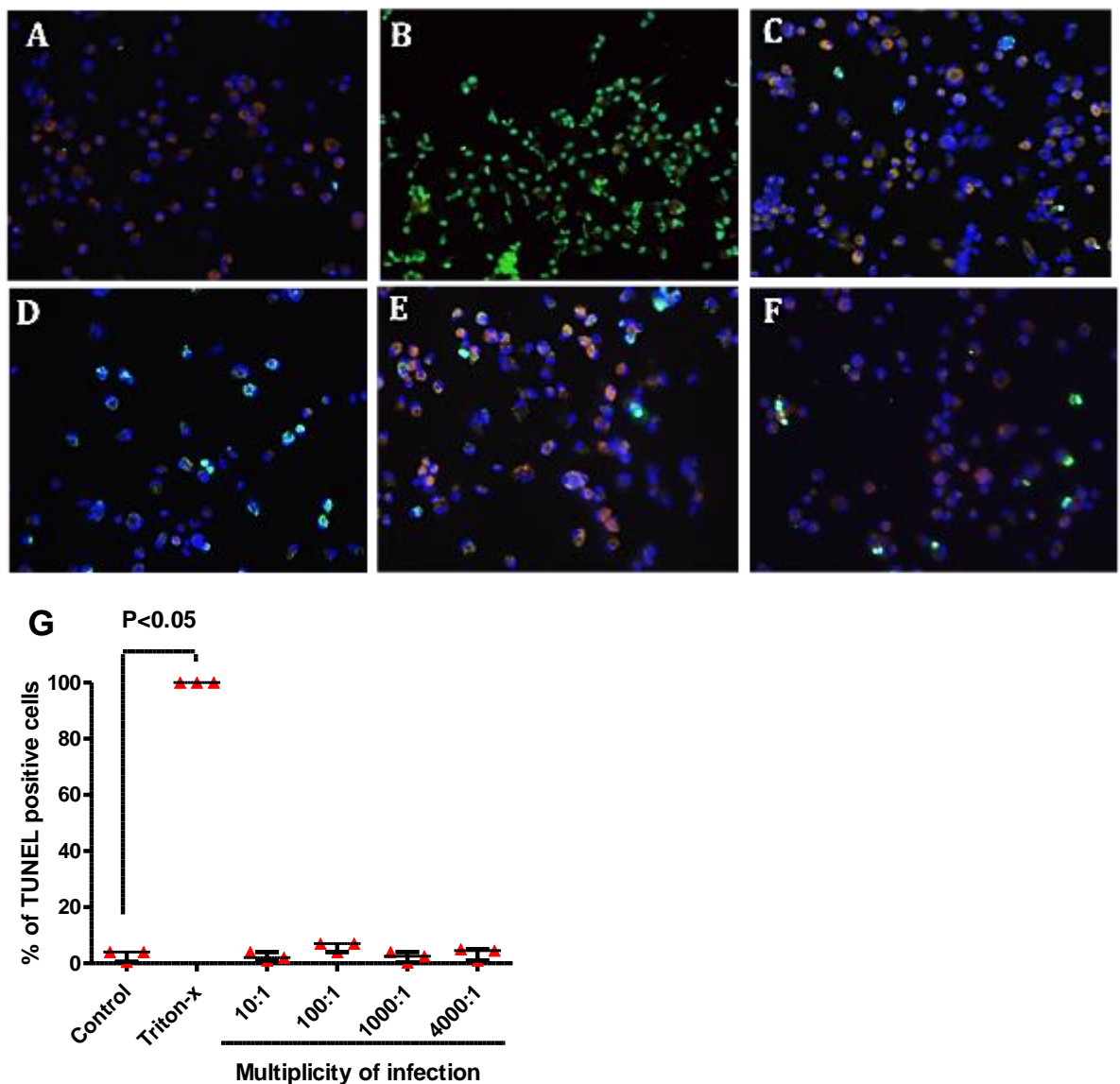
**Figure 3.3: Effect of NTHi infection on alveolar macrophage viability in the model.** Alveolar macrophages from 3 subjects (1 smoker and 2 COPD) were cultured on chamber slides (A) and treated with either Triton-X (0.1%) (B), live NTHi at 10:1 (C), 100:1 (D), 1000:1 (E) and 4000:1 (F) MOIs for 24 hours. Cells were stained with TUNEL stain and nuclei were counterstained with 4', 6-diamidino-2-phenylindole. The apoptotic cells (with green nuclei) were counted and the percentages of apoptotic cells from total cells per condition were calculated. The percentage of apoptotic cells for all conditions are presented in (G), data show individual subjects with median value represented as horizontal line and total range by error bars. Statistical significance is shown above corresponding bars (Friedman test with Dunn's multiple comparisons test). The pictures are representative of three different experiments. Magnification power is 20X.

### 3.3.5. NTHi survival in the *in vitro* model:

In this experiment, I sought to assess bacterial survival further in the model at three different time points, both extracellularly and intracellularly. Alveolar macrophages from 4 subjects (2 smokers and 2 COPD patients) were cultured and infected with live NTHi (R2846). Bacterial viability was checked at 0, 2, 6 and 24 hours of infection both extracellularly and intracellularly by Miles-Misra plate counting, as detailed in section 3.2.5.

The median initial NTHi count per well was $1.2 \times 10^6$ CFU (total range, 0.72-1.6 $\times 10^6$). This count was considered as 100% NTHi input at 0 hours or initial count. After 2 hours, the extracellular NTHi count was reduced to $0.65 \times 10^6$ CFU per well (total range, 0.5-0.8 $\times 10^6$) which equates to 54% of the initial count. At 6 hours, the bacterial count was $1.1 \times 10^6$ CFU per well (total range, 0.4-1.97 $\times 10^6$) or 92% of the initial bacterial count. After 24 hours, bacterial count decreased to $0.65 \times 10^6$ CFU per well (total range, 0.4-0.9 $\times 10^6$) or 54% of the initial input. However, at all-time points, the extracellular bacterial count was not different from the initial count per well (Figure 3.4 A, Table 3.4).

Active internalisation of NTHi was reported in the model. The initial intracellular count was $0.0001 \times 10^6$ CFU per well (total range, 0.0001-0.0002 $\times 10^6$) which equates to 0.008% of the initial count. The viable intracellular NTHi count increased after 2 and 6 hours of infection to $0.13 \times 10^6$ and $0.133 \times 10^6$ CFU per well respectively (total range, 0.05-0.26 $\times 10^6$ and 0.11-0.55 $\times 10^6$ respectively), which equates to 10.8% and 11.1% of the initial bacterial count per well respectively. This increase at 2 and 6 hours was significantly greater than the initial intracellular count at 0 hours ($p < 0.05$, $p < 0.01$ respectively). NTHi intracellular viability decreased after 24 hours to $0.007 \times 10^6$ CFU per well (total range, 0.0002-0.02 $\times 10^6$) or 1% of the

initial bacterial count, which was not different from the initial intracellular count (Figure 3.4 B, Table 3.4).



**A**

**Extracellular viable NTHi count**

**B**    **Intracellular viable NTHi count**
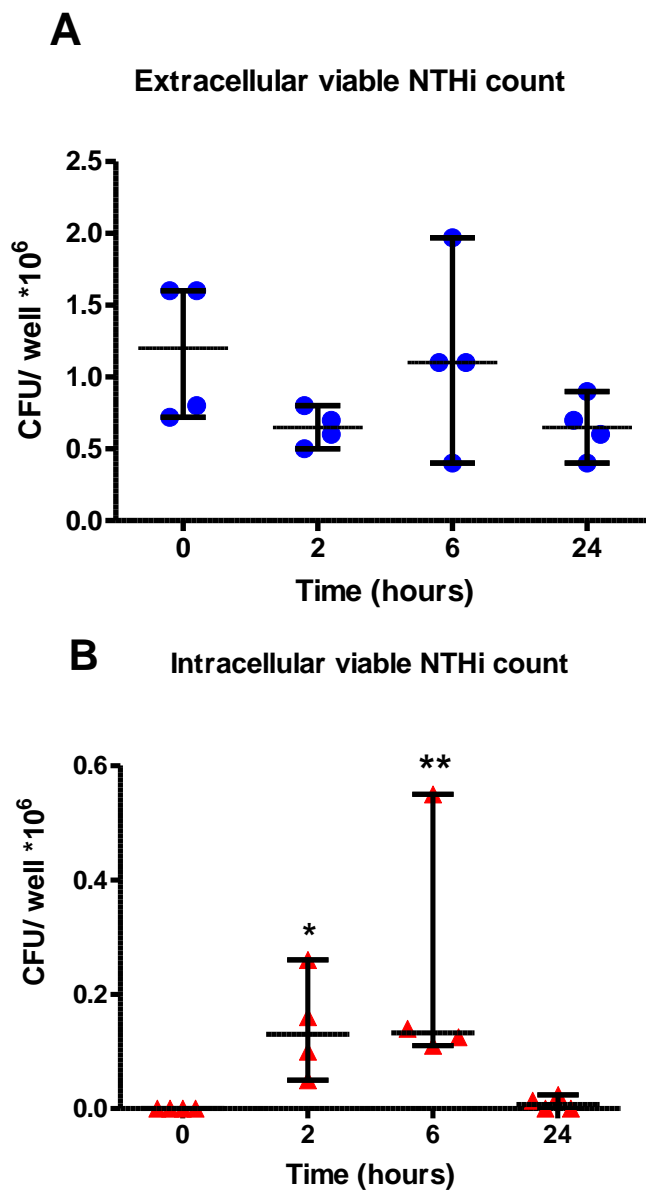
**Figure 3.4: NTHi survival in the *in vitro* model:** Alveolar macrophages from 4 subjects (2 smokers and 2 COPD) were infected with NTHi (R2846). At 0, 2, 6 and 24 hours of infection, the extracellular media and cell lysates were plated on chocolate agar plates for viable bacterial counting. The extracellular (A) and intracellular (B) viable NTHi counts per well were calculated and compared to the count at 0 hours. Data show individual subjects with median value represented as horizontal line and total range by error bars. *, ** represent significantly greater than 0 hours (initial) intracellular control ($p < 0.05$, $p < 0.01$ respectively, Friedman test followed by Dunn's multiple comparisons test).

**Table 3.4:** **Absolute count and percentage of viable NTHi in the *in vitro* model**

| Time (hours) | Extracellular/well | | Intracellular/well | | Total count/well | |
|---|---|---|---|---|---|---|
| | CFUx10$^6$ | % | CFUx10$^6$ | % | CFUx10$^6$ | % |
| **0** **(Initial)** | 1.2 (0.72-1.6) | 100% | 0.0001 (0.0001-0.0002) | 0.008% | 1.2 (0.72-1.6) | 100% |
| **2** | 0.65 (0.5-0.8) | 54.0% | 0.13 (0.05-0.26) * | 10.8% | 0.78 (0.55-1.06) | 64.8% |
| **6** | 1.1 (0.4-1.97) | 92.0% | 0.133 (0.11-0.55) ** | 11.1% | 1.233 (0.51-2.52) | 103.1% |
| **24** | 0.65 (0.4-0.9) | 54.0% | 0.007 (0.0002-0.02) | 1.00% | 0.657 (0.4-0.92) | 55.0% |

Data are presented as median (range), *, ** represent significantly greater than the initial intracellular NTHi count per well (p<0.05, p<0.01 respectively)

### 3.3.6. Isolation and biotyping of NTHi from sputum samples of stable COPD patients

Four NTHi clinical strains were isolated from induced sputum of 11 stable COPD patients. NTHi was diagnosed depending on colonial morphology and bacterial tests. Clinical isolates were described depending on the biotyping and antibiogram tests. NTHi (R2846) was also tested.

NTHi (R2846) and isolate 3 were biotype III. Meanwhile, isolates 1, 2 and 4 were all biotype II (Table 3.5).

NTHi (R2846) was sensitive to all tested antibiotics. Isolates 1 and 2 showed sensitivity to all antibiotic groups, but not the penicillin group. Isolate 3 showed resistances to penicillins and trimethoprim-sulfamethoxazole. Isolate 4 was resistant to ampicillin and trimethoprim-sulfamethoxazole (Table 3.6).

**Table 3.5:** **NTHi clinical isolates biotypes.**

| Bacterial isolate | Urease | Indole | Ornithine | Biotype |
|---|---|---|---|---|
| NTHi (R2846) | + | - | - | III |
| Isolate 1 | + | + | - | II |
| Isolate 2 | + | + | - | II |
| Isolate 3 | + | - | - | III |
| Isolate 4 | + | + | - | II |

**Table 3.6: Antibiotic sensitivity of NTHi clinical isolates.** R=resistance, S=sensitive, I=intermediate.

| Antimicrobial agent | NTHi (R2846) | Isolate 1 | Isolate 2 | Isolate 3 | Isolate 4 |
|---|---|---|---|---|---|
| **Penicillins** | | | | | |
| **Amoxicillin** | S | R | R | R | S |
| **Ampicillin** | S | R | R | R | R |
| **Amoxicillin-clavulanic acid** | S | R | R | R | S |
| **Cephalosporins** | | | | | |
| **Cefaclor** | S | S | S | S | S |
| **Cefotaxime** | S | S | S | S | S |
| **Ceftriaxone** | S | S | S | S | S |
| **Ceftazidime** | S | S | S | S | S |
| **Carbapenems** | | | | | |
| **Imipenem** | S | S | S | S | S |
| **Macrolides** | | | | | |
| **Azithromycin** | S | S | S | S | S |
| **Erythromycin** | S | S | S | S | S |
| **Clarithromycin** | S | S | S | S | S |
| **Quinolones** | | | | | |
| **Moxifloxacin** | S | S | S | S | S |
| **Ciprofloxacin** | S | S | S | S | S |
| **Levofloxacin** | S | S | S | S | S |
| **Tetracyclines** | | | | | |
| **Tetracyclin** | S | S | S | S | S |
| **Miscellaneous** | | | | | |
| **Chloramphenicol** | S | S | S | S | S |
| **Trimethoprim-Sulfamethoxazole** | S | S | S | R | R |

### 3.3.7. Alveolar macrophage inflammatory response to NTHi clinical isolates:

Each NTHi isolate was used to stimulate alveolar macrophages from 6 subjects (1 smoker and 5 COPD patients). Based on my previous experiment on NTHi (R2846), I decided to choose two MOIs which caused a significant submaximal TNF-$\alpha$, IL-6, CXCL8 and IL-10 release, which are 10:1 and 100:1MOI. Culture supernatants were aspirated at 2, 6 and 24 hours of infection and analysed for the TNF-$\alpha$, CXCL8, IL-6 and IL-10 release by ELISA. The previously studied NTHi (R2846) was run alongside the clinical isolates for further comparison.

All clinical isolates and NTHi (R2846) stimulated alveolar macrophages to release the inflammatory mediators in a time-dependent manner. The highest levels were detected after 24 hours (Figure 3.5). At 2, 6 and 24 hours, most NTHi clinical isolates as well as NTHi (R2846) caused a significantly greater release of TNF-$\alpha$, IL-6 and CXCL8 compared to time-matched unstimulated controls at both MOIs ($p < 0.05$, Figure 3.5 A-C). There was no difference between clinical isolates and NTHi (R2846) for TNF-$\alpha$, IL-6 and CXCL8 release.

IL-10 release after 2 hours was not induced by clinical isolates or NTHi (R2846) at both MOIs. At 6 hours and 24 hours, most clinical isolates and NTHi (R2846) provoked a significant IL-10 release at both MOIs ($p < 0.05$ versus time-matched unstimulated control). IL-10 release by isolate 4, at both MOIs, was not different from time-matched unstimulated control at 24 hours (Figure 3.5 D). Also, only isolate 4 caused significantly lower IL-10 release than NTHi (R2846) at 24 hours ($p < 0.05$).
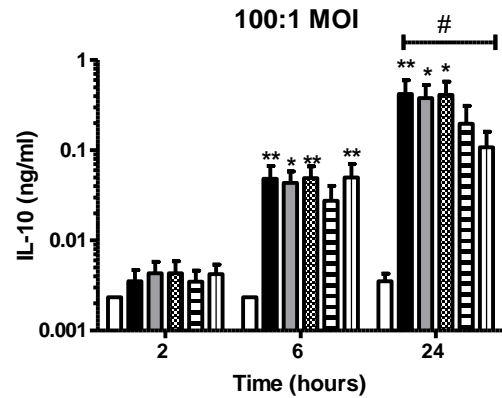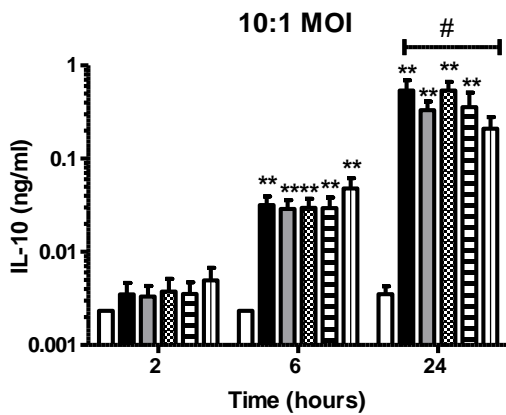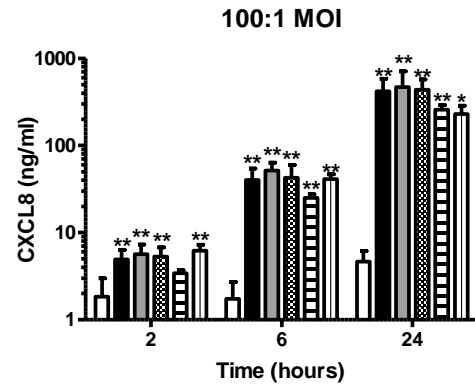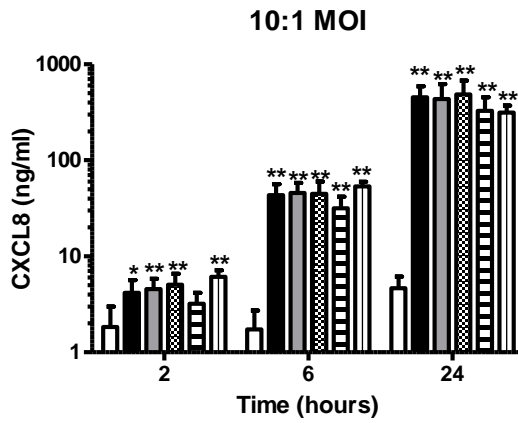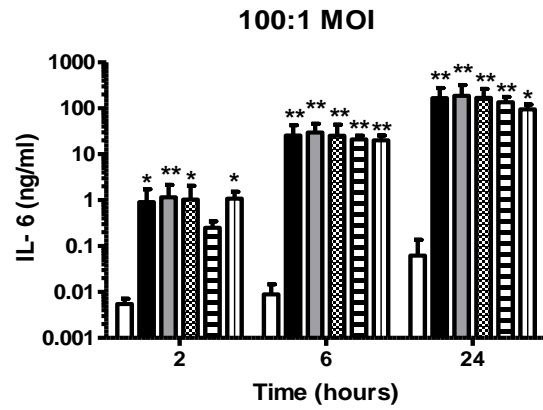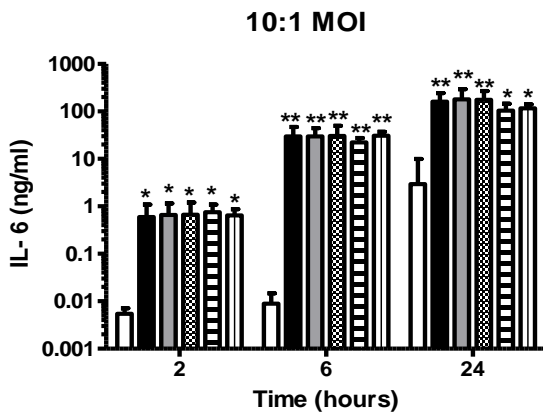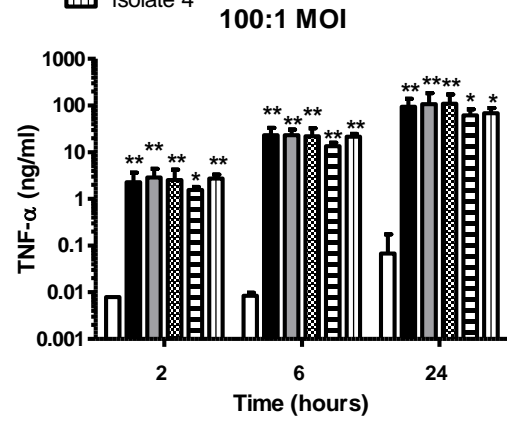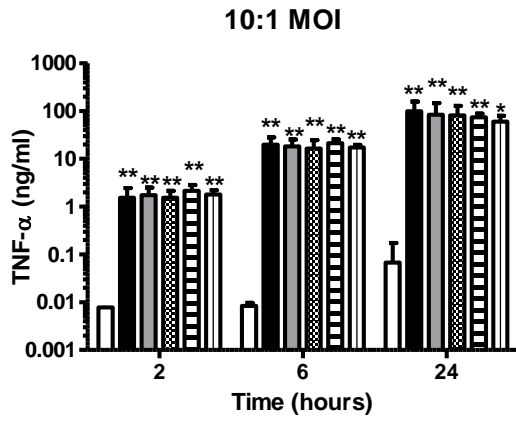
**Figure3.5: Alveolar macrophage cytokine release in response to NTHi clinical isolates.** Four NTHi strains were isolated from sputum samples of stable COPD patients. NTHi clinical isolates, as well as NTHi (R2846), were used to infect alveolar macrophages from 6 subjects (1 smoker and 5 COPD) at 100:1 and 10:1 MOI for 24 hours. Supernatants were aspirated at 2, 6 and 24 hours of infection and analysed for TNF-α (A), IL-6 (B), CXCL8 (C) and IL-10 (D)release by ELISA. Data are presented as mean+SEM. *, ** represent significantly greater than time-matched unstimulated control ($p < 0.05$, $< 0.001$ respectively, Repeated Measures ANOVA followed by Dunnett multiple comparisons test). # represents a significant difference from NTHi (R2846) ($p < 0.05$, Dunnett multiple comparisons test).

### 3.4. Discussion:

NTHi is a common colonising bacterium in the airways of COPD patients. In this chapter I have established an *in vitro* model of inflammation relevant to COPD, using whole live NTHi as a stimulus in human alveolar macrophages.

I investigated alveolar macrophage reactivity to live bacteria, by monitoring cytokine release over 24 hours. I have used live NTHi (R2846), also known as strain 12, which is a well-described and widely studied clinical isolate (318,373,375,377). LPS–induced inflammation is a well-established *in vitro* model in COPD (168,349,397,422). Therefore, I used LPS alongside the whole bacterial model for purpose of comparison. Furthermore, I used whole live *E. coli*, which is the source of LPS for further comparison. Both bacteria stimulated TNF-α release from alveolar macrophages. However, the pattern of TNF-α release was different between NTHi and *E. coli*. The higher *E. coli* concentrations (lower dilutions) failed to stimulate alveolar macrophages after 6 and 24 hours. Meanwhile, the higher NTHi concentrations (lower dilutions) caused more TNF-α release from alveolar macrophages after 24 hours. This observation implies that live NTHi caused different inflammatory profile from that caused by *E. coli*. To investigate the difference between the two bacteria further, I measured their viability in the culture medium. *E. coli* showed a continuous growth in the media over 24 hours. This might overwhelm alveolar macrophage defences and hence TNF-α levels were less after 24 hours. On the other hand, NTHi viability reduced over time, which suggests bacterial degradation in the culture media. NTHi degradation will result in the release of the potent cytoplasmic antigens (375,377), which might add to the antigenicity of the surface molecules (LOS and OMP). Also, the released LOS will potentially result in a more pro-inflammatory response (418). *E. coli* is less relevant

in COPD and it has different profile of stimulation and relative overgrowth in comparison to NTHi, therefor, only NTHi was chosen to be further investigated in this study.

LPS failed to induce TNF-α from alveolar macrophages in the preliminary experiment. However, it induced prominent cytokine release from alveolar macrophages in the subsequent experiment. This can be explained by lower sample size in the first experiment (N=4) and hence less statistical power.

Expressing bacterial load as a ratio of live bacteria to a cell, known as the multiplicity of infection (MOI), is widely applied in bacterial infection experiments (133,297). Therefore, I optimised a calculation for MOI in my culture and I set a range of target MOI from 1:1-1000:1. NTHi (R2846) at 1:1-1000:1 MOIs caused alveolar macrophages to release the pro-inflammatory cytokines TNF-α and IL-6. In addition, NTHi provoked CXCL8 release. CXCL8 attracts neutrophils and plays a significant role in lung tissue destruction and development of emphysema (66). Furthermore, IL-10, the anti-inflammatory cytokine and TNF-α antagonist (423), was also induced by NTHi.

Previous *in vitro* studies by Berenson and colleagues used NTHi antigens, specifically OMP P2, P6 and LOS, which were purified from a COPD clinical isolate. These antigens caused a significant release of TNF-α, CXCL8, IL-10 and IL-1β from alveolar macrophages and MDMs in COPD and non-COPD patients after 24 hours of stimulation (228,316). However, their reported levels were less than those reported in my model. This difference may be due to the use of whole live bacteria in the current study versus purified antigens. Alveolar macrophages in my model are subjected to a dynamic process of bacterial growth and turnover. Bacterial turnover will continuously release cytoplasmic antigenic molecules and surface antigens

164

(LOS and OMP). This scenario might be closer to the real life situation in human lungs.

In this model, I reported a time-dependent increase in TNF-α, CXCL8, IL-6 and IL-10, with maximal levels reached after 24 hours of infection. Increased inflammation over time might be due to the continuous bacterial turnover in the media, releasing its cytoplasmic and surface antigens. Nevertheless, Marti-Lliteras et al. (133) reported murine alveolar macrophage production of TNF-α plateaued after 4 hours of exposure to live NTHi. This difference from my finding might be attributed to using non-human cells with different culture conditions, and possibly different bacterial strain, (strain 398), versus NTHi (R2846) in this study.

Increased bacterial load in the lower airways has been linked to a higher airway inflammation, worse lung function and occurrence of exacerbation (164,215,421). Sethi et al (217), reported only a 7% difference in NTHi load between stable and exacerbation state, indicating that increased bacterial load per se in patients who are already colonised is unlikely to be the predominant mechanism of acute exacerbation in COPD. However, Abusriwil and Stockley (218) found a calculation error of the bacterial load in the Sethi study and recalculated the increase in NTHi load during exacerbation as 202% instead of 7%. This recalculation alters the conclusion to one which is, therefore, consistent to that of the previous studies mentioned above.

Previous *in vitro* studies applied only one bacterial load or MOI (100:1) (133,297,424). This study is the first to test the effect of an increasing bacterial load on *in vitro* inflammatory response. I observed no effect of increasing NTHi load on the pro-inflammatory cytokines (TNF-α, IL-6 and CXCL8). This finding indicates that the alveolar macrophage pro-inflammatory response is a relatively bacterial load-

independent phenomenon. Nonetheless, exacerbation can be precipitated by different factors other than an increase in bacterial load. This requires further investigation of the host-pathogen interaction.

In contrast, IL-10 showed an inverse correlation with bacterial load, with the highest levels induced by the lowest MOI (1:1). This observation suggests the role of IL-10 in the low-grade NTHi infection which might persist in the lower airways. It is well known that IL-10 release early in the course of infection, inhibits the pro-inflammatory immune response and cell apoptosis. The anti-inflammatory effect of IL-10 can result in bacterial persistence in the host and less tissue destruction (423). Moreover, the IL-10 release was identified as a mechanism of chronicity in mycobacterial infection (425,426). Taken together, the results presented here suggest that lower bacterial load causes a stronger anti-inflammatory response. This might encourage bacterial persistence in the lower airways, with relatively less clinical symptoms.

Investigation of alveolar macrophage viability in my model is important for two reasons. Firstly, high NTHi load might be lethal to the macrophages. Secondly, modulation of cell apoptosis by IL-10 might be one possible mechanism of NTHi survival and virulence (427,428). I, therefore, sought to assess alveolar macrophage viability throughout the infection experiment using TUNEL assay. I showed that NTHi did not induce macrophage apoptosis even at the highest MOI (4000:1). Therefore, the whole range of MOIs applied in this model is non-toxic to the cells. Whether NTHi impairs macrophage apoptosis to persist inside the cell and evade host immunity is beyond the scope of this study. However, it is a plausible mechanism of NTHi survival in the lung and requires further investigation.

Culturing live NTHi with alveolar macrophages was quite challenging. Hemin, an essential requirement for bacterial growth, can induce the anti-inflammatory enzyme heme oxygenase-1 (429–431), which might mask alveolar macrophage inflammatory response in my model. Therefore, I omitted hemin from the culture medium and monitored the NTHi growth in the model. Within 2 hours of NTHi inoculation, about 35% reduction in the NTHi viability was reported. However, bacterial growth surged at 6 hours and then sloped down towards the end of 24 hours, with more than 50% of the initial NTHi input is still viable. Therefore, the absence of NTHi nutritional requirement in the model had no significant impact on the NTHi survival during the experiment.

Some strains of NTHi were reported to resist the intracellular killing and persist inside the macrophages for more than 24 hours after phagocytosis (297). In my model, the NTHi phagocytosis and survival was monitored. The viable intracellular NTHi increased in the first 6 hours of inoculation to 11% of the initial NTHi load, which indicates active phagocytosis without killing. After 24 hours, almost all phagocytosed bacteria were killed. However, about $7x10^3$ viable bacteria (~1% of the initial NTHi input) were still viable inside the cells. These results agree with the previously reported NTHi survival in a mouse macrophage cell line (297). My findings suggest that *in vitro* NTHi infection is a dynamic process of growth, lysis, phagocytosis and intracellular survival. This bacterial behaviour in the model can explain the reported time-dependent release of inflammatory mediators over the 24 hours.

NTHi (R2846) is an otitis media clinical isolate (318,432). To characterise the relevance of this isolate in COPD, I compared the inflammatory response induced by NTHi (R2846) to that induced by NTHi isolated from COPD patients. Four strains of

NTHi were isolated from sputum samples of stable COPD patients. These isolates had different biotypes and antibiotic sensitivity (Tables 3.5 and 3.6). I used these COPD isolates in the same *in vitro* model using two MOIs (10:1 and 100:1). Most isolates showed pro-inflammatory responses similar to that reported for NTHi (R2846). However, there are some minor differences between strains in IL-10 release. Generally, the effect of different NTHi strains in this model appear similar, therefore, using NTHi (R2846) would be a relevant model of infection in COPD.

In conclusion, I characterised the pro-inflammatory effects of NTHi on COPD alveolar macrophages. NTHi provoked the release of TNF-$\alpha$, IL-6, CXCL8 and IL-10 resembling the inflammatory response that occurs in patients during bacterial infection. The experimental model described here is, therefore, suitable for further investigations of the pathophysiology of NTHi airway colonisation and COPD exacerbations.

# Chapter Four

# The Effects of Corticosteroids and Kinase Inhibitors on NTHi Stimulation in Human Alveolar Macrophages

## 4.1 introduction

The limited clinical response to corticosteroids has been recently investigated in COPD among other inflammatory diseases (433,434). Researchers have shown that inhaled corticosteroids at high doses failed to decrease the sputum inflammatory markers, or re-establish protease-antiprotease balance in stable COPD (395). In addition, *in vitro* studies have identified corticosteroids unresponsiveness in COPD neutrophils (399), macrophages (168) and lymphocytes (400).

Corticosteroids responsiveness is known to be cell and stimulus-specific (435,436). Since NTHi has been recently highlighted as an important inflammatory stimulus in COPD that contributes to disease progression (437), investigation of corticosteroid responsiveness of NTHi-induced inflammation in COPD would add more to the current understanding of steroid response during airway bacterial infection.

Studies in human epithelial cells have identified NF-κB and MAPK pathways as mediators of NTHi–induced airway inflammation and mucin production (373,375,377). However, the intracellular signalling pathways of NTHi have not yet been investigated in COPD alveolar macrophages.

Corticosteroids exert their action through binding to their intracellular receptors, the glucocorticoid receptors (GR). However, GR can be phosphorylated by agonist-dependent or independent manner. The GR phosphorylation status determines GR nuclear localisation and subsequent transcriptional activity of corticosteroids (388). ser 211 and ser 226 are the most identified phosphorylation sites in human GR. Phosphorylation of ser 211 has been linked to GR nuclear translocation and transcription of target genes. Meanwhile, phosphorylation at ser

226 is associated with GR nuclear exportation and steroid unresponsiveness (386,438). Recently, defective GR nuclear translocation has been identified in steroid insensitive asthma (406), which is found to be mediated by p38 MAPK-induced GR phosphorylation (346,348). Although GR phosphorylation in airways and alveolar macrophages of COPD patients was reported to be the same as in non-COPD controls (397), little is known about GR translocation in COPD in the presence of NTHi infection.

In this chapter, I used my established model of NTHi infection, to investigate corticosteroid responsiveness of NTHi-induced inflammation in COPD alveolar macrophages. Furthermore, I studied the signalling pathways activated by NTHi infection. I also examined the anti-inflammatory effect of combined corticosteroids and kinase inhibitors in the model. Moreover, I studied GR phosphorylation and translocation in NTHi-infected alveolar macrophages.

## 4.2. Materials and Methods:

### 4.2.1. Study subjects:

Thirty-five patients undergoing lung resection surgery for suspected or confirmed lung cancers were recruited for different experiments (see Table 4.1 and 4.2 for detailed demographics). Samples from subgroups of these patients were used for individual experiments, with numbers described in figure legends. Details of patients involved in each experiment are available in Table 4.3. Patients were categorised as either COPD (according to GOLD criteria) (38), smokers with normal lung function or non-smokers. Both COPD and smokers comprised of current and ex-smokers. Informed consents were obtained from all patients and the research was approved by South Manchester Research Ethics Committee.

**Table 4.1:** **Patients' demographic data.**

| Criteria | COPD | Smokers |
|---|---|---|
| **Smoking history (Current/Ex)** | (19/5) | (5/5) |
| **Gender (male/female)** | (16/8) | (7/3) |
| **Age (years)** | 68.5±6.2 | 72.8±6.9 |
| **FEV1 (L)** | 1.9±0.6 | 2.4±0.6 |
| **FEV1% predicted** | 71.6±20.8 | 103.8±23.7 |
| **FVC (L)** | 3.1±0.8 | 3.2±0.8 |
| **FEV1/FVC ratio (%)** | 56.8±10.4 | 78.5±8.7 |
| **Pack-year history** | 46.0±21.0 | 41.0±35.8 |

Data are presented as mean±SD. FEV1= Forced expiratory volume in 1 second, FVC= Forced vital capacity, L= Litre.

**Table 4.2:** **Patient's demographic data for glucocorticoid receptor translocation assay (N=1).**

| Category | Age (years) | Gender | FEV1 (L) | FEV1% predicted | FVC (L) | FEV1/FVC ratio (%) |
|---|---|---|---|---|---|---|
| **Non-smoker** | 85 | female | 1.73 | 134 | 2.21 | 78.29 |

FEV1= Forced expiratory volume in 1 second, FVC= Forced vital capacity, L= Litre.

**Table 4.3:** **Patient categorisation per experiments.**

| Experiment | COPD | Smokers | Non-smoker | Total |
|---|---|---|---|---|
| **Effect of dexamethasone on NTHi and LPS -induced cytokine release in alveolar macrophages** | 13 | 10 | 0 | 23 |
| **Signalling pathways of NTHi infection in alveolar macrophages** | 7 | 0 | 0 | 7 |
| **Effect of kinase inhibitors on NTHi-induced cytokine release in alveolar macrophages** | 6 | 0 | 0 | 6 |
| **Effect of kinase inhibitors and dexamethasone on NTHi-activated signalling pathways** | 4 | 0 | 0 | 4 |
| **Combination effect of dexamethasone and kinase inhibitors on NTHi-induced cytokines.** | 6 | 0 | 0 | 6 |
| **Effect of NTHi on glucocorticoid receptor phosphorylation** | 5 | 0 | 0 | 5 |
| **Glucocorticoid receptor translocation in alveolar macrophages** | 0 | 0 | 1 | 1 |

### 4.2.2. Effect of dexamethasone on NTHi and LPS-stimulated cytokine release by alveolar macrophages:

Alveolar macrophages were isolated from resected lung tissue of COPD and smokers and plated on flat bottom 96 well plates at $1x10^5$ cells per well. After overnight incubation, non-adherent cells were washed away and the adherent cells were treated with dexamethasone. Dexamethasone was reconstituted in dimethyl sulfoxide (DMSO) and diluted in supplemented RPMI1640 to give concentrations of 0.0001-1 μM and added to alveolar macrophages for 1 hour at 37 °C and 5% $CO_2$. Pretreated cells were stimulated with either NTHi (at 10:1 and 100:1 MOI) or LPS (1μg/ml). For vehicle control, DMSO (0.05%) was added for 1 hour before stimulation. After 24 hours of incubation, plates were spun and culture supernatants were aspirated and stored at -20 °C for future analysis of TNF-α, IL-6, CXCL8 and IL-10 by ELISA as described in materials and methods chapter in section 2.5.

### 4.2.3. Signalling pathways of NTHi in COPD alveolar macrophages:

Alveolar macrophages were isolated from lung tissue of COPD patients and plated on 6 well plates at $1x10^6$ cells per well. Following overnight incubation, non-adherent cells were washed away and the remaining cells were either stimulated with NTHi (at 10:1 MOI) or LPS (1μg/ml), or left unstimulated. Cells were lysed at 0, 10, 20, 40 and 60 minutes and the cell lysates were analysed for protein phosphorylation by Western blot as described in materials and methods chapter in section 2.6.

### 4.2.4. Effect of kinase inhibitors on NTHi-induced cytokine release by alveolar macrophages:

Alveolar macrophages were obtained from resected lungs of COPD patients and plated on flat bottom 96 well plates at a concentration of $1x10^5$ cells per well.

After overnight adhesion, cells were pretreated with either ERK MAPK inhibitor (AZD6244, Selleckchem), p38 MAPK inhibitor (BIRB-796, Selleckhem), IKK inhibitor (BMS-345541, Merck Millipore), or dexamethasone for 1 hour. The applied concentrations for each inhibitor were 0.0001- 1 μM, and for dexamethasone were 0.1 and 1 μM. After that, cells were incubated with NTHi at 10:1 MOI for 24 hours. Each of the inhibitors and dexamethasone was reconstituted in DMSO and diluted in RPMI1640 media. For a vehicle control, DMSO 0.05% was added for 1 hour followed by NTHi stimulation.

A subsequent experiment was conducted to study the combined anti-inflammatory effect of dexamethasone and kinase inhibitors. Alveolar macrophages from 6 COPD patients were treated with either dexamethasone (0.01 and 1 μM), BIRB-796 (1 μM), AZD6244 (1 μM) or the combination of either inhibitor with either dexamethasone concentration, for 1 hour followed by 24 hours stimulation with NTHi at 10:1 MOI.

After 24 hours incubation, plates were spun and the supernatants were aspirated for cytokine analysis by ELISA as detailed in materials and methods chapter in section 2.5.

## 4.2.5. Effect of kinase inhibitors and dexamethasone on NTHi-activated signalling pathways:

To test the pharmacological activity of the kinase inhibitors; alveolar macrophages from COPD patients were plated on 6 well culture plate at $1x10^6$ cells per well and incubated overnight at 37 °C and 5% $CO_2$. Alveolar macrophages were pretreated with BMS-345541, BIRB-796, AZD6244 or dexamethasone, each at 1 μM concentration, for 1 hour before stimulation with NTHi at 10:1 MOI for 20 minutes. At the end of incubation, cells were lysed and the lysates were assayed for

phosphorylated p65, p38 and ERK MAPK by Western blot as described in materials and methods chapter in section 2.6.

### 4.2.6. Glucocorticoid receptor (GR) phosphorylation:

Alveolar macrophages were isolated from COPD patients and plated onto 6 well culture plates at $1x10^6$ cells per well. After overnight incubation, cells were pretreated with dexamethasone (at 1µM) for 1 hour, followed by 20 minutes stimulation with either NTHi at 10:1 MOI or LPS (1µg/ml).

In a separate experiment to investigate the role of p38 MAPK in GR phosphorylation, alveolar macrophages were pretreated with BIRB-796 at 1µM for 1 hour followed by stimulation with NTHi (at 10:1 MOI) for 20 minutes.

At the end of incubation, alveolar macrophages were lysed and studied for phosphorylation of GR at ser 211 and ser 226 residues by Western blot.

### 4.2.7. GR translocation:

Alveolar macrophages were obtained from resected lung tissue of a non-smoker and were incubated onto chamber slides at a concentration of $3x10^5$ cells per chamber. Alveolar macrophages were incubated with NTHi (at 10:1 MOI), dexamethasone (1µM), or dexamethasone plus NTHi for 30 minutes.

A subsequent investigation of the role of p38 MAPK in GR translocation was conducted. Cells were pretreated with BIRB-796 for 30 minutes followed by the addition of NTHi, dexamethasone, or both for another 30 minutes. At the end of incubation time, cells were washed, fixed and stained for GR as detailed in materials and methods in section 2.8. Four hundred cells were counted per condition. Cells were classified according to GR localisation into nuclear (GR are localised in the

nucleus); cytoplasmic (GR are localised in the cytoplasm); or nuclear and cytoplasmic (GR are localised in the cytoplasm and the nucleus at the same time).

### 4.2.8. Statistics:

Normality of data was assessed by Kolmogorov-Smirnov test. Levels of cytokine release induced by NTHi and LPS in COPD and smokers were parametrically distributed. Unpaired t-tests (two-tailed) were performed to compare cytokine levels between COPD and smokers and to compare cytokine levels between NTHi and LPS treatment within each group. Dexamethasone and kinase inhibitors effect on NTHi-induced TNF-$\alpha$, IL-6, CXCL8 and IL-10 data were parametrically distributed. Dexamethasone and kinase inhibitors' treatment levels were compared and normalised to DMSO vehicle control using repeated measures ANOVA with Dunnett multiple comparisons test and levels were expressed as percentage inhibition of cytokine release. Differences between COPD and smokers' response to dexamethasone effect on NTHi-induced and LPS-induced cytokines were evaluated by unpaired t-test (two-tailed). Comparisons between dexamethasone percentage inhibition of cytokines induced by NTHi at 10:1, 100:1 MOIs and LPS were performed by unpaired t-test (two-tailed). Difference between combined inhibitory effect of kinase inhibitors and dexamethasone versus either treatment alone was assessed by repeated measures ANOVA with Dunnett multiple comparisons test

Data of NTHi-induced phosphorylation of NF-$\kappa$B and p38 MAPK pathways were parametrically distributed. Levels at each time point were compared to time-matched unstimulated control by repeated measures ANOVA with Dunnett multiple comparisons test. NTHi-induced ERK MAPK phosphorylation data were

nonparametrically distributed. Levels were compared to time-matched unstimulated control using Friedman test with Dunn's multiple comparisons test.

Inhibition of NTHi-activated pathways by kinase inhibitors and dexamethasone were parametrically distributed. Comparisons of the different treatments versus time-matched unstimulated control were performed by repeated measures ANOVA with Dunnett multiple comparisons test. Comparison of the effect of dexamethasone and kinase inhibitors pretreatment on NTHi-activated pathways was tested versus NTHi infected control by Dunnett multiple comparisons test.

Data of GR phosphorylation were parametrically distributed. Repeated measures ANOVA with Dunnett multiple comparisons test was performed to compare different treatments versus time-matched unstimulated control. Data of GR translocation was insufficient for statistical analyses (N=1).

When multiple testing was performed for intergroup or intragroup comparison, significance threshold was adjusted to account for multiple testing. For example, when comparing COPD and smokers at five different dexamethasone concentrations, significance threshold was adjusted to $p<0.01$. Also, when comparing LPS and NTHi (at 10:1 and 100:1 MOI) for cytokine release and dexamethasone sensitivity, significance threshold was adjuster to $p<0.025$. For all other comparisons $p<0.05$ was considered statistically significant.

## 4.3. Results:

### 4.3.1. Effect of dexamethasone on NTHi and LPS-induced inflammatory response in alveolar macrophages from COPD and smokers.

Alveolar macrophages from 23 subjects (10 smokers and 13 COPD) were pretreated with dexamethasone followed by NTHi or LPS stimulation. Culture supernatants were analysed for levels of TNF-α, IL-6, CXCL8 and IL-10 as detailed in methods section 4.2.2.

### 4.3.1.1. Comparison between NTHi and LPS-induced cytokine release in alveolar macrophages from COPD and smokers.

NTHi (at 100:1 and 10:1 MOI) induced a greater release of TNF-α than that induced by LPS in COPD patients (p=0.0003, p=0.005 respectively). In smokers, only 100:1 MOI caused a greater release of TNF- α than that caused by LPS (p=0.008). Also, NTHi (at 100:1 and 10:1 MOI) caused a greater release of IL-6 than that induced by LPS in COPD patients (p=0.009, p=0.004 respectively). There was no difference between NTHi and LPS-stimulated CXCL8 and IL-10 in both groups. Moreover, cytokines induction by NTHi and LPS was similar in COPD patients and smokers (Figure 4.1).

Significance threshold was adjusted to p<0.025 for comparison between LPS and NTHi (at 100:1 and 10:1 MOI) stimulation within each group. For comparison of LPS and NTHi (at 100:1 and 10:1 MOI) stimulation between COPD and smokers, significance threshold was adjusted to p<0.017. This adjustment have been made to account for multiple testing.
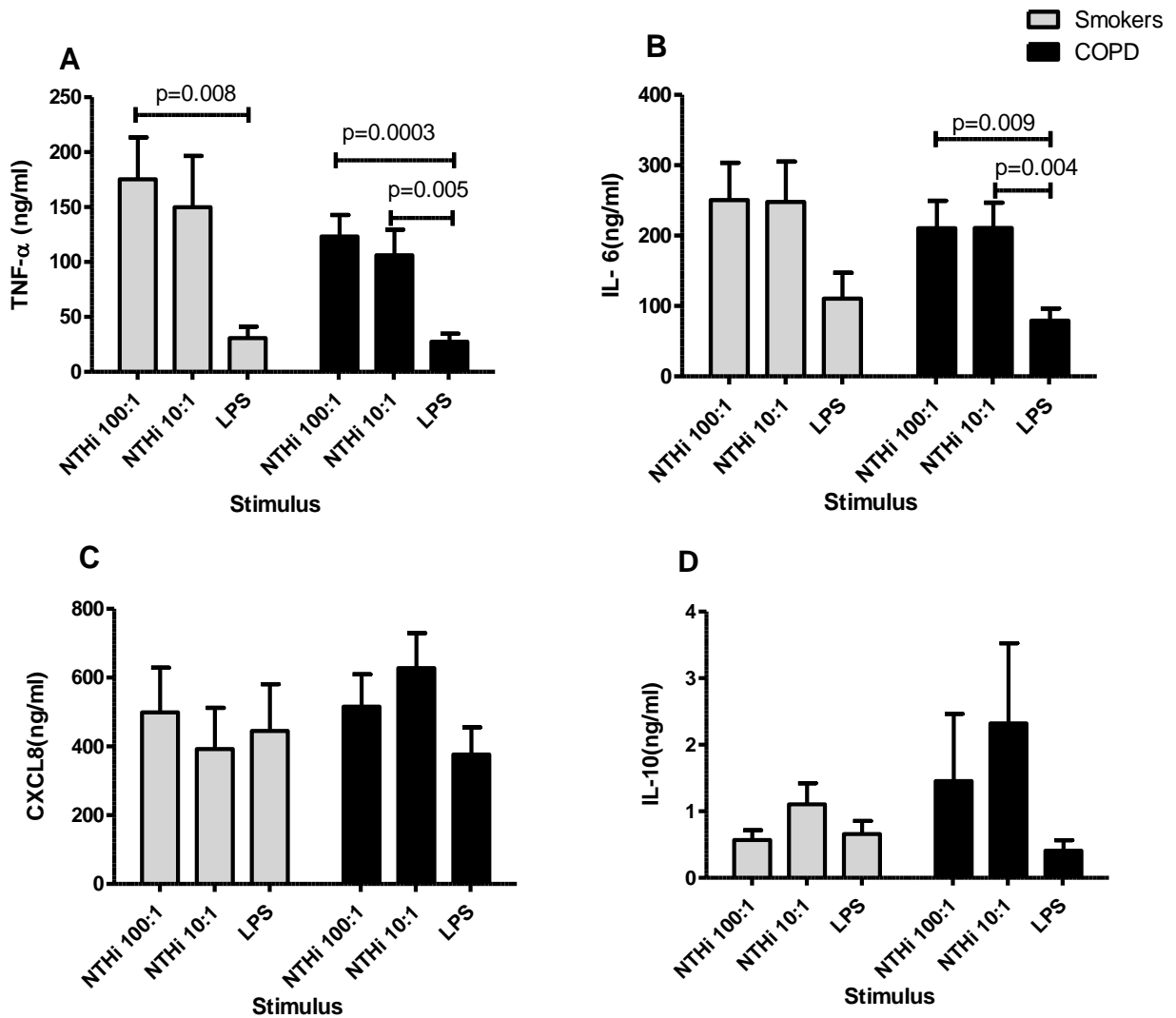
**Figure 4.1: Cytokine release in COPD and smokers' alveolar macrophages; NTHi versus LPS stimulation.** Alveolar macrophages from COPD and smokers were incubated with vehicle (DMSO 0.05%) for 1 hour before infection with either NTHi at 100:1 MOI (10 smokers and 13 COPD and), NTHi at 10:1 MOI (8 smokers and 12 COPD), or with LPS at 1μg/ml (7 smokers and 11 COPD). Supernatants were collected after 24 hours and assayed for TNF-α (A), IL-6 (B), CXCL8 (C) and IL-10 (D) release by ELISA. Data are presented as mean+SEM, the significant difference between groups are shown above bars (unpaired t-test).

### 4.3.1.2: Effect of dexamethasone on NTHi and LPS-induced TNF-α in alveolar macrophages from COPD and Smokers.

NTHi and LPS-induced TNF-α release was significantly inhibited by dexamethasone in a dose-dependent manner both in COPD and smokers ($p < 0.05$, Figure 4.2). The highest level of inhibition was achieved at 1 µM (up to 66% for NTHi-induced TNF-α) (Table 4.4). Interestingly, levels of TNF-α inhibition by 0.1-1µM dexamethasone was significantly higher in smokers than COPD in NTHi model at 100:1 MOI ($p = 0.009$). However, there was no difference between COPD and smokers in NTHi model (at 10:1 MOI) and in the LPS model (Figure 4.2). For this intergroup comparison, significance threshold was adjusted to $p < 0.01$ to account for multiple testing.
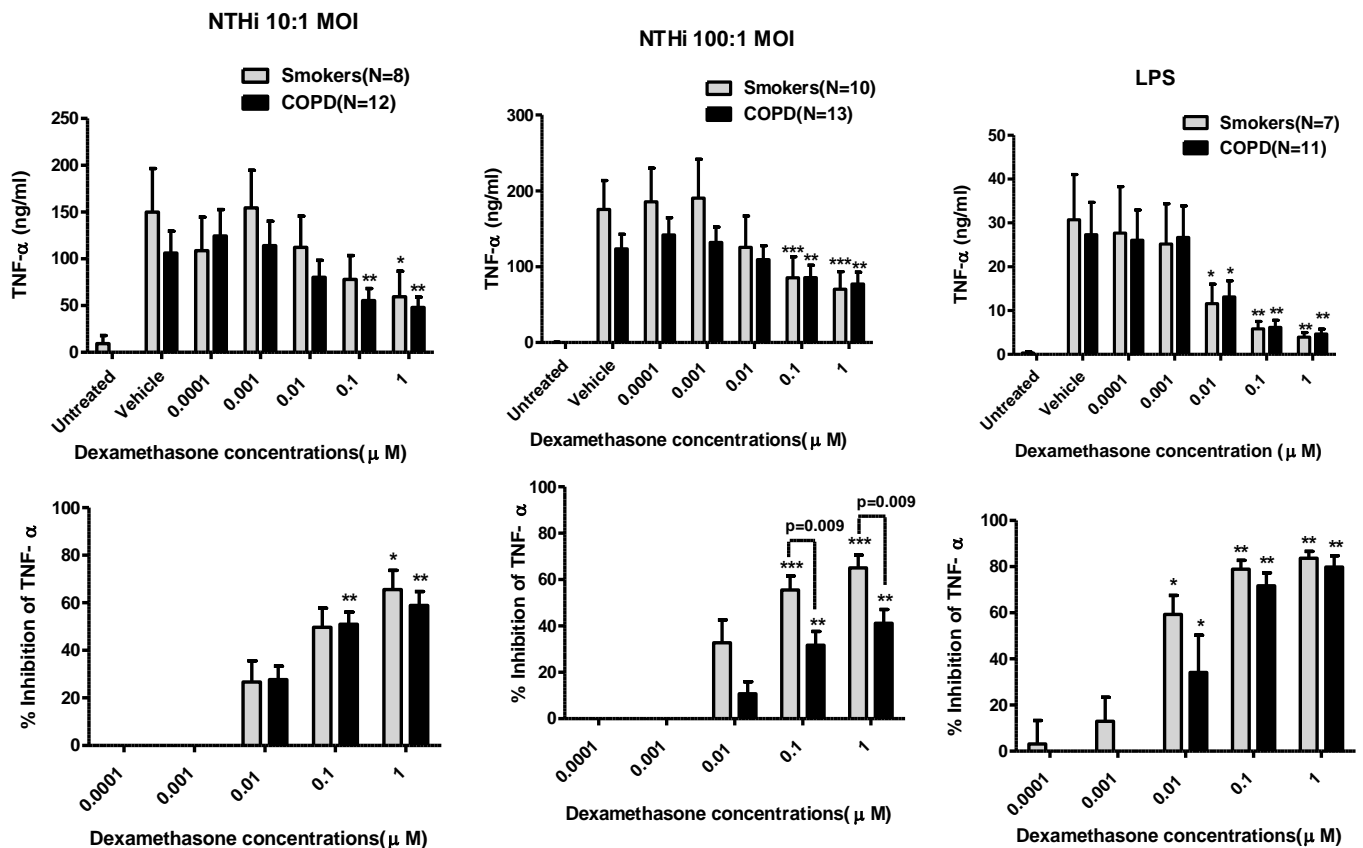
**Figure 4.2: Dexamethasone inhibition of NTHi and LPS-induced TNF-α release in alveolar macrophages from COPD and smokers.** Alveolar macrophages from 23 subjects (10 smokers and 13 COPD) were either pretreated with vehicle (DMSO 0.05%), dexamethasone (0.0001-1 μM) for 1 hour or left untreated. Pretreated cells were stimulated with either NTHi (at 10 and 100:1 MOI) or LPS (1μg/ml) for 24 hours. Untreated control means there was no NTHi or LPS stimulation. Vehicle control refers to vehicle for dexamethasone treatment. Culture supernatants were analysed for TNF-α levels by ELISA. Absolute levels (upper panel) were normalised to DMSO control to give percentage inhibition (lower panel). Data are presented as mean+SEM. *, **, *** represent significant inhibition below DMSO control (p<0.05, <0.01, <0.001 respectively, Repeated measures ANOVA followed by Dunnett multiple comparison test). p values shown above bars represent the difference between COPD and smokers (unpaired t-test).

### 4.3.1.3: Effect of dexamethasone on NTHi and LPS-induced IL-6 in alveolar macrophages from COPD and Smokers.

The IL-6 release was significantly and dose-dependently inhibited by dexamethasone in NTHi and LPS model both in COPD and smokers ($p < 0.05$, Figure 4.3), with the highest levels of inhibition detected at 1 µM (up to 41% for NTHi-induced IL-6) (Table 4.4). At 10:1 MOI, 0.01 µM dexamethasone concentration caused significantly greater inhibition of IL-6 in COPD than in smokers ($p = 0.009$). However, there was no difference between COPD and smokers in NTHi model (at 100:1 MOI) and in the LPS model of stimulation (Figure 4.3). For this intergroup comparison, significance threshold was adjusted to $p < 0.01$ to account for multiple testing.
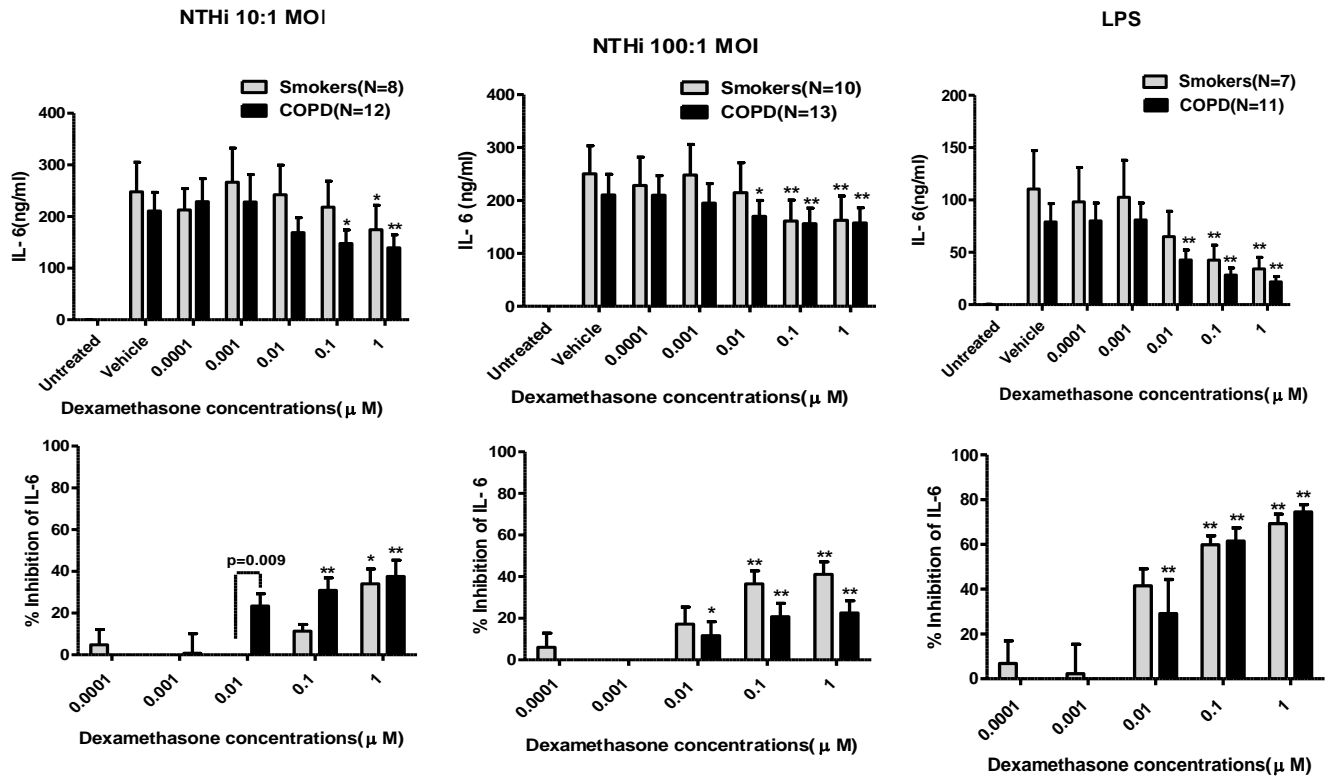
**Figure 4.3: Dexamethasone inhibition of NTHi and LPS-induced IL-6 release in alveolar macrophages from COPD and smokers.** Alveolar macrophages from 23 subjects (10 smokers and 13 COPD) were either pretreated with vehicle (DMSO 0.05%), dexamethasone (0.0001-1 µM) for 1 hour or left untreated. Pretreated cells were stimulated with either NTHi (at 10 and 100:1 MOI) or LPS (1µg/ml) for 24 hours. Untreated control means there was no NTHi or LPS stimulation. Vehicle control refers to vehicle for dexamethasone treatment. Culture supernatants were analysed for IL-6 levels by ELISA. Absolute levels (upper panel) were normalised to DMSO control to give percentage inhibition (lower panel). Data are presented as mean+SEM. *, ** represent significant inhibition below DMSO control ($p<0.05$, $<0.01$ respectively, Repeated measures ANOVA followed by Dunnett multiple comparison test). p values shown above bars represent the difference between COPD and smokers (unpaired t-test).

### 4.3.1.4: Effect of dexamethasone on NTHi and LPS-induced CXCL8 in alveolar macrophages from COPD and Smokers.

Dexamethasone did not inhibit NTHi-induced CXCL8 release in COPD and smokers at 10:1 and 100:1 MOI. At 100:1 MOI, there was significant induction of CXCL8 caused by dexamethasone at 0.001 and 1 µM (-22% and -30% respectively) ($p<0.05$, Figure 4.4, Table 4.4). On the other hand, LPS-induced CXCL8 was significantly and dose-dependently inhibited by dexamethasone in both COPD and smokers (up to 61%) ($p<0.05$, Figure 4.4). There was no difference in CXCL8 inhibition between COPD patients and smokers in NTHi and LPS models of stimulation. For this intergroup comparison, significance threshold was adjusted to $p<0.01$ to account for multiple testing.
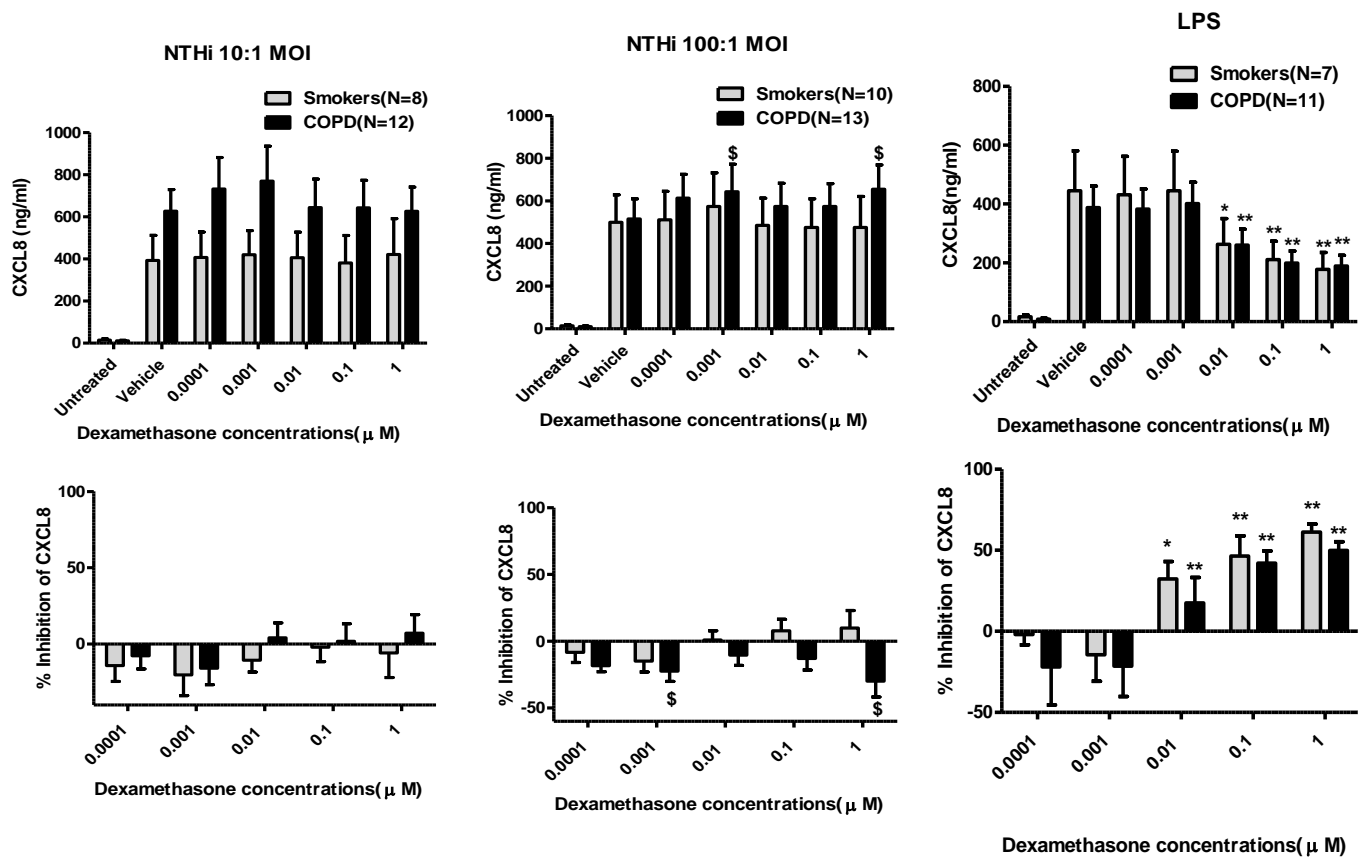
**Figure 4.4: Dexamethasone inhibition of NTHi and LPS-induced CXCL8 release in alveolar macrophages from COPD and smokers.** Alveolar macrophages from 23 subjects (10 smokers and 13 COPD) were either pretreated with vehicle (DMSO 0.05%), dexamethasone (0.0001-1 µM) for 1 hour or left untreated. Pretreated cells were stimulated with either NTHi (at 10 and 100:1 MOI) or LPS (1µg/ml) for 24 hours. Untreated control means there was no NTHi or LPS stimulation. Vehicle control refers to vehicle for dexamethasone treatment. Culture supernatants were analysed for CXCL8 levels by ELISA. Absolute levels (upper panel) were normalised to DMSO control to give percentage inhibition (lower panel). Data are presented as mean+SEM. *, ** represent significant inhibition below DMSO control (p<0.05, <0.01 respectively), $ represents significant increase above DMSO control (p<0.05, Repeated measures ANOVA followed by Dunnett multiple comparison test).

186

### 4.3.1.5: Effect of dexamethasone on NTHi and LPS-induced IL-10 in alveolar macrophages from COPD and Smokers.

IL-10 induced by NTHi and LPS was significantly inhibited by dexamethasone in a dose-dependent manner in COPD. In smokers, however, the inhibition was only significant at 100:1 MOI and LPS model ($p < 0.05$). Maximum inhibition achieved at 1μM dexamethasone was up to 53% for NTHi-induced IL-10 (Table 4.4). There was no difference between COPD and smokers in inhibition of LPS and NTHi-induced IL-10 (Figure 4.5). For this intergroup comparison, significance threshold was adjusted to $p < 0.01$ to account for multiple testing.
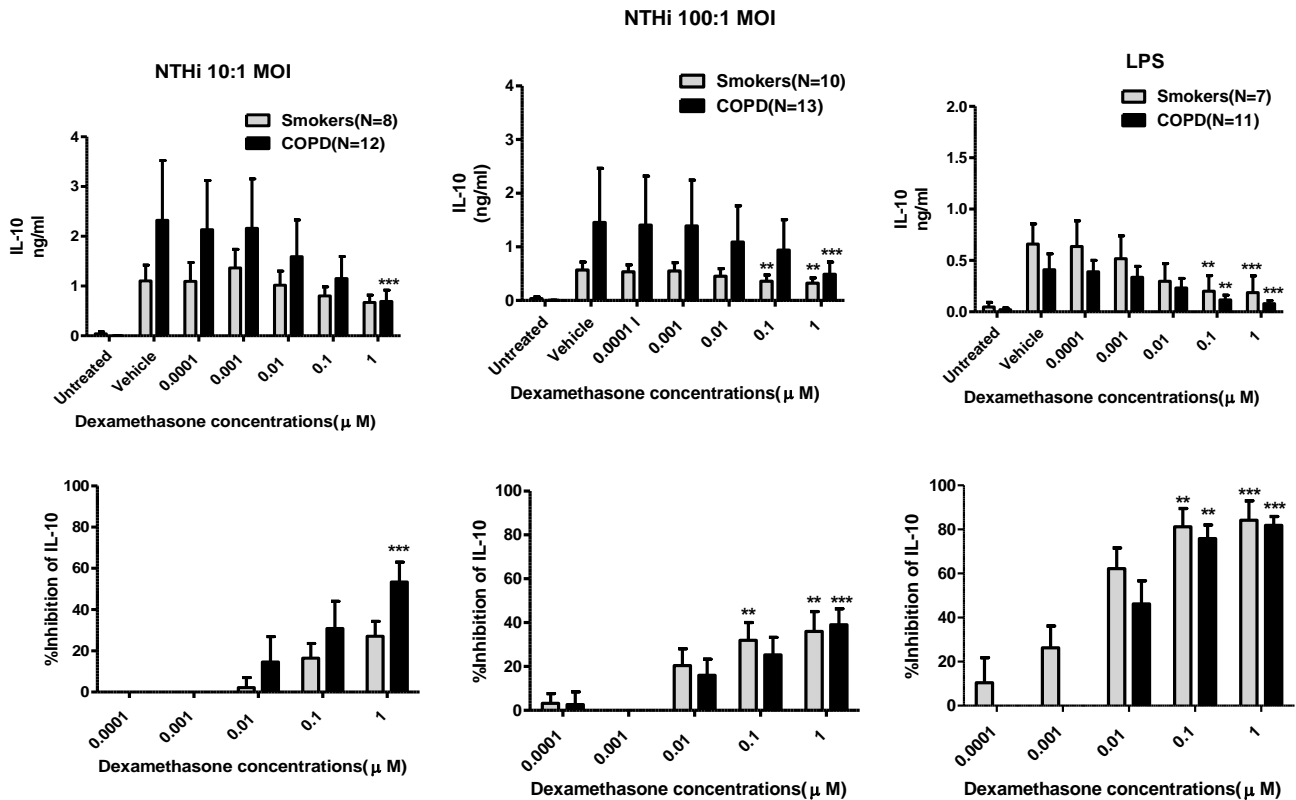
**Figure 4.5: Dexamethasone inhibition of NTHi and LPS-induced IL-10 release in alveolar macrophages from COPD and smokers.** Alveolar macrophages from 23 subjects (10 smokers and 13 COPD) were either pretreated with vehicle (DMSO 0.05%), dexamethasone (0.0001-1 µM) for 1 hour or left untreated. Pretreated cells were stimulated with either NTHi (at 10 and 100:1 MOI) or LPS (1µg/ml) for 24 hours. Untreated control means there was no NTHi or LPS stimulation. Vehicle control refers to vehicle for dexamethasone treatment. Culture supernatants were analysed for IL-10 levels by ELISA. Absolute levels (upper panel) were normalised to DMSO control to give percentage inhibition (lower panel). Data are presented as mean+SEM. **, *** represent significant inhibition below DMSO control ($p < 0.01$, $< 0.001$ respectively, Repeated measures ANOVA followed by Dunnett multiple comparison test)

## 4.3.1.6: Difference between NTHi and LPS models in corticosteroid responsiveness.

Dexamethasone inhibition of TNF-α was significantly greater in LPS model than NTHi model, at 10:1 and 100:1 MOI, in COPD (78% versus 59% and 41%) ($p < 0.025$), and at 100:1 MOI in smokers' macrophages (84% versus 65%) ($p = 0.02$,

Figure 4.6, Table 4.4). IL-6 inhibition was significantly greater in LPS model than NTHi, at 10:1 and 100:1 MOI, in COPD (75% versus 38% and 23%) and in smokers (69% versus 34% and 41%) (p<0.025). Dexamethasone inhibition of CXCL8 was significantly greater in LPS model than NTHi model, at 10:1 and 100:1 MOI, in both COPD (50% versus 7% and -30%) and smokers (61% versus -6% and 10%) (p<0.025). Similarly, IL-10 inhibition was significantly greater in LPS model than NTHi model, at 10:1 and 100:1 MOI, both in COPD (82% versus 53% and 39%) and smokers (84% versus 27% and 36%) (p<0.025, Figure 4.6, Table 4.4).

For these comparisons between dexamethasone inhibition of NTHi and LPS-induced cytokines, significance threshold was adjusted to p<0.025 to account for multiple testing.

**Table 4.4: Comparison between maximal dexamethasone inhibition of NTHi and LPS-induced cytokines in COPD and smokers' alveolar macrophages.**

| Cytokine | Dexamethasone percentage inhibition | | | | | | | |
|---|---|---|---|---|---|---|---|---|
| | COPD | | | | Smokers | | | |
| | NTHi 100:1 | NTHi 10:1 | LPS | P value | NTHi 100:1 | NTHi 10:1 | LPS | P value |
| **TNF-α** | 41% ** | 59% ** | 78% ** | †P<0.0001 ‡P=0.013 | 65% *** | 66% * | 84% ** | †P=0.02 ‡P>0.025 |
| **IL-6** | 23% ** | 38% ** | 75% ** | †p<0.0001 ‡P=0.004 | 41% ** | 34% * | 69% ** | †P=0.003 ‡P=0.001 |
| **CXCL8** | -30% $ | 7% | 50% ** | †P<0.0001 ‡P=0.005 | 10% | -6% | 61% ** | †P=0.007 ‡P=0.003 |
| **IL-10** | 39% *** | 53% *** | 82% *** | †P<0.0001 ‡P=0.02 | 36% ** | 27% | 84% *** | †P=0.002 ‡P=0.0002 |

Maximum inhibition achieved at 1μM dexamethasone concentration. Unpaired t-test was performed between NTHi at either MOI and LPS, †= LPS Versus NTHi (100:1 MOI), ‡= LPS Versus NTHI (10:1 MOI). *, **, ***= Significant inhibition below DMSO vehicle control (p<0.05, <0.01, <0.001 respectively). $= Significant induction above DMSO vehicle control (p<0.05).
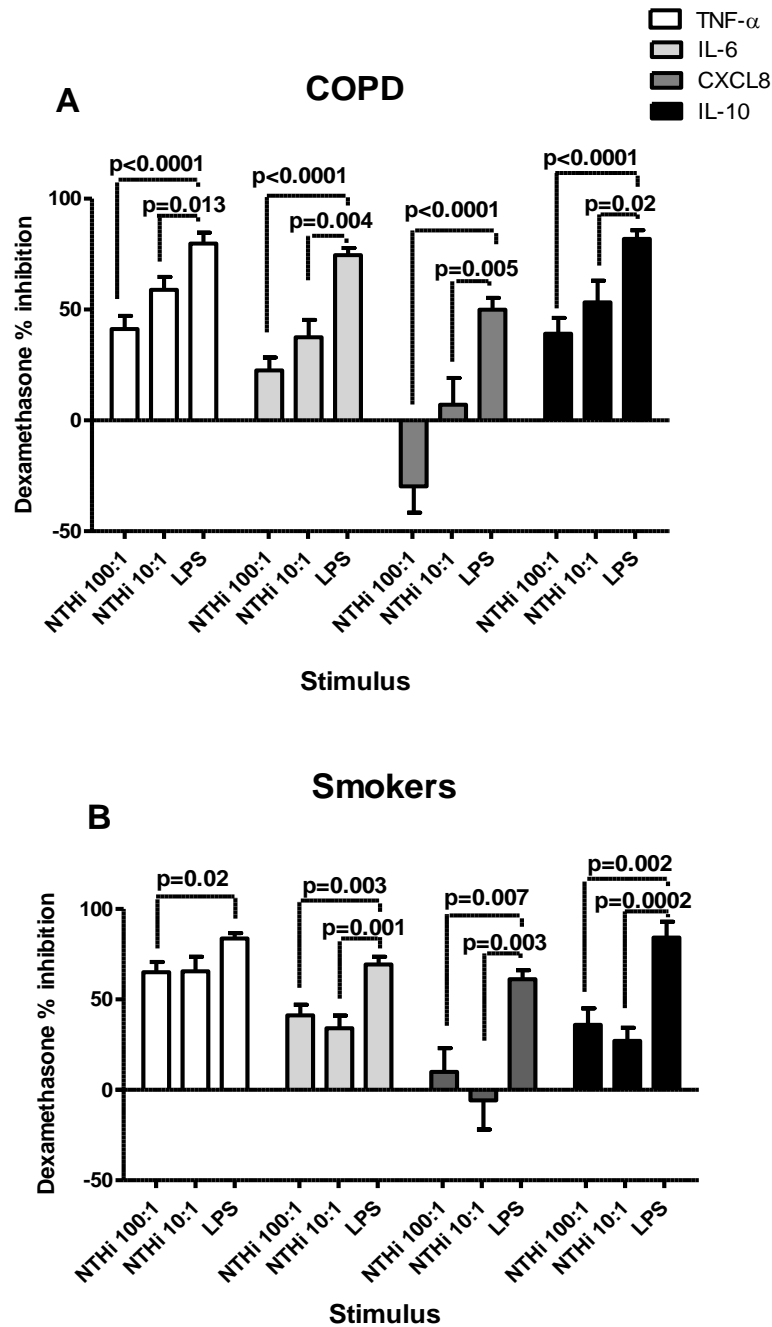
**Figure 4.6: Comparison between maximal dexamethasone percentage inhibition of NTHi and LPS-induced cytokines in smokers and COPD alveolar macrophages.** Alveolar macrophages from COPD (A) and smokers (B) were pretreated with dexamethasone (1 μM) or with vehicle (DMSO 0.05%) for 1 hour before infection with either NTHi at 100:1 MOI (10 smokers and 13 COPD), NTHi at 10:1 MOI (8 smokers and 12 COPD), or with LPS at 1μg/ml (7 smokers and 11 COPD). Supernatants were collected after 24 hours and assayed for TNF-α, IL-6, CXCL8 and IL-10 release by ELISA. Data are presented as mean+SEM. The significant difference between stimuli is shown above corresponding bars (unpaired t-test).

191

### 4.3.2: Signalling pathways of NTHi infection in COPD alveolar macrophages:

Alveolar macrophages from 7 COPD patients were either infected with NTHi (at 10:1 MOI) or stimulated with LPS (1µg/ml) for 1 hour, or left unstimulated. Cells were lysed at 0, 10, 20, 40 and 60 minutes and the phosphorylation of NF-kB subunit (p65), p38 MAPK and ERK MAPK was analysed by Western blot. Levels of induced phosphorylation were compared to time-matched unstimulated control.

NTHi significantly phosphorylated NF-kB subunit (p65) after 10 and 20 minutes of infection ($p<0.01$, $<0.05$ respectively). LPS caused significant phosphorylation of p65 (at 10-40 minutes) ($p<0.001$, $<0.05$, $<0.01$ respectively, Figure 4.7 A, refer to Appendix 2 A for individual blots). NTHi caused significant phosphorylation of p38 MAPK at 10-60 minutes ($p<0.05$). Similarly, LPS caused significant phosphorylation of p38 MAPK at all-time points up to 60 minutes ($p<0.05$, Figure 4.5 B, refer to Appendix 2 B for individual blots). ERK MAPK pathway was also phosphorylated by NTHi at 20 and 40 minutes of infection ($p<0.05$). Meanwhile, LPS phosphorylated ERK MAPK significantly at 20-60 minutes ($p<0.01$, Figure 4.7 C, refer to Appendix 2 C for individual blots).
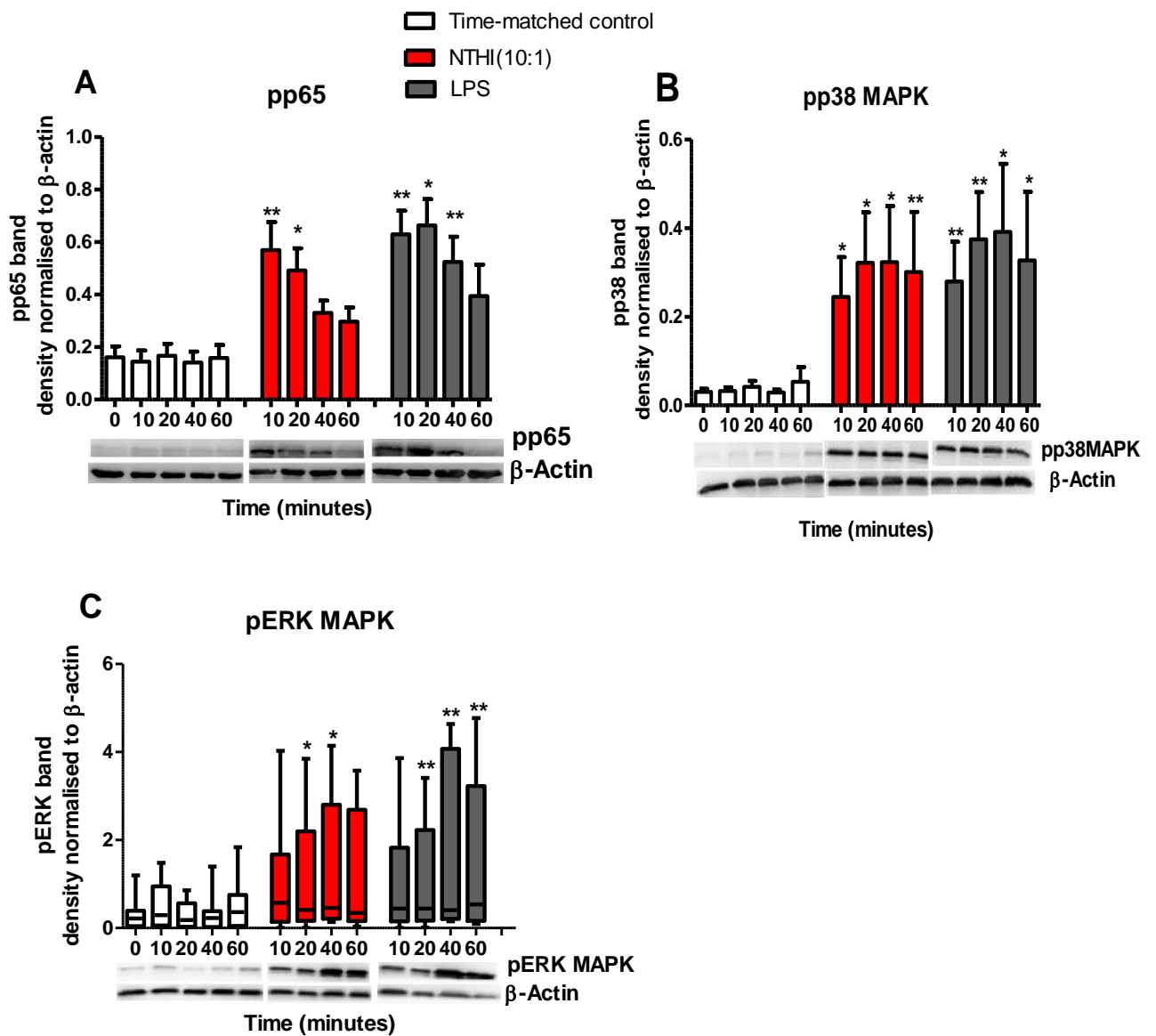
**Figure 4.7: Signalling pathways of NTHi infection in COPD alveolar macrophage.**
Alveolar macrophages from COPD patients (N=7) were either stimulated with NTHi (10:1 MOI), LPS (1µg/ml) or left unstimulated. Phosphorylation of NF-κB subunit (p65) (A), p38 MAPK (B) and ERK MAPK (C) was assessed at 0, 10, 20, 40 and 60 minutes of stimulation by Western blot. All blots were analysed by densitometry and bands density was normalised to β-Actin loading control. Representative blots are shown under matching conditions. Data are presented as mean+SEM for p65 and p38 MAPK and as median with interquartile range and total range for ERK MAPK. *, **, *** represent significantly greater than time-matched unstimulated control (p<0.05, <0.01, <0.001 respectively, Repeated measures ANOVA followed by Dunnett multiple comparison test or Friedman test followed by Dunn's multiple comparison test)

### 4.3.3. The effect of kinase inhibitors on NTHi-induced cytokine release in COPD alveolar macrophages:

Signalling pathways of NTHi infection in COPD alveolar macrophages were targeted by applying inhibitors of NF-κB (BMS-345541), p38 (BIRB-796) and ERK MAPK (AZD6244). Alveolar macrophages from COPD patient (N=6) were pretreated with either of the kinase inhibitors each at 0.0001-1 µM or dexamethasone at 0.1 and 1 µM before infection with NTHi (at 10:1 MOI) for 24 hours. Culture supernatants were analysed for TNF-α, IL-6, CXCL8 and IL-10 by ELISA.

TNF-α was significantly inhibited by AZD6244, BIRB-796 and dexamethasone in a dose dependent manner ($p<0.01$, $<0.05$ and $<0.01$ respectively), with the highest inhibition achieved at 1µM concentration of all compounds (40%, 41% and 68% respectively). However, BMS-345541 showed no effect on TNF-α release (Figure 4.8 A).

IL-6 was only significantly and dose-dependently inhibited by dexamethasone (up to 41%) ($p<0.05$). BIRB-796 caused inhibition by up to 19%. However, it was not significant. AZD6244 and BMS-345541 showed no effect on IL-6 release (Figure 4.8 B)

There was up to 26% and 24% inhibition of CXCL8 by AZD6244 and dexamethasone respectively (Figure 4.8 C). However, this inhibition did not reach statistical significance.

IL-10 was inhibited by dexamethasone (up to 33%), BIRB-796 (up to 14%) and AZD6244 (up to 40%), however, it was not statistically significant. BMS-345541 had no effect on IL-10 release (Figure 4.8 D)
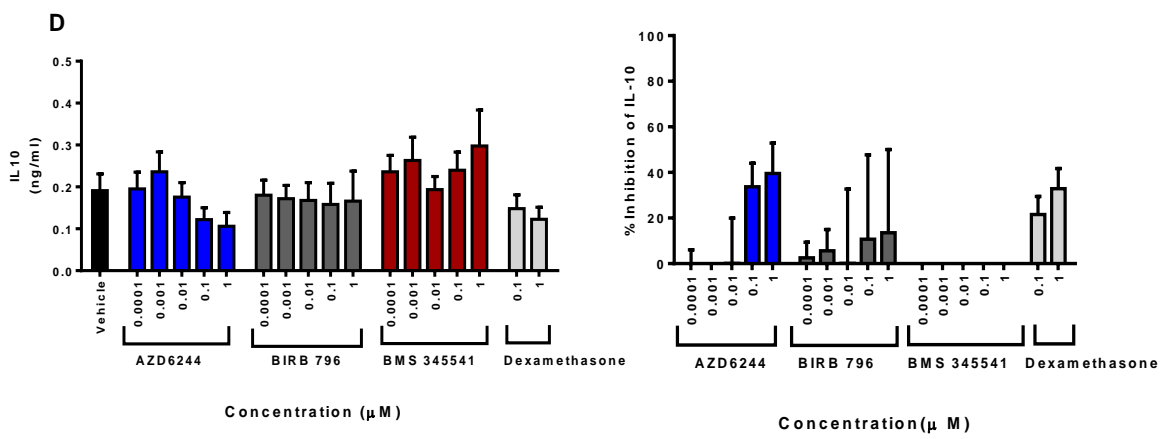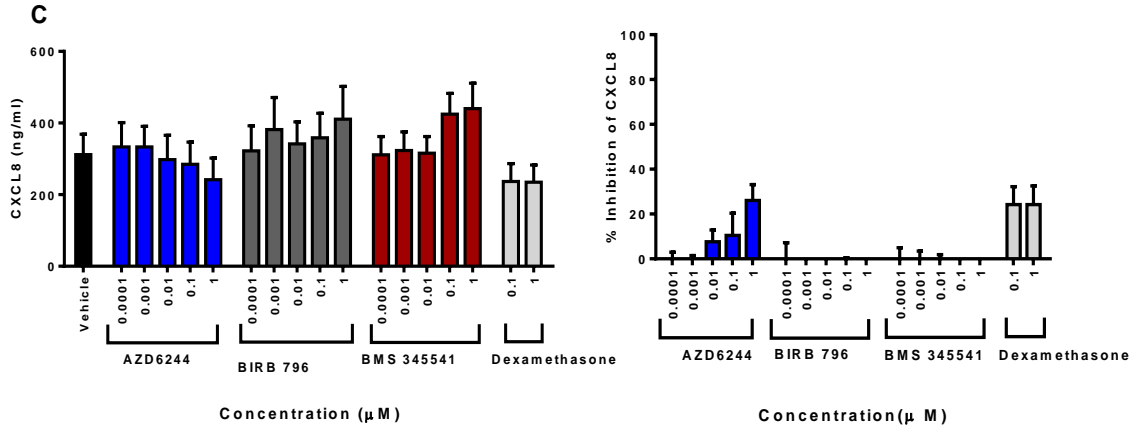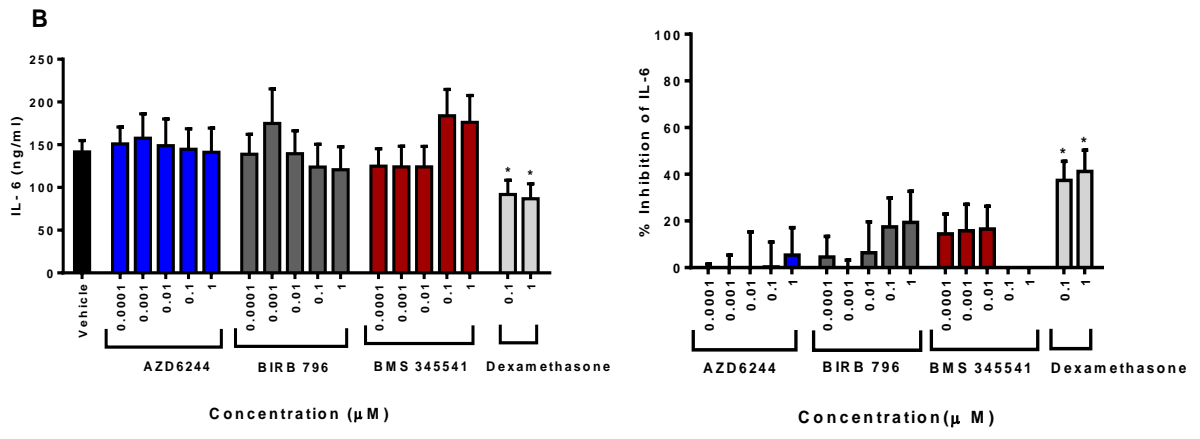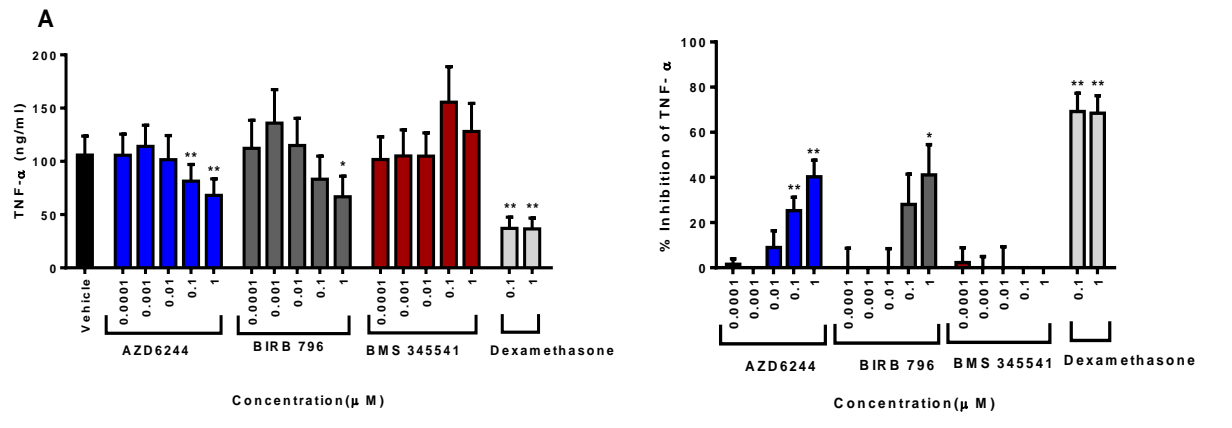
**Figure 4.8: The effect of kinase inhibitors on NTHi-induced TNF-α (A), IL-6 (B), CXCL8 (C) and IL-10 (D) in COPD alveolar macrophages.** Alveolar macrophages from COPD patients (N=6) were pretreated with either ERK inhibitor (AZD6244), p38 inhibitor (BIRB-796), IKK2 inhibitor (BMS-345541), each at (0.0001-1 μM), dexamethasone at (0.1 and 1 μM) or with vehicle (DMSO 0.05%) for 1 hour. The treatment was followed by NTHi infection at 10:1 MOI. Supernatants were collected after 24 hours and assayed for cytokine release by ELISA. Data are presented as mean+SEM. *, ** represent significant inhibition below DMSO control ($p < 0.05$, $< 0.01$ respectively, Repeated measures ANOVA followed by Dunnett multiple comparison test).

### 4.3.4. Effect of kinase inhibitors and dexamethasone on NTHi-activated signalling pathways:

Alveolar macrophages from 4 COPD patients were pretreated with either of kinase inhibitors, BMS-345541 (NF-κB inhibitor), BIRB-796 (p38 MAPK inhibitor), AZD6244 (ERK MAPK inhibitor) or dexamethasone, each at 1μM concentration for 1 hour. After that, cells were infected with NTHi at 10:1 MOI. Cells were lysed after 20 minutes of infection and the lysates were studied for phosphorylated p65, p38 and ERK MAPK by Western blot.

NTHi significantly phosphorylated p65 after 20 minutes ($p < 0.05$), this phosphorylation was not inhibited by BMS-345541 or dexamethasone in comparison with NTHi-stimulated level (Figure 4.9 A, refer to Appendix 3 A for individual blots). Moreover, neither dexamethasone nor BMS-345541 inhibited the unstimulated level of phosphorylated p65.

p38 MAPK was significantly phosphorylated by NTHi after 20 minutes ($p < 0.001$). Pretreatment with BIRB-796 significantly reduced NTHi phosphorylation of p38 MAPK ($p < 0.05$, Figure 4.9 B, refer to Appendix 3 B for individual blots). Dexamethasone pretreatment had no effect on NTHi-induced phosphorylation of p38 MAPK. There was no significant effect of dexamethasone and BIRB-796 on the unstimulated level of p38 phosphorylation.

NTHi caused significant phosphorylation of ERK MAPK ($p < 0.001$). AZD6244 caused significant inhibition of both unstimulated level ($p < 0.05$) and the NTHi-stimulated level of phosphorylated ERK MAPK ($p < 0.001$). Dexamethasone pretreatment had no effect on either unstimulated levels or NTHi-stimulated phosphorylation of ERK MAPK (Figure 4.9 C, refer to Appendix 3 C for individual blots)
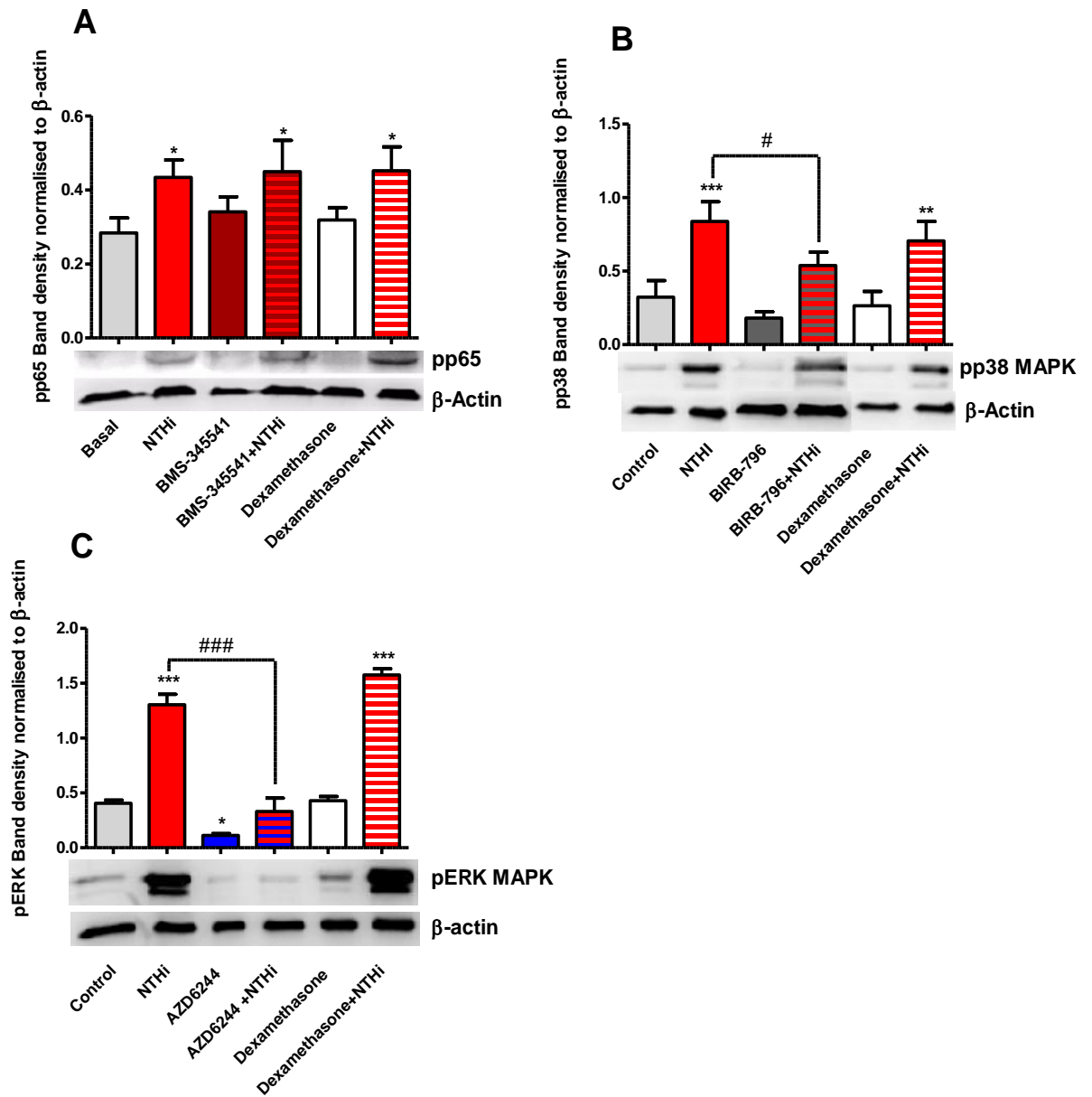
**Figure 4.9: The effect of kinase inhibitors and dexamethasone on NTHi-activated signalling pathways.** Alveolar macrophages from 4 COPD patients were pretreated with BMS-345541, BIRB-796, AZD6244 or dexamethasone, each at 1μM for 1 hour before stimulation with NTHi (10:1 MOI). After 20 minutes, cells were lysed and studied for phosphorylation of p65 (A), p38 (B) and ERK MAPK (C) by Western blot. All blots were analysed by densitometry and bands density was normalised to β-Actin loading control. Representative blots are shown under matching conditions. Data are presented as mean+SEM. *, **, *** represent a significant difference from time-matched unstimulated controls ($p<0.05$, $<0.01$, $<0.001$ respectively, Repeated measures ANOVA). #, ### represent significantly lower than NTHi stimulated level ($p<0.05$, $0.001$ respectively, Repeated measures ANOVA followed by Dunnett multiple comparison test).

### 4.3.5. Combination effect of dexamethasone and kinase inhibitors on NTHi-induced cytokine release in COPD alveolar macrophages:

After I had verified the pharmacological activity of AZD6244 and BIRB-796, I tried to investigate their combined anti-inflammatory effect with dexamethasone in my model of infection. Alveolar macrophages from 6 COPD patients were pretreated with dexamethasone (0.01 and 1μM), AZD6244, BIRB-796 (both at 1 μM), either alone or in combination for 1 hour. DMSO was run as a vehicle control. After that, cells were infected with NTHi for 24 hours. Culture supernatants were analysed for levels of TNF-α, IL-6, CXCL8 and IL-10 by ELISA.

NTHi-induced TNF-α and IL-6 were significantly inhibited by dexamethasone, AZD6244 and BIRB-796 either alone or in combination ($p < 0.05$). Combination of either BIRB-796 or AZD6244 with dexamethasone caused significant inhibition of TNF-α and IL-6, which was maximal with 1 μM dexamethasone ($p < 0.01$) and was greater than either compound alone ($p < 0.01$, Figure 4.10 A, B, Table 4.5)

Interestingly, dexamethasone, BIRB-796 and AZD6244 did not inhibit NTHi-induced CXCL8. However, the combination of BIRB-796 or AZD6244 with 1 μM dexamethasone caused significant inhibition of CXCL8 ($p < 0.01$) which was greater than either compound alone ($p < 0.05$, Figure 4.10 C, Table 4.5).

NTHi-induced IL-10 was significantly inhibited by dexamethasone, BIRB-796 and AZD6244 either alone or in combination at the tested doses ($p < 0.01$). Combination of 1 μM dexamethasone with BIRB-796 or AZD6244 caused greater inhibition than dexamethasone alone ($p < 0.01$), and each kinase inhibitor alone ($p < 0.05$, Figure 4.10 D, Table 4.5)

**Table 4.5:** **Inhibition of NTHi-induced cytokine release in COPD alveolar macrophages by dexamethasone and kinase inhibitors**

| Treatment | Percentage inhibition of NTHi-induced cytokines | | | |
|---|---|---|---|---|
| | TNF-α | IL-6 | CXCL8 | IL-10 |
| **Dexamethasone 0.01µM** | 57% * | 44% ** | 20% | 56% ** |
| **Dexamethasone 1µM** | 72% * | 59% ** | 35% | 67% ** |
| **BIRB-796 1µM** | 68% * | 53% ** | 10% | 76% ** |
| **AZD6244 1 µM** | 65% * | 32% ** | 15% | 70% ** |
| **Dexamethasone 0.01µM+BIRB-796 1 µM** | 84%** ## $$ | 69% ** ## $$ | 23% | 83% ** ## |
| **Dexamethasone 1µM+BIRB-796 1 µM** | 93% ** ### $$ | 84% ** ### $$ | 48% ** # $$ | 89% ** ### $ |
| **Dexamethasone 0.01µM+AZD6244 1 µM** | 80% ** ### ΔΔ | 49% ** Δ | 37% ** ΔΔ | 74% ** # |
| **Dexamethasone 1µM+AZD6244 1 µM** | 93% ** ### ΔΔ | 78% ** ## ΔΔ | 52% ** ## ΔΔ | 82% ** ## Δ |

*, ** = Significant inhibition below DMSO control (p<0.05, 0.01 respectively).

#, ##, ##= Significantly greater inhibition than corresponding dexamethasone concentration (p<0.05, <0.01, <0.001 respectively).

$, $$ = Significantly greater inhibition than BIRB-796 alone (p<0.05, <0.01 respectively).

Δ, Δ Δ = Significantly greater inhibition than AZD6244 alone (p<0.05, <0.01 respectively).

**A**

**B**

**C**
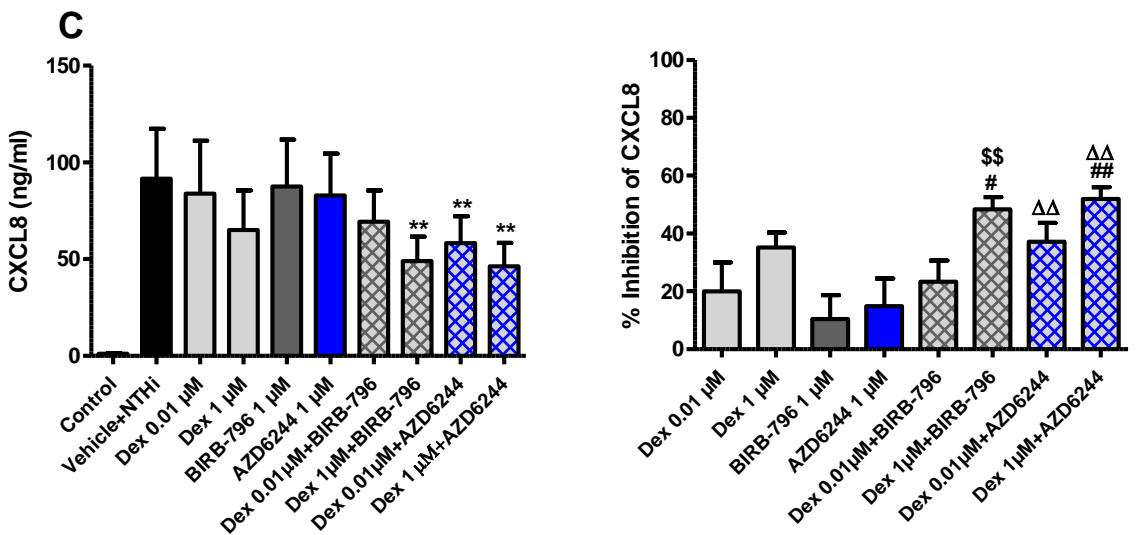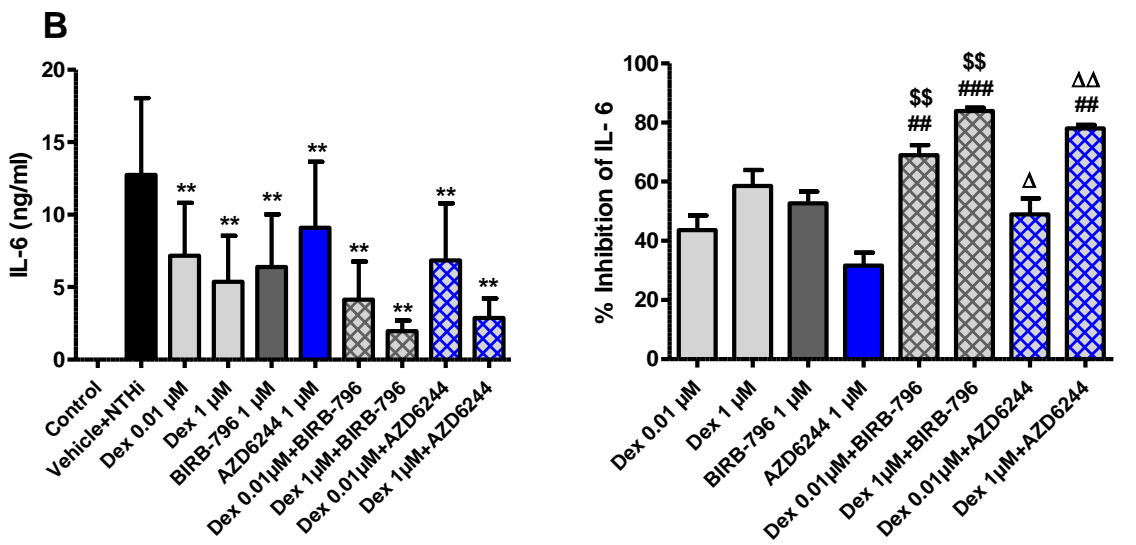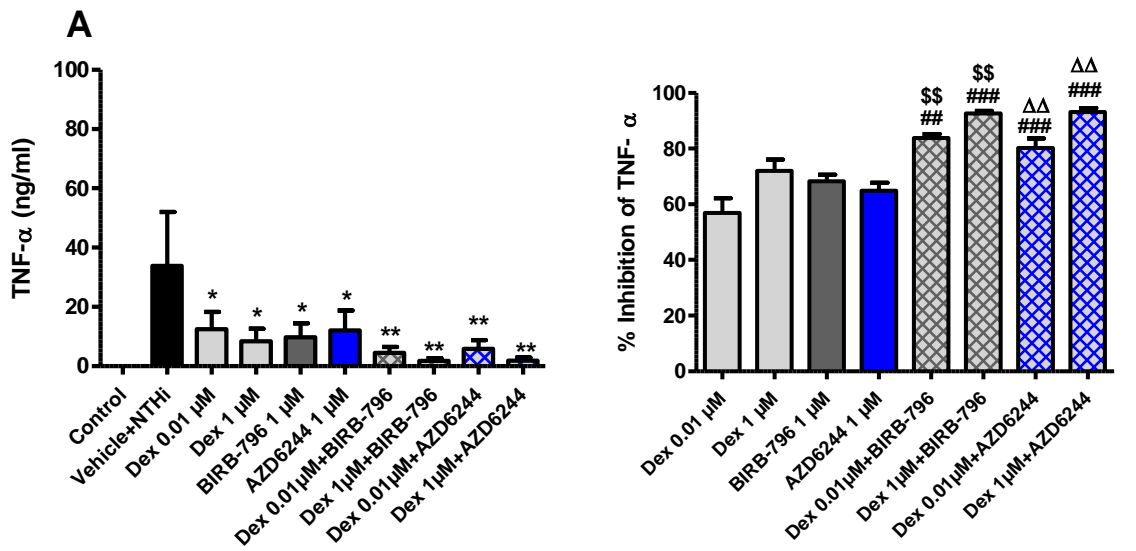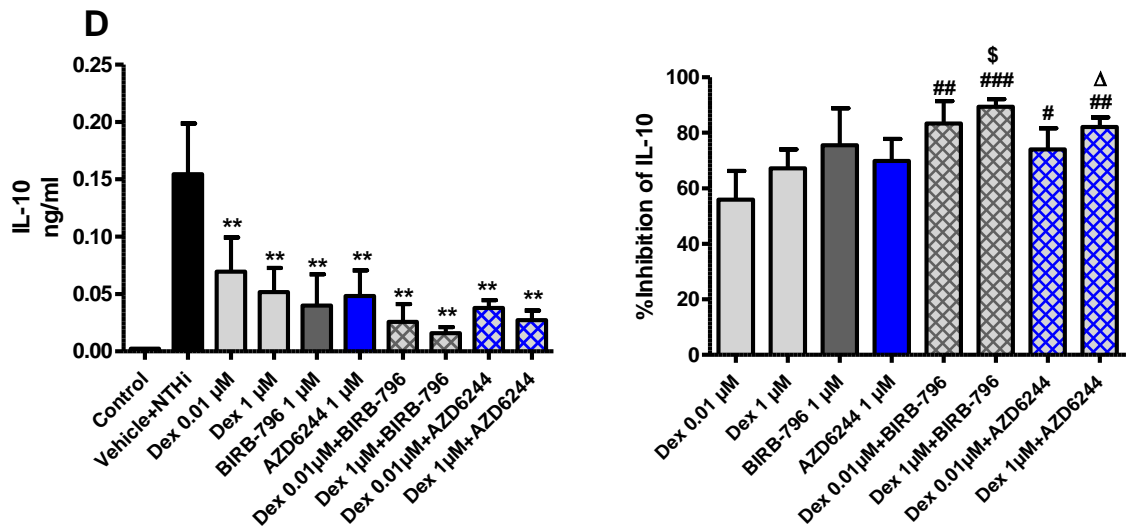
**Figure 4.10: Combination effect of dexamethasone and kinase inhibitors on NTHi-induced TNF-α (A), IL-6 (B), CXCL8 (C) and IL-10 (D) in COPD alveolar macrophages**. Alveolar macrophages from 6 COPD patients were pretreated with either dexamethasone (0.01 and 1μM), BIRB-796 (1μM), AZD6244 (1μM) alone or in combination, for 1 hour before NTHi (10:1 MOI) stimulation for 24 hours. DMSO 0.05% was used as vehicle control. Cytokines levels were measured by ELISA. Data are presented as mean+SEM. *, ** represent significant inhibition below DMSO control (p<0.05, <0.01 respectively). #, ##, ### represent significantly greater inhibition than corresponding dexamethasone concentration (p<0.05, <0.01, <0.001 respectively). $, $$ represent significantly greater inhibition than BIRB-796 alone, Δ, Δ Δ represent significantly greater inhibition than AZD6244 alone (p<0.05, <0.01 respectively, Repeated measures ANOVA followed by Dunnett multiple comparison test).

### 4.3.6. Effect of NTHi on glucocorticoid receptor phosphorylation in COPD alveolar macrophages:

Alveolar macrophages from 5 COPD patients were pretreated with dexamethasone at 1μM for 1 hour before stimulation with NTHi (10:1 MOI) or LPS for 20 minutes. Cells were lysed and the lysates were assessed for GR phosphorylation on ser 211 and ser 226 residues by Western blot.

Dexamethasone alone caused significant phosphorylation at ser 211 residue ($p < 0.01$). NTHi induced significant phosphorylation of GR at ser 226 ($p < 0.05$) but there was no phosphorylation at ser 211 residue. Dexamethasone pretreatment followed by NTHi caused significant phosphorylation at ser 226 and ser 211 ($p < 0.05$, Figure 4.11 A, B, refer to Appendix 4 A, B for individual blots).

LPS had no effect on GR ser 226 and ser 211 phosphorylation. However, dexamethasone and LPS caused significant phosphorylation at ser 211 residue ($p < 0.05$, Figure 4.11 B).
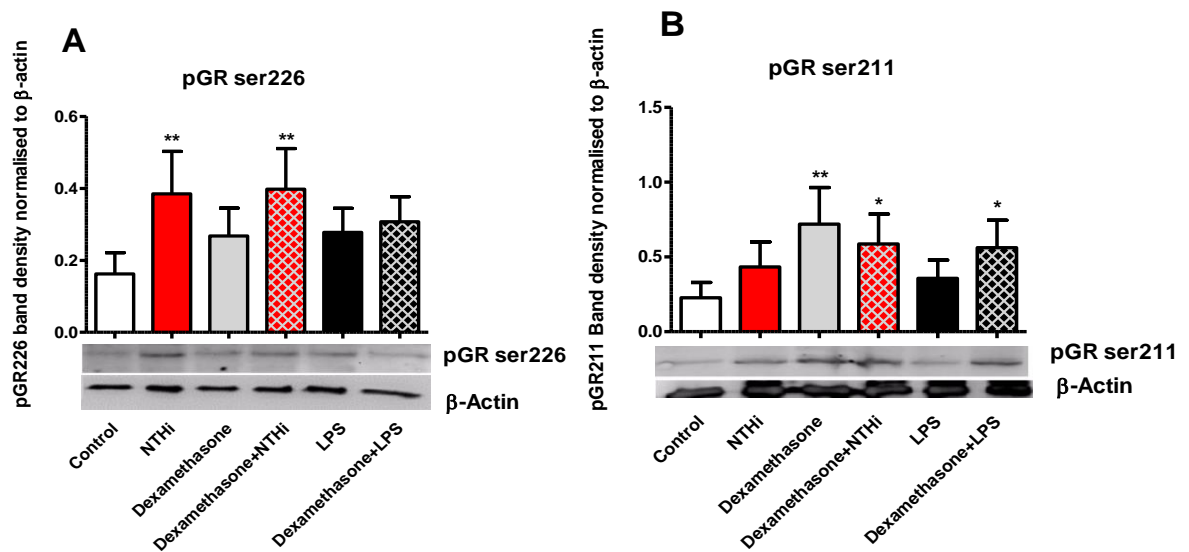
**Figure 4.11: Effect of NTHi on glucocorticoid receptor phosphorylation in COPD alveolar macrophages:** COPD alveolar macrophages (N=5) were either stimulated with NTHi (10:1MOI) or LPS (1µg/ml) for 20 minutes with or without 1-hour pretreatment with dexamethasone at 1µM. cells were lysed and assessed for GR phosphorylation at ser 226 (A) and ser 211 (B) by Western blot. All blots were analysed by densitometry and band density was normalised to β-actin loading control. Representative blots are shown under corresponding conditions. Data are presented as mean+SEM, *, ** represent significantly greater than time-matched unstimulated control (p<0.05, <0.01 respectively, Repeated measures ANOVA followed by Dunnett multiple comparison test).

### 4.3.7. The role of p38 MAPK in NTHi-induced GR phosphorylation:

Next I investigated the role of the p38MAPK pathway in NTHi-induced GR phosphorylation. Alveolar macrophages from 5 COPD patients were pretreated with BIRB-796 1μM for 1 hour before infection with NTHi (at 10:1 MOI) for 20 minutes. Cells were lysed and studied for GR phosphorylation by Western blot.

NTHi caused significant phosphorylation of GR ser 226 (p<0.05), but not GR ser 211. After pretreatment with BIRB-796, NTHi-induced phosphorylation at ser 226 residue was no longer significantly greater than the unstimulated control. BIRB-796 showed no effect on GR phosphorylation at ser 211 residue (Figure 12 A, B, refer to Appendix 5 A, B for individual blots).
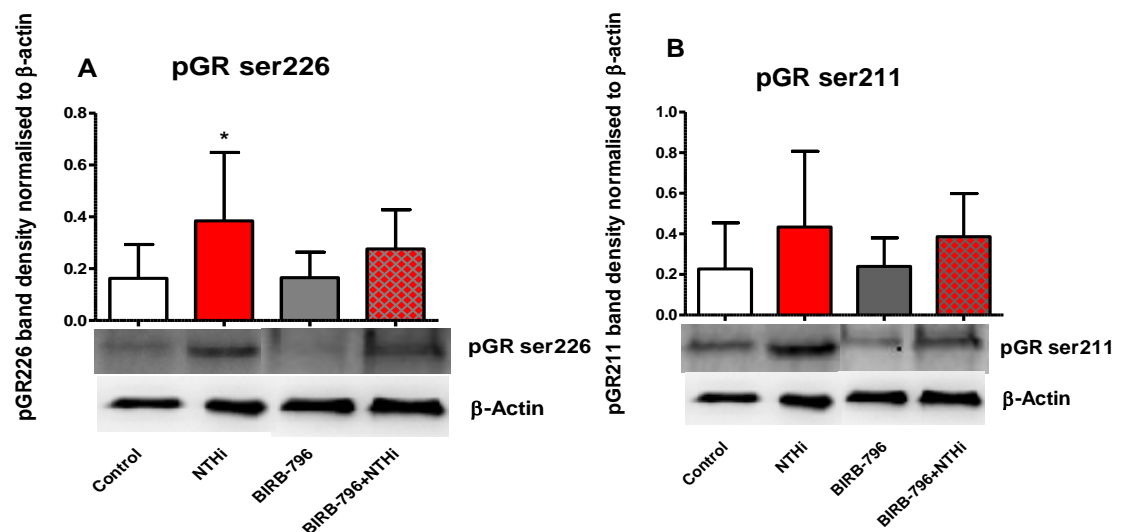


**Figure 4.12:** **Role of p38MAPK in NTHi-induced GR phosphorylation in COPD alveolar macrophages:** COPD alveolar macrophages (N=5) were pretreated with BIRB-796 for 1 hour before 20 minutes stimulation with NTHi (10:1 MOI). Cell lysates were analysed for GR phosphorylation at ser 226 (A) and ser 211 (B) residues by Western blot. All blots were analysed by densitometry and band density was normalised to β-actin loading control. Representative blots are shown under corresponding conditions. Data are presented as mean+SEM. * represents significantly greater than time-matched unstimulated control (p<0.05, Repeated measures ANOVA followed by Dunnett multiple comparison test).

### 4.3.8. Effect of NTHi on glucocorticoids receptor (GR) translocation in alveolar macrophages:

Alveolar macrophages from a non-smoker subject (N=1) were treated with dexamethasone (1µM) or NTHi (10:1 MOI) both alone and in combination for 30 minutes. Cells were also pretreated with or without BIRB-796 (1 µM) for 30 minutes before dexamethasone, NTHi or both. Cells were washed, fixed and stained for GR.

Under basal conditions 83% of cells stained for GR both in the cytoplasm and the nucleus with only 17% of cells staining for GR solely in the nucleus. Treatment with dexamethasone (1 µM) for 30 minutes caused GR nuclear translocation in 99% of cells with GR staining within the nucleus only (Table 4.6 and Figure 4.13 A, B).

NTHi stimulation for 30 minutes caused a decrease in the percentage of cells with nuclear only GR staining (5%) compared to unstimulated levels (17%). NTHi also decreased the effects of dexamethasone on nuclear GR translocation from 99% to 22% (Table 4.6 and Figure 4.13 C, D).

Pretreatment with BIRB-796 (1 µM) for 30 minutes reduced the effect of NTHi on dexamethasone-induced GR nuclear translocation increasing nuclear GR expression from 22% to 44% (Table 4.6 and Figure 4.13 H). Pretreatment with BIRB-796 had no effect on unstimulated GR staining (Figure 4.13 E) or dexamethasone-induced GR nuclear translocation (99%) (Figure 4.13 F) and NTHi induced cytoplasmic GR translocation (Figure 4.13 G).

**Table 4.6:** Glucocorticoid receptors (GR) translocation in the alveolar macrophage.

| Condition | Cytoplasmic | Nuclear and cytoplasmic | Nuclear |
|---|---|---|---|
| **Unstimulated time-matched control** | 0% | 83% | 17% |
| **Dexamethasone** | 0% | 1% | 99% |
| **NTHi** | 1% | 94% | 5% |
| **Dexamethasone+NTHi** | 0% | 78% | 22% |
| **BIRB-796** | 0.2% | 75.8% | 24% |
| **BIRB-796+dexamethasone** | 0% | 1% | 99% |
| **BIRB-796+NTHi** | 0% | 86% | 14% |
| **BIRB-796+dexamethasone+NTHi** | 0% | 56% | 44% |
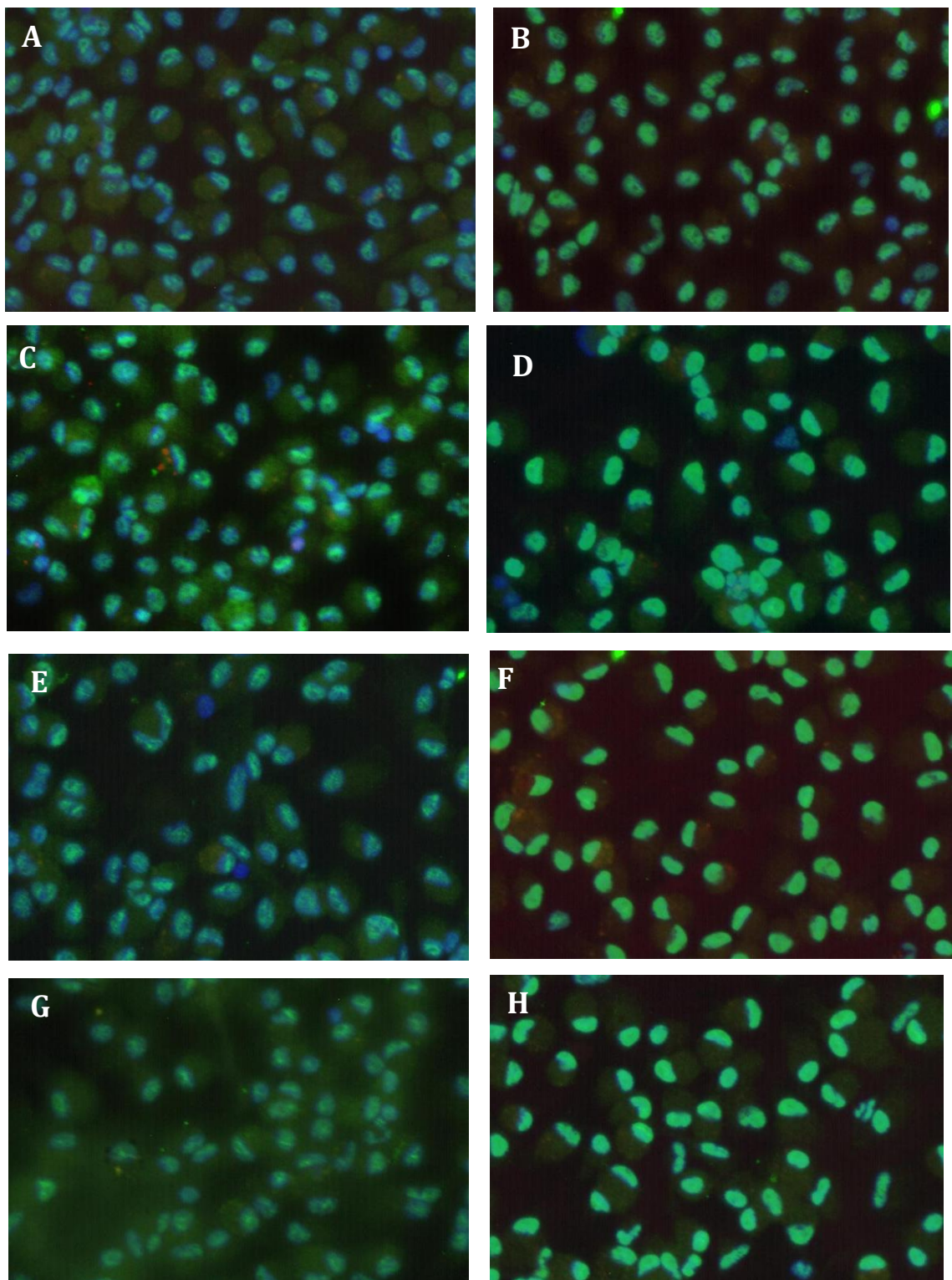
**Figure 4.13: Glucocorticoid receptors translocation in alveolar macrophages:** alveolar macrophages from a non-smoker subject (N=1) (A) were either pretreated with dexamethasone (1µM) (B), infected with NTHi (10:1 MOI) (C), or both (D). Cells were also pretreated with BIRB-796 (1µM) alone (E) or in combination with dexamethasone (F), BIRB-796 pretreated cells were infected with NTHi (G), and the combined BIRB-796 and dexamethasone pretreatment was also followed by NTHi infection (H). Cells were fixed and immunostained for glucocorticoid receptors. Cells nuclei were counterstained with 4', 6-diamidino-2-phenylindole (blue). GR Immunofluorescence (green) was detected by

fluorescence microscope and GR localisation in the cells was classified as cytoplasmic, cytoplasmic and nuclear or nuclear. Magnification power is 20X.

## 4.4. Discussion:

In this chapter, corticosteroid responsiveness of NTHi-induced inflammation in alveolar macrophages was investigated in my NTHi *in vitro* model of infection. LPS model was used alongside NTHi model, as it is a well-established model of inflammation in COPD and was previously tested for corticosteroid sensitivity (168,397). Dexamethasone is a synthetic corticosteroid and is widely used *in vitro* to investigate corticosteroid responsiveness of different inflammatory elements in COPD and asthma (133,168,349,422). I have demonstrated that both NTHi and LPS-induced TNF-α, IL-6 and IL-10 were corticosteroid-responsive cytokines both in COPD and smokers' alveolar macrophages. However, there was only "partial suppression" of these cytokines, even at high corticosteroid concentrations. LPS-induced cytokines showed significantly greater corticosteroid responsiveness than NTHi (Figure 4.6, Table 4.4). CXCL8, which is a known neutrophil chemoattractant (3), was not inhibited by dexamethasone in the NTHi model but was inhibited by more than 50% in LPS model. NTHi-induced CXCL8 from COPD alveolar macrophages was further induced by dexamethasone, however, the percentage induction was small. This effect on CXCL8 is an experimental variability as it is not consistent at different dexamethasone concentration. The reported CXCL8 relative insensitivity to dexamethasone agrees with other papers from our laboratory which show that LPS-stimulated CXCL8 secretion has a relatively poor sensitivity to corticosteroids in comparison to other cytokines including TNF-α, and that LPS-induced cytokines secretion is only "partially sensitive" to corticosteroids (168,349,350). In addition, one study using live clinical isolate of NTHi by Literas et al. have also reported corticosteroid responsiveness of NTHi-induced TNF-α in murine alveolar macrophages (133).

In the current study, there was no significant difference between alveolar macrophages from COPD and smokers in NTHi and LPS-induced cytokine release, which was similarly highlighted in LPS stimulated cytokines in alveolar macrophages from COPD and non-COPD controls (168,349,397). However, importantly, I have reported a difference in corticosteroid responsiveness between COPD and smokers in NTHi–induced cytokines at 100:1 MOI. I observed that TNF-α had less corticosteroid responsiveness in COPD alveolar macrophages than smokers' alveolar macrophages. These findings agree with previously reported lower corticosteroid responsiveness in COPD macrophages (167). In contrast, at 10:1 MOI, I reported more IL-6 corticosteroid responsiveness in COPD alveolar macrophages. Although the magnitude of these between-group differences was small (<20% approximately) and not consistently observed at each concentration, which might reflect sample size. Overall, these findings suggest no major difference in corticosteroid sensitivity between groups. Additionally, there was no difference in corticosteroid response between COPD and smokers in LPS model, which agrees with previous observations (168).

The dexamethasone response findings can be interpreted in the clinical context of corticosteroid therapy in the presence of NTHi infection, which may occur during the stable state (colonisation), or during exacerbations. Previous experiments using LPS have shown partial suppression of cytokines by corticosteroids. The LPS model probably overestimates corticosteroid effects "in real life", as my experiments using NTHi showed a lower effect of corticosteroids. Furthermore, CXCL8 secretion was completely corticosteroid insensitive, meaning that these drugs will not supress this mechanism that promotes neutrophilic inflammations. Overall, the experiments shown in this chapter using NTHi indicate

that corticosteroids have minimal effects on bacterial induced inflammatory response by macrophages. This is compatible with the anecdotal clinical observation that corticosteroids have no clinical benefit during bacterial infection.

Investigation of signalling pathways of NTHi infection in COPD would help in understanding the immunological basis of infection and could help to identify potential therapeutic targets. In COPD alveolar macrophages, I have used NTHi at 10:1 MOI as it showed significant inflammatory response. I observed that NTHi activated the transcription factor NF-κB at the beginning of infection, with more prolonged activation of p38 and ERK MAPK signalling pathways. My findings are in agreement with the previously reported NF-κB, p38 and ERK MAPK activation in human epithelial cells by NTHi lysate (373,375).

In human epithelial cells, NTHi activation of NF-κB has been linked to TNF-α, CXCL8 and IL-1β release (373). Meanwhile, NTHi activation of p38 and ERK MAPK was identified as a mediator for CXCL8 release (375). To further investigate the biological role of the NTHi-activated pathways in COPD alveolar macrophages, I used specific inhibitors of NF-κB, p38 and ERK MAPK pathways, the mode of their action is outlined in Figure (4.14).
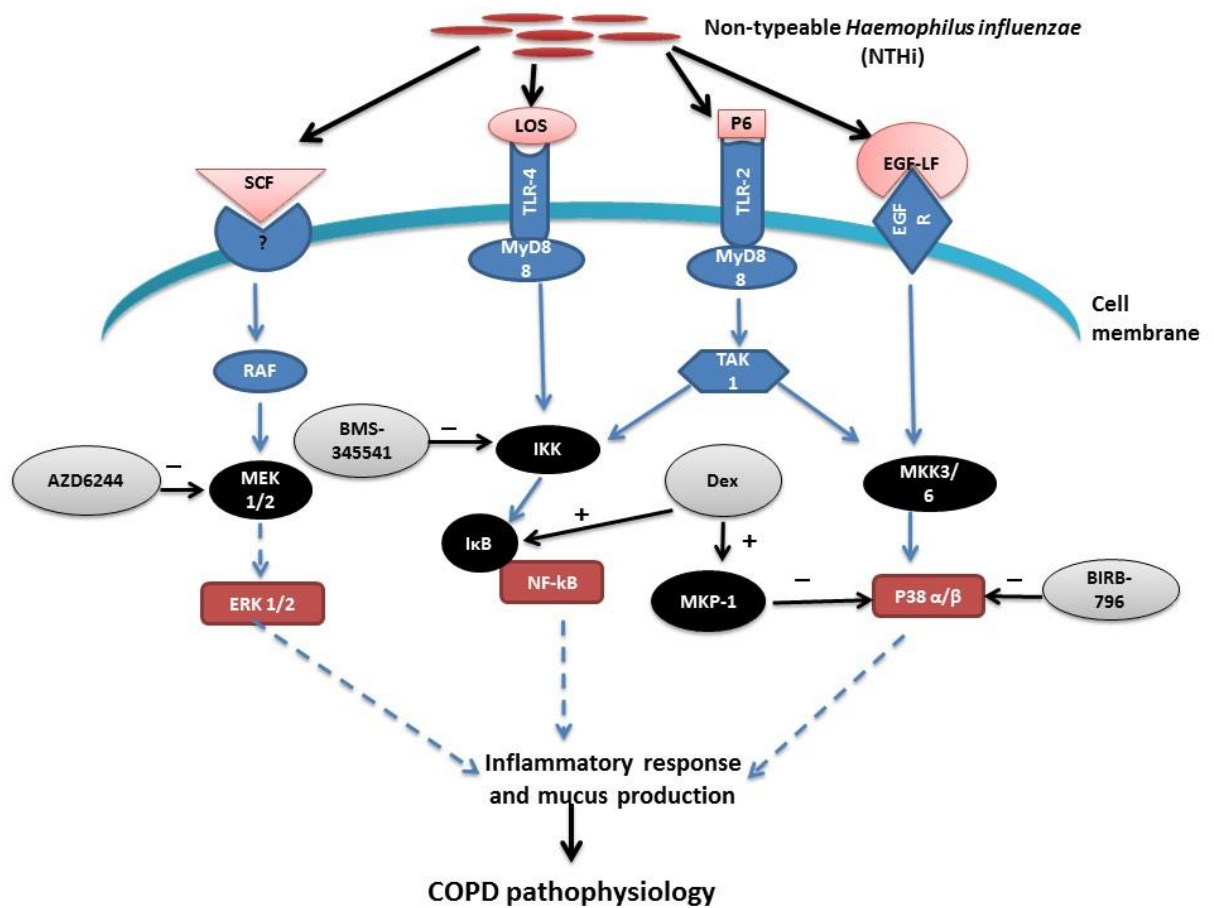
**Figure 4.14: Modulation of NTHi-activated signalling pathways by dexamethasone and kinase inhibitors**: The binding of NTHi ligands to different receptors on the cell membrane activates different intracellular signalling pathways. The activated pathways mediate airway inflammation. Dexamethasone might inhibit NF-κB and p38 MAPK through the transactivation of their inhibitory molecules, IκB and MKP-1 respectively. BIRB-796 inhibits the p38 MAPK pathway. AZD6244 inhibits MKK1/2, the upstream kinases of ERK MAPK. BMS345541 inhibits IKK, the upstream kinase of IκB resulting in the inhibition of NF-κB. += Activation, -= Inhibition, dashed arrows represent inhibited pathway. LOS= Lipooligosaccharide, SCF= Soluble cytoplasmic fraction, P6= Outer membrane protein P6, EGFLF= Epidermal growth factor like factor, TLR= Toll-like receptors, EGFR= Epidermal growth factor receptor, RAF= Rapidly accelerated fibrosarcoma kinase, ERK= Extracellular signal- regulated Kinase, IKK= IκB kinase, NF-κB= Nuclear factor-κB, TAK1= TGF-β activated kinase 1, MKK= Mitogen- activated protein kinase kinase.

BMS-345541 is a selective inhibitor of IKK2, the enzyme which activates NF-κB. The anti-inflammatory potency of BMS-345541 was experimentally proven *in vivo* and *in vitro* (439,440). In my model, BMS-345541 unexpectedly showed no pharmacological activity in inhibition of NTHi-induced p65 phosphorylation and cytokine release from COPD alveolar macrophages. Further assessment of the pharmacological activity of BMS-345541 in human alveolar macrophages is required. This might include testing the inhibitor activity in some models of inflammation that involve NF-κB activation like NTHi and LPS models. Also, assessment of BMS-345541 activity might involve testing a wider range of BMS-34551 concentration. In the view of the time limitation in the current study, I did not use this inhibitor in my further experiments

p38MAPK mediates inflammation in COPD, and is known to be upregulated in the COPD lung (329). *In vivo* inhibition of p38 MAPK inhibition by SB-681323 showed potential anti-inflammatory effect in COPD patients (441). Furthermore, *in vitro* inhibition of p38 MAPK by SB706504 significantly inhibited a panel of LPS-activated inflammatory genes in MDMs from COPD (350). In this model, I have used a p38 MAPK inhibitor (BIRB-796), which is a selective and potent inhibitor of p38MAPK (442,443). It showed pharmacological inhibition of NTHi-induced p38 phosphorylation. BIRB-796 caused inhibition of NTHi-induced TNF-α in COPD alveolar macrophages. Likewise, BIRB-796 was recently shown to inhibit LPS induced TNF-α, IL-6 and CXCL8 in COPD and non-COPD alveolar macrophages (349).

ERK MAPK inhibitor (AZD6244) is a highly selective inhibitor of MEK1/2, which are the upstream kinases of ERK. The biological potency of AZD6244 has been tested in cell lines and *in vivo* tumour models (444–446). In my model, I confirmed its pharmacological activity by inhibition of NTHi-induced ERK phosphorylation. I

observed that AZD6244 caused inhibition of NTHi-induced TNF-α. Similarly, Wang et al. have reported ERK inhibition by PD 98059 and UO 126 to decrease NTHi-induced CXCL8 release from human epithelial cells (375). My results imply that p38 and ERK MAPK are critical pathways in mediating NTHi-induced inflammation in COPD alveolar macrophages.

Corticosteroids exert their anti-inflammatory action by different mechanisms, involving transactivation and transrepression of the key inflammatory genes (447). Evidence supports the corticosteroid inhibitory effect on transcription factors, such as NF-κB, through the transactivation of its inhibitory molecule IκB. Moreover, corticosteroids transactivate MKP-1, which inactivates MAPK pathways (447,448). Based on these facts, I investigated dexamethasone effect on NTHi-activated pathways in my model. At the highest tested concentration, dexamethasone did not show any inhibitory effect on NTHi-activated p65, p38 and ERK MAPK phosphorylation, which could be one explanation for the limited dexamethasone effect in my NTHi infection model.

Long term corticosteroid therapy has been linked to some adverse effects like hypertension, glucose intolerance and cataract (2,55,449). The combination of lower doses of corticosteroids with other anti-inflammatory drugs could help to reduce the incidence of side effects (349). Previous *in vitro* study in asthma patient had reported a combined anti-inflammatory effect of dexamethasone and the p38 inhibitors, SD282 and GW-A, in alveolar macrophages and PBMCs (450). I next tried to test this strategy in my NTHi model of inflammation. I observed that the combination of dexamethasone and inhibitors of p38 (BIRB-796) and ERK (AZD6244) MAPK caused significantly higher cytokine inhibition than monotherapies. These results agreed with Armstrong et al. who reported a

synergistic anti-inflammatory effect of dexamethasone and BIRB-796 in LPS-stimulated COPD alveolar macrophages (349). These findings further confirm the important role of p38 and ERK MAPK in NTHi induced cytokine release in COPD alveolar macrophages.

Corticosteroid action is mediated by GR. It is well known that corticosteroids and different inflammatory stimuli cause GR phosphorylation at different sites (386). GR phosphorylation state would govern its cellular localisation, DNA binding, cofactor interaction and receptor stability (390). Thus, I studied the effect of NTHi on GR phosphorylation in my model. I found that NTHi (but not LPS) caused significant GR phosphorylation at serine 226 residue. This phosphorylation site was reported to reduce GR nuclear localisation, and hence less glucocorticoids transcriptional activity (386). This finding pointed to the possible effect of NTHi on GR cellular localisation. Therefore, I studied GR nuclear translocation in alveolar macrophages from a non-smoker subject. NTHi caused more cytoplasmic localisation of GR than the unstimulated state. Furthermore, NTHi impaired dexamethasone-induced GR nuclear localisation. These results concur with NTHi-induced GR phosphorylation at ser 226, and indicate that NTHi lower airway infection could reduce GR nuclear localisation and hence impair the anti-inflammatory effect of the administered corticosteroid. Nevertheless, the use of cells from a non-smoker in this experiment might not necessarily reflect the corticosteroid response in COPD patients. Therefore, further investigation of NTHi effect on GR translocation in COPD and normal smokers would be more disease relevant.

Evidence suggests the role of p38 MAPK in corticosteroid insensitive asthma patients, through p38 MAPK-mediated GR phosphorylation (346). Inhibition of p38

MAPK was found to improve dexamethasone sensitivity in PBMCs from severe asthmatics (348). In my model, I observed that NTHi-induced GR ser 226 phosphorylation could be, in part, p38 MAPK mediated. This observation was further confirmed by the combined effect of BIRB-796 with dexamethasone in improving GR nuclear translocation in alveolar macrophages infected with NTHi. The effect of BIRB-796 on GR translocation indicates that p38 MAPK is an important mediator of corticosteroid unresponsiveness, and inhibition of this pathway could synergistically improve corticosteroid responses in NTHi-induced inflammation in COPD.

Taken together, my results revealed the following:

- Impaired corticosteroid responsiveness of NTHi-induced inflammatory cytokines in COPD alveolar macrophages; CXCL8 was the most corticosteroid unresponsive cytokine.

- NTHi-induced GR phosphorylation at ser 226 is a possible mechanism of reduced corticosteroid responsiveness in COPD alveolar macrophages.

- p38 and ERK MAPK pathways mediated NTHi-induced inflammation in COPD alveolar macrophages.

- p38 MAPK modified GR phosphorylation and nuclear localisation in NTHi-infected alveolar macrophages. Therefore, inhibition of MAPK pathways improved corticosteroid unresponsiveness, either by synergistic or additive anti-inflammatory effect.

# Chapter Five

# Alveolar Macrophage Functional Polarisation in Response to NTHi Infection

---

## 5.1. Introduction:

Alveolar macrophage functional polarisation has been recently investigated in the pathogenesis of COPD (129,140). A growing body of evidence suggests dysregulated M1/M2 macrophage function in COPD. This macrophage dysfunction is characterised by ongoing inflammation and tissue damage, in parallel with impaired anti-inflammatory function, pathogen phagocytosis and efferocytosis (121,134,135,140). Nevertheless, all investigations have referred to cigarette smoking as the driving factor for modulated macrophage polarisation, without any reference to the role of airway bacterial pathogens (129,140).

M1 phenotype is characterised by the release of pro-inflammatory molecules like TNF-α, IL-6, CXCL8, and upregulation of the antigen presentation molecule HLA-DR. These molecules are important in bacterial recognition and killing (121,140,451,452). On the other hand, M2 phenotype is characterised by the release of anti-inflammatory molecules like IL-10 and TGFβ, and upregulation of phagocytic markers like MR and CD36. The M2 molecules are important in the resolution of inflammation (121,123,452,453).

Investigations of the molecular mechanism of different bacterial infections in humans have identified dysregulated macrophage phenotype at the site of infection, which is a key determinant of the fate of infection (122). The M1 signature was identified during the acute phase of some bacterial infections, which is believed to control infection by releasing pro-inflammatory cytokines and bactericidal molecules (454,455). Meanwhile, the M2 signature was identified during the chronic phase of infection which is believed to aid bacterial survival and evolution of the chronic infection state (456–458). In the context of lung diseases, *Mycobacterium tuberculosis* (the cause of pulmonary tuberculosis) was reported to modify

macrophage phenotype by inducing more immunoregulatory M2. This phenotype can permit bacterial intracellular survival and chronic persistence in the host (459). Apparently, no similar investigation has been carried out on NTHi pulmonary infection.

NTHi has a substantial role in COPD exacerbations and disease progression (213,420). It can overcome host innate immunity and persist in the lower airways, causing a state of chronic colonisation (437). However, the molecular mechanisms of NTHi chronicity are not fully understood.

In this chapter, I hypothesised that NTHi infection can modulate alveolar macrophage polarisation to facilitate survival inside the lung. The main aim was to study the effect of NTHi on the mRNA levels of a group of M1/M2 markers. Moreover, I aimed to investigate the effect of NTHi airway infection on the polarisation of sputum macrophages from NTHi-colonised COPD patients versus non-infected control subjects.

## 5.2. Materials and Methods:

### 5.2.1. Study subjects:

Patients were recruited for two sets of experiments. In the first set, lung alveolar macrophage phenotypes were investigated the *in vitro* model of NTHi infection. For this experiment, six COPD patients undergoing lung resection surgery for suspected or confirmed lung cancer were recruited (see Table 5.1 for full demographics). In the second set, sputum macrophage phenotypes in NTHi-infected COPD patients and non-infected controls were studied. For this experiment, eight healthy non-smokers and fifteen COPD patients were recruited for sputum induction (see Table 5.2 for full demographics). In either set of experiments, patients were diagnosed as COPD (according to GOLD criteria) (38) and they were mixed population of current and ex-smokers. In the sputum macrophage experiment, COPD patients were sub-grouped according to presence or absence of NTHi infection in the sputum sample. Written informed consents were obtained from all patients and the research was approved by South Manchester Research Ethics Committee.

**Table 5.1:** **Patients' demographic data** (alveolar macrophage phenotype experiment).

| Criteria | COPD |
|---|---|
| COPD history (COPD/non-COPD) | (6/0) |
| Smoking history (Current/Ex) | (4/2) |
| Gender (male/female) | (4/2) |
| Age (years) | 67.3±3.9 |
| FEV1 (L) | 2.1±0.6 |
| FEV1% predicted | 72.8±13.1 |
| FVC (L) | 3.5±0.5 |
| FEV1/FVC ratio (%) | 53.9±11.2 |
| Pack-year history | 39.6±6.0 |

Data are presented as mean±SD. FEV1= Forced expiratory volume in 1 second, FVC= Forced vital capacity, L= Litre.

**Table 5.2:** **Patients' demographic data** (sputum macrophage phenotype experiment).

| Criteria | COPD | | P value | Non-smokers (HNS) | P value |
|---|---|---|---|---|---|
| | NTHi-infected | Non infected | NTHi-infected Vs non-infected COPD | | HNS Vs COPD |
| Number | 8 | 7 | | 8 | |
| Smoking history (Current/Ex) | (1/7) | (2/5) | | NA | |
| Gender (male/female) | (8/0) | (6/1) | | (6/2) | |
| Age (years) | 71.25±5.7 | 68.14±3.9 | NS | 53.38±15.9 | P<0.05 |
| Pack-year history | 45.46±14.7 | 50.04±26.6 | NS | NA | |
| Exacerbation history in last 12 months | 1.4±1 | 1.6±0.7 | NS | NA | |
| Steroid use (yes/No) | (7/1) | (5/2) | | NA | |
| Sputum bacterial load (CFU/ml of sample) | 4.45x10$^7$±4.5 | NA | | NA | |
| **Pre- bronchodilator lung function** | | | | | |
| FEV1 (L) | 1.31±0.4 | 1.40±0.5 | NS | 3.84±0.9 | P<0.001 |
| FEV1% predicted | 42.82±10.5 | 53.63±22.4 | NS | 115.61±16.8 | P<0.001 |
| FVC (L) | 3.11 ±0.4 | 3.18±0.8 | NS | 4.91±0.99 | P<0.001 Vs NTHi infected P<0.01 Vs non-infected |
| FEV1/FVC ratio (%) | 41.44 ±8.5 | 43.60±10.0 | NS | 77.75±5.9 | P<0.001 |

Data are presented as mean±SD. Difference between groups was assessed by unpaired t-test. FEV1= Forced expiratory volume in 1 second, FVC= Forced vital capacity, HNS= Healthy non-smoker, NA= Not applicable, NS= Non-significant, L= Litre.

## 5.2.2. Effect of NTHi on *in vitro* alveolar macrophage M1/M2 phenotype markers expression:

Alveolar macrophages from COPD patients were cultured on 24 well culture plates at $4 \times 10^5$ cells per well and incubated at $37\ ^{o}C$ and 5% $CO_2$ for 24 hours. Non-adherent cells were washed with pre-warmed RPMI 1640 media without antibiotics. Adherent cells were incubated with NTHi (R2846) (at 10:1 and 100:1 MOI), LPS (1μg/ml), or left untreated for 24 hours at $37\ ^{o}C$ and 5% $CO_2$. After 2, 6 and 24 hours of incubation, cells were lysed by RLT lysis buffer containing 1% 2-mercaptoethanol. The cell lysates were stored at $-80\ ^{o}C$ for future RNA extraction and analysis of M1/M2 markers' mRNA by qPCR, as detailed in materials and methods chapter in section 2.7. mRNA levels were normalised to the housekeeping gene GAPDH, and levels after stimulation were compared to unstimulated levels and expressed as fold change from time-matched unstimulated control using Δ Δ Ct method.

## 5.2.3. Effect of airway NTHi infection on sputum macrophage M1/M2 phenotype markers expression:

Sputum was induced from COPD patients and healthy non-smokers. Alveolar macrophages were isolated as detailed in materials and methods chapter in section 2.1.2. Cells were plated on 6 well culture plates at a concentration of $1 \times 10^6$ cells per well and cultured for 24 hours at $37\ ^{\circ}C$, 5% CO2 to enable macrophage adherence. Non-adherent cells were washed by supplemented RPMI 1640 and the adherent macrophages were lysed by RLT lysis buffer containing 1% 2-mercaptoethanol. The lysates were frozen at $-80\ ^{\circ}C$ for future RNA extraction and M1/M2 mRNA analysis by qPCR as detailed in materials and methods chapter in section 2.7. Relative expression levels were determined using the ΔCt method normalising to the housekeeping gene (GAPDH).

### 5.2.4. Statistics:

Normality of data was assessed by Kolmogorov-Smirnov test. Comparison of demographic data between NTHi-infected COPD and non-infected controls was performed by unpaired t-test (two-tailed). Data of TNF-$\alpha$, CXCL8, CD38, HLA-DR, IL-10, CD36, CD206, CD14 and CD163 markers mRNA level were nonparametrically distributed. The NTHi and LPS effects on these markers were assessed separately. For each model, the mRNA levels of M1/M2 markers at 2, 6 and 24 hours were compared versus time-matched unstimulated control by Friedman test with Dunn's multiple comparisons test. The difference between LPS and NTHi-induced mRNA levels of all markers were assessed by Friedman test with Dunn's multiple comparisons test.

Data for all sputum macrophage markers were nonparametrically distributed, except for HLA-DR. Differences between COPD and healthy controls, and between NTHi-infected and non-infected COPD were assessed by Mann-Whitney test (two-tailed). The difference between groups in HLA-DR mRNA levels was assessed by unpaired t-test (two-tailed). For all comparisons, $p < 0.05$ was considered statistically significant.

## 5.3. Results:

### 5.3.1. Effect of NTHi on M1/M2 markers' mRNA levels in COPD alveolar macrophages:

Alveolar macrophages from COPD patients (N=6) were incubated with NTHi (R2846) (at 10:1 and 100:1), LPS (1µg/ml) or left untreated. Cells were lysed after 2, 6 and 24 hours of stimulation, and studied for a panel of M1/M2 markers' mRNA levels by RT-PCR. The studied M1/M2 markers are: the pro-inflammatory cytokines (TNF-α and CXCL8), CD38, HLA-DR, the anti-inflammatory cytokine (IL-10) and the scavenger receptors (CD36, Mannose receptor C1 (MRC1or CD206), CD14 and CD163).

### 5.3.1.1. Effect of NTHi on pro-inflammatory cytokines' (TNF-α and CXCL8) mRNA levels:

NTHi (at both MOIs) caused significant upregulation of TNF-α mRNA level after 2 hours, and after 6 hours in comparison to time-matched unstimulated control ($p<0.05$, $p<0.001$ respectively, Figure 5.1 A). Similarly, LPS increased TNF-α mRNA level after 2 hours and 6 hours ($p<0.05$, $p<0.01$ respectively).

NTHi (at both MOIs) increased CXCL8 mRNA level significantly after 6 and 24 hours in comparison to time-matched unstimulated control ($p<0.05$, $p<0.01$ respectively, Figure 5.1 B). Also, LPS caused significant upregulation of CXCL8 mRNA level after 6 and 24 hours ($p<0.01$).
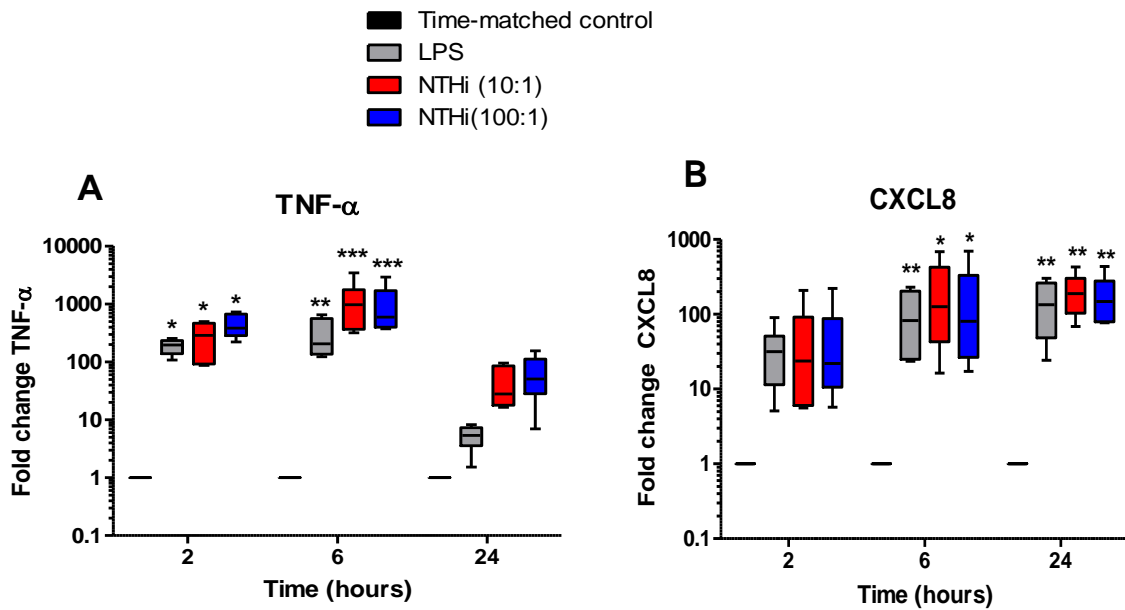
**Figure 5.1: Effect of NTHi on TNF-α and CXCL8 mRNA levels in COPD alveolar macrophages**. Alveolar macrophages from COPD patients (N=6) were infected with NTHi (at MOI of 10:1 and 100:1), stimulated with LPS (1μg/ml) or left untreated. Cells were lysed at 2, 6 and 24 hours of infection. RNAs were extracted and mRNA levels of TNF-α (A), CXCL8 (B) were assessed by RT-PCR. Data are presented as median with interquartile range and total range. *, **, *** represent a significant difference from time-matched unstimulated control ($p<0.05$, $<0.01$, $<0.001$ respectively, Friedman test followed by Dunn's multiple comparisons test). Relative expression levels were determined using the ΔΔCt method normalising to the housekeeping gene (GAPDH).

### 5.3.1.2. Effect of NTHi on CD38 mRNA levels.

NTHi (at both MOIs) significantly upregulated CD38 mRNA levels compared to time-matched unstimulated control after 6 hours of infection (p<0.01). After 24 hours, NTHi at 10:1 significantly increased CD38 mRNA level above time-matched unstimulated control (p<0.05, Figure 5.2). LPS stimulation caused a significant increase in CD38 mRNA levels at 6 and 24 hours (p<0.05, p<0.001 respectively). LPS-induced CD38 mRNA levels were significantly greater compared to that induced by NTHi (at 100:1 MOI) after 24 hours (p<0.05).
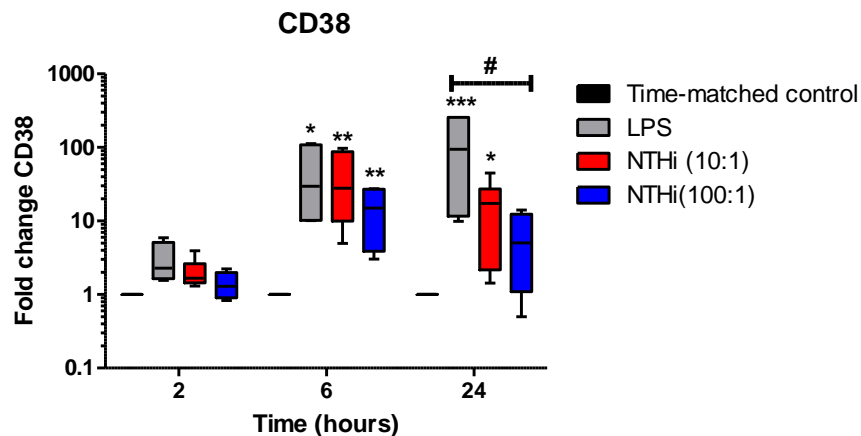


**Figure 5.2:** **Effect of NTHi on CD38 mRNA levels in COPD alveolar macrophages**. Alveolar macrophages from COPD patients (N=6) were infected with NTHi (at MOI of 10:1 and 100:1), stimulated with LPS (1µg/ml) or left untreated. Cells were lysed at 2, 6 and 24 hours of infection. RNAs were extracted and CD38 mRNA levels were assessed by RT-PCR. Data are presented as median with interquartile range and total range. *, **, *** represent a significant difference from time-matched unstimulated control (p<0.05, <0.01, <0.001 respectively, Friedman test followed by Dunn's multiple comparisons test). # represents a significant difference between LPS and NTHi models (p<0.05, Friedman test followed by Dunn's multiple comparisons test). Relative expression levels were determined using the ΔΔCt method normalising to the housekeeping gene (GAPDH).

### 5.3.1.3. Effect of NTHi on HLA-DR mRNA levels.

HLA-DR mRNA levels were significantly reduced below time-matched control after 24 hours by NTHi (at both MOI) ($p < 0.05$, Figure 5.3). LPS did not alter HLA-DR mRNA level levels at any time point.
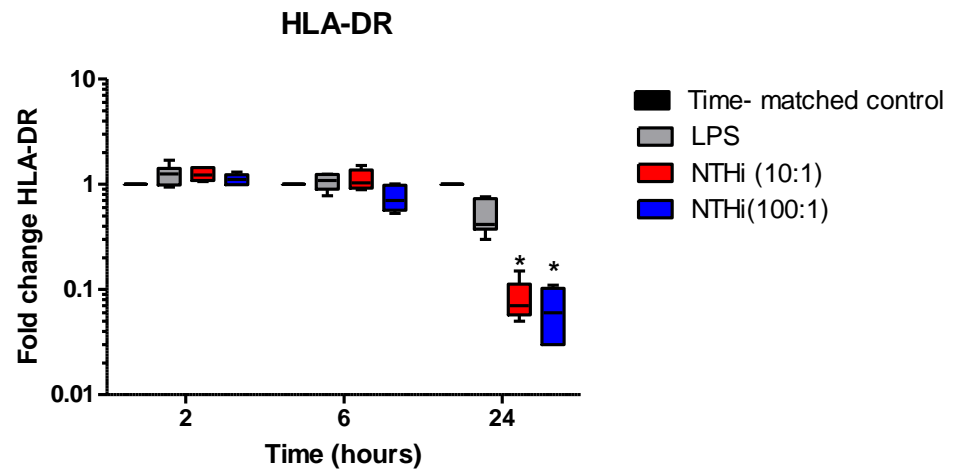


**Figure 5.3: Effect of NTHi on HLA-DR mRNA levels in COPD alveolar macrophages.** Alveolar macrophages from COPD patients (N=6) were infected with NTHi (at MOI of 10:1 and 100:1), stimulated with LPS (1µg/ml) or left untreated. Cells were lysed at 2, 6 and 24 hours of infection. RNAs were extracted and HLA-DR mRNA levels were assessed by RT-PCR. Data are presented as median with interquartile range and total range. * represent a significant difference from time-matched unstimulated control ($p < 0.05$, Friedman test followed by Dunn's multiple comparisons test). Relative expression levels were determined using the ΔΔCt method normalising to the housekeeping gene (GAPDH).

### 5.3.1.4. Effect of NTHi on IL-10 mRNA levels.

NTHi *in vitro* infection resulted in a significant upregulation of IL-10 mRNA levels above time-matched unstimulated control after 6hours (at both MOI) ($p<0.01$) and after 24 hours (at 10:1 MOI) ($p<0.05$, Figure 5.4). LPS caused significant increase in IL-10 mRNA levels above time-matched unstimulated control at 6 hours ($p<0.01$).
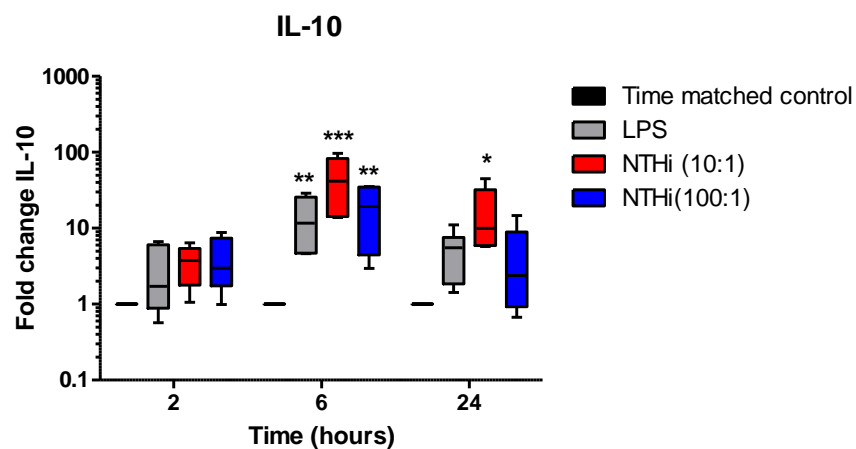


**Figure 5.4:** **Effect of NTHi on IL-10 mRNA levels in COPD alveolar macrophages**. Alveolar macrophages from COPD patients (N=6) were infected with NTHi (at MOI of 10:1 and 100:1), stimulated with LPS (1µg/ml) or left untreated. Cells were lysed at 2, 6 and 24 hours of infection. RNAs were extracted and IL-10 mRNA levels were assessed by RT-PCR. Data are presented as median with interquartile range and total range. *, **, *** represent a significant difference from time-matched unstimulated control ($p<0.05$, $<0.01$, $<0.001$ respectively, Friedman test followed by Dunn's multiple comparisons test). Relative expression levels were determined using the ΔΔCt method normalising to the housekeeping gene (GAPDH).

### 5.3.1.5. Effect of NTHi on scavenger receptors (CD36, MRC1 (CD206), CD14 and CD163) mRNA levels.

CD36 and mannose receptor (CD206) mRNA levels were significantly downregulated compared to time-matched unstimulated controls by NTHi (at both MOI) after 24 hours ($p < 0.05$, Figure 5.5 A, B respectively). LPS caused a significant decrease in CD36 mRNA level at 24 hours compared to time-matched unstimulated controls ($p < 0.05$, Figure 5.5 A).

CD14 mRNA levels were significantly downregulated compared to time-matched unstimulated controls at 24 hours by NTHi at both MOI ($p < 0.05$, Figure 5.5 C). In contrast, LPS appeared to increased CD14 mRNA levels by 2.4 fold (range 0.5-4.1) at 24 hours, however, this increase did not reach statistical significance. LPS-induced CD14 mRNA levels were significantly greater than those induced by NTHi (at 100:1 MOI) after 24 hours ($p < 0.001$).

CD163 mRNA levels were significantly downregulated by NTHi (at both MOI) as compared to time-matched unstimulated controls after 24 hours ($p < 0.05$, Figure 5.5 D). Meanwhile, LPS did not affect CD163 mRNA levels at all-time points.
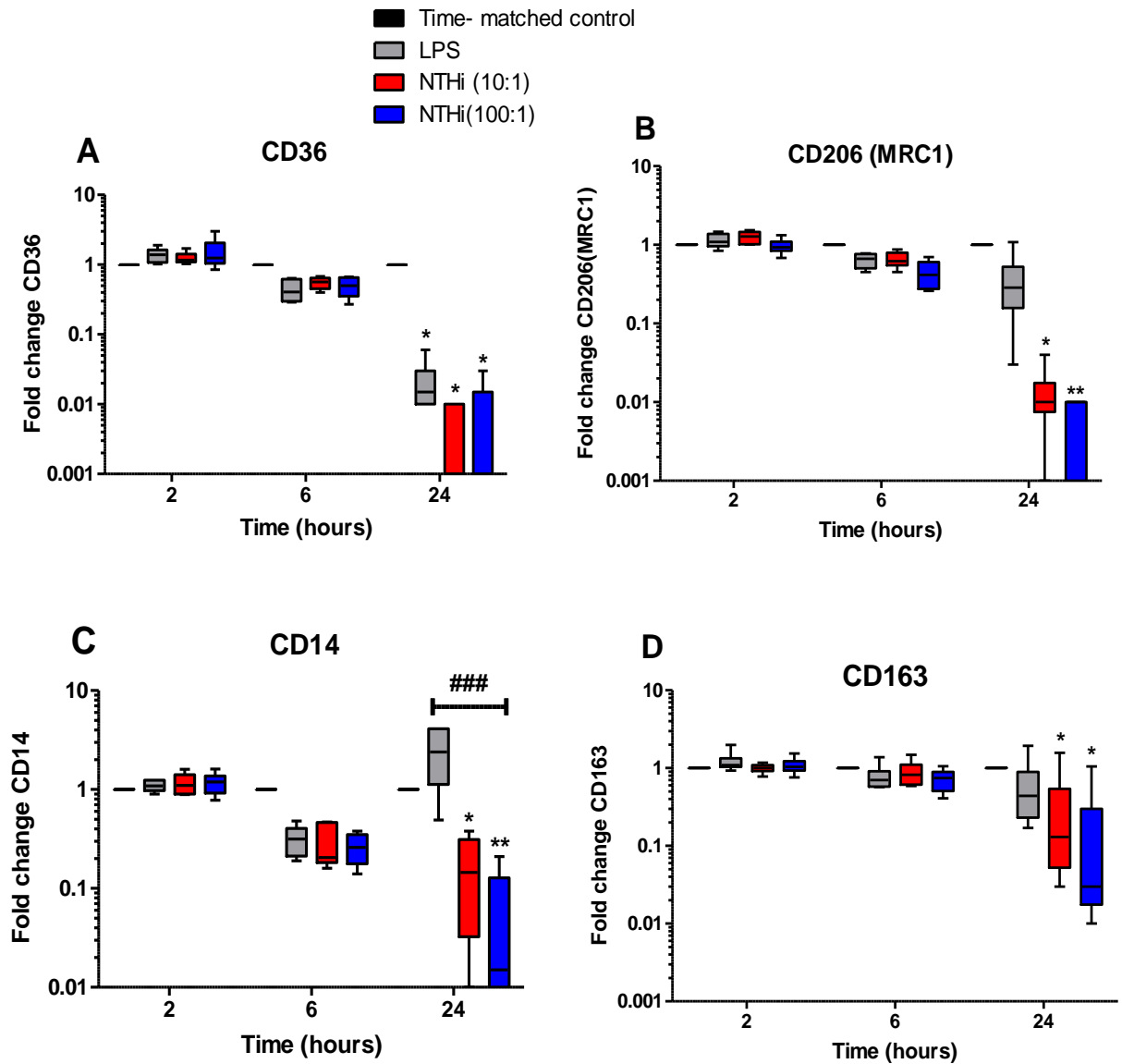
**Figure 5.5: Effect of NTHi on scavenger receptors' mRNA levels in COPD alveolar macrophages**. Alveolar macrophages from COPD patients (N=6) were infected with NTHi (at MOI of 10:1 and 100:1), stimulated with LPS (1μg/ml) or left untreated. Cells were lysed at 2, 6 and 24 hours of infection. RNAs were extracted and the mRNA levels of CD36 (A), CD206 (MRC1) (B), CD14 (C) and CD163 (D) were assessed by RT-PCR. Data are presented as median with interquartile range and total range. *, ** represent a significant difference from time-matched unstimulated control (p<0.05, <0.01 respectively Friedman test followed by Dunn's multiple comparisons test. ### represents a significant difference between LPS and NTHi models (p<0.001, Friedman test followed by Dunn's multiple comparisons test). Relative expression levels were determined using the ΔΔCt method normalising to the housekeeping gene (GAPDH).

232

### 5.3.2. Effect of NTHi airway infection on M1/M2 markers' mRNA levels in sputum macrophages from COPD and healthy controls.

Macrophages were isolated from induced sputum samples of COPD patients (N=15) and healthy non-smokers (N=8). Eight out of fifteen COPD patients were confirmed to have NTHi infection as detailed in materials and methods chapter in section 2.3. The remaining seven COPD patients as well as the healthy controls showed no growth of potentially pathogenic bacteria. Sputum macrophages were lysed and studied by qPCR for M1/M2 markers' mRNA levels as detailed in methods chapter in section 2.7.

### 5.3.2.1. TNF-α and CXCL8 mRNA levels in NTHi-infected COPD patients and non-infected controls:

There was no difference in TNF-α mRNA levels between COPD subjects and healthy non-smokers (Figure 5.6 A). Similarly, there was no difference between NTHi-infected and non-infected COPD in TNF-α mRNA levels (Figure 5.6 B).



**Figure 5.6:** **Effect of NTHi airway infection on TNF-α mRNA levels in sputum macrophages from COPD and healthy controls**. Macrophages were isolated from induced sputum of 15 COPD and 8 HNS (A). COPD subjects were categorised into NTHi-infected COPD (N=8) and non-infected COPD (N=7) (B). RNAs were extracted and the mRNA levels of TNF- α were assessed by RT-PCR. Data are presented as median with interquartile range and total range. Comparison between COPD and HNS, NTHi-infected and Non-infected COPD was performed by Mann-Whitney test. Relative expression levels were determined using the ΔCt method normalising to the housekeeping gene (GAPDH). HNS= healthy non-smoker.

CXCL8 mRNA levels were not different between COPD and healthy non-smokers (Figure 5.7 A). In addition, there was no difference between NTHi-infected and non-infected COPD subjects (Figure 5.7 B).
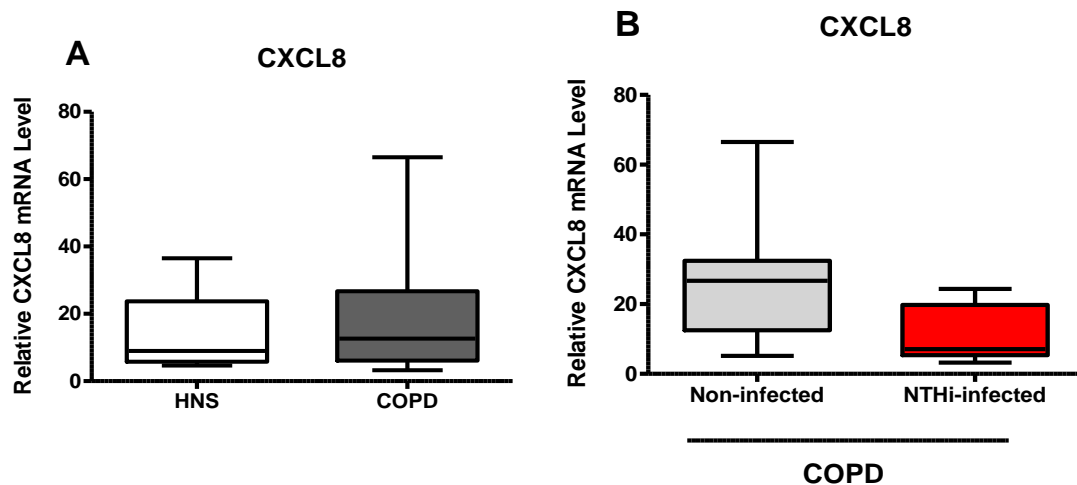


**Figure 5.7:** **Effect of NTHi airway infection on CXCL8 mRNA levels in sputum macrophages from COPD and healthy controls**. Macrophages were isolated from induced sputum of 15 COPD and 8 healthy non-smokers (A). COPD subjects were categorised into NTHi-infected COPD (N=8) and non-infected COPD (N=7) (B). RNAs were extracted and the mRNA levels of CXCL8 were assessed by RT-PCR. Data are presented as median with interquartile range and total range. Comparison between COPD and HNS, NTHi-infected and Non-infected COPD was performed by Mann-Whitney test. Relative expression levels were determined using the ΔCt method normalising to the housekeeping gene (GAPDH). HNS= healthy non-smoker.

### 5.3.2.2. CD38 mRNA levels in NTHi-infected COPD patients and non-infected controls:

There was no difference in CD38 mRNA levels in sputum macrophages from COPD subjects compared to healthy non-smokers (Figure 5.8 A). In addition, there was no difference in sputum macrophage CD38 mRNA levels between NTHi-infected and non-infected COPD patients (Figure 5.8 B).
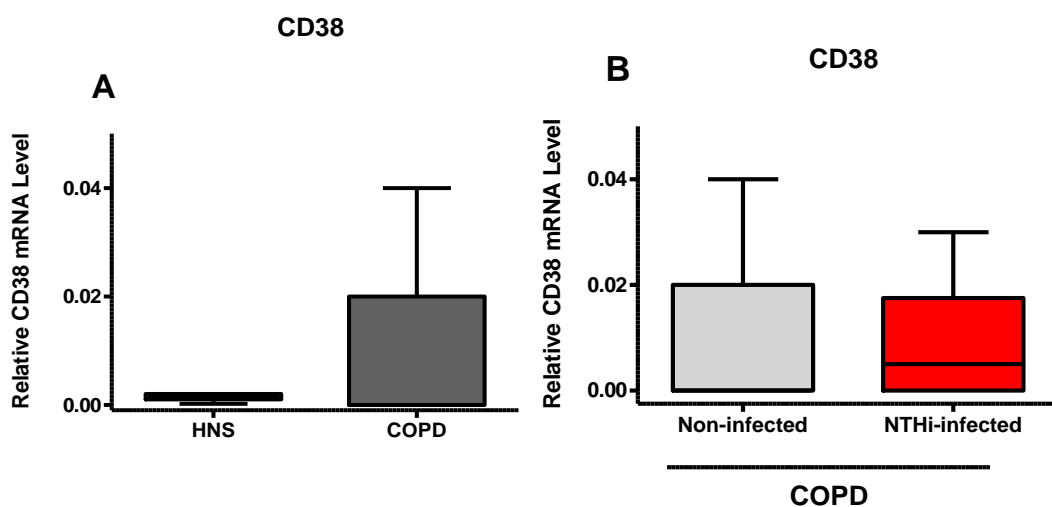


**Figure 5.8:** **Effect of NTHi airway infection on CD38 mRNA levels in sputum macrophages from COPD and healthy controls**. Macrophages were isolated from induced sputum of 15 COPD and 8 healthy non-smokers (A). COPD subjects were categorised into NTHi-infected COPD (N=8) and non-infected COPD (N=7) (B). RNAs were extracted and the mRNA levels of CD38 were assessed by RT-PCR. Data are presented as median with interquartile range and total range. Comparison between COPD and HNS, NTHi-infected and Non-infected COPD was performed by Mann-Whitney test. Relative expression levels were determined using the ΔCt method normalising to the housekeeping gene (GAPDH). HNS= healthy non-smoker.

### 5.3.2.3. HLA-DR mRNA levels in NTHi-infected COPD patients and non-infected controls:

COPD sputum macrophages HLA-DR mRNA levels were not different from healthy non-smokers (Figure 5.9 A). However, NTHi-infected COPD subjects showed significantly lower HLA-DR mRNA levels than non-infected COPD (p=0.02, Figure 5.9 B).
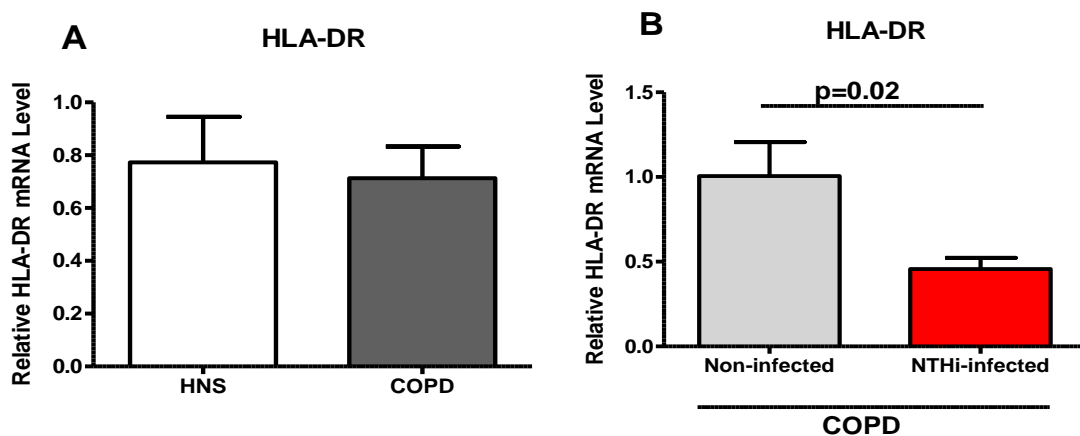


**Figure 5.9:** **Effect of NTHi airway infection on HLA-DR mRNA levels in sputum macrophages from COPD and healthy controls**. Macrophages were isolated from induced sputum of 15 COPD and 8 healthy non-smokers (A). COPD subjects were categorised into NTHi-infected COPD (N=8) and non-infected COPD (N=7) (B). RNAs were extracted and the mRNA levels of HLA-DR were assessed by RT-PCR. Data are presented as mean+SEM. Comparison between COPD and HNS, NTHi-infected and Non-infected COPD was performed by unpaired t-test test. Relative expression levels were determined using the ΔCt method normalising to the housekeeping gene (GAPDH). HNS= healthy non-smoker.

### 5.3.2.4. IL-10 mRNA levels in NTHi-infected COPD patients and non-infected controls:

There was no difference between groups in IL-10 mRNA levels (Figure 5.10 A, B)
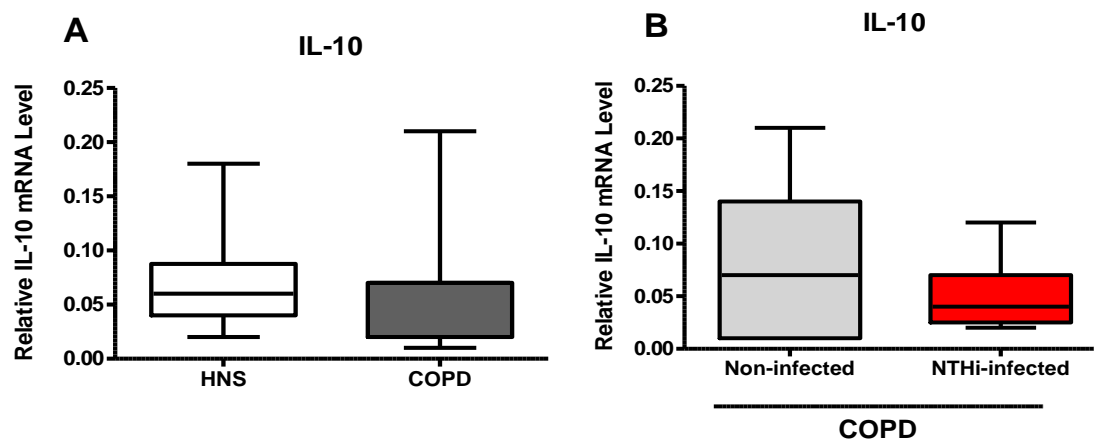


**Figure 5.10: Effect of NTHi airway infection on IL-10 mRNA levels in sputum macrophages from COPD and healthy controls**. Macrophages were isolated from induced sputum of 15 COPD and 8 healthy non-smokers (A). COPD subjects were categorised into NTHi-infected COPD (N=8) and non-infected COPD (N=7) (B). RNAs were extracted and the mRNA levels of IL-10 were assessed by RT-PCR. Data are presented as median with interquartile range and total range. Comparison between COPD and HNS, NTHi-infected and Non-infected COPD was performed by Mann-Whitney test. Relative expression levels were determined using the ΔCt method normalising to the housekeeping gene (GAPDH). HNS= healthy non-smoker.

.

### 5.3.2.5. Scavenger receptors (CD36, MRC1 (CD206), CD14 and CD163) mRNA levels in NTHi-infected COPD patients and non-infected controls:

CD36 mRNA levels in COPD sputum macrophages were not different from healthy non-smokers (Figure 5.11 A). However, CD36 mRNA levels in NTHi-infected COPD subjects were significantly lower than non-infected COPD (p=0.04, Figure 5.11 B).
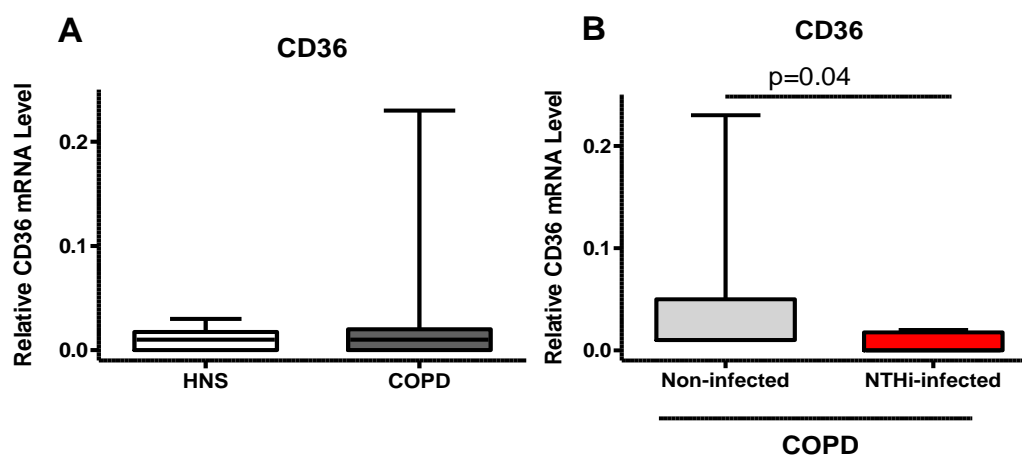


**Figure 5.11: Effect of NTHi airway infection on CD36 mRNA levels in sputum macrophages from COPD and healthy controls**. Macrophages were isolated from induced sputum of 15 COPD and 8 healthy non-smokers (A). COPD subjects were categorised into NTHi-infected COPD (N=8) and non-infected COPD (N=7) (B). RNAs were extracted and the mRNA levels of CD36 were assessed by RT-PCR. Data are presented as median with interquartile range and total range. Comparison between COPD and HNS, NTHi-infected and Non-infected COPD was performed by Mann-Whitney test. Relative expression levels were determined using the ΔCt method normalising to the housekeeping gene (GAPDH). HNS= healthy non-smoker.

COPD sputum macrophages showed significantly higher MRC1 (CD206) mRNA levels than healthy non-smokers (p=0.04, Figure 5.12 A). However, there was no difference between NTHi-infected COPD and non-infected COPD patients (Figure 5.12 B).
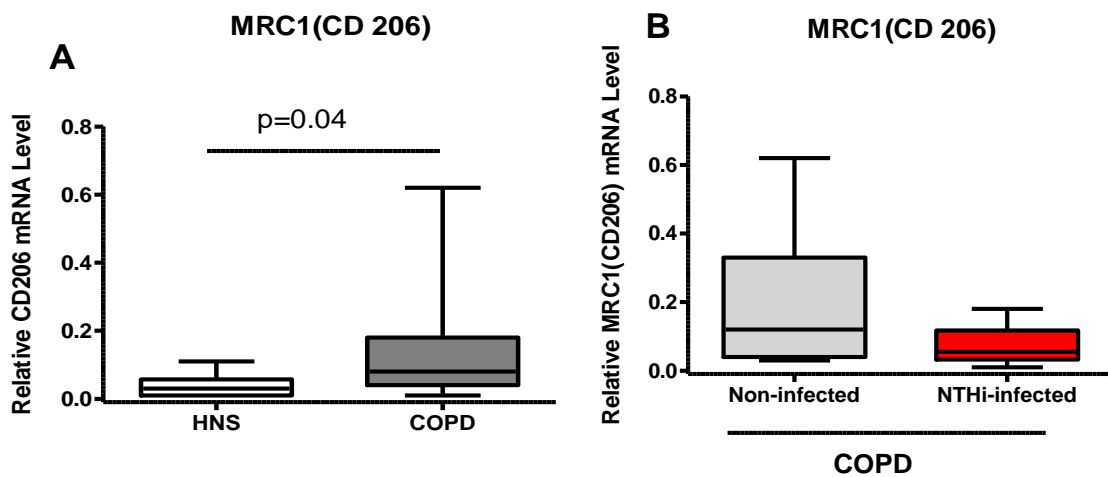


**Figure 5.12:** **Effect of NTHi airway infection on CD206 (MRC1) mRNA levels in sputum macrophages from COPD and healthy controls**. Macrophages were isolated from induced sputum of 15 COPD and 8 healthy non-smokers (A). COPD subjects were categorised into NTHi-infected COPD (N=8) and non-infected COPD (N=7) (B). RNAs were extracted and the mRNA levels of MRC1 (CD206) were assessed by RT-PCR. Data are presented as median with interquartile range and total range. Comparison between COPD and HNS, NTHi-infected and Non-infected COPD was performed by Mann-Whitney test. Relative expression levels were determined using the ΔCt method normalising to the housekeeping gene (GAPDH). HNS= healthy non-smoker.

There was no difference between groups in CD14 mRNA level (Figure 5.13 A, B).
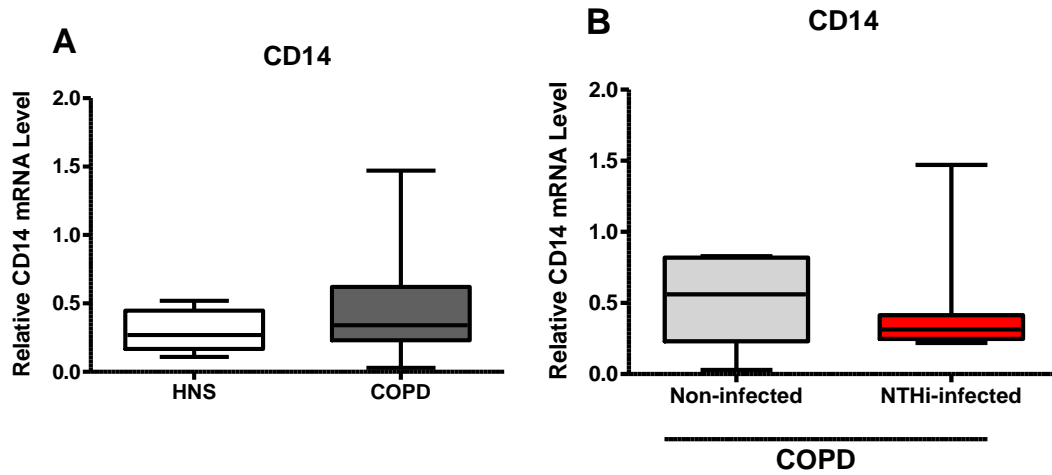


**Figure 5.13:** **Effect of NTHi airway infection on CD14 mRNA levels in sputum macrophages from COPD and healthy controls**. Macrophages were isolated from induced sputum of 15 COPD and 8 healthy non-smokers (A). COPD subjects were categorised into NTHi-infected COPD (N=8) and non-infected COPD (N=7) (B). RNAs were extracted and the mRNA levels of CD14 were assessed by RT-PCR. Data are presented as median with interquartile range and total range. Comparison between COPD and HNS, NTHi-infected and Non-infected COPD was performed by Mann-Whitney test. Relative expression levels were determined using the ΔCt method normalising to the housekeeping gene (GAPDH). HNS= healthy non-smoker.

CD163 mRNA was significantly upregulated in COPD patients as compared to healthy non-smokers (p=0.009, Figure 5.14 A). Nonetheless, there was no difference between NTHi-infected and non-infected COPD patients in CD163 mRNA levels (Figure 5.14 B).
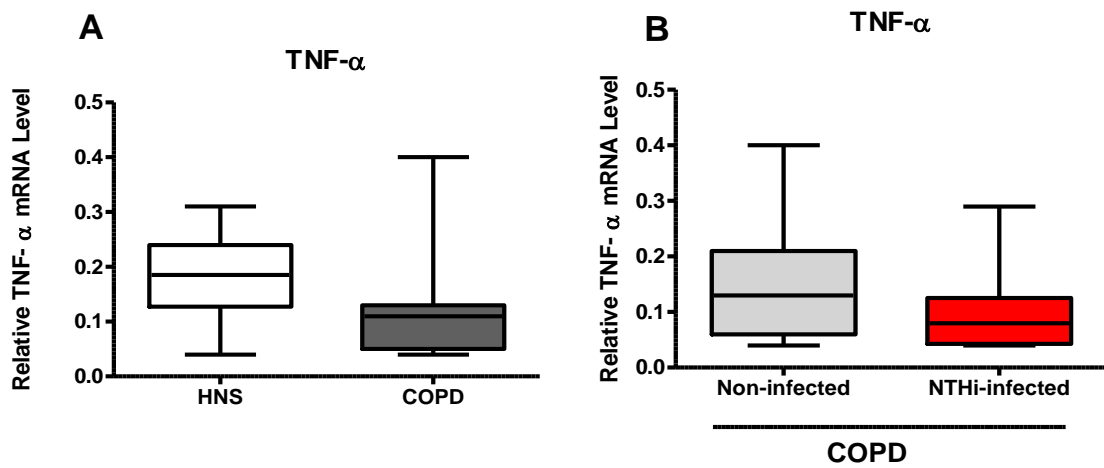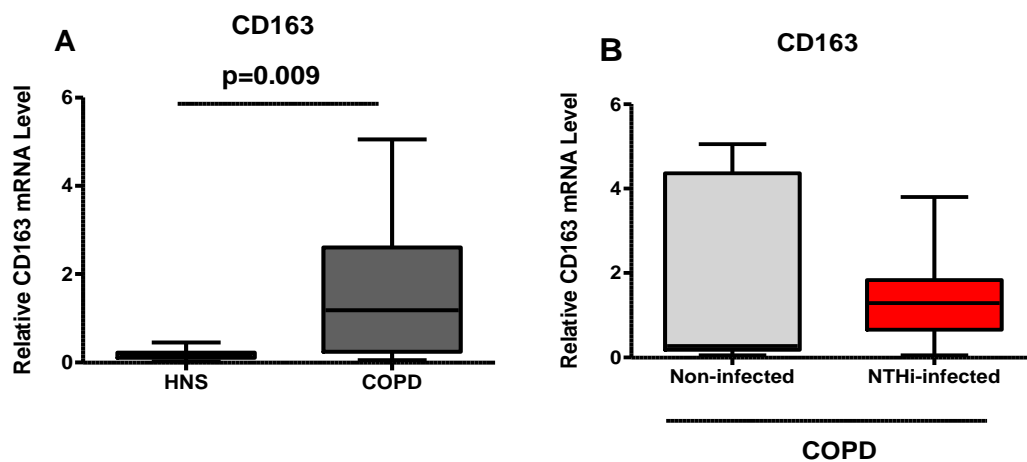


**Figure 5.14:** **Effect of NTHi airway infection on CD163 mRNA levels in sputum macrophages from COPD and healthy controls**. Macrophages were isolated from induced sputum of 15 COPD and 8 healthy non-smokers (A). COPD subjects were categorised into NTHi-infected COPD (N=8) and non-infected COPD (N=7) (B). RNAs were extracted and the mRNA levels of CD163 were assessed by RT-PCR. Data are presented as median with interquartile range and total range. Comparison between COPD and HNS, NTHi-infected and Non-infected COPD was performed by Mann-Whitney test. Relative expression levels were determined using the $\Delta Ct$ method normalising to the housekeeping gene (GAPDH). HNS= healthy non-smoker.

## 5.4. Discussion:

In this chapter, I have studied alveolar macrophage functional programming in response to NTHi infection. In my *in vitro* model of infection, NTHi induced alveolar macrophage dysfunction through modification of M1/M2 related molecules. Of these modified molecules, HLA-DR and CD36 were also identified in sputum macrophages from NTHi-infected COPD subjects.

In some human infections, bacterial pathogens have the tendency to overcome the host innate immune response and survive its hostile environment. These bacteria can cause chronic diseases which might represent a treatment challenge. Investigations of mechanisms behind the chronicity of important human infections, like *M.tuberculosis, Salmonella typhi* and *Brucella abortus* revealed the ability of the bacteria to interfere with the microbicidal M1 function (460–462), and might induce M2 immunoregulatory program to survive inside the host (459). Nonetheless, no similar investigations were performed in airway bacterial infection relevant to COPD.

I monitored a group of markers which reflect a plethora of M1/M2 functions in response to NTHi infection. To do that, I ran two parallel settings of NTHi infection in COPD. Firstly, I used my clinically relevant *in vitro* model to monitor the first 24 hours of NTHi infection, which could represent the acute phase response to infection. Secondly, I have studied sputum macrophages phenotype markers in COPD patients who had positive sputum culture for NTHi. Those patients were not exacerbating at the time of sampling in spite of positive NTHi culture. Therefore, I considered those patients as chronically infected with NTHi.

Pro-inflammation is a hallmark of M1 phenotype that is characterised by the release of pro-inflammatory cytokines and chemokines to protect the host against

the invading pathogen. I reported an upregulation of the pro-inflammatory mediators, TNF-α and CXCL8, during the first 24 hours of NTHi infection. These findings parallel my previously reported time-dependent release of these cytokines (refer to chapter three), and in agreement with the reported M1 polarisation in the acute phase of mycobacterial infection in mice (463). In addition, it is well known that macrophages show a robust M1 response to a diverse group of bacteria. This response is called core response to infection (122,464). These data indicate that alveolar macrophages respond to acute NTHi infection by expressing M1 related molecules, which could control the early stage of infection. In contrast to the *in vitro* findings, I did not observe any upregulation in TNF-α and CXCL8 mRNA levels in NTHi-infected COPD patients versus non-infected controls. As mentioned above, my COPD cohort had no exacerbation at the time of sampling. So I speculate that NTHi is resident in the airways for a relatively longer period of time and hence less reported acute phase M1 markers.

CD38 is transmembrane glycoprotein which has an enzymatic function involved in regulation of intracellular calcium levels (465). CD38 is expressed by various cells as macrophages (466), neutrophils (467), lymphocytes (466) and airway smooth muscle cells (468). Evidence suggests that CD38 plays a role in macrophage phagocytosis (469), cytokine release (470), neutrophil chemotaxis (467) and smooth muscle contraction (471). Moreover, CD38 was found to mediate airway hyperresponsiveness and airway inflammation in asthma studies (470,471). However, the role of CD38 in COPD pathogenesis is not fully described. I showed that NTHi upregulated CD38 mRNA levels in COPD alveolar macrophages *in vitro.* Moreover, LPS caused more upregulation of CD38 mRNA level than that induced by NTHi. This observation agrees with the previous finding by Lee et al, who

demonstrated that LPS caused time-dependent upregulation of CD38 genes in murine alveolar macrophages (466). On the other hand, CD38 expression in NTHi-infected COPD sputum macrophages was not different from non-infected controls. These data suggest that NTHi could only activate CD38 during the early phase of infection causing more pro-inflammatory response.

HLA-DR is a cell surface glycoprotein expressed by macrophages, and it is involved in antigen presentation (472,473). HLA-DR expression by macrophages reflect their activation state (474), and downregulation of HLA-DR was linked to the development of immune tolerance (143). I found that NTHi caused significant downregulation of HLA-DR mRNA levels in COPD alveolar macrophages. Furthermore, sputum macrophages from COPD patients were not different from non-smokers in HLA-DR mRNA levels. However, NTHi-infected COPD patients showed significantly lower expression of HLA-DR than non-infected COPD patients. My results differ from that by Pons and colleagues (141). They reported reduced HLA-DR surface expression in BAL-derived COPD alveolar macrophages in comparison to smokers and non-smokers. However, they did not refer to the airway colonisation state in their work, which might be one contributing factor for the reduced HLA-DR expression (141). My data indicate that NTHi exposure caused HLA-DR downregulation over time, which could favour NTHi persistence in the lower airways.

M2 macrophages are known for their anti-inflammatory function, which is reflected by the release of anti-inflammatory mediators like IL-10 and TGF-β (452,453). The role of M2 derived IL-10 has been recognised in the chronic development of human mycobacterial infections (457,458). NTHi caused IL-10 upregulation in COPD alveolar macrophages *in vitro*. However, IL-10 expression by

sputum macrophages from NTHi-infected patients was similar to non-infected controls. This suggests that NTHi could stimulate IL-10 only to modulate the early acute pro-inflammatory response to survive in the airways.

Another function of M2 macrophage is phagocytosis of pathogens, debris and apoptotic cells (efferocytosis). A number of surface receptors are implicated in this function, including CD36, MRC1 (CD206), CD14 and CD163 (475–478).

CD36 is a membrane scavenger receptor involved in phagocytosis of pathogens (476,479), apoptotic neutrophils and epithelial cells  (efferocytosis) (480,481). This process is essential in limiting tissue damage and in the resolution of inflammation. Efferocytosis was reported to be impaired in COPD (140,185). However, lung tissue, MDMs and alveolar macrophages expression of CD36 in COPD was similar to healthy controls(134,141,482). I reported that NTHi infection *in vitro* caused downregulation of CD36 mRNA levels in COPD alveolar macrophages. In addition, sputum macrophages from NTHi-infected COPD patients had lower expression of CD36 than non-infected controls. These findings disagree with Sharif et al, who reported CD36 expression to be increased by *Streptococcus pneumoniae* in murine alveolar macrophages especially after 24 hours of infection (476). This contradicting finding might be explained by the use of different cell type and bacterial species in this study. My results suggest that NTHi could perpetuate airway inflammation by negative regulation of macrophage efferocytosis.

MRC1 (CD206) is implicated in pathogen phagocytosis (483) and efferocytosis (484). Moreover, evidence suggested its immunoregulatory role in *Pneumocystis* infection in human (475). The expression of CD206 was found to be impaired in COPD alveolar macrophages (484). However, it was identified to be overexpressed in severe COPD and thought to play a role in disease pathogenesis

(485). NTHi *in vitro* infection caused significant reduction inCD206 mRNA Levels in COPD alveolar macrophages. On the other hand, sputum macrophages from COPD subjects showed higher expression of CD206 than healthy non-smokers, with no difference between NTHi-infected and non-infected COPD patients. These data suggest that CD206 downregulation could be one virulent mechanism adapted by NTHi to resist bacterial clearance during the acute phase of infection and persist inside the airways for a longer period of time. Furthermore, CD206 upregulation in sputum macrophages could be attributed to the disease process in the COPD lung rather than NTHi chronic lower airway infection.

CD14 is another macrophage receptor implicated in the recognition of bacterial LPS and internalisation of bacteria (477,486,487). In addition, it mediates bacteria-induced airway inflammation and lung injury (488). The soluble form of CD14 was found to be increased in BAL fluid from COPD patients (487). In the data presented here, NTHi caused significant downregulation of CD14 mRNA levels in COPD alveolar macrophages. This finding was similar to that of Francis et al, who highlighted the effect of NTHi on reduced mRNA levels of CD14 in COPD monocytes and polymorphonuclear leukocytes (489). On the other hand, I did not find a difference in CD14 mRNA levels in sputum macrophages from NTHi-infected and non-infected controls, which is in agreement with the previous reports in alveolar macrophages and MDMs from COPD and healthy controls (134,141). I speculate that downregulation of CD14 during the early NTHi infection could be another mechanism of its airway colonisation. Of note, LPS caused upregulation of CD14 mRNA levels which was significantly greater than the NTHi effect. The latter finding suggests different mechanisms of modulating macrophage function in LPS versus NTHi models of inflammation.

CD163 scavenger receptor is known for its homeostatic functions by removing free haemoglobin and protecting the tissue from its damaging effect (490). Also, it has been identified as an innate immune sensor of gram positive and gram negative bacteria and mediator of bacteria-induced inflammation (478). CD163 positive macrophages were identified in tuberculous granulomas in monkeys (491). Moreover, higher CD163 expression by COPD macrophages was negatively correlated to FEV1 (485). I observed that NTHi caused downregulation of CD163 mRNA levels in COPD alveolar macrophages. This could be one possible mechanism to evade innate immune response early in the course of infection. Sputum macrophages from COPD patients showed higher CD163 expression than non-smokers with no difference between NTHi-infected and non-infected COPD. These findings agree with Kaku et al., who observed higher CD163 expression in macrophages from COPD lungs than healthy controls. However, they did not investigate the possible role of airway bacterial infection in their findings (485). My results suggest that NTHi is still recognised by alveolar macrophages in the COPD lung by CD163 in spite of impaired phagocytosis, and this might be responsible for ongoing airway inflammation with persistence of NTHi.

Overall, my findings suggest that NTHi could change alveolar macrophage phenotype markers and ultimately function at the site of infection to evade innate immune response and persist in the airways. Impaired phagocytosis and antigen presentation functions of alveolar macrophages could be one mechanism adapted by NTHi to survive in the airways. In addition, NTHi could impair efferocytosis function of alveolar macrophages which might result in ongoing airway inflammation and, may be, disease progression.

# Chapter Six

# General Discussion

## 6.1. Thesis aim:

COPD is an airway inflammatory disease where many patients have recurrent lower airway bacterial infection, often NTHi (420,437). Corticosteroids are the most widely used anti-inflammatory drugs in COPD; their primary role is exacerbation reduction (50,391,394). Previous *in vitro* studies using alveolar macrophages that focused on corticosteroid responsiveness in COPD have generally not considered the role of airway NTHi infection.

The general aim of this thesis was to investigate NTHi-induced inflammation in COPD alveolar macrophages using a clinically relevant *in vitro* model and to test corticosteroid responsiveness in this model. Furthermore, I studied NTHi- induced alveolar macrophage phenotype modification as a possible virulence mechanism in COPD.

## 6.2. NTHi versus LPS model in alveolar macrophage studies

Investigations of bacterial infection using COPD alveolar macrophages have previously applied bacterial antigens as an inflammatory stimulus. The most commonly applied bacterial antigen in COPD studies is LPS, which is purified from *E. coli* (168,350,397). In chapter three of this thesis, I have established a clinically relevant *in vitro* model of NTHi infection, using a live clinical isolate (R2846) in human alveolar macrophage cell cultures. Live NTHi (R2846) caused greater cytokine secretion than LPS, possibly due to the dynamic growth of NHTi. The NTHi model is obviously resembles the real life situation more closely than using LPS. To further validate my model, I tested the alveolar macrophage inflammatory response to four NTHi isolates from the airways of stable COPD patients. Cytokine induction

by clinical isolates was generally similar to that induced by the standard strain (R2846).

My results in chapter four showed that NTHi-infected alveolar macrophages were less corticosteroid-responsive than LPS-stimulated cells (Table 4.4, Figure 4.6). NTHi-induced CXCL8 was a particularly unresponsive cytokine. NTHi, but not LPS, caused GR phosphorylation at ser 226 residue, which would encourage GR exportation from the nucleus. These differences indicate that the inflammatory mechanism of live NTHi infection is different from LPS, causing a different corticosteroid response between the two models.

The NTHi modulation of M1/M2 markers' mRNA levels is distinct from that induced by LPS. Chapter five data showed that LPS caused upregulation of CD38 mRNA levels more than the upregulation caused by NTHi. In addition, NTHi downregulated HLA-DR, CD206 and CD163 mRNA. Meanwhile, LPS had not effect on these markers. Notably, NTHi downregulated CD14 mRNA in contrast to LPS which appeared to increase CD14 mRNA levels. My overall findings in chapter three, four and five add weight to the clinical relevance of the NTHi model versus LPS model in COPD research

The differences between LPS and NTHi *in vitro* models might be attributed to various bacterial elements (LOS, OMP P6, SCF, EGFLF and TGFLF) which bind to different cell surface receptors (TLR2, TLR4, EGFR, TGFβR and PAF). The activation of these receptors will, in turn, activate various intracellular signaling pathways. This could result in the reported different inflammatory response between the two models. The main differences between the two models are summarised in Figure 6.1.
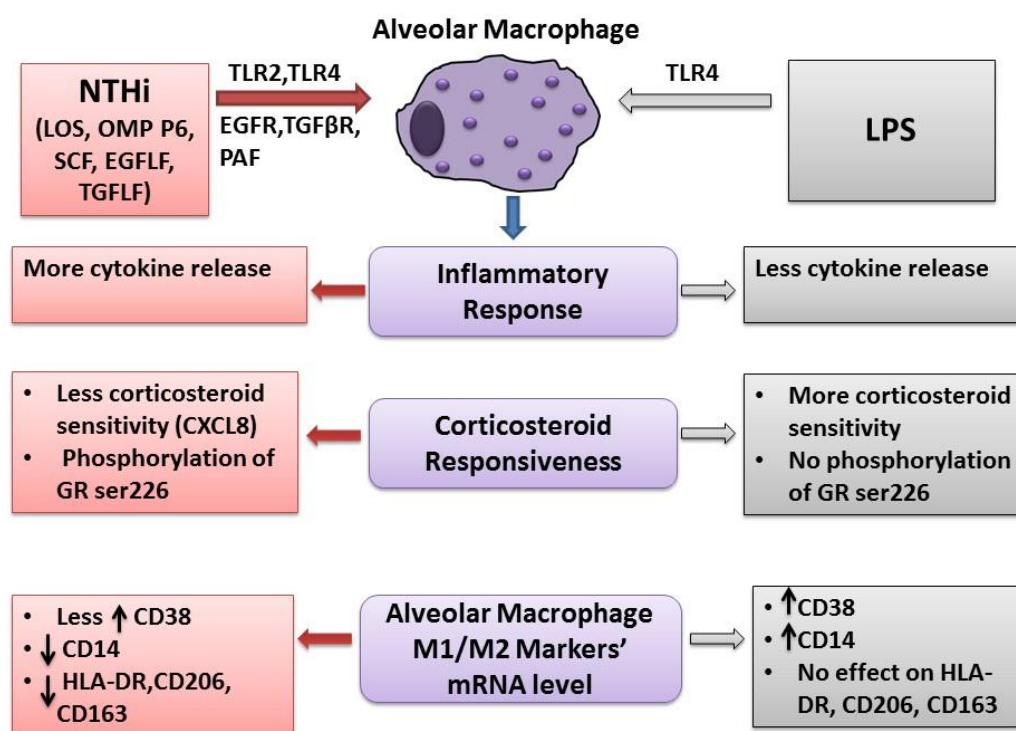
**Figure 6.1: LPS versus NTHi *in vitro* models of stimulation in the human alveolar macrophage.** LPS induces cytokine release from alveolar macrophages by binding to TLR4 receptors. The LPS-induced cytokines are relatively corticosteroid sensitive. NTHi antigenic molecules (LOS, OMP P6, SCF, EGFLF and TGFLF) bind to different cell receptors including TLR2, TLR4, EGFR, TGF-βR and PAF receptors. The activation of these receptors by NTHi ligands might be the cause of higher cytokine release than the LPS model. The NTHi-induced cytokines are less corticosteroid sensitive, CXCL8 is completely corticosteroid resistant. NTHi modulation of M1/M2 markers mRNA levels is different from the modulation induced by LPS. NTHi causes downregulation of HLA-DR and scavenger receptors. LPS= Lipopolysaccharide, NTHi= Nontypeable *Haemophilus influenzae,* LOS= Lipooligosaccharide, OMP P6= Outer membrane protein P6, SCF= Soluble cytoplasmic fraction, EGFLF= Epidermal growth factor like factor, TGFLF= Transforming growth factor like factor, PAF= Platelet-activating factor, TLR= Toll-like receptors, EGFR= Epidermal growth factor receptor, TGF-βR= Transforming growth factor-β receptor, GR= Glucocorticoid receptor, ser 226= Serine 226 residue, CXCL8= Chemokine C-X-C Motif Ligand 8, CD= Cluster of differentiation, HLA-DR= Human leukocyte antigen-DR.

252

## 6.3. The practicability of NTHi *in vitro* model of stimulation.

NTHi is a fastidious microorganism (195), requiring consistent growth conditions throughout the experiment. Accidental changes in the incubator temperature or rotation rate during incubation time can affect bacterial growth. Also, extra caution should be taken while handling more than one bacterial species (NTHi and *E. coli*), or when processing sputum samples and pure NTHi cultures at the same time, to avoid contamination of pure culture plates. Another practical point is the relatively longer time of preparation of NTHi suspension; at least two days are required to grow NTHi from frozen stock to bacterial suspension in the stationary phase of growth. This relatively long time of preparation resulted in less chance of running experiments per week than LPS model. Therefore, NTHi *in vitro* model of stimulation is feasible but less practicable than LPS model. On the other hand, LPS is less clinically relevant to COPD than NTHi.

## 6.4. IL-10; possible role in NTHi lower airway colonisation.

IL-10 is known for its immunoregulatory role in the lung. It antagonises TNF-α and inhibits cell apoptosis (423). Some bacteria exploit IL-10 to survive the hostile host environment (425,426). In chapter three, I showed an inverse correlation between NTHi load and IL-10 release; lower MOIs caused more IL-10 release than higher MOIs. This finding implies that NTHi at lower concentrations could stimulate considerable IL-10 release in the lung to subvert the pro-inflammatory host response. Furthermore, IL-10 could help in the intracellular survival of NTHi by reducing cell apoptosis (427,428). Therefore, IL-10 could be further investigated as a mechanism that promotes lower airway colonisation by NTHi in COPD.

## 6.5. NTHi infection impairs corticosteroid responsiveness in COPD patients.

Previous clinical and *in vitro* studies highlighted the corticosteroid unresponsiveness of inflammatory cells in COPD airways (167,168,395), but no attention was paid to the possibility of lower airway NTHi infection in corticosteroid unresponsive patients. In chapter four, I showed that NTHi-induced cytokines from alveolar macrophages were less corticosteroid-responsive, particularly CXCL8, which showed minimal response to corticosteroids. This finding suggests that the lungs of NTHi-infected COPD patients have an ongoing recruitment of neutrophils in spite of corticosteroid therapy, causing progressive tissue damage and airway obstruction. I further confirmed the role of NTHi in possible corticosteroid unresponsiveness by showing its phosphorylation of GR at ser 226 residue and its impairment of corticosteroid-induced GR nuclear localisation. From the above findings, it would be important to consider NTHi lower airway infection in the investigation of corticosteroid unresponsiveness in COPD.

COPD patients with NTHi-associated neutrophilic airway inflammation may prove to be corticosteroid-unresponsive in real life, and the data in this thesis shows mechanisms by which alveolar macrophages promote this corticosteroid insensitivity. Bacterial colonisation in COPD probably requires targeted treatment; this is a personalised medicine approach.

## 6.6. MAPK pathway is a candidate therapeutic target in NTHi-infected COPD patients

MAPK pathway is a potential therapeutic target in COPD; p38 MAPK inhibitors showed synergistic anti-inflammatory effect with corticosteroids in LPS-stimulated alveolar macrophages (349). However, no similar investigation has been performed in NTHi infection in COPD.

In chapter four of this thesis, NTHi-induced *in vitro* inflammatory response was associated with p38 and ERK MAPK activation. Inhibitors of these pathways (BIRB-796 and AZD6244 respectively) showed significant inhibition of NTHi-induced TNF-α release from COPD alveolar macrophages. Moreover, these inhibitors showed a combined anti-inflammatory effect with corticosteroids. CXCL8, shown in this thesis to be corticosteroid-unresponsive, was significantly inhibited when MAPK inhibitors were combined with the corticosteroid, suggesting a possible role of these inhibitors in reducing airways neutrophilia associated with bacterial infections. In addition, p38 MAPK inhibitor (BIRB-796) improved corticosteroid-induced GR nuclear translocation in NTHi-infected alveolar macrophages.

These findings further confirmed the role of the MAPK pathway in COPD pathophysiology. The potential role of MAPK inhibitors in NTHi-infected COPD is worthy of further investigation. The next step would be to determine whether the anti-inflammatory effect of MAPK inhibitors is synergistic or additive to corticosteroids and whether ERK inhibition could also improve the GR nuclear localisation in NTHi-infected cells. However, the possible anti-inflammatory effect of MAPK inhibitors should be weighed versus possible systemic adverse effects. The use of p38 MAPK inhibitors in inflammatory diseases including COPD has undergone clinical trials. A clinical trial in COPD patients showed that a p38 MAPK inhibitor improved lung function (492). Meanwhile, other trials on patients with rheumatoid arthritis reported some drawbacks of p38 MAPK inhibitors, including hepatotoxicity and transient anti-inflammatory effect (493,494). Moreover, the effect of MAPK inhibitors on bacterial survival in the host is unknown. Therefore, investigation of MAPK inhibitors in NTHi-infected patients would be interesting, and would inform us of the potential of this class of drug to enhance corticosteroid effects, and to

investigate the possibility of bacterial persistence with this type of anti-inflammatory therapies.

## 6.7. NTHi- induced modification of alveolar macrophage phenotype is a possible mechanism of chronic infection.

Changes in alveolar macrophage phenotype have been investigated during acute and chronic bacterial human infections like mycobacterial diseases, salmonellosis and brucellosis (460–462). It is well accepted that bacterial-induced M2 macrophage programming results in chronicity of infection (122). However, no similar investigation has previously been performed on NTHi lower airway infection in COPD.

In chapter five, I have investigated this concept in two different settings of NTHi infection. My *in vitro* model served as a model of acute NTHi infection, and sputum samples from clinically stable COPD patients with NTHi infection used as a model of chronic infection. NTHi infection resulted in a mixed M1/M2 macrophage phenotype during the early acute phase of infection, rather than inducing a distinct polarisation of the cells. NTHi caused an upregulation of the mRNA levels of the pro-inflammatory markers (TNF-α, CXCL8 and CD38), while also upregulated the anti-inflammatory marker (IL-10). Also, it resulted in a downregulation of the mRNA levels of the antigen presentation molecule (HLA-DR) and scavenger receptors (CD36, CD206, CD14 and CD163). These findings indicate that NTHi starts to modulate different functions of alveolar macrophages during the early phase of infection, by upregulation or downregulation of some surface molecules. This might favour NTHi survival and persistence in the host.

Sputum macrophage markers in NTHi-infected COPD patients, showed a less dramatic difference in comparison to non-infected controls. The most important finding was the downregulation of HLA-DR and CD36 mRNA levels. The downregulation of HLA-DR suggests a reduced antigen presentation potential of the macrophages which might increase the possibility of chronic infection. Furthermore, the reduced CD36 mRNA level suggests reduced efferocytosis function which could result in more tissue destruction and disease progression. Although NTHi was the most predominant bacteria in the sputum samples of infected COPD patients, care should be taken while interpreting these findings as most samples were infected with lower concentrations of different bacterial species.

The above results indicate that NTHi modification of macrophage phenotype needs to be considered as a possible mechanism of lower airway NTHi colonisation in COPD patients.

## 6.8. Study limitations.

Although my study has reached its aim, there were some unavoidable limitations. First, due to limited time, relatively small populations of COPD and healthy controls were recruited for each of my experiments. The small sample size for some of my experiments resulted in less statistical power. My preliminary experiments were particularly of small sample size, this caused non statistically significant results for some sets of data which visually look significant (see Figure 3.1, Figure 3.4). Therefore, interpretation of my findings on the general population should consider this limitation.

Second, subjects in my population were not matched in terms of age, gender, severity of the disease, smoking history and corticosteroid therapy. This limitation

was due to the use of surgically resected lung tissue from suspected lung cancer patients, and because of limited time, it was difficult to recruit demographically matched patients for each experiment.

The above limitations were mainly due to limited time-frame for this study. Recruitment of bigger number of demographically matched subjects will increase the statistical power and give sounder conclusion which might be interpreted on the wider scale of general population.

Third, using frozen alveolar macrophages in some of my experiments might give a different response from freshly isolated macrophages. In GR phosphorylation and translocation assay, some frozen cells were poorly adherent to culture plates or chamber slides resulting in lower sample size for these experiments and may be a less detected response.

The access to fresh cells was not possible during some of my work. However, the limitation of using frozen cells could be overcome by validation of using these cells versus freshly isolated cells. For example, frozen then thawed macrophages could be tested for response to LPS, cells adherence and viability, and compared to fresh cells. Additionally, cells can be examined at different time-points to assess the effect of storage conditions on these cells over time.

Fourth, the activity of the compounds used in this study were not been verified due to the time limitation. BIRB-796 and AZD6244 showed pharmacological activity in my model, which suggested these compounds to be active. On the other hand, BMS-345541 did not show pharmacological activity and did not inhibit the NTHi-activated NF-κB. This indicated BMS-345541 might be an inactive compound in my model.

Verification of the compounds activity before their application in my model could be performed by testing these compounds in a relevant experimental model. Previously documented models could be used. The activity of BMS-345541 could be tested by inhibition of LPS-induced TNF-α, CXCL8 and IL-6 in THP-1 cells (439). Alternatively, this compound could be tested in mice for inhibition of LPS-induced TNF-α (439). BIRB-796 activity could be assayed in THP-1 cells for inhibition of LPS-induced CXCL8 (495). Also, the binding of fluorescently labeled BIRB-796 to recombinant human p38 MAPK could be monitored to verify the activity of BIRB-796 (442). AZD6244 inhibition of MEK1/2 could be assessed by measuring the phosphorylation state of basal and epidermal growth factor–induced ERK MAPK in Malme-3M (human melanoma cell line) or PBMCs (444).

## 6.9. Recommendations for Future Research.

Applying whole live NTHi in COPD research is less practicable than LPS. Alternatively, using purified NTHi antigens could improve the practicability of NTHi model. The OMP P6 would be a successful candidate antigen, due to its chemical conservation among strains (227,229) and its potential antigenicity *in vitro* (228). This would require purification of OMP P6 from a standard NTHi strain, and comparison of OMP P6-induced inflammatory response *in vitro* to that induced by live NTHi and LPS models. Validation of such model would be more disease relevant than LPS model. Nevertheless, the whole bacterial model is more realistic.

This study revealed some molecular aspects in NTHi airway infection in COPD. NTHi is capable of inducing robust cytokine release from alveolar macrophages through the activation of NF-κB and MAPK pathway. However, studying other intracellular pathways of inflammation in the setting of NTHi

259

infection would improve our understanding of the infection pathogenesis, TGF-β-SMAD signaling pathways could be the next pathways to be considered due to its role in airway remodeling in COPD patients (496) .

Although NTHi is the most common bacterial infection in COPD, other bacterial species, like *Moraxella catarrhalis*, *Streptococcus pneumoniae* and *Pseudomonas aeruginosa*, were involved in disease exacerbation and chronic colonisation. Therefore, investigation of airway inflammatory response to other COPD-relevant bacterial pathogens would be of clinical value. This would involve using live clinical isolates of different bacterial species in a model similar to my NTHi model. The resultant response could be compared to NTHi and LPS model. Investigation of the intracellular signaling pathways of these pathogens would be valuable to understand the molecular mechanism of each bacterial infection in COPD.

The possible role of p38 MAPK in NTHi-induced corticosteroid unresponsiveness in COPD alveolar macrophages require further investigation; bigger sample size and using freshly isolated cells could be tried to confirm the p38 MAPK role in NTHi-induced GR phosphorylation and translocation. Moreover, the role of ERK MAPK in NTHi-induced corticosteroid unresponsiveness needs to be studied as well.

Linking NTHi infection, neutrophilic airway inflammation and steroid unresponsiveness in COPD might be one example of the multi-dimensional approach in disease phenotyping. This might be performed by investigating NTHi presence in sputum or BAL fluid from COPD patients during stable and exacerbated state. Samples from NTHi positive patients can be further examined for the

inflammatory profile, and the measurements linked to the patient's clinical response to corticosteroids.

NTHi modulates alveolar macrophage marker mRNA levels to survive inside the airways. However, assessment of surface expression of these markers by flow cytometry would further confirm the NTHi-induced phenotype changes. I observed a reduction in CD36 and HLA-DR mRNA levels in alveolar macrophages from NTHi-infected COPD patients. The next step in this investigation is to confirm the functional relevance of these markers in COPD. This can be achieved by studying the efferocytosis and T-cell proliferation functions of alveolar macrophages in the presence of NTHi infection.

## 6.10. General conclusion:

NTHi provoked cytokine release from alveolar macrophages *in vitro* through activation of NF-κB and MAPK pathways. NTHi- induced inflammatory responses were more corticosteroid unresponsive than LPS-induced responses. NTHi-induced CXCL8 was the most corticosteroid unresponsive cytokine. My results highlighted the role of NTHi in GR phosphorylation and reduced GR nuclear localisation. Inhibitors of p38 and ERK MAPK pathways showed potential synergistic anti-inflammatory effects with corticosteroids in suppressing NTHi-induced cytokines release from alveolar macrophages. Furthermore, NTHi modified alveolar macrophage phenotype markers to persist inside the lung. CD36 and HLA-DR were particularly downregulated by NTHi.

My thesis focused on alveolar macrophages. My results suggest the role of NTHi infection in corticosteroid unresponsiveness in COPD, through CXCL8 production. This unresponsiveness could be improved by inhibitors of MAPK

pathway. Modification of alveolar macrophage functional polarisation by NTHi could be one mechanism of NTHi chronicity and could contribute to disease progression.

# References:

1. Chronic obstructive pulmonary disease | working-definition-of-copd | Guidance and guidelines | NICE [Internet]. [cited 2014 Nov 27]. Available from: https://www.nice.org.uk/guidance/cg101/chapter/working-definition-of-copd

2. GOLD. Global Strategy For The Diagnosis, Management and prevention of COPD.available at http://www.goldcopd.org/guidelines-global-strategy-for-diagnosis-management.html. 2014.

3. Barnes PJ. Mediators of Chronic Obstructive Pulmonary Disease. Pharmacol Rev. 2004 Dec 1;56(4):515–48.

4. Terzano C, Conti V, Di Stefano F, Petroianni A, Ceccarelli D, Graziani E, et al. Comorbidity, hospitalization, and mortality in COPD: results from a longitudinal study. Lung. 2010 Aug;188(4):321–9.

5. Paul D. Scanlon. the pathogenesis and pathology of COPD: identifying risk factors and improving morbidity and mortality. Adv Stud Med. 2004;volume 4:S744–9.

6. Simon PM, Schwartzstein RM, Weiss JW, Fencl V, Teghtsoonian M, Weinberger SE. Distinguishable types of dyspnea in patients with shortness of breath. Am Rev Respir Dis. 1990 Nov;142(5):1009–14.

7. Mannino DM, Ford ES, Redd SC. Obstructive and restrictive lung disease and markers of inflammation: data from the Third National Health and Nutrition Examination. Am J Med. 2003 Jun 15;114(9):758–62.

8. Burge S, Wedzicha JA. COPD exacerbations: definitions and classifications. Eur Respir J Suppl. 2003 Jun;41:46s – 53s.

9. Rodriguez-Roisin R. Toward a consensus definition for COPD exacerbations. Chest. 2000;117(5 Suppl 2):398S – 401S.

10. Seemungal TA, Donaldson GC, Bhowmik A, Jeffries DJ, Wedzicha JA. Time course and recovery of exacerbations in patients with chronic obstructive pulmonary disease. Am J Respir Crit Care Med. 2000 May;161(5):1608–13.

11. Papi A, Luppi F, Franco F, Fabbri LM. Pathophysiology of Exacerbations of Chronic Obstructive Pulmonary Disease. Proc Am Thorac Soc. 2006 May 1;3:245–51.

12. Veeramachaneni SB, Sethi S. Pathogenesis of bacterial exacerbations of COPD. COPD. 2006 Jun;3:109–15.

13. Eller J, Ede A, Schaberg T, Niederman MS, Mauch H, Lode H. Infective exacerbations of chronic bronchitis: relation between bacteriologic etiology and lung function. Chest. 1998 Jun;113(6):1542–8.

14. Fagon JY, Chastre J, Trouillet JL, Domart Y, Dombret MC, Bornet M, et al. Characterization of distal bronchial microflora during acute exacerbation of chronic bronchitis. Use of the protected specimen brush technique in 54 mechanically ventilated patients. Am Rev Respir Dis. 1990 Nov;142(5):1004–8.

15. Pela R, Marchesani F, Agostinelli C, Staccioli D, Cecarini L, Bassotti C, et al. Airways microbial flora in COPD patients in stable clinical conditions and during exacerbations: a bronchoscopic investigation. Monaldi Arch Chest Dis Arch Monaldi Mal Torace Fondazione Clin Lav IRCCS Ist Clin Tisiol E Mal Appar Respir Univ Napoli Secondo Ateneo. 1998 Jun;53(3):262–7.

16. Sanjay Sethi. Bacteria in Acute Exacerbations and in Stable COPD. PCCSU Artic. 2007 Aug 15;

17. MacNee W. Pathology, pathogenesis, and pathophysiology. BMJ. 2006 May 20;332(7551):1202–4.

18. Cosio MG, Saetta M, Agusti A. Immunologic aspects of chronic obstructive pulmonary disease. N Engl J Med. 2009 Jun 4;360(23):2445–54.

19. Kukkonen MK, Tiili E, Vehmas T, Oksa P, Piirilä P, Hirvonen A. Association of genes of protease-antiprotease balance pathway to lung function and emphysema subtypes. BMC Pulm Med. 2013 Jun 4;13(1):36.

20. Abboud RT, Vimalanathan S. Pathogenesis of COPD. Part I. The role of protease-antiprotease imbalance in emphysema. Int J Tuberc Lung Dis Off J Int Union Tuberc Lung Dis. 2008 Apr;12(4):361–7.

21. Lesser M, Padilla ML, Cardozo C. Induction of emphysema in hamsters by intratracheal instillation of cathepsin B. Am Rev Respir Dis. 1992 Mar;145(3):661–8.

22. Lucey EC, Keane J, Kuang P-P, Snider GL, Goldstein RH. Severity of elastase-induced emphysema is decreased in tumor necrosis factor-alpha and interleukin-1beta receptor-deficient mice. Lab Investig J Tech Methods Pathol. 2002 Jan;82(1):79–85.

23. Kao RC, Wehner NG, Skubitz KM, Gray BH, Hoidal JR. Proteinase 3. A distinct human polymorphonuclear leukocyte proteinase that produces emphysema in hamsters. J Clin Invest. 1988 Dec;82(6):1963–73.

24. Wright JL, Farmer SG, Churg A. Synthetic serine elastase inhibitor reduces cigarette smoke-induced emphysema in guinea pigs. Am J Respir Crit Care Med. 2002 Oct 1;166(7):954–60.

25. Fujita J, Nelson NL, Daughton DM, Dobry CA, Spurzem JR, Irino S, et al. Evaluation of elastase and antielastase balance in patients with chronic bronchitis and pulmonary emphysema. Am Rev Respir Dis. 1990 Jul;142(1):57–62.

26. Hautamaki RD, Kobayashi DK, Senior RM, Shapiro SD. Requirement for macrophage elastase for cigarette smoke-induced emphysema in mice. Science. 1997 Sep 26;277(5334):2002–4.

27. Finlay GA, O'Driscoll LR, Russell KJ, D'Arcy EM, Masterson JB, FitzGerald MX, et al. Matrix metalloproteinase expression and production by alveolar macrophages in emphysema. Am J Respir Crit Care Med. 1997 Jul;156:240–7.

28. Segura-Valdez L, Pardo A, Gaxiola M, Uhal BD, Becerril C, Selman M. Upregulation of gelatinases A and B, collagenases 1 and 2, and increased parenchymal cell death in COPD. Chest. 2000 Mar;117(3):684–94.

29. Döring G. The Role of Neutrophil Elastase in Chronic Inflammation. Am J Respir Crit Care Med. 1994 Dec 1;150(6_pt_2):S114–7.

30. Laurell C-B, Eriksson S. The electrophoretic α1-globulin pattern of serum in α1-antitrypsin deficiency. 1963. COPD. 2013 Mar;10 Suppl 1:3–8.

31. Stockley RA. Alpha-1-antitrypsin deficiency: what next? Thorax. 2000 Jul 1;55(7):614–8.

32. Hill AT, Bayley D, Stockley RA. The interrelationship of sputum inflammatory markers in patients with chronic bronchitis. Am J Respir Crit Care Med. 1999 Sep;160(3):893–8.

33. Rahman I. The role of oxidative stress in the pathogenesis of COPD: implications for therapy. Treat Respir Med. 2005;4:175–200.

34. Malhotra D, Thimmulappa R, Navas-Acien A, Sandford A, Elliott M, Singh A, et al. Decline in NRF2-regulated antioxidants in chronic obstructive pulmonary disease lungs due to loss of its positive regulator, DJ-1. Am J Respir Crit Care Med. 2008 Sep 15;178(6):592–604.

35. Jackson AD. Airway goblet-cell mucus secretion. Trends Pharmacol Sci. 2001 Jan 1;22(1):39–45.

36. Peinado VI, Pizarro S, Barberà JA. Pulmonary vascular involvement in COPD. Chest. 2008 Oct;134(4):808–14.

37. GOLD. Global strategy for the Diagnosis, Management and prevention of COPD. available at http://www.goldcopd.org/Guidelines/guidelines-global-strategy-for-diagnosis-management-2007-3.html.

38. GOLD. Global strategy for the Diagnosis, Management and prevention of COPD. available at http://www.goldcopd.org/Guidelines/guidelines-global-strategy-for-diagnosis-management-2011-3.html.

39. Sestini P, Cappiello V, Aliani M, Martucci P, Sena A, Vaghi A, et al. Prescription bias and factors associated with improper use of inhalers. J Aerosol Med Off J Int Soc Aerosols Med. 2006;19(2):127–36.

40. Calverley PMA, Anderson JA, Celli B, Ferguson GT, Jenkins C, Jones PW, et al. Salmeterol and Fluticasone Propionate and Survival in Chronic Obstructive Pulmonary Disease. N Engl J Med. 2007 Feb 22;356(8):775–89.

41. Boyd G, Morice AH, Pounsford JC, Siebert M, Peslis N, Crawford C. An evaluation of salmeterol in the treatment of chronic obstructive pulmonary disease (COPD). Eur Respir J. 1997 Apr;10(4):815–21.

42. Tashkin DP, Fabbri LM. Long-acting beta-agonists in the management of chronic obstructive pulmonary disease: current and future agents. Respir Res. 2010;11:149.

43. van Noord JA, Bantje TA, Eland ME, Korducki L, Cornelissen PJ. A randomised controlled comparison of tiotropium nd ipratropium in the treatment of chronic obstructive pulmonary disease. The Dutch Tiotropium Study Group. Thorax. 2000 Apr;55(4):289–94.

44. Barr RG, Bourbeau J, Camargo CA, Ram FSF. Inhaled tiotropium for stable chronic obstructive pulmonary disease. Cochrane Database Syst Rev. 2005;(2):CD002876.

45. Vincken W, van Noord JA, Greefhorst APM, Bantje TA, Kesten S, Korducki L, et al. Improved health outcomes in patients with COPD during 1 yr's treatment with tiotropium. Eur Respir J. 2002 Feb;19(2):209–16.

46. Routine nebulized ipratropium and albuterol together are better than either alone in COPD. The COMBIVENT Inhalation Solution Study Group. Chest. 1997 Dec;112(6):1514–21.

47. Bateman ED, Ferguson GT, Barnes N, Gallagher N, Green Y, Henley M, et al. Dual bronchodilation with QVA149 versus single bronchodilator therapy: the SHINE study. Eur Respir J. 2013 Dec;42(6):1484–94.

48. Pauwels RA, Buist AS, Calverley PMA, Jenkins CR, Hurd SS. Global Strategy for the Diagnosis, Management, and Prevention of Chronic Obstructive Pulmonary Disease. Am J Respir Crit CARE Med. 2001 Apr 1;163:1256–76.

49. Calverley P, Pauwels R, Vestbo J, Jones P, Pride N, Gulsvik A, et al. Combined salmeterol and fluticasone in the treatment of chronic obstructive pulmonary disease: a randomised controlled trial. Lancet. 2003 Feb 8;361(9356):449–56.

50. Jones PW, Willits LR, Burge PS, Calverley PMA, Inhaled Steroids in Obstructive Lung Disease in Europe study investigators. Disease severity and the effect of fluticasone propionate on chronic obstructive pulmonary disease exacerbations. Eur Respir J. 2003 Jan;21(1):68–73.

51. Mahler DA, Wire P, Horstman D, Chang C-N, Yates J, Fischer T, et al. Effectiveness of fluticasone propionate and salmeterol combination delivered via the Diskus device in the treatment of chronic obstructive pulmonary disease. Am J Respir Crit Care Med. 2002 Oct 15;166(8):1084–91.

52. Burge PS, Calverley PM, Jones PW, Spencer S, Anderson JA, Maslen TK. Randomised, double blind, placebo controlled study of fluticasone propionate

in patients with moderate to severe chronic obstructive pulmonary disease: the ISOLDE trial. BMJ. 2000 May 13;320(7245):1297–303.

53. Vestbo J, Sørensen T, Lange P, Brix A, Torre P, Viskum K. Long-term effect of inhaled budesonide in mild and moderate chronic obstructive pulmonary disease: a randomised controlled trial. Lancet. 1999 May 29;353(9167):1819–23.

54. Singh S, Loke YK. An overview of the benefits and drawbacks of inhaled corticosteroids in chronic obstructive pulmonary disease. Int J Chron Obstruct Pulmon Dis. 2010;5:189–95.

55. Johnell O, Pauwels R, Löfdahl CG, Laitinen LA, Postma DS, Pride NB, et al. Bone mineral density in patients with chronic obstructive pulmonary disease treated with budesonide Turbuhaler. Eur Respir J. 2002 Jun;19(6):1058–63.

56. Ram FS, Jones PW, Castro AA, De Brito JA, Atallah AN, Lacasse Y, et al. Oral theophylline for chronic obstructive pulmonary disease. Cochrane Database Syst Rev. 2002;(4):CD003902.

57. Calverley PMA, Rabe KF, Goehring U-M, Kristiansen S, Fabbri LM, Martinez FJ, et al. Roflumilast in symptomatic chronic obstructive pulmonary disease: two randomised clinical trials. Lancet. 2009 Aug 29;374(9691):685–94.

58. Rennard SI, Calverley PMA, Goehring UM, Bredenbröker D, Martinez FJ. Reduction of exacerbations by the PDE4 inhibitor roflumilast--the importance of defining different subsets of patients with COPD. Respir Res. 2011;12:18.

59. Fabbri LM, Calverley PMA, Izquierdo-Alonso JL, Bundschuh DS, Brose M, Martinez FJ, et al. Roflumilast in moderate-to-severe chronic obstructive pulmonary disease treated with longacting bronchodilators: two randomised clinical trials. Lancet. 2009 Aug 29;374(9691):695–703.

60. Celli BR, MacNee W, ATS/ERS Task Force. Standards for the diagnosis and treatment of patients with COPD: a summary of the ATS/ERS position paper. Eur Respir J. 2004 Jun;23(6):932–46.

61. Leuppi JD, Schuetz P, Bingisser R, Bodmer M, Briel M, Drescher T, et al. Short-term vs conventional glucocorticoid therapy in acute exacerbations of chronic obstructive pulmonary disease: the REDUCE randomized clinical trial. JAMA. 2013 Jun 5;309(21):2223–31.

62. Ram FSF, Rodriguez-Roisin R, Granados-Navarrete A, Garcia-Aymerich J, Barnes NC. Antibiotics for exacerbations of chronic obstructive pulmonary disease. Cochrane Database Syst Rev. 2006;(2):CD004403.

63. Quon BS, Gan WQ, Sin DD. Contemporary management of acute exacerbations of COPD: a systematic review and metaanalysis. Chest. 2008 Mar;133(3):756–66.

64. Voelkel NF, Tuder R. COPD: exacerbation. Chest. 2000 May;117(5 Suppl 2):376S – 9S.

65. Barnes PJ. Alveolar macrophages as orchestrators of COPD. COPD. 2004 Apr;1:59–70.

66. Tanino M, Betsuyaku T, Takeyabu K, Tanino Y, Yamaguchi E, Miyamoto K, et al. Increased levels of interleukin-8 in BAL fluid from smokers susceptible to pulmonary emphysema. Thorax. 2002 May 1;57:405–11.

67. Traves SL, Culpitt SV, Russell REK, Barnes PJ, Donnelly LE. Increased levels of the chemokines GROalpha and MCP-1 in sputum samples from patients with COPD. Thorax. 2002 Jul;57(7):590–5.

68. Lacoste JY, Bousquet J, Chanez P, Van Vyve T, Simony-Lafontaine J, Lequeu N, et al. Eosinophilic and neutrophilic inflammation in asthma, chronic bronchitis, and chronic obstructive pulmonary disease. J Allergy Clin Immunol. 1993 Oct;92(4):537–48.

69. Keatings VM, Collins PD, Scott DM, Barnes PJ. Differences in interleukin-8 and tumor necrosis factor-alpha in induced sputum from patients with chronic obstructive pulmonary disease or asthma. Am J Respir Crit Care Med. 1996 Feb;153:530–4.

70. Di Stefano A, Capelli A, Lusuardi M, Balbo P, Vecchio C, Maestrelli P, et al. Severity of airflow limitation is associated with severity of airway inflammation in smokers. Am J Respir Crit Care Med. 1998 Oct;158(4):1277–85.

71. Finkelstein R, Fraser RS, Ghezzo H, Cosio MG. Alveolar inflammation and its relation to emphysema in smokers. Am J Respir Crit Care Med. 1995 Nov;152:1666–72.

72. de Jong JW, van der Belt-Gritter B, Koëter GH, Postma DS. Peripheral blood lymphocyte cell subsets in subjects with chronic obstructive pulmonary disease: association with smoking, IgE and lung function. Respir Med. 1997 Feb;91(2):67–76.

73. Kim W-D, Kim W-S, Koh Y, Lee S-D, Lim C-M, Kim D-S, et al. Abnormal peripheral blood T-lymphocyte subsets in a subgroup of patients with COPD. Chest. 2002 Aug;122(2):437–44.

74. Saetta M, Baraldo S, Corbino L, Turato G, Braccioni F, Rea F, et al. CD8+ve cells in the lungs of smokers with chronic obstructive pulmonary disease. Am J Respir Cirt Care Med. 1999;160:711–7.

75. Majo J, Ghezzo H, Cosio MG. Lymphocyte population and apoptosis in the lungs of smokers and their relation to emphysema. Eur Respir J. 2001 May;17(5):946–53.

76. Retamales I, Elliott WM, Meshi B, Coxson HO, Pare PD, Sciurba FC, et al. Amplification of inflammation in emphysema and its association with latent adenoviral infection. Am J Respir Crit Care Med. 2001 Aug 1;164(3):469–73.

77. Curtis JL, Freeman CM, Hogg JC. The Immunopathogenesis of Chronic Obstructive Pulmonary Disease. Proc Am Thorac Soc. 2007 Oct 1;4(7):512–21.

78. Cosio MG, Majo J, Cosio MG. Inflammation of the airways and lung parenchyma in COPD: role of T cells. Chest. 2002 May;121(5 Suppl):160S – 165S.

79. Brightling CE, Monteiro W, Ward R, Parker D, Morgan MD, Wardlaw AJ, et al. Sputum eosinophilia and short-term response to prednisolone in chronic obstructive pulmonary disease: a randomised controlled trial. Lancet. 2000 Oct 28;356(9240):1480–5.

80. Turato G, Zuin R, Saetta M. Pathogenesis and pathology of COPD. Respir Int Rev Thorac Dis. 2001;68(2):117–28.

81. Saetta M, Di Stefano A, Maestrelli P, Turato G, Ruggieri MP, Roggeri A, et al. Airway eosinophilia in chronic bronchitis during exacerbations. Am J Respir Crit Care Med. 1994 Dec;150(6 Pt 1):1646–52.

82. Saetta M, Di Stefano A, Maestrelli P, Turato G, Mapp CE, Pieno M, et al. Airway eosinophilia and expression of interleukin-5 protein in asthma and in exacerbations of chronic bronchitis. Clin Exp Allergy J Br Soc Allergy Clin Immunol. 1996 Jul;26(7):766–74.

83. Papi A, Romagnoli M, Baraldo S, Braccioni F, Guzzinati I, Saetta M, et al. Partial reversibility of airflow limitation and increased exhaled NO and sputum eosinophilia in chronic obstructive pulmonary disease. Am J Respir Crit Care Med. 2000 Nov;162(5):1773–7.

84. Mio T, Romberger DJ, Thompson AB, Robbins RA, Heires A, Rennard SI. Cigarette smoke induces interleukin-8 release from human bronchial epithelial cells. Am J Respir Crit Care Med. 1997 May;155(5):1770–6.

85. Hellermann GR, Nagy SB, Kong X, Lockey RF, Mohapatra SS. Mechanism of cigarette smoke condensate-induced acute inflammatory response in human bronchial epithelial cells. Respir Res. 2002;3(1):22.

86. Floreani AA, Wyatt TA, Stoner J, Sanderson SD, Thompson EG, Allen-Gipson D, et al. Smoke and C5a induce airway epithelial intercellular adhesion molecule-1 and cell adhesion. Am J Respir Cell Mol Biol. 2003 Oct;29(4):472–82.

87. Takizawa H, Tanaka M, Takami K, Ohtoshi T, Ito K, Satoh M, et al. Increased expression of transforming growth factor-beta1 in small airway epithelium from tobacco smokers and patients with chronic obstructive pulmonary disease (COPD). Am J Respir Crit Care Med. 2001 May;163(6):1476–83.

88. Adler KB, Li Y. Airway epithelium and mucus: intracellular signaling pathways for gene expression and secretion. Am J Respir Cell Mol Biol. 2001 Oct;25(4):397–400.

89. Jacquot J, Spilmont C, de Bentzmann S, Dupuit F, Puchelle E. [Structure and secretory functions of the respiratory epithelium]. Arch Int Physiol Biochim Biophys. 1992 Aug;100(4):A41–6.

90. Franklin WA, Veve R, Hirsch FR, Helfrich BA, Bunn PA. Epidermal growth factor receptor family in lung cancer and premalignancy. Semin Oncol. 2002 Feb;29(1 Suppl 4):3–14.

91. Bathoorn E, Kerstjens H, Postma D, Timens W, MacNee W. Airways inflammation and treatment during acute exacerbations of COPD. Int J Chron Obstruct Pulmon Dis. 2008;3(2):217–29.

92. Bhowmik A, Seemungal TAR, Sapsford RJ, Wedzicha JA. Relation of sputum inflammatory markers to symptoms and lung function changes in COPD exacerbations. Thorax. 2000 Feb 1;55:114–20.

93. Fujimoto K, Yasuo M, Urushibata K, Hanaoka M, Koizumi T, Kubo K. Airway inflammation during stable and acutely exacerbated chronic obstructive pulmonary disease. Eur Respir J. 2005 Apr;25(4):640–6.

94. Tsoumakidou M, Tzanakis N, Chrysofakis G, Kyriakou D, Siafakas NM. Changes in sputum T-lymphocyte subpopulations at the onset of severe exacerbations of chronic obstructive pulmonary disease. Respir Med. 2005 May;99(5):572–9.

95. Mercer PF, Shute JK, Bhowmik A, Donaldson GC, Wedzicha JA, Warner JA. MMP-9, TIMP-1 and inflammatory cells in sputum from COPD patients during exacerbation. Respir Res. 2005;6:151.

96. Qiu Y, Zhu J, Bandi V, Atmar RL, Hattotuwa K, Guntupalli KK, et al. Biopsy Neutrophilia, Neutrophil Chemokine and Receptor Gene Expression in Severe Exacerbations of Chronic Obstructive Pulmonary Disease. Am J Respir Crit CARE Med. 2003 Oct 15;168:968–75.

97. Stockley RA, Bayley D, Hill SL, Hill AT, Crooks S, Campbell EJ. Assessment of airway neutrophils by sputum colour: correlation with airways inflammation. Thorax. 2001 May;56(5):366–72.

98. Gompertz S, O'Brien C, Bayley DL, Hill SL, Stockley RA. Changes in bronchial inflammation during acute exacerbations of chronic bronchitis. Eur Respir J. 2001 Jun;17(6):1112–9.

99. Drost EM, Skwarski KM, Sauleda J, Soler N, Roca J, Agusti A, et al. Oxidative stress and airway inflammation in severe exacerbations of COPD. Thorax. 2005 Apr;60(4):293–300.

100. Saetta M, Stefano AD, Turato G, Facchini FM, Corbino L, Mapp CE, et al. CD8 T-Lymphocytes in peripheral airways of smokers with chronic obstructive pulmonary disease. Am J Respir Cirt Care Med. 1998;157:822–6.

101. O'Shaughnessy TC, Ansari TW, Barnes C, Jeffery PK. Inflammation in bronchial biopsies of subjects with chronic bronchitis: inverse relationship of CD8+ T lymphocytes with FEV1. Am J Respir Crit Care Med. 1997;155:852–7.

102. Barnes PJ. Mechanisms in COPD: differences from asthma. Chest. 2000;117:Suppl:10S – 14S.

103. Bocchino V, Bertorelli G, Bertrand CP, Ponath PD, Newman W, Franco C, et al. Eotaxin and CCR3 are up-regulated in exacerbations of chronic bronchitis. Allergy. 2002 Jan;57(1):17–22.

104. Rohde G, Gevaert P, Holtappels G, Fransen L, Borg I, Wiethege A, et al. Soluble interleukin-5 receptor alpha is increased in acute exacerbation of chronic obstructive pulmonary disease. Int Arch Allergy Immunol. 2004 Sep;135(1):54–61.

105. Zhu J, Qiu YS, Majumdar S, Gamble E, Matin D, Turato G, et al. Exacerbations of Bronchitis: bronchial eosinophilia and gene expression for interleukin-4, interleukin-5, and eosinophil chemoattractants. Am J Respir Crit Care Med. 2001 Jul 1;164(1):109–16.

106. Aaron SD, Angel JB, Lunau M, Wright K, Fex C, Le Saux N, et al. Granulocyte inflammatory markers and airway infection during acute exacerbation of chronic obstructive pulmonary disease. Am J Respir Crit Care Med. 2001 Feb;163(2):349–55.

107. Calikoglu M, Sahin G, Unlu A, Ozturk C, Tamer L, Ercan B, et al. Leptin and TNF-alpha levels in patients with chronic obstructive pulmonary disease and their relationship to nutritional parameters. Respir Int Rev Thorac Dis. 2004 Feb;71(1):45–50.

108. Balbi B, Bason C, Balleari E, Fiasella F, Pesci A, Ghio R, et al. Increased bronchoalveolar granulocytes and granulocyte/macrophage colony-stimulating factor during exacerbations of chronic bronchitis. Eur Respir J. 1997 Apr;10(4):846–50.

109. Wedzicha JA, Seemungal TA, MacCallum PK, Paul EA, Donaldson GC, Bhowmik A, et al. Acute exacerbations of chronic obstructive pulmonary disease are accompanied by elevations of plasma fibrinogen and serum IL-6 levels. Thromb Haemost. 2000 Aug;84(2):210–5.

110. Wedzicha JA. Exacerbations: etiology and pathophysiologic mechanisms. Chest. 2002 May;121(5 Suppl):136S – 141S.

111. Smallman LA, Hill SL, Stockley RA. Reduction of ciliary beat frequency in vitro by sputum from patients with bronchiectasis: a serine proteinase effect. Thorax. 1984 Sep;39(9):663–7.

112. Nadel JA. Role of neutrophil elastase in hypersecretion during COPD exacerbations, and proposed therapies. Chest. 2000;117:386S – 389S.

113. Tetley TD. Macrophages and the pathogenesis of COPD. Chest. 2002 May;121:156S – 159S.

114. Jeffery PK. Structural and inflammatory changes in COPD: a comparison with asthma. Thorax. 1998 Feb;53:129–36.

115. Marques LJ, Teschler H, Guzman J, Costabel U. Smoker's lung transplanted to a nonsmoker. Long-term detection of smoker's macrophages. Am J Respir Crit Care Med. 1997 Nov;156(5):1700–2.

116. de Boer WI, Sont JK, van Schadewijk A, Stolk J, van Krieken JH, Hiemstra PS. Monocyte chemoattractant protein 1, interleukin 8, and chronic airways inflammation in COPD. J Pathol. 2000 Apr;190(5):619–26.

117. Tomita K, Caramori G, Lim S, Ito K, Hanazawa T, Oates T, et al. Increased p21(CIP1/WAF1) and B cell lymphoma leukemia-x(L) expression and reduced apoptosis in alveolar macrophages from smokers. Am J Respir Crit Care Med. 2002 Sep 1;166(5):724–31.

118. Bitterman PB, Saltzman LE, Adelberg S, Ferrans VJ, Crystal RG. Alveolar macrophage replication. One mechanism for the expansion of the mononuclear phagocyte population in the chronically inflamed lung. J Clin Invest. 1984 Aug;74(2):460–9.

119. Smaldone GC, Foster WM, O'Riordan TG, Messina MS, Perry RJ, Langenback EG. Regional impairment of mucociliary clearance in chronic obstructive pulmonary disease. Chest. 1993 May;103(5):1390–6.

120. Bhowmik A, Chahal K, Austin G, Chakravorty I. Improving mucociliary clearance in chronic obstructive pulmonary disease. Respir Med. 2009 Apr;103(4):496–502.

121. Boorsma CE, Draijer C, Melgert BN. Macrophage heterogeneity in respiratory diseases. Mediators Inflamm. 2013;2013:769214.

122. Benoit M, Desnues B, Mege JL. Macrophage polarization in bacterial infections. J Immunol. 2008 Sep 15;181:3733–9.

123. Mosser DM, Edwards JP. Exploring the full spectrum of macrophage activation. Nat Rev Immunol. 2008 Dec;8:958–69.

124. Mantovani A, Sica A, Sozzani S, Allavena P, Vecchi A, Locati M. The chemokine system in diverse forms of macrophage activation and polarization. Trends Immunol. 2004;25:677–86.

125. O'Reilly M, Newcomb DE, Remick D. Endotoxin, sepsis, and the primrose path. Shock. 1999;12:411–20.

126. Mosser DM. The many faces of macrophage activation. J Leukoc Biol. 2003 Feb;73(2):209–12.

127. Harris J, De Haro SA, Master SS, Keane J, Roberts EA, Delgado M, et al. T helper 2 cytokines inhibit autophagic control of intracellular Mycobacterium tuberculosis. Immunity. 2007 Sep;27(3):505–17.

128. Benoit M, Barbarat B, Bernard A, Olive D, Mege J-L. Coxiella burnetii, the agent of Q fever, stimulates an atypical M2 activation program in human macrophages. Eur J Immunol. 2008 Apr;38(4):1065–70.

129. Shaykhiev R, Krause A, Salit J, Strulovici-Barel Y, Harvey B-G, O'Connor TP, et al. Smoking-dependent reprogramming of alveolar macrophage polarization: implication for pathogenesis of chronic obstructive pulmonary disease. J Immunol Baltim Md 1950. 2009 Aug 15;183(4):2867–83.

130. Alberts B, Johnson A, Lewis J, Raff M, Roberts K, Walter P. Helper T Cells and Lymphocyte Activation. 2002 [cited 2014 Dec 8]; Available from: http://www.ncbi.nlm.nih.gov/books/NBK26827/

131. Mosser DM. Receptors on phagocytic cells involved in microbial recognition. Immunol Ser. 1994;60:99–114.

132. Gordon SB, Read RC. Macrophage defences against respiratory tract infections. Br Med Bull. 2002 Mar 1;61:45–61.

133. Marti-Lliteras P, Regueiro V, Morey P, Hood DW, Saus C, Sauleda J, et al. Nontypeable Haemophilus influenzae clearance by alveolar macrophages is impaired by exposure to cigarette smoke. Infect Immun. 2009 Oct;77:4232–42.

134. Taylor AE, Finney-Hayward TK, Quint JK, Thomas CM, Tudhope SJ, Wedzicha JA, et al. Defective macrophage phagocytosis of bacteria in COPD. Eur Respir J. 2010 May;35:1039–47.

135. Berenson CS, Garlipp MA, Grove LJ, Maloney J, Sethi S. Impaired Phagocytosis of Nontypeable Haemophilus influenzae by Human Alveolar Macrophages in Chronic Obstructive Pulmonary Disease. J Infect Dis. 2006 Nov 15;194:1375–84.

136. Gordon S, Taylor PR. Monocyte and macrophage heterogeneity. Nat Rev Immunol. 2005;5:953–64.

137. Unanue ER. Antigen-Presenting Function of the Macrophage. Annu Rev Immunol. 1984;2(1):395–428.

138. Blumenthal RL, Campbell DE, Hwang P, DeKruyff RH, Frankel LR, Umetsu DT. Human alveolar macrophages induce functional inactivation in antigen-specific CD4 T cells. J Allergy Clin Immunol. 2001 Feb;107(2):258–64.

139. Chelen CJ, Fang Y, Freeman GJ, Secrist H, Marshall JD, Hwang PT, et al. Human alveolar macrophages present antigen ineffectively due to defective expression of B7 costimulatory cell surface molecules. J Clin Invest. 1995 Mar;95(3):1415–21.

140. Hodge S, Matthews G, Mukaro V, Ahern J, Shivam A, Hodge G, et al. Cigarette Smoke-Induced Changes to Alveolar Macrophage Phenotype and Function Are Improved by Treatment with Procysteine. Am J Respir Cell Mol Biol. 2011 May 1;44:673–81.

141. Pons AR, Noguera A, Blanquer D, Sauleda J, Pons J, Agustí AGN. Phenotypic characterisation of alveolar macrophages and peripheral blood monocytes in COPD. Eur Respir J. 2005 Apr 1;25:647–52.

142. Muehlstedt SG, Lyte M, Rodriguez JL. Increased IL-10 production and HLA-DR suppression in the lungs of injured patients precede the development of nosocomial pneumonia. Shock Augusta Ga. 2002 Jun;17(6):443–50.

143. Odeberg J, Soderberg-Naucler C. Reduced Expression of HLA Class II Molecules and Interleukin-10- and Transforming Growth Factor ?1- Independent Suppression of T-Cell Proliferation in Human Cytomegalovirus-Infected Macrophage Cultures. J Virol. 2001 Jun;75(11):5174–81.

144. MacMicking J, Xie QW, Nathan C. Nitric oxide and macrophage function. Annu Rev Immunol. 1997;15:323–50.

145. Xu S, Cooper A, Sturgill-Koszycki S, van Heyningen T, Chatterjee D, Orme I, et al. Intracellular trafficking in Mycobacterium tuberculosis and Mycobacterium avium-infected macrophages. J Immunol Baltim Md 1950. 1994 Sep 15;153(6):2568–78.

146. Aberdein JD, Cole J, Bewley MA, Marriott HM, Dockrell DH. Alveolar macrophages in pulmonary host defence the unrecognized role of apoptosis as a mechanism of intracellular bacterial killing. Clin Exp Immunol. 2013 Nov;174(2):193–202.

147. Dockrell DH, Marriott HM, Prince LR, Ridger VC, Ince PG, Hellewell PG, et al. Alveolar macrophage apoptosis contributes to pneumococcal clearance in a resolving model of pulmonary infection. J Immunol Baltim Md 1950. 2003 Nov 15;171(10):5380–8.

148. Martin Bewley, Richard Budd, Dave Singh, Peter J. Barnes, Louise E. Donnelly, Moira K.B. Whyte, et al. Alveolar Macrophages During COPD Demonstrate Reduced Apoptosis-Associated Bacterial Killing And Reduced Mitochondrial Reactive Oxygen Species-Dependent Killing. In: B39 COPD EXACERBATIONS: PRECIPITATING FACTORS, PREVENTION, AND OUTCOME [Internet]. American Thoracic Society; 2014 [cited 2014 Dec 4]. p. A2862–A2862. (American Thoracic Society International Conference Abstracts). Available from: http://www.atsjournals.org/doi/abs/10.1164/ajrccm-conference.2014.189.1_MeetingAbstracts.A2862

149. Stow JL, Low PC, Offenhäuser C, Sangermani D. Cytokine secretion in macrophages and other cells: pathways and mediators. Immunobiology. 2009;214(7):601–12.

150. Hume DA. The mononuclear phagocyte system. Curr Opin Immunol. 2006 Feb;18(1):49–53.

151. Pedroza M, Schneider DJ, Karmouty-Quintana H, Coote J, Shaw S, Corrigan R, et al. Interleukin-6 Contributes to Inflammation and Remodeling in a Model of Adenosine Mediated Lung Injury. PLoS ONE. 2011 Jul 25;6(7):e22667.

152. Pantelidis P, Fanning GC, Wells AU, Welsh KI, Du Bois RM. Analysis of tumor necrosis factor-alpha, lymphotoxin-alpha, tumor necrosis factor receptor II, and interleukin-6 polymorphisms in patients with idiopathic pulmonary fibrosis. Am J Respir Crit Care Med. 2001 May;163(6):1432–6.

153. Bucchioni E, Kharitonov SA, Allegra L, Barnes PJ. High levels of interleukin-6 in the exhaled breath condensate of patients with COPD. Respir Med. 2003;97:1299–302.

154. Aldonyte R, Jansson L, Piitulainen E, Janciauskiene S. Circulating monocytes from healthy individuals and COPD patients. Respir Res. 2003 Sep 22;4(1):11.

155. Russell RE, Thorley A, Culpitt SV, Dodd S, Donnelly LE, Demattos C, et al. Alveolar macrophage-mediated elastolysis: roles of matrix metalloproteinases, cysteine, and serine proteases. Am J Physiol Lung Cell Mol Physiol. 2002 Oct;283:L867–73.

156. Kusano K, Miyaura C, Inada M, Tamura T, Ito A, Nagase H, et al. Regulation of matrix metalloproteinases (MMP-2, -3, -9, and -13) by interleukin-1 and interleukin-6 in mouse calvaria: association of MMP induction with bone resorption. Endocrinology. 1998 Mar;139(3):1338–45.

157. Singh B, Arora S, Khanna V. Association of severity of COPD with IgE and interleukin-1 beta. Monaldi Arch Chest Dis Arch Monaldi Mal Torace Fondazione Clin Lav IRCCS Ist Clin Tisiol E Mal Appar Respir Univ Napoli Secondo Ateneo. 2010 Jun;73(2):86–7.

158. Chung KF. Cytokines in chronic obstructive pulmonary disease. Eur Respir J Suppl. 2001 Dec;34:50s – 59s.

159. Hirani N, Antonicelli F, Strieter RM, Wiesener MS, Ratcliffe PJ, Haslett C, et al. The regulation of interleukin-8 by hypoxia in human macrophages--a potential role in the pathogenesis of the acute respiratory distress syndrome (ARDS). Mol Med. 2001 Oct;7:685–97.

160. Saetta M, Mariani M, Panina-Bordignon P, Turato G, Buonsanti C, Baraldo S, et al. Increased expression of the chemokine receptor CXCR3 and its ligand CXCL10 in peripheral airways of smokers with chronic obstructive pulmonary disease. Am J Respir Crit Care Med. 2002 May 15;165:1404–9.

161. Yamamoto C, Yoneda T, Yoshikawa M, Fu A, Tokuyama T, Tsukaguchi K, et al. Airway inflammation in COPD assessed by sputum levels of interleukin-8. Chest. 1997 Aug;112(2):505–10.

162. Nocker RE, Schoonbrood DF, van de Graaf EA, Hack CE, Lutter R, Jansen HM, et al. Interleukin-8 in airway inflammation in patients with asthma and chronic obstructive pulmonary disease. Int Arch Allergy Immunol. 1996 Feb;109(2):183–91.

163. Crooks SW, Bayley DL, Hill SL, Stockley RA. Bronchial inflammation in acute bacterial exacerbations of chronic bronchitis: the role of leukotriene B4. Eur Respir J. 2000 Feb;15(2):274–80.

164. Hill AT, Campbell EJ, Hill SL, Bayley DL, Stockley RA. Association between airway bacterial load and markers of airway inflammation in patients with stable chronic bronchitis. Am J Med. 2000 Sep;109(4):288–95.

165. Patel IS, Seemungal TAR, Wilks M, Lloyd-Owen SJ, Donaldson GC, Wedzicha JA. Relationship between bacterial colonisation and the frequency, character, and severity of COPD exacerbations. Thorax. 2002 Sep 1;57:759–64.

166. Cosio BG, Tsaprouni L, Ito K, Jazrawi E, Adcock IM, Barnes PJ. Theophylline restores histone deacetylase activity and steroid responses in COPD macrophages. J Exp Med. 2004 Sep 6;200(5):689–95.

167. Culpitt SV, Rogers DF, Shah P, De Matos C, Russell REK, Donnelly LE, et al. Impaired inhibition by dexamethasone of cytokine release by alveolar macrophages from patients with chronic obstructive pulmonary disease. Am J Respir Crit Care Med. 2003 Jan 1;167(1):24–31.

168. Armstrong J, Sargent C, Singh D. Glucocorticoid sensitivity of lipopolysaccharide-stimulated chronic obstructive pulmonary disease alveolar macrophages. Clin Exp Immunol. 2009;158:74–83.

169. Gaschler GJ, Zavitz CCJ, Bauer CMT, Skrtic M, Lindahl M, Robbins CS, et al. Cigarette smoke exposure attenuates cytokine production by mouse alveolar macrophages. Am J Respir Cell Mol Biol. 2008 Feb;38(2):218–26.

170. Ouyang Y, Virasch N, Hao P, Aubrey MT, Mukerjee N, Bierer BE, et al. Suppression of human IL-1beta, IL-2, IFN-gamma, and TNF-alpha production by cigarette smoke extracts. J Allergy Clin Immunol. 2000 Aug;106(2):280–7.

171. Kent L, Smyth L, Clayton C, Scott L, Cook T, Stephens R, et al. Cigarette smoke extract induced cytokine and chemokine gene expression changes in COPD macrophages. Cytokine. 2008 May;42(2):205–16.

172. Culpitt SV, Rogers DF, Fenwick PS, Shah P, Matos CD, Russell REK, et al. Inhibition by red wine extract, resveratrol, of cytokine release by alveolar macrophages in COPD. Thorax. 2003 Nov 1;58(11):942–6.

173. Birrell MA, Wong S, Catley MC, Belvisi MG. Impact of tobacco-smoke on key signaling pathways in the innate immune response in lung macrophages. J Cell Physiol. 2008 Jan;214(1):27–37.

174. Shamsuddin M, Chen E, Anderson J, Smith LJ. Regulation of leukotriene and platelet-activating factor synthesis in human alveolar macrophages. J Lab Clin Med. 1997 Dec;130:615–26.

175. Biernacki WA, Kharitonov SA, Barnes PJ. Increased leukotriene B4 and 8-isoprostane in exhaled breath condensate of patients with exacerbations of COPD. Thorax. 2003 Apr;58(4):294–8.

176. Woolhouse IS, Bayley DL, Stockley RA. Sputum chemotactic activity in chronic obstructive pulmonary disease: effect of alpha(1)-antitrypsin deficiency and the role of leukotriene B(4) and interleukin 8. Thorax. 2002 Aug;57(8):709–14.

177. Hackett TL, Holloway R, Holgate ST, Warner JA. Dynamics of pro-inflammatory and anti-inflammatory cytokine release during acute inflammation in chronic obstructive pulmonary disease: an ex vivo study. Respir Res. 2008;9:47.

178. Armstrong L, Jordan N, Millar A. Interleukin 10 (IL-10) regulation of tumour necrosis factor alpha (TNF-alpha) from human alveolar macrophages and peripheral blood monocytes. Thorax. 1996 Feb;51(2):143–9.

179. Lacraz S, Nicod LP, Chicheportiche R, Welgus HG, Dayer JM. IL-10 inhibits metalloproteinase and stimulates TIMP-1 production in human mononuclear phagocytes. J Clin Invest. 1995 Nov;96(5):2304–10.

180. Mostafa Mtairag E, Chollet-Martin S, Oudghiri M, Laquay N, Jacob MP, Michel JB, et al. Effects of interleukin-10 on monocyte/endothelial cell adhesion and MMP-9/TIMP-1 secretion. Cardiovasc Res. 2001 Mar;49(4):882–90.

181. Takanashi S, Hasegawa Y, Kanehira Y, Yamamoto K, Fujimoto K, Satoh K, et al. Interleukin-10 level in sputum is reduced in bronchial asthma, COPD and in smokers. Eur Respir J. 1999 Aug;14:309–14.

182. Zhang L, Cheng Z, Liu W, Wu K. Expression of interleukin (IL)-10, IL-17A and IL-22 in serum and sputum of stable chronic obstructive pulmonary disease patients. COPD. 2013 Aug;10(4):459–65.

183. McCubbrey AL, Curtis JL. Efferocytosis and lung disease. Chest. 2013 Jun;143(6):1750–7.

184. Schmidt EP, Tuder RM. Role of Apoptosis in Amplifying Inflammatory Responses in Lung Diseases. J Cell Death. 2010 Jul 20;2010(3):41–53.

185. Hodge S, Hodge G, Scicchitano R, Reynolds PN, Holmes M. Alveolar macrophages from subjects with chronic obstructive pulmonary disease are deficient in their ability to phagocytose apoptotic airway epithelial cells. Immunol Cell Biol. 2003 Aug;81(4):289–96.

186. Hodge S, Hodge G, Ahern J, Jersmann H, Holmes M, Reynolds PN. Smoking Alters Alveolar Macrophage Recognition and Phagocytic Ability. Am J Respir Cell Mol Biol. 2007 Dec 1;37:748–55.

187. Churg A, Zhou S, Preobrazhenska O, Tai H, Wang R, Wright JL. Expression of profibrotic mediators in small airways versus parenchyma after cigarette smoke exposure. Am J Respir Cell Mol Biol. 2009 Mar;40(3):268–76.

188. Davidson JM. Biochemistry and turnover of lung interstitium. Eur Respir J. 1990 Oct;3(9):1048–63.

189. Cardozo C, Padilla ML, Choi HS, Lesser M. Goblet cell hyperplasia in large intrapulmonary airways after intratracheal injection of cathepsin B into hamsters. Am Rev Respir Dis. 1992 Mar;145(3):675–9.

190. Werb Z, Banda MJ, McKerrow JH, Sandhaus RA. Elastases and elastin degradation. J Invest Dermatol. 1982 Jul;79 Suppl 1:154s – 159s.

191. Russell RE, Culpitt SV, DeMatos C, Donnelly L, Smith M, Wiggins J, et al. Release and activity of matrix metalloproteinase-9 and tissue inhibitor of metalloproteinase-1 by alveolar macrophages from patients with chronic

obstructive pulmonary disease. Am J Respir Cell Mol Biol. 2002 May;26:602–9.

192. Salazar LM, Herrera AM. Fibrotic response of tissue remodeling in COPD. Lung. 2011 Apr;189(2):101–9.

193. Khalil N, O'Connor RN, Unruh HW, Warren PW, Flanders KC, Kemp A, et al. Increased production and immunohistochemical localization of transforming growth factor-beta in idiopathic pulmonary fibrosis. Am J Respir Cell Mol Biol. 1991 Aug;5(2):155–62.

194. Vignola AM, Chanez P, Chiappara G, Merendino A, Zinnanti E, Bousquet J, et al. Release of transforming growth factor-beta (TGF-beta) and fibronectin by alveolar macrophages in airway diseases. Clin Exp Immunol. 1996 Oct;106(1):114–9.

195. King P. Haemophilus influenzae and the lung (Haemophilus and the lung). Clin Transl Med. 2012 Jun 14;1:10.

196. Eskola J, Käyhty H, Takala AK, Peltola H, Rönnberg PR, Kela E, et al. A randomized, prospective field trial of a conjugate vaccine in the protection of infants and young children against invasive Haemophilus influenzae type b disease. N Engl J Med. 1990 Nov 15;323(20):1381–7.

197. http://www.cdc.gov/.

198. http://www.microbiologyinpictures.com/haemophilus%20influenzae.html.

199. Kilian, M. Haemophilus. In A. Balows, K. L. Herrmann, H. D. Isenberg, and J. J. Shadomy (ed.), Manual of clinical microbiology. American Society for Microbiology, Washington, DC.p. 463-470. 1991.

200. Ward JI. Haemophilus influenzae vaccines In: Vaccines, Plotkin, SA, Orienstein, WA (Eds),. third ed. WB Saunders Company, Philadelphia, Pennsylvania; 1999.

201. Mukundan D, Ecevit Z, Patel M, Marrs CF, Gilsdorf JR. Pharyngeal Colonization Dynamics of Haemophilus influenzae and Haemophilus haemolyticus in Healthy Adult Carriers. J Clin Microbiol. 2007 Oct 1;45(10):3207–17.

202. Sunakawa K, Takeuchi Y, Iwata S. [Nontypeable Haemophilus influenzae (NTHi) epidemiology]. Kansenshōgaku Zasshi J Jpn Assoc Infect Dis. 2011 May;85(3):227–37.

203. Faden H, Duffy L, Williams A, Krystofik DA, Wolf J. Epidemiology of Nasopharyngeal Colonization with Nontypeable Haemophilus influenzae in the First 2 Years of Life. J Infect Dis. 1995 Jul 1;172(1):132–5.

204. Murphy TF, Brauer AL, Schiffmacher AT, Sethi S. Persistent Colonization by Haemophilus influenzae in Chronic Obstructive Pulmonary Disease. Am J Respir Crit CARE Med. 2004 Aug 1;170:266–72.

205. King PT, Hutchinson PE, Johnson PD, Holmes PW, Freezer NJ, Holdsworth SR. Adaptive Immunity to Nontypeable Haemophilus influenzae. Am J Respir Crit Care Med. 2003 Feb 15;167(4):587–92.

206. Bandi V, Apicella MA, Mason E, Murphy TF, Siddiqi A, Atmar RL, et al. Nontypeable Haemophilus influenzae in the lower respiratory tract of patients with chronic bronchitis. Am J Respir Crit Care Med. 2001 Dec 1;164(11):2114–9.

207. Soler N, Ewig S, Torres A, Filella X, Gonzalez J, Zaubet A. Airway inflammation and bronchial microbial patterns in patients with stable chronic obstructive pulmonary disease. Eur Respir J. 1999 Nov;14(5):1015–22.

208. Sethi S, Maloney J, Grove L, Wrona C, Berenson CS. Airway Inflammation and Bronchial Bacterial Colonization in Chronic Obstructive Pulmonary Disease. Am J Respir Crit CARE Med. 2006 May 1;173:991–8.

209. Bresser P, Out TA, van Alphen L, Jansen HM, Lutter R. Airway inflammation in nonobstructive and obstructive chronic bronchitis with chronic haemophilus influenzae airway infection. Comparison with noninfected patients with chronic obstructive pulmonary disease. Am J Respir Crit Care Med. 2000 Sep;162(3 Pt 1):947–52.

210. Banerjee D, Khair OA, Honeybourne D. Impact of sputum bacteria on airway inflammation and health status in clinical stable COPD. Eur Respir J. 2004 May 1;23:685–91.

211. Eldika N, Sethi S. Role of nontypeable Haemophilus influenzae in exacerbations and progression of chronic obstructive pulmonary disease. Curr Opin Pulm Med. 2006 Mar;12(2):118–24.

212. Moghaddam SJ, Clement CG, De la Garza MM, Zou X, Travis EL, Young HWJ, et al. Haemophilus influenzae Lysate Induces Aspects of the Chronic Obstructive Pulmonary Disease Phenotype. Am J Respir Cell Mol Biol. 2008 Jun 1;38:629–38.

213. Sethi S, Murphy TF. Infection in the Pathogenesis and Course of Chronic Obstructive Pulmonary Disease. N Engl J Med. 2008;359:2355–65.

214. Sethi S, Wrona C, Grant BJB, Murphy TF. Strain-specific immune response to Haemophilus influenzae in chronic obstructive pulmonary disease. Am J Respir Crit Care Med. 2004 Feb 15;169(4):448–53.

215. Garcha DS, Thurston SJ, Patel ARC, Mackay AJ, Goldring JJP, Donaldson GC, et al. Changes in prevalence and load of airway bacteria using quantitative PCR in stable and exacerbated COPD. Thorax. 2012 Dec 1;67:1075–80.

216. Rosell A, Monso E, Soler N, Torres F, Angrill J, Riise G, et al. Microbiologic determinants of exacerbation in chronic obstructive pulmonary disease. Arch Intern Med. 2005;165:891–7.

217. Sethi S, Sethi R, Eschberger K, Lobbins P, Cai X, Grant BJB, et al. Airway Bacterial Concentrations and Exacerbations of Chronic Obstructive Pulmonary Disease. Am J Respir Crit CARE Med. 2007 Aug 15;176:356–61.

218. Abusriwil H, Stockley RA. Bacterial Load and Exacerbations of COPD. Am J Respir Crit Care Med. 2008 May 1;177(9):1048–9.

219. Tager I, Speizer FE. Role of Infection in Chronic Bronchitis. N Engl J Med. 1975;292:563–71.

220. Sethi S, Evans N, Grant BJB, Murphy TF. New Strains of Bacteria and Exacerbations of Chronic Obstructive Pulmonary Disease. N Engl J Med. 2002;347:465–71.

221. Kilbourn JP, Haas H, Morris JF, Samson S. Hemophilus Influenzae Biotypes and Chronic Bronchitis. Am Rev Respir Dis. 1983 Dec 1;128(6):1093–4.

222. Joseph W. St Geme. Molecular and cellular determinants of non-typeable Haemophilus influenzae adherence and invasion. Cell Microbiol. 2002;4(4),:191–200.

223. Reddy MS, Bernstein JM, Murphy TF, Faden HS. Binding between outer membrane proteins of nontypeable Haemophilus influenzae and human nasopharyngeal mucin. Infect Immun. 1996 Apr;64(4):1477–9.

224. Hill DJ, Toleman MA, Evans DJ, Villullas S, Van Alphen L, Virji M. The variable P5 proteins of typeable and non-typeable Haemophilus influenzae target human CEACAM1. Mol Microbiol. 2001 Feb;39(4):850–62.

225. Hansen EJ, Hart DA, McGehee JL, Toews GB. Immune enhancement of pulmonary clearance of nontypable Haemophilus influenzae. Infect Immun. 1988 Jan;56(1):182–90.

226. Forbes KJ, Bruce KD, Ball A, Pennington TH. Variation in length and sequence of porin (ompP2) alleles of non-capsulate Haemophilus influenzae. Mol Microbiol. 1992 Aug;6(15):2107–12.

227. Nelson MB, Apicella MA, Murphy TF, Vankeulen H, Spotila LD, Rekosh D. Cloning and sequencing of Haemophilus influenzae outer membrane protein P6. Infect Immun. 1988 Jan;56(1):128–34.

228. Berenson CS, Murphy TF, Wrona CT, Sethi S. Outer Membrane Protein P6 of Nontypeable Haemophilus influenzae Is a Potent and Selective Inducer of Human Macrophage Proinflammatory Cytokines. Infect Immun. 2005 May;73(5):2728–35.

229. Murphy TF, Bartos LC, Campagnari AA, Nelson MB, Apicella MA. Antigenic characterization of the P6 protein of nontypable Haemophilus influenzae. Infect Immun. 1986 Dec;54(3):774–9.

230. Badr WH, Loghmanee D, Karalus RJ, Murphy TF, Thanavala Y. Immunization of mice with P6 of nontypeable Haemophilus influenzae: kinetics of the antibody response and IgG subclasses. Vaccine. 1999 Aug 20;18:29–37.

231. Abe Y, Murphy TF, Sethi S, Faden HS, Dmochowski J, Harabuchi Y, et al. Lymphocyte proliferative response to P6 of Haemophilus influenzae is associated with relative protection from exacerbations of chronic obstructive pulmonary disease. Am J Respir Crit Care Med. 2002 Apr 1;165(7):967–71.

232. Murphy TF, Kirkham C, Lesse AJ. Construction of a mutant and characterization of the role of the vaccine antigen P6 in outer membrane integrity of nontypeable Haemophilus influenzae. Infect Immun. 2006 Sep;74(9):5169–76.

233. Johnson AP, Inzana TJ. Loss of ciliary activity in organ cultures of rat trachea treated with lipo-oligosaccharide from Haemophilus influenzae. J Med Microbiol. 1986 Nov;22(3):265–8.

234. Masoud H, Moxon ER, Martin A, Krajcarski D, Richards JC. Structure of the variable and conserved lipopolysaccharide oligosaccharide epitopes expressed by Haemophilus influenzae serotype b strain Eagan. Biochemistry (Mosc). 1997 Feb 25;36(8):2091–103.

235. Risberg A, Masoud H, Martin A, Richards JC, Moxon ER, Schweda EK. Structural analysis of the lipopolysaccharide oligosaccharide epitopes expressed by a capsule-deficient strain of Haemophilus influenzae Rd. Eur J Biochem FEBS. 1999 Apr;261(1):171–80.

236. Campagnari AA, Gupta MR, Dudas KC, Murphy TF, Apicella MA. Antigenic diversity of lipooligosaccharides of nontypable Haemophilus influenzae. Infect Immun. 1987 Apr;55(4):882–7.

237. Zwahlen A, Winkelstein JA, Moxon ER. Surface determinants of Haemophilus influenzae pathogenicity: comparative virulence of capsular transformants in normal and complement-depleted rats. J Infect Dis. 1983 Sep;148(3):385–94.

238. Zhang YH, Takahashi K, Jiang GZ, Zhang XM, Kawai M, Fukada M, et al. In vivo production of heat shock protein in mouse peritoneal macrophages by administration of lipopolysaccharide. Infect Immun. 1994 Oct;62(10):4140–4.

239. Nelson S, Bagby GJ, Bainton BG, Wilson LA, Thompson JJ, Summer WR. Compartmentalization of intraalveolar and systemic lipopolysaccharide-induced tumor necrosis factor and the pulmonary inflammatory response. J Infect Dis. 1989 Feb;159(2):189–94.

240. Lysenko ES, Gould J, Bals R, Wilson JM, Weiser JN. Bacterial phosphorylcholine decreases susceptibility to the antimicrobial peptide LL-37/hCAP18 expressed in the upper respiratory tract. Infect Immun. 2000 Mar;68(3):1664–71.

241. Pang B, Winn D, Johnson R, Hong W, West-Barnette S, Kock N, et al. Lipooligosaccharides Containing Phosphorylcholine Delay Pulmonary Clearance of Nontypeable Haemophilus influenzae. Infect Immun. 2008 May;76:2037–43.

242. Hong W, Pang B, West-Barnette S, Swords WE. Phosphorylcholine Expression by Nontypeable Haemophilus influenzae Correlates with Maturation of Biofilm Communities In Vitro and In Vivo. J Bacteriol. 2007 Nov;189(22):8300–7.

243. Swords WE, Buscher BA, Ver Steeg Ii K, Preston A, Nichols WA, Weiser JN, et al. Non-typeable Haemophilus influenzae adhere to and invade human bronchial epithelial cells via an interaction of lipooligosaccharide with the PAF receptor. Mol Microbiol. 2000;37:13–27.

244. Gilsdorf JR, McCrea KW, Marrs CF. Role of pili in Haemophilus influenzae adherence and colonization. Infect Immun. 1997 Aug;65(8):2997–3002.

245. Euba B, Moleres J, Viadas C, Ruiz de los Mozos I, Valle J, Bengoechea JA, et al. Relative Contribution of P5 and Hap Surface Proteins to Nontypable Haemophilus influenzae Interplay with the Host Upper and Lower Airways. PLoS ONE [Internet]. 2015 Apr 20 [cited 2015 Dec 16];10(4). Available from: http://www.ncbi.nlm.nih.gov/pmc/articles/PMC4403991/

246. Avadhanula V, Rodriguez CA, Ulett GC, Bakaletz LO, Adderson EE. Nontypeable Haemophilus influenzae adheres to intercellular adhesion molecule 1 (ICAM-1) on respiratory epithelial cells and upregulates ICAM-1 expression. Infect Immun. 2006 Feb;74(2):830–8.

247. Geme JWS, Falkow S, Barenkamp SJ. High-molecular-weight proteins of nontypable Haemophilus influenzae mediate attachment to human epithelial cells. Proc Natl Acad Sci. 1993 Apr 1;90(7):2875–9.

248. Kubiet M, Ramphal R, Weber A, Smith A. Pilus-Mediated Adherence of Haemophilus influenzae to Human Respiratory Mucins. Infect Immun. 2000 Jun;68(6):3362–7.

249. Carruthers MD, Tracy EN, Dickson AC, Ganser KB, Munson RS, Bakaletz LO. Biological roles of nontypeable Haemophilus influenzae type IV pilus proteins encoded by the pil and com operons. J Bacteriol. 2012 Apr;194(8):1927–33.

250. Henderson IR. Virulence functions of autotransporter proteins. Infect Immun. 2001;69:1231–43.

251. Ahren IL, Williams DL, Rice PJ, Forsgren A, Riesbeck K. The importance of a beta-glucan receptor in the nonopsonic entry of nontypeable Haemophilus influenzae into human monocytic and epithelial cells. J Infect Dis. 2001 Jul 15;184:150–8.

252. Ronander E, Brant M, Eriksson E, Mörgelin M, Hallgren O, Westergren-Thorsson G, et al. Nontypeable Haemophilus influenzae adhesin protein E: Characterization and Biological Activity. J Infect Dis. 2009 Feb 15;199(4):522–31.

253. Fink DL, Buscher AZ, Green B, Fernsten P, St Geme JW. The Haemophilus influenzae Hap autotransporter mediates microcolony formation and adherence to epithelial cells and extracellular matrix via binding regions in

the C-terminal end of the passenger domain. Cell Microbiol. 2003 Mar;5(3):175–86.

254. St Geme JW, de la Morena ML, Falkow S. A Haemophilus influenzae IgA protease-like protein promotes intimate interaction with human epithelial cells. Mol Microbiol. 1994 Oct;14(2):217–33.

255. Fink DL, Green BA, St Geme JW. The Haemophilus influenzae Hap autotransporter binds to fibronectin, laminin, and collagen IV. Infect Immun. 2002 Sep;70(9):4902–7.

256. Kerr MA. Function of immunoglobulin A in immunity. Gut. 2000 Dec 1;47(6):751–2.

257. Kerr MA. The structure and function of human IgA. Biochem J. 1990 Oct 15;271(2):285–96.

258. Pilette C, Ouadrhiri Y, Godding V, Vaerman J-P, Sibille Y. Lung mucosal immunity: immunoglobulin-A revisited. Eur Respir J. 2001 Sep 1;18(3):571–88.

259. Kilian M, Mestecky J, Schrohenloher RE. Pathogenic species of the genus Haemophilus and Streptococcus pneumoniae produce immunoglobulin A1 protease. Infect Immun. 1979 Oct;26(1):143–9.

260. Plaut AG, Qiu J, Grundy F, Wright A. Growth of Haemophilus influenzae in human milk: synthesis, distribution, and activity of IgA protease as determined by study of iga+ and mutant iga- cells. J Infect Dis. 1992 Jul;166(1):43–52.

261. Mistry DV, Stockley RA. The cleavage specificity of an IgA1 protease from Haemophilus influenzae. Virulence. 2011 Mar 1;2(2):103–10.

262. Vitovski S, Dunkin KT, Howard AJ, Sayers JR. Nontypeable Haemophilus influenzae in carriage and disease: a difference in IgA1 protease activity levels. JAMA. 2002 Apr 3;287(13):1699–705.

263. Fernaays MM, Lesse AJ, Cai X, Murphy TF. Characterization of igaB, a second immunoglobulin A1 protease gene in nontypeable Haemophilus influenzae. Infect Immun. 2006 Oct;74(10):5860–70.

264. Fernaays MM, Lesse AJ, Sethi S, Cai X, Murphy TF. Differential genome contents of nontypeable Haemophilus influenzae strains from adults with chronic obstructive pulmonary disease. Infect Immun. 2006 Jun;74(6):3366–74.

265. St Geme JW. The pathogenesis of nontypable Haemophilus influenzae otitis media. Vaccine. 2000 Dec 8;19 Suppl 1:S41–50.

266. Hendrixson DR, St Geme JW. The Haemophilus influenzae Hap serine protease promotes adherence and microcolony formation, potentiated by a soluble host protein. Mol Cell. 1998 Dec;2(6):841–50.

267. van Ham SM, van Alphen L, Mooi FR, van Putten JP. Phase variation of H. influenzae fimbriae: transcriptional control of two divergent genes through a variable combined promoter region. Cell. 1993 Jun 18;73(6):1187–96.

268. Gilsdorf JR. Antigenic diversity and gene polymorphisms in Haemophilus influenzae. Infect Immun. 1998;66:5053–9.

269. Duim B, Vogel L, Puijk W, Jansen HM, Meloen RH, Dankert J, et al. Fine mapping of outer membrane protein P2 antigenic sites which vary during persistent infection by Haemophilus influenzae. Infect Immun. 1996 Nov 1;64:4673–9.

270. Costerton JW, Stewart PS, Greenberg EP. Bacterial biofilms: a common cause of persistent infections. Science. 1999 May 21;284:1318–22.

271. O'Toole G, Kaplan HB, Kolter R. Biofilm formation as microbial development. Annu Rev Microbiol. 2000;54:49–79.

272. Meluleni GJ, Grout M, Evans DJ, Pier GB. Mucoid Pseudomonas aeruginosa growing in a biofilm in vitro are killed by opsonic antibodies to the mucoid exopolysaccharide capsule but not by antibodies produced during chronic lung infection in cystic fibrosis patients. J Immunol. 1995 Aug 15;155:2029–38.

273. Evans DJ, Allison DG, Brown MR, Gilbert P. Susceptibility of Pseudomonas aeruginosa and Escherichia coli biofilms towards ciprofloxacin: effect of specific growth rate. J Antimicrob Chemother. 1991 Feb;27:177–84.

274. Post JC, Preston RA, Aul JJ, Larkins-Pettigrew M, Rydquist-White J, Anderson KW, et al. Molecular analysis of bacterial pathogens in otitis media with effusion. JAMA. 1995 May 24;273(20):1598–604.

275. Slinger R, Chan F, Ferris W, Yeung S-W, St Denis M, Gaboury I, et al. Multiple combination antibiotic susceptibility testing of nontypeable Haemophilus influenzae biofilms. Diagn Microbiol Infect Dis. 2006 Nov;56(3):247–53.

276. Starner TD, Zhang N, Kim G, Apicella MA, McCray PB. Haemophilus influenzae forms biofilms on airway epithelia: implications in cystic fibrosis. Am J Respir Crit Care Med. 2006 Jul 15;174(2):213–20.

277. Murphy TF, Kirkham C. Biofilm formation by nontypeable Haemophilus influenzae: strain variability, outer membrane antigen expression and role of pili. BMC Microbiol. 2002 Apr 15;2:7.

278. Swords WE, Moore ML, Godzicki L, Bukofzer G, Mitten MJ, VonCannon J. Sialylation of lipooligosaccharides promotes biofilm formation by nontypeable Haemophilus influenzae. Infect Immun. 2004 Jan;72(1):106–13.

279. Bouchet V, Hood DW, Li J, Brisson J-R, Randle GA, Martin A, et al. Host-derived sialic acid is incorporated into Haemophilus influenzae lipopolysaccharide and is a major virulence factor in experimental otitis media. Proc Natl Acad Sci U S A. 2003 Jul 22;100(15):8898–903.

280. Novotny LA, Adams LD, Kang DR, Wiet GJ, Cai X, Sethi S, et al. Epitope mapping immunodominant regions of the PilA protein of nontypeable Haemophilus influenzae (NTHI) to facilitate the design of two novel chimeric vaccine candidates. Vaccine. 2009 Dec 10;28(1):279–89.

281. Webster P, Wu S, Gomez G, Apicella M, Plaut AG, St Geme JW. Distribution of bacterial proteins in biofilms formed by non-typeable Haemophilus influenzae. J Histochem Cytochem Off J Histochem Soc. 2006 Jul;54(7):829–42.

282. Jurcisek JA, Bakaletz LO. Biofilms formed by nontypeable Haemophilus influenzae in vivo contain both double-stranded DNA and type IV pilin protein. J Bacteriol. 2007 May;189(10):3868–75.

283. Rouvière-Yaniv J, Gros F. Characterization of a novel, low-molecular-weight DNA-binding protein from Escherichia coli. Proc Natl Acad Sci U S A. 1975 Sep;72(9):3428–32.

284. Goodman SD, Obergfell KP, Jurcisek JA, Novotny LA, Downey JS, Ayala EA, et al. Biofilms can be dispersed by focusing the immune system on a common family of bacterial nucleoid-associated proteins. Mucosal Immunol. 2011 Nov;4(6):625–37.

285. Rutherford ST, Bassler BL. Bacterial Quorum Sensing: Its Role in Virulence and Possibilities for Its Control. Cold Spring Harb Perspect Med. 2012 Nov 1;2(11):a012427.

286. Ng W-L, Bassler BL. Bacterial quorum-sensing network architectures. Annu Rev Genet. 2009;43:197–222.

287. Asad S, Opal SM. Bench-to-bedside review: Quorum sensing and the role of cell-to-cell communication during invasive bacterial infection. Crit Care Lond Engl. 2008;12(6):236.

288. Bassler BL. Small Talk: Cell-to-Cell Communication in Bacteria. Cell. 2002 May 17;109(4):421–4.

289. Harrison A, Dyer DW, Gillaspy A, Ray WC, Mungur R, Carson MB, et al. Genomic sequence of an otitis media isolate of nontypeable Haemophilus influenzae: comparative study with H. influenzae serotype d, strain KW20. J Bacteriol. 2005 Jul;187(13):4627–36.

290. Armbruster CE, Hong W, Pang B, Dew KE, Juneau RA, Byrd MS, et al. LuxS promotes biofilm maturation and persistence of nontypeable haemophilus influenzae in vivo via modulation of lipooligosaccharides on the bacterial surface. Infect Immun. 2009 Sep;77(9):4081–91.

291. Armbruster CE, Hong W, Pang B, Weimer KED, Juneau RA, Turner J, et al. Indirect pathogenicity of Haemophilus influenzae and Moraxella catarrhalis in polymicrobial otitis media occurs via interspecies quorum signaling. mBio. 2010;1(3).

292. Clementi C, Murphy T. Non-typeable Haemophilus influenzae invasion and persistence in the human respiratory tract. Front Cell Infect Microbiol. 2011;1:1.

293. Clementi CF, Håkansson AP, Murphy TF. Internalization and Trafficking of Nontypeable Haemophilus influenzae in Human Respiratory Epithelial Cells and Roles of IgA1 Proteases for Optimal Invasion and Persistence. Infect Immun. 2014 Jan;82(1):433–44.

294. Morey P, Cano V, Martí-Lliteras P, López-Gómez A, Regueiro V, Saus C, et al. Evidence for a non-replicative intracellular stage of nontypable Haemophilus influenzae in epithelial cells. Microbiol Read Engl. 2011 Jan;157(Pt 1):234–50.

295. Swanson JA, Watts C. Macropinocytosis. Trends Cell Biol. 1995 Nov;5(11):424–8.

296. van Schilfgaarde M, Eijk P, Regelink A, van Ulsen P, Everts V, Dankert J, et al. Haemophilus influenzae localized in epithelial cell layers is shielded from antibiotics and antibody-mediated bactericidal activity. Microb Pathog. 1999 May;26(5):249–62.

297. Craig JE, Cliffe A, Garnett K, High NJ. Survival of nontypeable Haemophilus influenzae in macrophages. FEMS Microbiol Lett. 2001;203:55–61.

298. Forsgren J, Samuelson A, Ahlin A, Jonasson J, Rynnel-Dagöö B, Lindberg A. Haemophilus influenzae resides and multiplies intracellularly in human adenoid tissue as demonstrated by in situ hybridization and bacterial viability assay. Infect Immun. 1994 Feb;62(2):673–9.

299. Ketterer MR, Shao JQ, Hornick DB, Buscher B, Bandi VK, Apicella MA. Infection of primary human bronchial epithelial cells by Haemophilus influenzae: macropinocytosis as a mechanism of airway epithelial cell entry. Infect Immun. 1999 Aug;67:4161–70.

300. Veiga E, Guttman JA, Bonazzi M, Boucrot E, Toledo-Arana A, Lin AE, et al. Invasive and adherent bacterial pathogens co-Opt host clathrin for infection. Cell Host Microbe. 2007 Nov 15;2(5):340–51.

301. Swords WE, Ketterer MR, Shao J, Campbell CA, Weiser JN, Apicella MA. Binding of the non-typeable Haemophilus influenzae lipooligosaccharide to the PAF receptor initiates host cell signalling. Cell Microbiol. 2001;3:525–36.

302. Donaldson JG, Porat-Shliom N, Cohen LA. Clathrin-Independent Endocytosis: A unique Platform for Cell Signaling and PM Remodeling. Cell Signal. 2009 Jan;21(1):1–6.

303. Duncan MJ, Shin J-S, Abraham SN. Microbial entry through caveolae: variations on a theme. Cell Microbiol. 2002 Dec 1;4(12):783–91.

304. van Schilfgaarde M, van Alphen L, Eijk P, Everts V, Dankert J. Paracytosis of Haemophilus influenzae through cell layers of NCI-H292 lung epithelial cells. Infect Immun. 1995 Dec;63(12):4729–37.

305. Farley MM, Stephens DS, Mulks MH, Cooper MD, Bricker JV, Mirra SS, et al. Pathogenesis of IgA1 protease-producing and -nonproducing Haemophilus influenzae in human nasopharyngeal organ cultures. J Infect Dis. 1986 Nov;154(5):752–9.

306. Möller LV, Timens W, van der Bij W, Kooi K, de Wever B, Dankert J, et al. Haemophilus influenzae in lung explants of patients with end-stage pulmonary disease. Am J Respir Crit Care Med. 1998 Mar;157(3 Pt 1):950–6.

307. St. Geme JW. Nontypeable Haemophilus influenzae disease: epidemiology, pathogenesis, and prospects for prevention. Infect Agents Dis. 1993;2:1–16.

308. Gilligan PH. Microbiology of airway disease in patients with cystic fibrosis. Clin Microbiol Rev. 1991;4:35–51.

309. Chipps BE, Talamo RC, Winkelstein JA. IgA deficiency, recurrent pneumonias, and bronchiectasis. Chest. 1978 Apr;73(4):519–26.

310. Hanson LA, Söderström R, Avanzini A, Bengtsson U, Björkander J, Söderström T. Immunoglobulin subclass deficiency. Pediatr Infect Dis J. 1988 May;7(5 Suppl):S17–21.

311. Musher DM, Wallace RJ. Bacteremic infections caused by nontypable Haemophilus influenzae in patients with dysgammaglobulinemia. J Clin Microbiol. 1983 Jan;17(1):143–5.

312. Read RC, Wilson R, Rutman A, Lund V, Todd HC, Brain AP, et al. Interaction of nontypable Haemophilus influenzae with human respiratory mucosa in vitro. J Infect Dis. 1991 Mar;163(3):549–58.

313. Denny FW. Effect of a toxin produced by Haemophilus influenzae on ciliated respiratory epithelium. J Infect Dis. 1974;129:93–100.

314. Kopp EB. The Toll-receptor family and control of innate immunity. Curr Opin Immunol. 1999;11:13.

315. Kurita S, Koyama J, Onizuka S, Motomura K, Watanabe H, Watanabe K, et al. Dynamics of dendritic cell migration and the subsequent induction of protective immunity in the lung after repeated airway challenges by nontypeable Haemophilus influenzae outer membrane protein. Vaccine. 2006 Jul 26;24(31-32):5896–903.

316. Berenson CS, Wrona CT, Grove LJ, Maloney J, Garlipp MA, Wallace PK, et al. Impaired Alveolar Macrophage Response to Haemophilus Antigens in Chronic Obstructive Lung Disease. Am J Respir Crit CARE Med. 2006 Jul 1;174:31–40.

317. Wang X, Moser C, Louboutin J-P, Lysenko ES, Weiner DJ, Weiser JN, et al. Toll-Like Receptor 4 Mediates Innate Immune Responses to Haemophilus influenzae Infection in Mouse Lung. J Immunol. 2002 Jan 15;168:810–5.

318. Wieland CW, Florquin S, Maris NA, Hoebe K, Beutler B, Takeda K, et al. The MyD88-Dependent, but Not the MyD88-Independent, Pathway of TLR4

Signaling Is Important in Clearing Nontypeable Haemophilus influenzae from the Mouse Lung. J Immunol. 2005 Nov 1;175:6042–9.

319. King PT, Ngui J, Gunawardena D, Holmes PW, Farmer MW, Holdsworth SR. Systemic humoral immunity to non-typeable Haemophilus influenzae. Clin Exp Immunol. 2008 Sep;153(3):376–84.

320. King PT, Ngui J, Farmer MW, Hutchinson P, Holmes PW, Holdsworth SR. Cytotoxic T lymphocyte and natural killer cell responses to non-typeable Haemophilus influenzae. Clin Exp Immunol. 2008 Jun;152(3):542–51.

321. King P, Ngui J, Oppedisano F, Robins-Browne R, Holmes P, Holdsworth S. Effect of interferon gamma and CD40 ligation on intracellular monocyte survival of nontypeable Haemophilus influenzae. APMIS. 2008;116(12):1043–9.

322. Lee I-T, Yang C-M. Inflammatory Signalings Involved in Airway and Pulmonary Diseases. Mediators Inflamm. 2013 Apr 4;2013:e791231.

323. Newton K, Dixit VM. Signaling in Innate Immunity and Inflammation. Cold Spring Harb Perspect Biol. 2012 Mar 1;4(3):a006049.

324. Widmann C, Gibson S, Jarpe MB, Johnson GL. Mitogen-activated protein kinase: conservation of a three-kinase module from yeast to human. Physiol Rev. 1999 Jan;79(1):143–80.

325. Mercer BA, D'Armiento JM. Emerging role of MAP kinase pathways as therapeutic targets in COPD. Int J Chron Obstruct Pulmon Dis. 2006 Jun;1(2):137–50.

326. Cargnello M, Roux PP. Activation and Function of the MAPKs and Their Substrates, the MAPK-Activated Protein Kinases. Microbiol Mol Biol Rev. 2011 Mar 1;75:50–83.

327. Jiang Y, Li Z, Schwarz EM, Lin A, Guan K, Ulevitch RJ, et al. Structure-Function Studies of p38 Mitogen-activated Protein Kinase: LOOP 12 INFLUENCES SUBSTRATE SPECIFICITY AND AUTOPHOSPHORYLATION, BUT NOT UPSTREAM KINASE SELECTION. J Biol Chem. 1997 Apr 25;272:11096–102.

328. Cuadrado A, Nebreda AR. Mechanisms and functions of p38 MAPK signalling. Biochem J. 2010 Aug 1;429(3):403–17.

329. Gaffey K, Reynolds S, Plumb J, Kaur M, Singh D. Increased phosphorylated p38 mitogen-activated protein kinase in COPD lungs. Eur Respir J. 2013 Jul 1;42(1):28–41.

330. Salvador JM, Mittelstadt PR, Guszczynski T, Copeland TD, Yamaguchi H, Appella E, et al. Alternative p38 activation pathway mediated by T cell receptor-proximal tyrosine kinases. Nat Immunol. 2005 Apr;6(4):390–5.

331. Karin M. Nuclear factor-kappaB in cancer development and progression. Nature. 2006 May 25;441(7092):431–6.

332. Buxade M, Parra-Palau JL, Proud CG. The Mnks: MAP kinase-interacting kinases (MAP kinase signal-integrating kinases). Front Biosci J Virtual Libr. 2008;13:5359–73.

333. Winzen R, Kracht M, Ritter B, Wilhelm A, Chen CY, Shyu AB, et al. The p38 MAP kinase pathway signals for cytokine-induced mRNA stabilization via MAP kinase-activated protein kinase 2 and an AU-rich region-targeted mechanism. EMBO J. 1999 Sep 15;18(18):4969–80.

334. Brook M, Tchen CR, Santalucia T, McIlrath J, Arthur JSC, Saklatvala J, et al. Posttranslational regulation of tristetraprolin subcellular localization and protein stability by p38 mitogen-activated protein kinase and extracellular signal-regulated kinase pathways. Mol Cell Biol. 2006 Mar;26(6):2408–18.

335. Newton R, Holden N. Inhibitors of p38 mitogen-activated protein kinase: potential as anti-inflammatory agents in asthma? BioDrugs Clin Immunother Biopharm Gene Ther. 2003;17(2):113–29.

336. Kim C, Sano Y, Todorova K, Carlson BA, Arpa L, Celada A, et al. The kinase p38 alpha serves cell type-specific inflammatory functions in skin injury and coordinates pro- and anti-inflammatory gene expression. Nat Immunol. 2008 Sep;9(9):1019–27.

337. Renda T, Baraldo S, Pelaia G, Bazzan E, Turato G, Papi A, et al. Increased activation of p38 MAPK in COPD. Eur Respir J. 2008 Jan 1;31:62–9.

338. Meja KK, Seldon PM, Nasuhara Y, Ito K, Barnes PJ, Lindsay MA, et al. p38 MAP kinase and MKK-1 co-operate in the generation of GM-CSF from LPS-stimulated human monocytes by an NF-kappa B-independent mechanism. Br J Pharmacol. 2000 Nov;131(6):1143–53.

339. Koch A, Giembycz M, Stirling RG, Lim S, Adcock I, Wassermann K, et al. Effect of smoking on MAP kinase-induced modulation of IL-8 in human alveolar macrophages. Eur Respir J. 2004 Jun;23(6):805–12.

340. Woo C-H, Lim J-H, Kim J-H. Lipopolysaccharide induces matrix metalloproteinase-9 expression via a mitochondrial reactive oxygen species-p38 kinase-activator protein-1 pathway in Raw 264.7 cells. J Immunol Baltim Md 1950. 2004 Dec 1;173(11):6973–80.

341. Huang C, Xie M, He X, Gao H. Activity of sputum p38 MAPK is correlated with airway inflammation and reduced FEV1 in COPD patients. Med Sci Monit Int Med J Exp Clin Res. 2013 Dec 31;19:1229–35.

342. Heit B, Tavener S, Raharjo E, Kubes P. An intracellular signaling hierarchy determines direction of migration in opposing chemotactic gradients. J Cell Biol. 2002 Oct 14;159(1):91–102.

343. Heuertz RM, Tricomi SM, Ezekiel UR, Webster RO. C-reactive protein inhibits chemotactic peptide-induced p38 mitogen-activated protein kinase activity and human neutrophil movement. J Biol Chem. 1999 Jun 18;274(25):17968–74.

344. Langlois A, Chouinard F, Flamand N, Ferland C, Rola-Pleszczynski M, Laviolette M. Crucial implication of protein kinase C (PKC)-delta, PKC-zeta, ERK-1/2, and p38 MAPK in migration of human asthmatic eosinophils. J Leukoc Biol. 2009 Apr;85(4):656–63.

345. Li F, Zhang M, Hussain F, Triantaphyllopoulos K, Clark AR, Bhavsar PK, et al. Inhibition of p38 MAPK-dependent bronchial contraction after ozone by corticosteroids. Eur Respir J. 2011 Apr;37(4):933–42.

346. Irusen E, Matthews JG, Takahashi A, Barnes PJ, Chung KF, Adcock IM. p38 Mitogen-activated protein kinase–induced glucocorticoid receptor phosphorylation reduces its activity: Role in steroid-insensitive asthma. J Allergy Clin Immunol. 2002 Apr;109(4):649–57.

347. Bhavsar P, Hew M, Khorasani N, Torrego A, Barnes PJ, Adcock I, et al. Relative corticosteroid insensitivity of alveolar macrophages in severe asthma compared with non-severe asthma. Thorax. 2008 Sep;63(9):784–90.

348. Mercado N, Hakim A, Kobayashi Y, Meah S, Usmani OS, Chung KF, et al. Restoration of Corticosteroid Sensitivity by p38 Mitogen Activated Protein Kinase Inhibition in Peripheral Blood Mononuclear Cells from Severe Asthma. PLoS ONE. 2012 Jul 23;7(7):e41582.

349. Armstrong J, Harbron C, Lea S, Booth G, Cadden P, Wreggett KA, et al. Synergistic effects of p38 mitogen-activated protein kinase inhibition with a corticosteroid in alveolar macrophages from patients with chronic obstructive pulmonary disease. J Pharmacol Exp Ther. 2011;338:732–40.

350. Kent LM, Smyth LJC, Plumb J, Clayton CL, Fox SM, Ray DW, et al. Inhibition of Lipopolysaccharide-Stimulated Chronic Obstructive Pulmonary Disease Macrophage Inflammatory Gene Expression by Dexamethasone and the p38 Mitogen-Activated Protein Kinase Inhibitor N-cyano-N′-(2-{[8-(2,6-difluorophenyl)-4-(4-fluoro-2-methylphenyl)-7-oxo-7,8-dihydropyrido[2,3-d] pyrimidin-2-yl]amino}ethyl)guanidine (SB706504). J Pharmacol Exp Ther. 2009 Feb 1;328:458–68.

351. Boulton TG, Nye SH, Robbins DJ, Ip NY, Radziejewska E, Morgenbesser SD, et al. ERKs: a family of protein-serine/threonine kinases that are activated and tyrosine phosphorylated in response to insulin and NGF. Cell. 1991 May 17;65(4):663–75.

352. Raman M, Chen W, Cobb MH. Differential regulation and properties of MAPKs. Oncogene. 2007 May 14;26(22):3100–12.

353. Sebolt-Leopold JS, Dudley DT, Herrera R, Van Becelaere K, Wiland A, Gowan RC, et al. Blockade of the MAP kinase pathway suppresses growth of colon tumors in vivo. Nat Med. 1999 Jul;5(7):810–6.

354. Mercer BA, Kolesnikova N, Sonett J, D'Armiento J. Extracellular Regulated Kinase/Mitogen Activated Protein Kinase Is Up-regulated in Pulmonary Emphysema and Mediates Matrix Metalloproteinase-1 Induction by Cigarette Smoke. J Biol Chem. 2004 Apr 23;279:17690–6.

355. Gensch E, Gallup M, Sucher A, Li D, Gebremichael A, Lemjabbar H, et al. Tobacco smoke control of mucin production in lung cells requires oxygen radicals AP-1 and JNK. J Biol Chem. 2004 Sep 10;279(37):39085–93.

356. Schuh K, Pahl A. Inhibition of the MAP kinase ERK protects from lipopolysaccharide-induced lung injury. Biochem Pharmacol. 2009;77:1827–34.

357. Miller AL, Garza AS, Johnson BH, Thompson EB. Pathway interactions between MAPKs, mTOR, PKA, and the glucocorticoid receptor in lymphoid cells. Cancer Cell Int. 2007 Mar 28;7(1):3.

358. Bode AM, Dong Z. The functional contrariety of JNK. Mol Carcinog. 2007 Aug;46(8):591–8.

359. Bogoyevitch MA, Ngoei KRW, Zhao TT, Yeap YYC, Ng DCH. c-Jun N-terminal kinase (JNK) signaling: recent advances and challenges. Biochim Biophys Acta. 2010 Mar;1804(3):463–75.

360. Angel P, Karin M. The role of Jun, Fos and the AP-1 complex in cell-proliferation and transformation. Biochim Biophys Acta. 1991 Dec 10;1072(2-3):129–57.

361. Dhanasekaran DN, Reddy EP. JNK signaling in apoptosis. Oncogene. 2008 Oct 20;27(48):6245–51.

362. Sabapathy K, Hochedlinger K, Nam SY, Bauer A, Karin M, Wagner EF. Distinct roles for JNK1 and JNK2 in regulating JNK activity and c-Jun-dependent cell proliferation. Mol Cell. 2004 Sep 10;15(5):713–25.

363. Hoshino S, Yoshida M, Inoue K, Yano Y, Yanagita M, Mawatari H, et al. Cigarette smoke extract induces endothelial cell injury via JNK pathway. Biochem Biophys Res Commun. 2005 Apr 1;329(1):58–63.

364. Tuyt LM, Dokter WH, Birkenkamp K, Koopmans SB, Lummen C, Kruijer W, et al. Extracellular-regulated kinase 1/2, Jun N-terminal kinase, and c-Jun are involved in NF-kappa B-dependent IL-6 expression in human monocytes. J Immunol Baltim Md 1950. 1999 Apr 15;162(8):4893–902.

365. Itoh M, Adachi M, Yasui H, Takekawa M, Tanaka H, Imai K. Nuclear export of glucocorticoid receptor is enhanced by c-Jun N-terminal kinase-mediated phosphorylation. Mol Endocrinol Baltim Md. 2002 Oct;16(10):2382–92.

366. Szatmáry Z, Garabedian MJ, Vilček J. Inhibition of Glucocorticoid Receptor-mediated Transcriptional Activation by p38 Mitogen-activated Protein (MAP) Kinase. J Biol Chem. 2004 Oct 15;279:43708–15.

367. Lee I-T, Yang C-M. Role of NADPH oxidase/ROS in pro-inflammatory mediators-induced airway and pulmonary diseases. Biochem Pharmacol. 2012 Sep 1;84(5):581–90.

368. Edwards MR, Bartlett NW, Clarke D, Birrell M, Belvisi M, Johnston SL. Targeting the NF-kappaB pathway in asthma and chronic obstructive pulmonary disease. Pharmacol Ther. 2009 Jan;121(1):1–13.

369. Caramori G, Romagnoli M, Casolari P, Bellettato C, Casoni G, Boschetto P, et al. Nuclear localisation of p65 in sputum macrophages but not in sputum neutrophils during COPD exacerbations. Thorax. 2003 Apr;58(4):348–51.

370. Di Stefano A, Caramori G, Oates T, Capelli A, Lusuardi M, Gnemmi I, et al. Increased expression of nuclear factor-kappaB in bronchial biopsies from smokers and patients with COPD. Eur Respir J. 2002 Sep;20(3):556–63.

371. Hatada EN, Krappmann D, Scheidereit C. NF-kappaB and the innate immune response. Curr Opin Immunol. 2000 Feb;12(1):52–8.

372. Texereau J, Chiche JD, Taylor W, Choukroun G, Comba B, Mira JP. The importance of Toll-like receptor 2 polymorphisms in severe infections. Clin Infect Dis. 2005 Nov 15;41 Suppl 7:S408–15.

373. Shuto T, Xu H, Wang B, Han J, Kai H, Gu XX, et al. Activation of NF-kappa B by nontypeable Hemophilus influenzae is mediated by toll-like receptor 2-TAK1-dependent NIK-IKK alpha /beta-I kappa B alpha and MKK3/6-p38 MAP kinase signaling pathways in epithelial cells. Proc Natl Acad Sci U A. 2001;98:8774–9.

374. Xu X, Steere RR, Fedorchuk CA, Pang J, Lee JY, Lim JH, et al. Activation of epidermal growth factor receptor is required for NTHi-induced NF-kappaB-dependent inflammation. PLoS One. 2011;6:23.

375. Wang B, Cleary PP, Xu H, Li JD. Up-regulation of interleukin-8 by novel small cytoplasmic molecules of nontypeable Haemophilus influenzae via p38 and extracellular signal-regulated kinase pathways. Infect Immun. 2003;71:5523–30.

376. Jono H, Shuto T, Xu H, Kai H, Lim DJ, Gum JR, et al. Transforming growth factor-beta -Smad signaling pathway cooperates with NF-kappa B to mediate nontypeable Haemophilus influenzae-induced MUC2 mucin transcription. J Biol Chem. 2002 Nov 22;277:45547–57.

377. Wang B, Lim DJ, Han J, Kim YS, Basbaum CB, Li JD. Novel cytoplasmic proteins of nontypeable Haemophilus influenzae up-regulate human MUC5AC mucin transcription via a positive p38 mitogen-activated protein kinase pathway and a negative phosphoinositide 3-kinase-Akt pathway. J Biol Chem. 2002;277:949–57.

378. Barnes PJ. Corticosteroid Resistance in Airway Disease. Proc Am Thorac Soc. 2004 Nov 1;1:264–8.

379. Rhen T, Cidlowski JA. Antiinflammatory action of glucocorticoids--new mechanisms for old drugs. N Engl J Med. 2005 Oct 20;353(16):1711–23.

380. Ito K, Barnes PJ, Adcock IM. Glucocorticoid Receptor Recruitment of Histone Deacetylase 2 Inhibits Interleukin-1β-Induced Histone H4 Acetylation on Lysines 8 and 12. Mol Cell Biol. 2000 Sep 15;20:6891–903.

381. Clark AR. MAP kinase phosphatase 1: a novel mediator of biological effects of glucocorticoids? J Endocrinol. 2003 Jul;178(1):5–12.

382. Barnes PJ, Adcock IM. How Do Corticosteroids Work in Asthma? Ann Intern Med. 2003 Sep 2;139(5_Part_1):359–70.

383. Barnes PJ, Adcock IM, Ito K. Histone acetylation and deacetylation: importance in inflammatory lung diseases. Eur Respir J. 2005 Mar;25(3):552–63.

384. Kharwanlang B, Sharma R. Molecular interaction between the glucocorticoid receptor and MAPK signaling pathway: a novel link in modulating the anti-inflammatory role of glucocorticoids. Indian J Biochem Biophys. 2011 Aug;48(4):236–42.

385. Lewis-Tuffin LJ, Cidlowski JA. The physiology of human glucocorticoid receptor beta (hGRbeta) and glucocorticoid resistance. Ann N Y Acad Sci. 2006 Jun;1069:1–9.

386. Galliher-Beckley AJ, Cidlowski JA. Emerging roles of glucocorticoid receptor phosphorylation in modulating glucocorticoid hormone action in health and disease. IUBMB Life. 2009 Oct 1;61(10):979–86.

387. Zhou J, Cidlowski JA. The human glucocorticoid receptor: one gene, multiple proteins and diverse responses. Steroids. 2005 Jun;70(5-7):407–17.

388. Ismaili N, Garabedian MJ. Modulation of glucocorticoid receptor function via phosphorylation. Ann N Y Acad Sci. 2004 Jun;1024:86–101.

389. Leung DY, Bloom JW. Update on glucocorticoid action and resistance. J Allergy Clin Immunol. 2003;111:3–22.

390. Wang Z, Frederick J, Garabedian MJ. Deciphering the phosphorylation "code" of the glucocorticoid receptor in vivo. J Biol Chem. 2002 Jul 19;277(29):26573–80.

391. Suissa S, Ernst P, Vandemheen KL, Aaron SD. Methodological issues in therapeutic trials of COPD. Eur Respir J. 2008 May;31(5):927–33.

392. Llewellyn-Jones CG, Harris TA, Stockley RA. Effect of fluticasone propionate on sputum of patients with chronic bronchitis and emphysema. Am J Respir Crit Care Med. 1996 Feb;153(2):616–21.

393. Llewellyn-Jones CG, Hill SL, Stockley RA. Effect of fluticasone propionate on neutrophil chemotaxis, superoxide generation, and extracellular proteolytic activity in vitro. Thorax. 1994 Mar;49(3):207–12.

394. Bourbeau J, Christodoulopoulos P, Maltais F, Yamauchi Y, Olivenstein R, Hamid Q. Effect of salmeterol/fluticasone propionate on airway inflammation in COPD: a randomised controlled trial. Thorax. 2007 Nov;62(11):938–43.

395. Culpitt SV, Maziak W, Loukidis S, Nightingale JA, Matthews JL, Barnes PJ. Effect of High Dose Inhaled Steroid on Cells, Cytokines, and Proteases in Induced Sputum in Chronic Obstructive Pulmonary Disease. Am J Respir Crit CARE Med. 1999 Nov 1;160:1635–9.

396. Wilkinson TMA, Patel IS, Wilks M, Donaldson GC, Wedzicha JA. Airway bacterial load and FEV1 decline in patients with chronic obstructive pulmonary disease. Am J Respir Crit Care Med. 2003 Apr 15;167(8):1090–5.

397. Plumb J, Robinson L, Lea S, Banyard A, Blaikley J, Ray D, et al. Evaluation of glucocorticoid receptor function in COPD lung macrophages using beclomethasone-17-monopropionate. PLoS One. 2013;8.

398. Cowburn AS, Condliffe AM, Farahi N, Summers C, Chilvers ER. Advances in neutrophil biology: clinical implications. Chest. 2008 Sep;134(3):606–12.

399. Plumb J, Gaffey K, Kane B, Malia-Milanes B, Shah R, Bentley A, et al. Reduced glucocorticoid receptor expression and function in airway neutrophils. Int Immunopharmacol. 2012 Jan;12(1):26–33.

400. Manminder Kaur et al. T lymphocyte insensitivity to corticosteroids in chronic obstructive pulmonary disease. Respir Res. 2012;13:20 doi:10.1186/1465-9921-13-20.

401. Peter J Barnes. How corticosteroids control inflammation. Br J Pharmacol 1483 245–254. 2006;

402. Ito K, Ito M, Elliott WM, Cosio B, Caramori G, Kon OM, et al. Decreased Histone Deacetylase Activity in Chronic Obstructive Pulmonary Disease. N Engl J Med. 2005;352:1967–76.

403. Barnes PJ, Ito K, Adcock IM. Corticosteroid resistance in chronic obstructive pulmonary disease: inactivation of histone deacetylase. The Lancet. 2004 Feb 28;363(9410):731–3.

404. Ito K, Lim S, Caramori G, Chung KF, Barnes PJ, Adcock IM. Cigarette smoking reduces histone deacetylase 2 expression, enhances cytokine expression, and inhibits glucocorticoid actions in alveolar macrophages. FASEB J [Internet]. 2001 Feb 5 [cited 2015 May 6]; Available from: http://www.fasebj.org/content/early/2001/04/02/fj.00-0432fje

405. Hakim A, Adcock IM, Usmani OS. Corticosteroid Resistance and Novel Anti-Inflammatory Therapies in Chronic Obstructive Pulmonary Disease: Current Evidence and Future Direction. Drugs. 2012;72:1299–312 10.2165/11634350–000000000 – 00000.

406. Matthews JG, Ito K, Barnes PJ, Adcock IM. Defective glucocorticoid receptor nuclear translocation and altered histone acetylation patterns in glucocorticoid-resistant patients. J Allergy Clin Immunol. 2004 Jun;113(6):1100–8.

407. Barenkamp SJ, Leininger E. Cloning, expression, and DNA sequence analysis of genes encoding nontypeable Haemophilus influenzae high-molecular-weight

surface-exposed proteins related to filamentous hemagglutinin of Bordetella pertussis. Infect Immun. 1992;60:1302–13.

408. Coleman HN, Daines DA, Jarisch J, Smith AL. Chemically Defined Media for Growth of Haemophilus influenzae Strains. J Clin Microbiol. 2003 Sep 1;41:4408–10.

409. Miles AA, Misra SS, Irwin JO. The estimation of the bactericidal power of the blood. J Hyg (Lond). 1938 Nov;38(6):732–49.

410. BSAC Methods for Antimicrobial Susceptibility Testing, version 12 May 2013.

411. Arends MJ, Morris RG, Wyllie AH. Apoptosis. The role of the endonuclease. Am J Pathol. 1990 Mar;136(3):593–608.

412. Bortner CD, Oldenburg NBE, Cidlowski JA. The role of DNA fragmentation in apoptosis. Trends Cell Biol. 1995;5:21–6.

413. http://www.biotool.com/product/tunel-apo-green-detection-kit.html.

414. Laan M, Palmberg L, Larsson K, Lindén A. Free, soluble interleukin-17 protein during severe inflammation in human airways. Eur Respir J. 2002 Mar 1;19:534–7.

415. Livak KJ, Schmittgen TD. Analysis of relative gene expression data using real-time quantitative PCR and the 2(-Delta Delta C(T)) Method. Methods San Diego Calif. 2001 Dec;25(4):402–8.

416. Applied Biosystem User Bulletin No. 2 P/N 4303859.

417. St Geme JW, Falkow S. Haemophilus influenzae adheres to and enters cultured human epithelial cells. Infect Immun. 1990 Dec;58:4036–44.

418. Gu XX, Tsai CM, Apicella MA, Lim DJ. Quantitation and biological properties of released and cell-bound lipooligosaccharides from nontypeable Haemophilus influenzae. Infect Immun. 1995 Oct 1;63:4115–20.

419. Marin A, Garcia-Aymerich J, Sauleda J, Belda J, Millares L, Garcia-Nunez M, et al. Effect of bronchial colonisation on airway and systemic inflammation in stable COPD. COPD. Apr;9:121–30.

420. Sethi S, Murphy TF. Bacterial Infection in Chronic Obstructive Pulmonary Disease in 2000: a State-of-the-Art Review. Clin Microbiol Rev. 2001 Apr 1;14:336–63.

421. Marin A, Monsó E, Garcia-Nuñez M, Sauleda J, Noguera A, Pons J, et al. Variability and effects of bronchial colonisation in patients with moderate COPD. Eur Respir J. 2010 Feb 1;35:295–302.

422. Kane B, Kolsum U, Southworth T, Armstrong J, Woodcock A, Singh D. THe effects of smoking on the lipopolysaccharide response and glucocorticoid sensitivity of alveolar macrophages of patients with asthma. Chest. 2009 Jul 1;136(1):163–70.

423. Couper KN, Blount DG, Riley EM. IL-10: The Master Regulator of Immunity to Infection. J Immunol. 2008 May 1;180:5771–7.

424. Metcalfe HJ, Lea S, Hughes D, Khalaf R, Abbott-Banner K, Singh D. Effects of cigarette smoke on TLR activation of COPD macrophages. Clin Exp Immunol. 2014;DOI: 10.1111/cei.12289:n/a – n/a.

425. Roque S, Nobrega C, Appelberg R, Correia-Neves M. IL-10 Underlies Distinct Susceptibility of BALB/c and C57BL/6 Mice to Mycobacterium avium Infection and Influences Efficacy of Antibiotic Therapy. J Immunol. 2007 Jun 15;178:8028–35.

426. Balcewicz-Sablinska MK, Gan H, Remold HG. Interleukin 10 produced by macrophages inoculated with Mycobacterium avium attenuates mycobacteria-induced apoptosis by reduction of TNF-alpha activity. J Infect Dis. 1999;180:1230–7.

427. Lancellotti M, Pereira RFC, Cury GG, Hollanda LM de. Pathogenic and opportunistic respiratory bacteria-induced apoptosis. Braz J Infect Dis. 2009;13:226–31.

428. Gallelli L, Pelaia G, Fratto D, Muto V, Falcone D, Vatrella A, et al. Effects of budesonide on P38 MAPK activation, apoptosis and IL-8 secretion, induced by TNF-alpha and Haemophilus influenzae in human bronchial epithelial cells. Int J Immunopathol Pharmacol. 2010;23:471–9.

429. Shibahara S, Yoshida T, Kikuchi G. Induction of heme oxygenase by hemin in cultured pig alveolar macrophages. Arch Biochem Biophys. 1978;188:243–50.

430. Lang D, Reuter S, Buzescu T, August C, Heidenreich S. Heme-induced heme oxygenase-1 (HO-1) in human monocytes inhibits apoptosis despite caspase-3 up-regulation. Int Immunol. 2005 Feb 1;17:155–65.

431. Hualin C, Wenli X, Dapeng L, Xijing L, Xiuhua P, Qingfeng P. The Anti-inflammatory Mechanism of Heme Oxygenase-1 Induced by Hemin in Primary Rat Alveolar Macrophages. Inflammation. 2012;35:1087–93.

432. Erwin AL, Nelson KL, Mhlanga-Mutangadura T, Bonthuis PJ, Geelhood JL, Morlin G, et al. Characterization of Genetic and Phenotypic Diversity of Invasive Nontypeable Haemophilus influenzae. Infect Immun. 2005 Sep;73(9):5853–63.

433. Price D, Yawn B, Brusselle G, Rossi A. Risk-to-benefit ratio of inhaled corticosteroids in patients with COPD. Prim Care Respir J. 2013;22:92–100.

434. Soriano JB, Sin DD, Zhang X, Camp PG, Anderson JA, Anthonisen NR, et al. A pooled analysis of FEV1 decline in COPD patients randomized to inhaled corticosteroids or placebo. Chest. 2007;131:682–9.

435. Necela BM, Cidlowski JA. Mechanisms of Glucocorticoid Receptor Action in Noninflammatory and Inflammatory Cells. Proc Am Thorac Soc. 2004 Nov 1;1(3):239–46.

436. Ogawa S, Lozach J, Benner C, Pascual G, Tangirala RK, Westin S, et al. Molecular determinants of crosstalk between nuclear receptors and toll-like receptors. Cell. 2005 Sep 9;122(5):707–21.

437. Sethi S. Infection as a comorbidity of COPD. Eur Respir J. 2010 Jun 1;35:1209–15.

438. Kumar R, Calhoun WJ. Differential regulation of the transcriptional activity of the glucocorticoid receptor through site-specific phosphorylation. Biol Targets Ther. 2008 Dec;2(4):845–54.

439. Burke JR, Pattoli MA, Gregor KR, Brassil PJ, MacMaster JF, McIntyre KW, et al. BMS-345541 Is a Highly Selective Inhibitor of IκB Kinase That Binds at an Allosteric Site of the Enzyme and Blocks NF-κB-dependent Transcription in Mice. J Biol Chem. 2003 Jan 17;278:1450–6.

440. McIntyre KW, Shuster DJ, Gillooly KM, Dambach DM, Pattoli MA, Lu P, et al. A highly selective inhibitor of IκB kinase, BMS-345541, blocks both joint inflammation and destruction in collagen-induced arthritis in mice. Arthritis Rheum. 2003;48:2652–9.

441. Singh D, Smyth L, Borrill Z, Sweeney L, Tal-Singer R. A Randomized, Placebo-Controlled Study of the Effects of the p38 MAPK Inhibitor SB-681323 on Blood Biomarkers of Inflammation in COPD Patients. J Clin Pharmacol. 2010;50:94–100.

442. Pargellis C, Tong L, Churchill L, Cirillo PF, Gilmore T, Graham AG, et al. Inhibition of p38 MAP kinase by utilizing a novel allosteric binding site. Nat Struct Biol. 2002 Apr;9(4):268–72.

443. Regan J, Pargellis CA, Cirillo PF, Gilmore T, Hickey ER, Peet GW, et al. The kinetics of binding to p38MAP kinase by analogues of BIRB 796. Bioorg Med Chem Lett. 2003;13:3101–4.

444. Yeh TC, Marsh V, Bernat BA, Ballard J, Colwell H, Evans RJ, et al. Biological characterization of ARRY-142886 (AZD6244), a potent, highly selective mitogen-activated protein kinase kinase 1/2 inhibitor. Clin Cancer Res Off J Am Assoc Cancer Res. 2007 Mar 1;13(5):1576–83.

445. Uitdehaag JC, Verkaar F, Alwan H, de Man J, Buijsman RC, Zaman GJ. A guide to picking the most selective kinase inhibitor tool compounds for pharmacological validation of drug targets. Br J Pharmacol. 2012 Jun;166(3):858–76.

446. Uitdehaag JC, Zaman GJ. A theoretical entropy score as a single value to express inhibitor selectivity. BMC Bioinformatics. 2011 Apr 12;12(1):94.

447. Barnes PJ. Corticosteroid effects on cell signalling. Eur Respir J. 2006 Feb 1;27(2):413–26.

448. Lasa M, Abraham SM, Boucheron C, Saklatvala J, Clark AR. Dexamethasone Causes Sustained Expression of Mitogen-Activated Protein Kinase (MAPK)

Phosphatase 1 and Phosphatase-Mediated Inhibition of MAPK p38. Mol Cell Biol. 2002 Nov 15;22(22):7802–11.

449. Roland NJ, Bhalla RK, Earis J. The local side effects of inhaled corticosteroids*: Current understanding and review of the literature. Chest. 2004 Jul 1;126(1):213–9.

450. Bhavsar P, Khorasani N, Hew M, Johnson M, Chung KF. Effect of p38 MAPK inhibition on corticosteroid suppression of cytokine release in severe asthma. Eur Respir J. 2010 Apr;35(4):750–6.

451. Biswas SK, Mantovani A. Macrophage plasticity and interaction with lymphocyte subsets: cancer as a paradigm. Nat Immunol. 2010 Oct;11(10):889–96.

452. Edwards JP, Zhang X, Frauwirth KA, Mosser DM. Biochemical and functional characterization of three activated macrophage populations. J Leukoc Biol. 2006 Dec;80:1298–307.

453. Martinez FO, Gordon S. The M1 and M2 paradigm of macrophage activation: time for reassessment. F1000Prime Rep [Internet]. 2014 Mar 3 [cited 2014 Nov 18];6. Available from: http://f1000.com/prime/reports/b/6/13/

454. Chacón-Salinas R, Serafín-López J, Ramos-Payán R, Méndez-Aragón P, Hernández-Pando R, Van Soolingen D, et al. Differential pattern of cytokine expression by macrophages infected in vitro with different Mycobacterium tuberculosis genotypes. Clin Exp Immunol. 2005 Jun;140(3):443–9.

455. Jouanguy E, Doffinger R, Dupuis S, Pallier A, Altare F, Casanova JL. IL-12 and IFN-gamma in host defense against mycobacteria and salmonella in mice and men. Curr Opin Immunol. 1999;11:346–51.

456. Sieling PA, Modlin RL. Cytokine patterns at the site of mycobacterial infection. Immunobiology. 1994;191:378–87.

457. Bleharski JR, Li H, Meinken C, Graeber TG, Ochoa M-T, Yamamura M, et al. Use of genetic profiling in leprosy to discriminate clinical forms of the disease. Science. 2003 Sep 12;301(5639):1527–30.

458. Kiszewski AE, Becerril E, Aguilar LD, Kader ITA, Myers W, Portaels F, et al. The local immune response in ulcerative lesions of Buruli disease. Clin Exp Immunol. 2006 Mar;143(3):445–51.

459. Raju B, Hoshino Y, Belitskaya-Lévy I, Dawson R, Ress S, Gold JA, et al. Gene expression profiles of bronchoalveolar cells in pulmonary TB. Tuberc Edinb Scotl. 2008 Jan;88(1):39–51.

460. Vazquez-Torres A, Xu Y, Jones-Carson J, Holden DW, Lucia SM, Dinauer MC, et al. Salmonella pathogenicity island 2-dependent evasion of the phagocyte NADPH oxidase. Science. 2000 Mar 3;287(5458):1655–8.

461. Miller BH, Fratti RA, Poschet JF, Timmins GS, Master SS, Burgos M, et al. Mycobacteria inhibit nitric oxide synthase recruitment to phagosomes during macrophage infection. Infect Immun. 2004 May;72(5):2872–8.

462. Fernandes DM, Jiang X, Jung JH, Baldwin CL. Comparison of T cell cytokines in resistant and susceptible mice infected with virulent Brucella abortus strain 2308. FEMS Immunol Med Microbiol. 1996;16:193–203.

463. Ehrt S, Schnappinger D, Bekiranov S, Drenkow J, Shi S, Gingeras TR, et al. Reprogramming of the macrophage transcriptome in response to interferon-gamma and Mycobacterium tuberculosis: signaling roles of nitric oxide synthase-2 and phagocyte oxidase. J Exp Med. 2001;194:1123–40.

464. Nau GJ, Richmond JFL, Schlesinger A, Jennings EG, Lander ES, Young RA. Human macrophage activation programs induced by bacterial pathogens. Proc Natl Acad Sci U S A. 2002 Feb 5;99(3):1503–8.

465. Lee HC. Structure and Enzymatic Functions of Human CD38. Mol Med. 2006;12(11-12):317–23.

466. Lee C-U, Song E-K, Yoo C-H, Kwak Y-K, Han M-K. Lipopolysaccharide induces CD38 expression and solubilization in J774 macrophage cells. Mol Cells. 2012 Dec 1;34(6):573–6.

467. Partida-Sánchez S, Cockayne DA, Monard S, Jacobson EL, Oppenheimer N, Garvy B, et al. Cyclic ADP-ribose production by CD38 regulates intracellular calcium release, extracellular calcium influx and chemotaxis in neutrophils and is required for bacterial clearance in vivo. Nat Med. 2001 Nov;7(11):1209–16.

468. Deshpande DA, White TA, Dogan S, Walseth TF, Panettieri RA, Kannan MS. CD38/cyclic ADP-ribose signaling: role in the regulation of calcium homeostasis in airway smooth muscle. Am J Physiol Lung Cell Mol Physiol. 2005 May;288(5):L773–88.

469. Kang J, Park K-H, Kim J-J, Jo E-K, Han M-K, Kim U-H. The role of CD38 in Fcγ receptor (FcγR)-mediated phagocytosis in murine macrophages. J Biol Chem. 2012 Apr 27;287(18):14502–14.

470. Tliba O, Panettieri RA, Tliba S, Walseth TF, Amrani Y. Tumor necrosis factor-alpha differentially regulates the expression of proinflammatory genes in human airway smooth muscle cells by activation of interferon-beta-dependent CD38 pathway. Mol Pharmacol. 2004 Aug;66(2):322–9.

471. Amrani Y, Tliba O, Deshpande DA, Walseth TF, Kannan MS, Panettieri RA. Bronchial hyperresponsiveness: insights into new signaling molecules. Curr Opin Pharmacol. 2004 Jun;4(3):230–4.

472. Benacerraf B. Role of MHC gene products in immune regulation. Science. 1981 Jun 12;212(4500):1229–38.

473. Unanue ER, Beller DI, Lu CY, Allen PM. Antigen presentation: comments on its regulation and mechanism. J Immunol Baltim Md 1950. 1984 Jan;132(1):1–5.

474. Viksman MY, Liu MC, Bickel CA, Schleimer RP, Bochner BS. Phenotypic analysis of alveolar macrophages and monocytes in allergic airway inflammation. I. Evidence for activation of alveolar macrophages, but not peripheral blood monocytes, in subjects with allergic rhinitis and asthma. Am J Respir Crit Care Med. 1997 Mar 1;155(3):858–63.

475. Zhang J, Tachado SD, Patel N, Zhu J, Imrich A, Manfruelli P, et al. Negative regulatory role of mannose receptors on human alveolar macrophage proinflammatory cytokine release in vitro. J Leukoc Biol. 2005 Sep;78(3):665–74.

476. Sharif O, Matt U, Saluzzo S, Lakovits K, Haslinger I, Furtner T, et al. The scavenger receptor CD36 downmodulates the early inflammatory response while enhancing bacterial phagocytosis during pneumococcal pneumonia. J Immunol Baltim Md 1950. 2013 Jun 1;190(11):5640–8.

477. Schiff DE, Kline L, Soldau K, Lee JD, Pugin J, Tobias PS, et al. Phagocytosis of gram-negative bacteria by a unique CD14-dependent mechanism. J Leukoc Biol. 1997;62:786–94.

478. Fabriek BO, Dijkstra CD, van den Berg TK. The macrophage scavenger receptor CD163. Immunobiology. 2005;210:153–60.

479. Stuart LM, Deng J, Silver JM, Takahashi K, Tseng AA, Hennessy EJ, et al. Response to Staphylococcus aureus requires CD36-mediated phagocytosis triggered by the COOH-terminal cytoplasmic domain. J Cell Biol. 2005;170:477–85.

480. Savill J, Hogg N, Ren Y, Haslett C. Thrombospondin cooperates with CD36 and the vitronectin receptor in macrophage recognition of neutrophils undergoing apoptosis. J Clin Invest. 1992 Oct;90(4):1513–22.

481. Fadok VA, Warner ML, Bratton DL, Henson PM. CD36 is required for phagocytosis of apoptotic cells by human macrophages that use either a phosphatidylserine receptor or the vitronectin receptor (alpha v beta 3). J Immunol Baltim Md 1950. 1998 Dec 1;161(11):6250–7.

482. Noguera A, Gomez C, Faner R, Cosio B, González-Périz A, Clària J, et al. An investigation of the resolution of inflammation (catabasis) in COPD. Respir Res. 2012;13:101.

483. Zhang J, Zhu J, Imrich A, Cushion M, Kinane TB, Koziel H. Pneumocystis activates human alveolar macrophage NF-kappaB signaling through mannose receptors. Infect Immun. 2004 Jun;72(6):3147–60.

484. Hodge S, Hodge G, Jersmann H, Matthews G, Ahern J, Holmes M, et al. Azithromycin Improves Macrophage Phagocytic Function and Expression of Mannose Receptor in Chronic Obstructive Pulmonary Disease. Am J Respir Crit CARE Med. 2008 Jul 15;178:139–48.

485. Kaku Y, Imaoka H, Morimatsu Y, Komohara Y, Ohnishi K, Oda H, et al. Overexpression of CD163, CD204 and CD206 on Alveolar Macrophages in the

Lungs of Patients with Severe Chronic Obstructive Pulmonary Disease. PLoS ONE. 2014 Jan 30;9(1):e87400.

486. Devitt A, Moffatt OD, Raykundalia C, Capra JD, Simmons DL, Gregory CD. Human CD14 mediates recognition and phagocytosis of apoptotic cells. Nature. 1998;392:505–9.

487. Regueiro V, Campos MA, Morey P, Sauleda J, Agustí AGN, Garmendia J, et al. Lipopolysaccharide-binding protein and CD14 are increased in the bronchoalveolar lavage fluid of smokers. Eur Respir J. 2009 Feb 1;33(2):273–81.

488. Brass DM, Hollingsworth JW, McElvania-Tekippe E, Garantziotis S, Hossain I, Schwartz DA. CD14 is an essential mediator of LPS-induced airway disease. Am J Physiol - Lung Cell Mol Physiol. 2007 Jul 1;293(1):L77–83.

489. Francis SMS, Tan ME, Fung PR, Shaw JG, Semmler AB, Nataatmadja M, et al. Peripheral compartment innate immune response to Haemophilus influenzae and Streptococcus pneumoniae in chronic obstructive pulmonary disease patients. Innate Immun. 2013 Aug 1;19(4):428–37.

490. Kristiansen M, Graversen JH, Jacobsen C, Sonne O, Hoffman HJ, Law SK, et al. Identification of the haemoglobin scavenger receptor. Nature. 2001 Jan 11;409(6817):198–201.

491. Mattila JT, Ojo OO, Kepka-Lenhart D, Marino S, Kim JH, Eum SY, et al. Microenvironments in tuberculous granulomas are delineated by distinct populations of macrophage subsets and expression of nitric oxide synthase and arginase isoforms. J Immunol Baltim Md 1950. 2013 Jul 15;191(2):773–84.

492. MacNee W, Allan RJ, Jones I, De Salvo MC, Tan LF. Efficacy and safety of the oral p38 inhibitor PH-797804 in chronic obstructive pulmonary disease: a randomised clinical trial. Thorax. 2013 Aug;68(8):738–45.

493. Genovese MC, Cohen SB, Wofsy D, Weinblatt ME, Firestein GS, Brahn E, et al. A 24-week, randomized, double-blind, placebo-controlled, parallel group study of the efficacy of oral SCIO-469, a p38 mitogen-activated protein kinase inhibitor, in patients with active rheumatoid arthritis. J Rheumatol. 2011 May;38(5):846–54.

494. Hammaker D, Firestein GS. "Go upstream, young man": lessons learned from the p38 saga. Ann Rheum Dis. 2010 Jan;69 Suppl 1:i77–82.

495. Ryoo S, Choi J, Kim J, Bae S, Hong J, Jo S, et al. BIRB 796 has Distinctive Anti-inflammatory Effects on Different Cell Types. Immune Netw. 2013 Dec;13(6):283–8.

496. Zandvoort A, Postma DS, Jonker MR, Noordhoek JA, Vos JTWM, Geld YM van der, et al. Altered expression of the Smad signalling pathway: implications for COPD pathogenesis. Eur Respir J. 2006 Sep 1;28(3):533–41.

**A**

COPD (N=4)    Smokers (N=7)

□ 2 hr
■ 6 hr
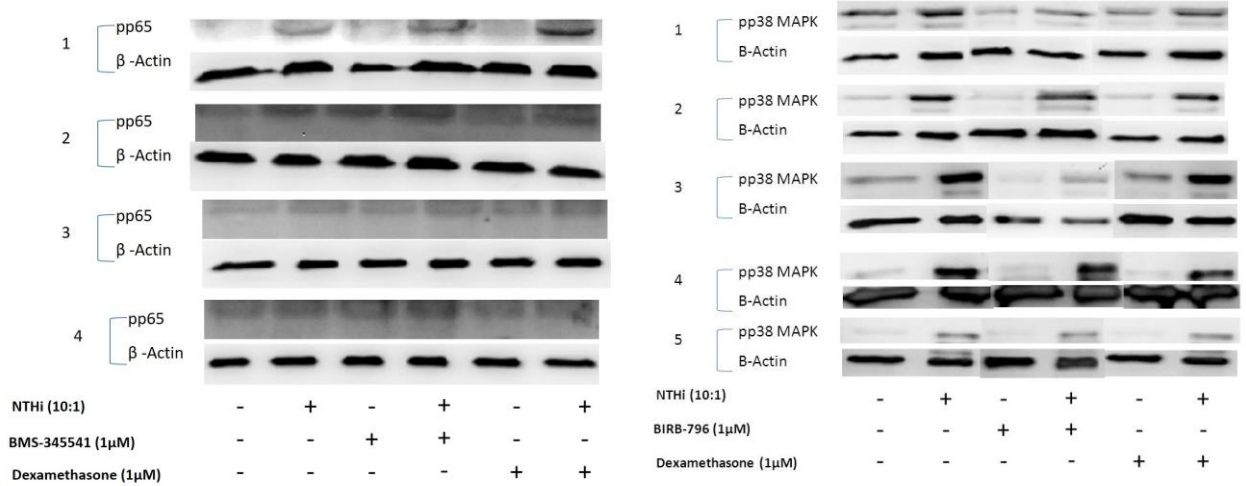■ 24 hr

**B**

**C**

**D**
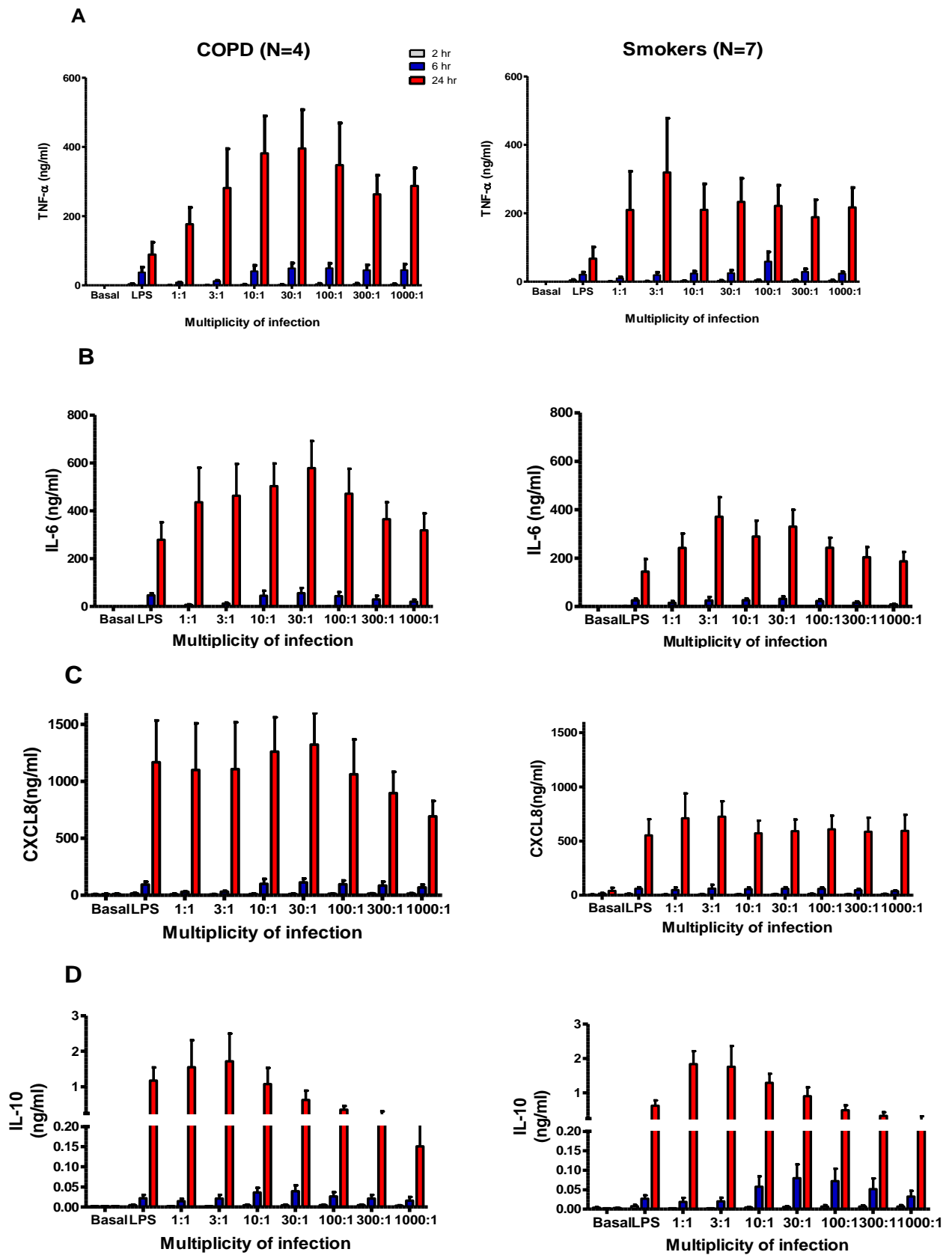
**NTHi provokes cytokine release from human alveolar macrophages; COPD versus smokers.** Alveolar macrophages from COPD (N=4) and smokers (N=7) were either infected with live NTHi (R2846) at MOI of 1:1-1000:1 or stimulated with LPS (1µg/ml). TNF-α (A), IL-6 (B), CXCL8 (C) and IL-10 (D) release was measured by ELISA at 2,6 and 24 hours of infection. Data are presented as Mean±SEM.
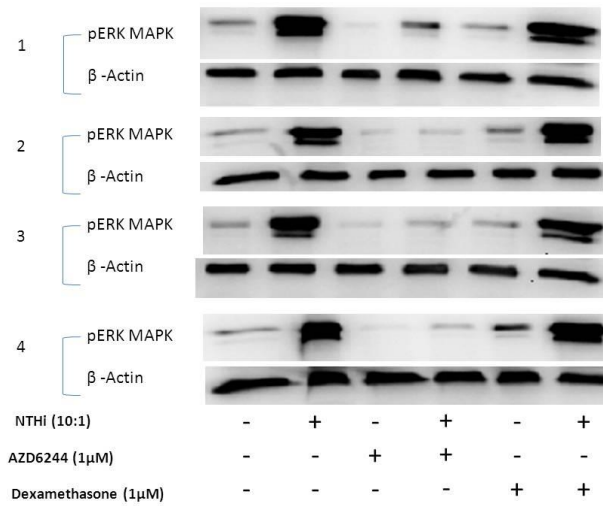
## Appendix 2:
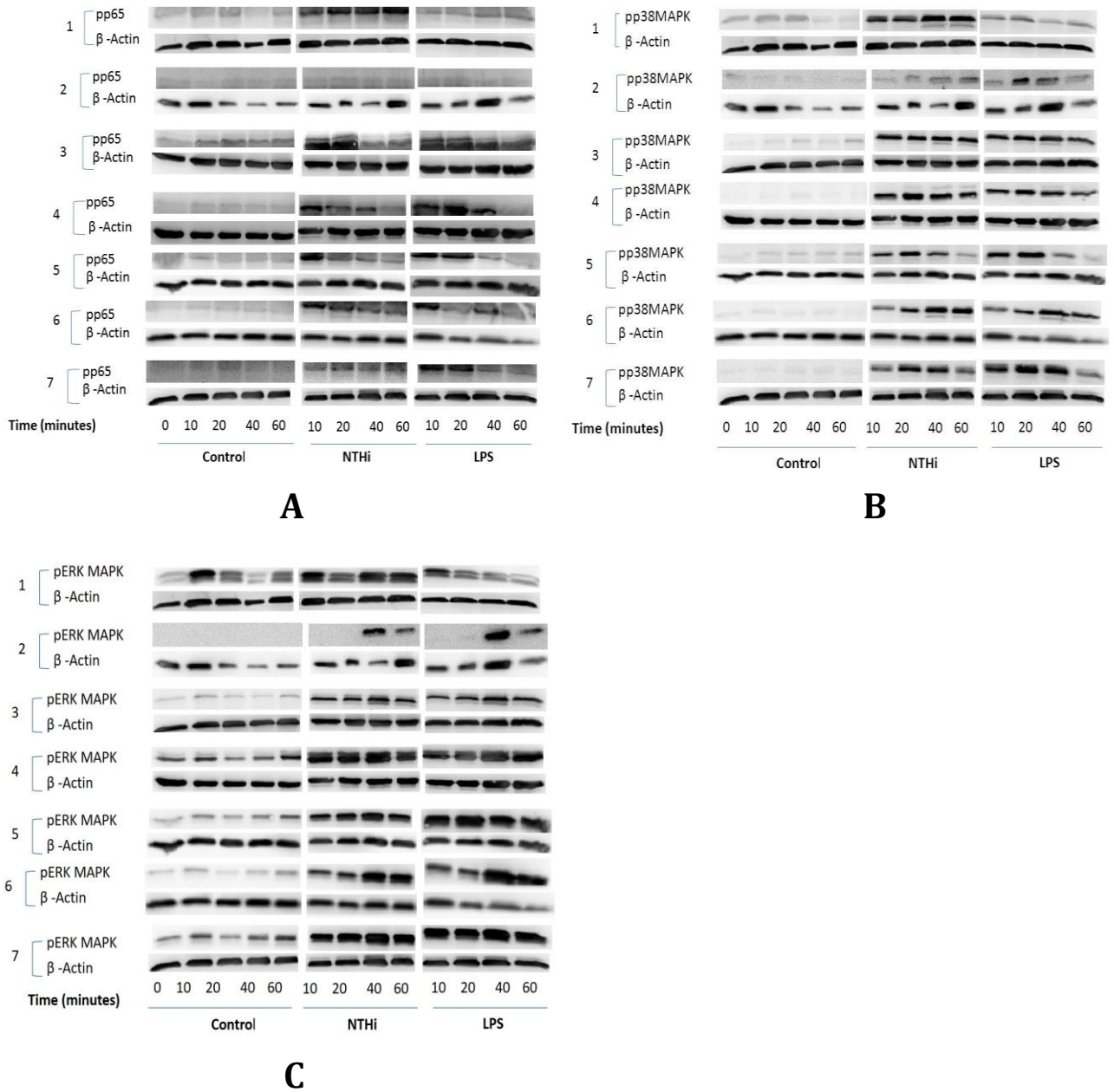


**A**



**B**



**C**

**Signalling pathways of NTHi in COPD alveolar macrophage:** Alveolar macrophages from COPD patients (N=7) were either stimulated with NTHi (10:1 MOI), LPS (1µg/ml) or left unstimulated. Phosphorylation of NF-κB subunit (p65) (A), p38 MAPK (B) and ERK MAPK (C) was assessed at 0, 10, 20, 40 and 60 minutes of stimulation by western blot. Individual blots are shown. β-Actin was used as a loading control.
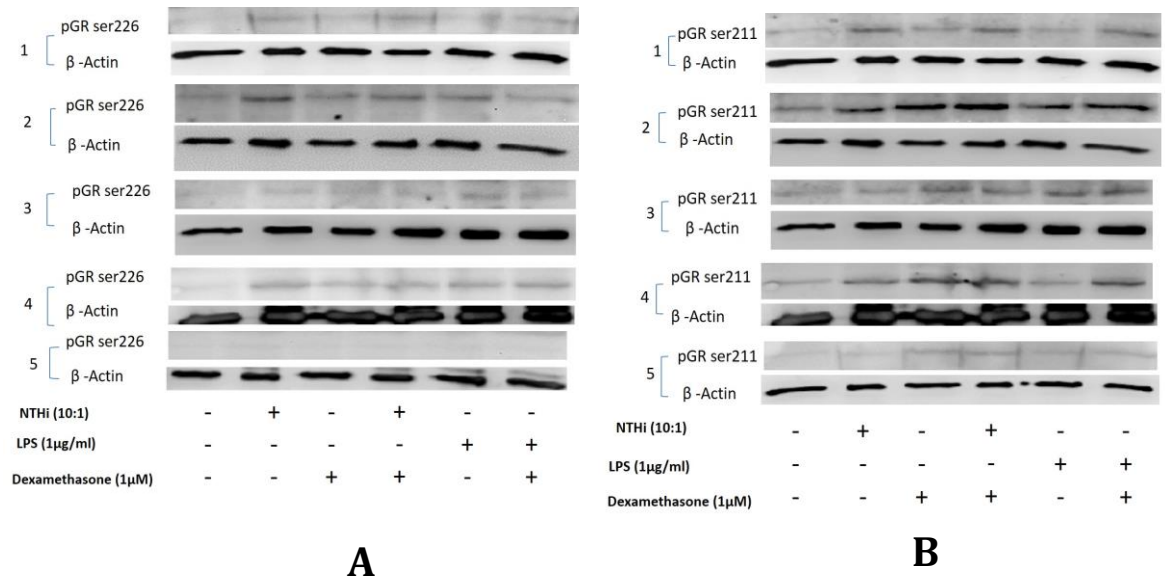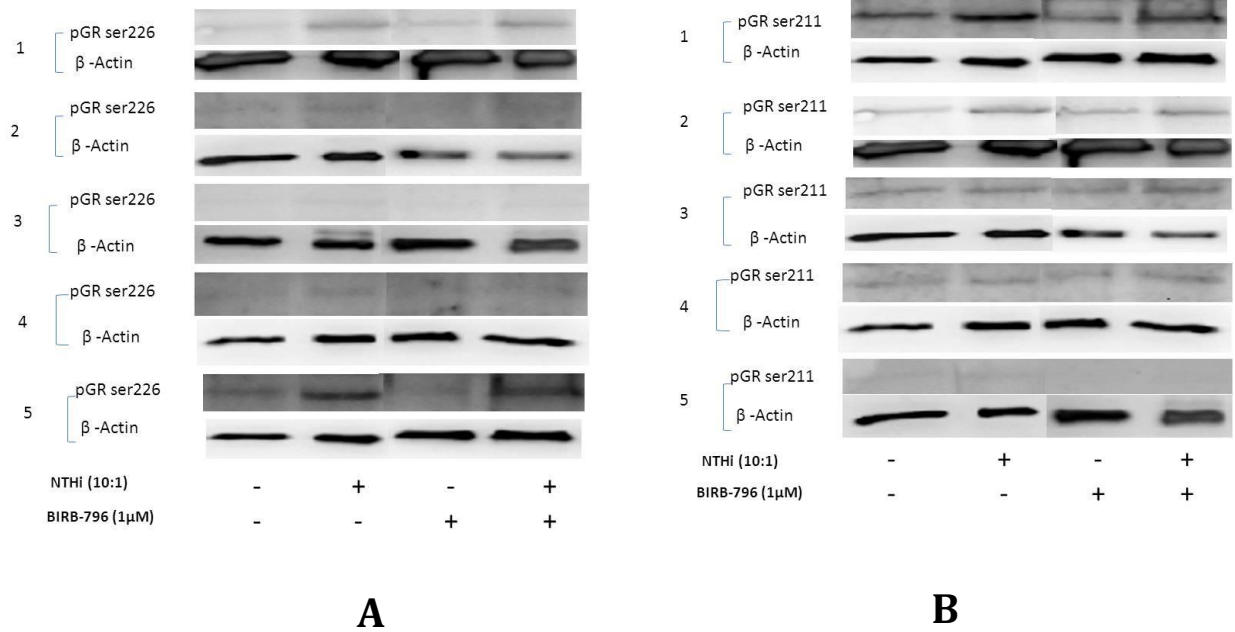
304

**A**



**B**



**C**

**The effect of kinase inhibitors and dexamethasone on NTHi-activated signalling pathways:** Alveolar macrophages from 4 COPD patients were pretreated with BMS-345541, BIRB-796, AZD6244 or dexamethasone, each at 1µM for 1 hour before stimulation with NTHi (10:1 MOI). After 20 minutes, cells were lysed and studied for phosphorylation of p65 (A), p38 (B) and ERK MAPK (C) by western blot. Individual blots are shown. β-Actin was used as a loading control.

# Appendix 4:



**Effect of NTHi on glucocorticoid receptor phosphorylation in COPD alveolar macrophages:** COPD alveolar macrophages (N=5) were either stimulated with NTHi (10:1MOI) or LPS (1μg/ml) for 20 minutes with or without 1-hour pretreatment with dexamethasone at 1μM. cells were lysed and assessed for GR phosphorylation at ser 226 (A) and ser 211 (B) by Western blot. Individual blots are shown. β-Actin was used as a loading control.

**A**



**B**

**Role of p38MAPK in NTHi-induced GR phosphorylation in COPD alveolar macrophages:** COPD alveolar macrophages (N=5) were pretreated with BIRB-796 for 1 hour before 20 minutes stimulation with NTHi (10:1 MOI). Cell lysates were analysed for GR phosphorylation at ser 226 (A) and ser 211 (B) residues by western blot. Individual blots are shown. β-Actin was used as a loading control.